12-19-2016 12:00 AM

Liquid Phase Nano Metal Catalyzed Dechlorination of Chlorinated Organic Compounds

Omneya El-Sharnouby
The University of Western Ontario

Supervisor
Dr. Denis O'Carroll
The University of Western Ontario

Graduate Program in Civil and Environmental Engineering
A thesis submitted in partial fulfillment of the requirements for the degree in Doctor of Philosophy

Abstract

1,2-Dichloroethane (1,2-DCA) is among the most prevalent groundwater chlorinated organic compounds (COCs) found at hazardous sites throughout the world. Given its pervasive contamination and adverse health effects, there is considerable interest in developing novel remediation technologies for successfully treating 1,2-DCA along with other COCs from water sources. Chemical reduction by nano zero valent iron (monometallic (nZVI) or bimetallic (Pd-nZVI)) has proven to be a successful field applicable technology, yet it has failed in degrading such a recalcitrant compound as 1,2-DCA.

In this study, the development of a field applicable nano metal based technology capable of degrading 1,2-DCA was carried out. For the first and the second studies, the feasibility of catalyzed dechlorination of 1,2-DCA using borohydride as a Hydrogen (H_2) source over nano palladium (nPd) and nano copper (nCu) in the liquid phase at room temperature was investigated. Complete removal of 1,2-DCA in a matter of days or hours was achieved by either nPd or nCu particles coupled with borohydride. The novel dechlorination system produced mainly ethane as the dechlorination byproduct, without formation of toxic chlorinated intermediates. This phase also examined the influence of different experimental parameters including: metal loading, 1,2-DCA loading, nanoparticle synthesis parameters and groundwater solutes on the dechlorination kinetics. It was found that experimental parameters affect the chemical composition as well as oxidation state of the nanoparticles, which controls the dechlorination reaction rate. For the third study, the efficiency of the developed novel technology, along with nZVI, Pd-nZVI, and nZVI-dithionite in remediating a suite of COCs, including 1,2-DCA, in a groundwater sample from an industrial site in Australia was assessed. nZVI, Pd-nZVI, and nZVI-dithionite were able to break down COCs with the exception of 1,2-DCA. nZVI-dithionite was able to breakdown about 20% of 1,2-DCA. nPd or nCu coupled with borohydride degraded 55% and 94%, respectively, of 1,2-DCA along with complete removal of all other COCs. The presence of groundwater solutes was found to adversely affect dechlorination efficiency of the treatments.

Overall, this thesis presents a novel nano metal based remediation technology capable of reducing 1,2-DCA. The results suggest that the developed nano metal based technology can be

an effective remediation approach for multi-COCs contaminated groundwater depending upon site conditions.

Keywords

1,2-Dichloroethane, Dechlorination, Palladium, Copper, Liquid-Phase, Borohydride, Hydrogen, Groundwater Solutes.

Co-Authorship Statement

The thesis was written in accordance with the guidelines and regulations for an Integrated Article format stipulated by the School of Graduate and Postdoctoral Studies at the University of Western Ontario. The candidate designed, conducted and analyzed all of the experimental work in this thesis under the supervision of Dr. Denis O'Carroll and the guidance of Dr. Hardiljeet K. Boparai.

Chapter 2: Literature Review

Contributions:

Omneya El-Sharnouby: primary author/writer, developed outline, reviewed/revised chapter, reviewed references.

Denis O'Carroll: reviewed/revised chapter.

Chapter 3: Liquid Phase Nano Palladium Catalyzed Hydrodechlorination of 1,2-Dichloroethane

Contributions:

Omneya El-Sharnouby: primary author/writer, designed and developed experimental methodology, planned and conducted experiments, conducted laboratory analyses, synthesized nanoparticles, interpreted and analyzed the collected data.

Denis O'Carroll: assisted in experimental design, data interpretation, and reviewed and revised chapter.

Hardiljeet K. Boparai: assisted in experimental design, laboratory analyses, data interpretation, reviewed and revised chapter.

Jose Herrera: provided supervision and discussions on part of the experimental design and data interpretation.

Chapter 4: Impact of Solution Chemistry on Nano Copper Catalyzed Dechlorination of 1,2-Dichloroethane

Contributions:

Omneya El-Sharnouby: primary author/writer, designed and developed experimental methodology, planned and conducted experiments, conducted laboratory analyses, synthesized nanoparticles, interpreted and analyzed the collected data.

Denis O'Carroll: assisted in experimental design, data interpretation, and reviewed and revised chapter.

Hardiljeet K. Boparai: assisted in experimental design, laboratory analyses, data interpretation, reviewed and revised chapter.

Jose Herrera: provided supervision and discussions on part of the experimental design, and data interpretation.

Chapter 5: Nano Metal Based Technologies for Treating Chlorinated Organic Compounds Mixtures in Groundwater

Contributions:

Omneya El-Sharnouby: primary author/writer, designed and developed experimental methodology, planned and conducted experiments, conducted laboratory analyses, synthesized nanoparticles, interpreted and analyzed the collected data.

Denis O'Carroll: provided groundwater samples, assisted in data interpretation, reviewed and revised chapter.

Hardiljeet K. Boparai: assisted in experimental design, conducting experiments, laboratory analyses, data interpretation, reviewed and revised chapter.

Acknowledgments

First and foremost, I thank and praise God for giving me the strength, the energy, and the faith to complete this research.

I would like to express my deepest appreciation and gratitude to my supervisor Dr. Denis O'Carroll for his guidance, support, tolerance, infinite patience, and endless encouragement. I have enjoyed working under your supervision for the past few years. Thank you for believing in me, for every time you told me "it's a learning process, you can do it", for always being there for advice and guidance not on the scientific level only, but also on the human level. You have been my mentor, you have been a support, you have been a great teacher, and I'll always be proud that I am your student. I am infinitely grateful to you. Thank you.

Hardiljeet K. Boparai, thank you for your tremendous help throughout my research. Thank you for your comments, suggestions, reviews, laboratory teachings, advices, ideas, meetings, discussions, and for the faith you have always put in me. Thank you, thank you, thank you. Thank you for your tolerance, understanding, support, kindness, and caring. I would have never been able to finish this work without your help. I would have never continued my studies with you next to me. You are a true inspiration to me on all levels. I will never forget all the kind things that you have done, and I hope one day I can return it to you.

I would also like to thank everyone who I have worked with in the laboratory, or have helped me throughout my study years. Dr. Ahmed Chowdhury, Dr. Cjestmir de Boer, Ariel Nunez Garcia, Caitlin Marshal, Mark Biesinger, Dr. Gardiner, Dr. Jose Herrera, Dr. Nakhla, Dr. El Naggar, Dr. Kopp, Dr. Hrymak, Dr. El Damatty, Rose Aquino, Whitney Barret, Kristen Edwards, Gureet Chandhok, thanks a lot for your help, thanks for always being there when needed.

Thanks to all the Restore members, thank you for being always nice, warm, and welcoming. Thank you for the ice cream socials, for the baking socials, for the thanksgiving gatherings, for the Christmas parties, birthday parties, group meetings, and for all the great times. You guys are the best group ever. Special thanks to Dr. Denis O'Carroll, Dr. Jason Gerhard, and Dr. Clare Robinson for holding the group meetings, and sending me to RENEW annual meetings, workshops, and seminars, I have learned a lot through these meetings, thanks a lot for your

devotion to your group, all the support through the years, and for always smiling and always creating friendly environments. Thank you.

Thanks to my friends who have supported me along this journey. A big thank you to Bilal Al-Bataina, thank you for always encouraging me, advising me, for all the coffee breaks every day (even though I rarely drank coffee!) and for always being there when I needed to talk, you are a true friend. You have always told me to just eat fruits and everything will turn out okay! Guess what? I ate fruits and everything turned out okay! From the bottom of my heart thanks to my friend Issam Gebril, thank you for being so calm always whenever I am complaining or struggling with my research, thank you for the long talks and walks, thank you for reading to me whenever I needed! You had the ability to adsorb any kind of negative energy or down feelings I had, and put a smile on my face at the worst times. You are the best thing that ever happened to me. When you are next to me, I can reach the stars! Thank you from here to the moon and back.

A special thank you to my uncle Reda, thank you for the international calls, for the midnight talks, thank you for your prayers, you have been with me all the way through, comforting me, and pushing me to accomplish this. You are my rock, thank you.

A very special acknowledgment goes to my brothers, sister in law, nephews, and my cat (Mr. Jojo!). Thank you for being in Canada, thank you for all the visits, Christmas gatherings, thank you for making this journey easier because you were in it. Special thanks to Mecckey. You are and have been always my role model. I always look up to you, and always try to follow your footsteps, from the day I joined Engineering School, Civil and Environmental Department, and years later Western University. All I am missing now is to marry someone from Poland (at least from a different nationality ;)) to be totally on your track! May be one day, who knows!

To my Mom and Dad, no words would ever be enough to express my gratitude. Dad, you were the first one to believe in me and encourage me to apply for a PhD at Western. Thank you for being you, a loving caring supporting encouraging and always laughing Dad. Mom, you have always dedicated your life for me and my brothers, and you have done more than anyone can imagine to help and support me through my studies, thank you for being with me all the way through day by day from day one, I would not have done it without your support, thank you for being a one of a kind Mom. Mom and dad I dedicate this thesis to you.

Table of Contents

List of Tables

List of Figures

List of Acronyms

1,1,2-TCA	1,1,2-Trichloroethane
1,1-DCE	1,1-Dichloroethene
1,2-DCA	1,2-Dichloroethane
B-nCu	Bare Nano Scale Copper
B-nPd	Bare Nano Scale Palladium
C-1,2-DCE	Cis-1,2-Dichloroethene
C-nCu	CMC stabilized Nano-scale Copper
C-nPd	CMC stabilized Nano-Scale Palladium
CMC	Carboxymethyl cellulose
COCs	Chlorinated volatile organic compounds
DCM	Dichloromethane
DLS	Dynamic Light Scattering
EDX	Energy Dispersive X-Ray Spectroscopy
H_2	Hydrogen Gas
JCPDS	Joint Committee on Powder Diffraction Standards
k_{obs}	Pseudo First Order Reaction Rate Constant
k_{sa}	Surface Area Normalized k_{obs}
$NaBH_4$	Sodium Borohydride
NAPL	Non aqueous Phase Liquids
nZVI	Nano-scale zero valent iron
ORP	Oxidation reduction potential
PCE	Perchloroethene/Tetrachloroethene
SEM	Scanning Electron Microscopy
TCE	Trichloroethene
TCM	Trichloromethane
TEM	Transmission Electron Microscopy
T-1,2-DCE	Trans-1,2-Dichloroethene
VC	Vinyl Chloride
XPS	X-ray Photoelectron Spectroscopy
XRD	X-ray Diffraction

Chapter 1

1 Introduction

1.1 Overview

Chlorinated organic compounds (COCs) are ubiquitously utilized for a number of industrial applications such as: pesticides, detergents, wood preservation, paint removers, dyes, solvents, and as intermediates in the manufacture of other chemicals (O'Carroll et al., 2013; Tobiszewski and Namieśnik, 2012). Upon release to the environment, these compounds are persistent over relatively long periods of time due to resistance to natural degradation processes (Lien and Zhang, 2005; Schüth et al., 2004; Song and Carraway, 2005b). Trichloromethane (TCM), dichloromethane (DCM), 1,1,2-trichloroethane (1,1,2-TCA), 1,2-dichloroethane (1,2-DCA), tetrachloroethene (PCE), trichloroethene (TCE), and vinyl chloride (VC) are among the most prevalent COCs at the contaminated sites (Zhang et al., 1998). Due to their preservative nature and possible carcinogenic effects, these compounds have been classified as priority pollutants by the U.S. Environmental Protection Agency and the Agency for Toxic Substances and Disease Registry (ATSDR, 2015; USEPA, 2015).

One of the most persistent COCs in the environment is 1,2-Dichloroethane (1,2-DCA, $C_2H_4Cl_2$) (Dewulf et al., 1995). 1,2-DCA is a dense non aqueous phase liquid (DNAPL) chlorinated aliphatic hydrocarbon (Atisha, 2011; Barbash and Reinhard, 1989b; Bejankiwar et al., 2005; Liu et al., 2014b). 1,2-DCA has good solubility in water (8.9 g L^{-1}), a low sorption coefficient (log K_{oc} = 1.28) and a low Henry's coefficient ($1.1x10^{-3}$ atm m^3 mol^{-1}) making it very stable in the environment (Dewulf et al., 1995). The predominant use of 1,2-DCA is in the synthesis of polyvinyl chloride (PVC), but it is also widely used as a solvent to remove lead from gasoline or extract oil from pesticides and pharmaceuticals (Liu et al., 2014b). 1,2-DCA causes circulatory and respiratory failure associated with neurological disorders in human beings (Humans et al., 1999) and has been determined to be a probable human carcinogen by the U.S. Environmental Protection Agency (EPA) and the International Agency for Cancer Research (IARC) (Liu et al., 2014b). The maximum

contamination level (MCL) for 1,2-DCA in drinking water is set as 5 μg L^{-1} by the U.S. EPA and the maximum contaminant level goal (MCLG) is set as zero. Thus, there is considerable interest in developing field applicable technologies to treat the subsurface from 1,2-DCA.

Many technologies have been implemented to remove 1,2-DCA from soil and groundwater. Physical treatments such as adsorption onto activated carbon and air stripping processes are applied. However, these physical treatments only transfer the contaminants from water to another phase, and disposal or further contaminant treatment is required thereafter (Crittenden et al., 2012). Biodegradation has been proven capable of degrading 1,2-DCA under both aerobic and anaerobic conditions (Alpaslan Kocamemi and Cecen, 2010; Dinglasan-Panlilio et al., 2006; Smidt and de Vos, 2004). However, biodegradation of 1,2-DCA is often incomplete and leads to the accumulation of more hazardous byproducts (e.g. VC) (Le and Coleman, 2011). Several studies have shown that 1,2-DCA can be successfully degraded by chemical methods such as: reduction with hydrogen sulfide (Barbash and Reinhard, 1989b), electrochemical degradation on stainless-steel electrodes (Bejankiwar et al., 2005), or Fenton's oxidation process (Vilve et al., 2010). Nonetheless, the application of these techniques is hampered due to drawbacks associated with their implementation, high cost, incomplete and slow degradation, as well as complex process control, rendering them impractical. Thus, there is an immediate need to develop effective field applicable technologies for 1,2-DCA remediation.

The reduction of chlorinated aliphatic hydrocarbons in the presence of electron donors is thermodynamically feasible under ambient conditions (Atisha, 2011; O'Carroll et al., 2013). Given this, the degradation of COCs by direct reduction using zero-valent iron (nZVI) technology has received great interest (Atisha, 2011; Elliott and Zhang, 2001; O'Carroll et al., 2013; Zhang et al., 1998). The very small dimensions of nZVI allow them to be injected in the form of a water slurry into the contaminated zone requiring treatment (Elliott and Zhang, 2001; O'Carroll et al., 2013).

A wide variety of chlorinated compounds (e.g. PCE, TCE, and 1,1,2-TCA) are easily degraded using nZVI (Arnold et al., 1999; Atisha, 2011; VanStone et al., 2007). Thus, over

the last decade, liquid-phase chemical reduction by nZVI has become a very promising subsurface remediation technology (O'Carroll et al., 2013). Nonetheless, although thermodynamically feasible, so far 1,2-DCA has been found to be almost absolutely resistant to reduction by nZVI (Atisha, 2011; Nunez Garcia et al., 2016b; Song and Carraway, 2005b). 1,2-DCA degradation could be achieved only when nZVI is coupled with dithionite, a very strong reductant, however with relatively slow reduction rates (Nunez Garcia et al., 2016b). Moreover, although doping nZVI with catalysts (i.e. palladium) has been reported to enhance nZVI reactivity and increase dechlorination rates for many chlorinated compounds, yet it has been found unable to enhance nZVI reactivity towards 1,2-DCA (Atisha, 2011; Song and Carraway, 2005b).

On the other hand, catalyzed reductive hydrodechlorination in the gas phase has been found to effectively dechlorinate 1,2-DCA via activated hydrogen gas (H_2) on catalyst surfaces (Borovkov et al., 2003; Job et al., 2005; Kaminska and Srebowata, 2015; Lambert et al., 2005; Lambert et al., 2004; Legawiec-Jarzyna et al., 2004; Li et al., 2009; Luebke et al., 2002; Śrębowata et al., 2007; Śrębowata et al., 2011; Xie et al., 2008). The catalyst activates the H_2 into atomic hydrogen (Equation 1-1), a robust reductant, which in turn reduces the COCs adsorbed on adjacent sites (Equation 1-2) (Álvarez-Montero et al., 2010; Chaplin et al., 2012; Tavoularis and Keane, 1999). A wide variety of group VIII and Ib catalysts are utilized to catalyze gas phase hydrodechlorination reactions (Bozzelli et al., 1992; Heinrichs et al., 1997b; Śrębowata et al., 2007; Xie et al., 2008). Group VIII catalysts (e.g. Pd, Pt, Ni) are expensive but have strong H_2 activation properties with the ability to replace adsorbed chlorine atoms by hydrogen atoms resulting in high dechlorination efficiencies (Fung and Sinfelt, 1987; Kulkarni et al., 1999b; Urbano and Marinas, 2001). On the other hand, group Ib catalysts (e.g. Cu, Ag, Au) are cheaper and can form strong bonds with the chlorides of the COCs (halogens in general) facilitating the dechlorination reaction (Bonarowska et al., 2010; Borovkov et al., 2003; Lambert et al., 2005; Luebke et al., 2002; Meshesha et al., 2013; Pardey et al., 2005; Vadlamannati et al., 1999; Vadlamannati et al., 2000; Xie et al., 2008). Among all utilized hydrodechlorination catalysts, Pd is the most effective and commonly used one for hydrodechlorination reactions (Bonarowska et al., 2010; Chen, 2003; Kulkarni et al., 1999b; Urbano and Marinas, 2001).

$$H_2 \xrightarrow{Catalyst} 2H^{\cdot} \quad \text{(Equation 1-1)}$$

$$RCl + H_2 \xrightarrow{Catalyst} RH + HCl \quad \text{(Equation 1-2)}$$

Where RCL is a chlorinated hydrocarbon.

Gas-phase reductive hydrodechlorination is carried out at high temperatures (>200ºC) and uses a direct H_2 gas stream which makes it impractical for in-situ applications (Urbano and Marinas, 2001). Thus, research was devoted into applying catalyzed reductive dechlorination in the liquid phase. Recently, liquid-phase catalyzed reductive hydrodechlorination on Pd and Cu catalysts emerged as a water and wastewater treatment technology (Aramendia et al., 2002; Chaplin et al., 2012; Gómez-Sainero et al., 2002; Kopinke et al., 2004; Kovenklioglu et al., 1992; Lowry and Reinhard, 1999; Mackenzie et al., 2006; McNab Jr and Ruiz, 1998; Yuan and Keane, 2003; Zhang et al., 2015; Zhao et al., 2008), using a range of alternative hydrogen sources (e.g. potassium formate, formic acid, 2-propanol, sodium borohydride, and hydrazine) (Anwer et al., 1989; Aramendia et al., 2000; Huang et al., 2011; Kopinke et al., 2004; Ukisu and Miyadera, 1997; Wiener et al., 1991). The technology has been found capable of rapidly dehalogenating a variety of common halogenated contaminants such as: chlorinated ethenes, chlorinated methanes, chlorinated aromatic compounds, chlorinated biphenyls, chlorofluorocarbons, and even halogenated pesticides, without the formation of substantial amounts of chlorinated intermediate compounds (e.g. (Aramendia et al., 2002; Chaplin et al., 2012; Gómez-Sainero et al., 2002; Kopinke et al., 2004; Kovenklioglu et al., 1992; Lowry and Reinhard, 1999; Mackenzie et al., 2006; McNab Jr and Ruiz, 1998; Yuan and Keane, 2003; Zhang et al., 2015; Zhao et al., 2008)). Moreover, a few field application studies of the technology were found effective (Davie et al., 2008; Mcnab et al., 2000; Schüth et al., 2004). Nonetheless, to date limited work has been devoted to the liquid phase catalyzed reductive hydrodechlorination of 1,2-DCA. To our knowledge, with the only exception being the study by Huang et al., studies on the catalytic hydrodechlorination of 1,2-DCA in the liquid phase were limited and not successful (Huang et al., 2011; Lowry and Reinhard, 1999; McNab Jr and Ruiz, 1998).

Therefore, the main aim of this work is to study the feasibility and develop a nano metal based catalyzed reductive dechlorination technology capable of reducing 1,2-DCA in the liquid phase. Since borohydride is already standardly used in excess amounts for the nano metal synthesis, this excess borohydride or freshly added borohydride is utilized as the H_2 source in this study (Equation 1-3) (Gómez-Lahoz et al., 1993; Huang et al., 2011), making the technology more economical and feasible.

$$\boldsymbol{BH_4^- + 2H_2O \rightarrow BO_2^- + 4H_2 \uparrow} \qquad \text{(Hydrolysis)} \qquad \text{(Equation 1-3)}$$

1.2 Research Objectives

The overall objective of this study was to develop a nano metal based field applicable technology capable of reducing 1,2-DCA in the liquid phase.

The first objective was to develop and investigate the effectiveness of Pd nano metals (nPd) in catalyzing the dechlorination of 1,2-DCA in the liquid phase, in the presence of residual borohydride after particles synthesis as the H_2 source. Moreover, this phase also examined the influence of different experimental parameters including: metal loading, 1,2-DCA loading, and nPd particle synthesis parameters on the dechlorination kinetics. In addition to that, the effect of the different particles synthesis parameters on the surface and catalytic properties of the Pd nanoparticles was evaluated.

The second objective was to investigate the effectiveness of Cu nano (nCu) particles compared to nPd particles in catalyzing the dechlorination of 1,2-DCA in the presence of residual borohydride as the H_2 source. Similar to the first objective, this phase evaluated the effect of the different experimental parameters on the dechlorination kinetics. Moreover, this study assessed the effect of the commonly encountered groundwater solutes on the developed treatment efficiency in catalytically reducing 1,2-DCA.

The third objective was to assess the efficiency of the developed novel technology in remediating a suite of COCs including 1,2-DCA in a groundwater sample from an industrial site in Australia. Moreover, this phase evaluated and correlated dechlorination efficiencies of already existing dechlorination technologies: nZVI, nZVI-Pd, nZVI-dithionite, and dithionite in remediating the same groundwater sample.

1.3 Thesis Outline

This thesis is written in "Integrated Article" format and comprises of 6 chapters including the current chapter. A brief description of the next five chapters is presented below:

Chapter 2 provides a survey of the existing literature on reductive dechlorination technologies. This includes a review on nZVI technologies and both gas and liquid phase catalytic hydrodechlorination technologies.

Chapter 3 presents the development of nPd particles coupled with borohydride treatment. This includes the effect of the different experimental parameters on 1,2-DCA dechlorination kinetics.

Chapter 4 evaluates nCu particles coupled with borohydride treatment efficiency in catalytically reducing 1,2-DCA under different experimental conditions and examines the impact of different groundwater solutes on the dechlorination kinetics.

Chapter 5 assesses the effectiveness of the developed treatments from chapter 3 and 4 in degrading a suite of COCs in a groundwater sample from an industrial site in Australia. Moreover, this phase investigates the efficiency of other reductive dechlorination technologies in remediating the same groundwater sample.

Chapter 6 briefly summarizes the main conclusions drawn from this thesis as well as the thesis implications and discusses the limitations requiring future research.

1.4 References

Alpaslan Kocamemi, B. and Cecen, F., 2010. Cometabolic degradation and inhibition kinetics of 1, 2-dichloroethane (1, 2-DCA) in suspended-growth nitrifying systems. Environmental technology, 31(3): 295-305.

Álvarez-Montero, M., Gómez-Sainero, L., Juan-Juan, J., Linares-Solano, A. and Rodriguez, J., 2010. Gas-phase hydrodechlorination of dichloromethane with activated carbon-supported metallic catalysts. Chemical Engineering Journal, 162(2): 599-608.

Anwer, M.K., Sherman, D., Roney, J.G. and Spatola, A.F., 1989. Applications of ammonium formate catalytic transfer hydrogenation. 6. Analysis of catalyst, donor quantity, and solvent effects upon the efficacy of dechlorination. The Journal of Organic Chemistry, 54(6): 1284-1289.

Aramendia, M. et al., 2002. Liquid-phase hydrodechlorination of chlorobenzene over palladium-supported catalysts: Influence of HCl formation and NaOH addition. Journal of Molecular Catalysis A: Chemical, 184(1): 237-245.

Aramendia, M. et al., 2000. Hydrodehalogenation of aryl halides by hydrogen gas and hydrogen transfer in the presence of palladium catalysts. Studies in Surface Science and Catalysis, 130: 2003-2008.

Arnold, W.A., Ball, W.P. and Roberts, A.L., 1999. Polychlorinated ethane reaction with zero-valent zinc: pathways and rate control. Journal of Contaminant Hydrology, 40(2): 183-200.

Atisha, A., 2011. Degradation of 1,2-Dichloroethane With Nano-Scale Zero Valent Iron Particles, Western Ontario, 111 pp.

ATSDR, 2015. Detailed data table for the 2015 priority list of hazardous substances that will be the subject of toxicological profiles. Agency for Toxic Substances and Disease Registry, Atlanta, GA. https://www.atsdr.cdc.gov/spl/resources/atsdr_2015_spl_detailed_data_table.pdf. Accessed 19 May, 2016.

Barbash, J.E. and Reinhard, M., 1989b. Abiotic dehalogenation of 1,2-dichloroethane and 1,2-dibromoethane in aqueous solution containing hydrogen sulfide. Environmental Science & Technology, 23(11): 1349-1358.

Bejankiwar, R., Lalman, J.A., Seth, R. and Biswas, N., 2005. Electrochemical degradation of 1,2-dichloroethane (DCA) in a synthetic groundwater medium using stainless-steel electrodes. Water Research, 39(19): 4715-4724.

Bonarowska, M., Śrębowata, A. and Karpiński, Z., 2010. Synergistic effects in hydrodechlorination of organic compounds catalyzed by metals. Annales UMCS, Chemistry, 65(1): 1-8.

Borovkov, V.Y., Luebke, D.R., Kovalchuk, V.I. and d'Itri, J.L., 2003. Hydrogen-assisted 1, 2-dichloroethane dechlorination catalyzed by Pt-Cu/SiO2: Evidence for different functions of Pt and Cu sites. The Journal of Physical Chemistry B, 107(23): 5568-5574.

Bozzelli, J.W., Chen, Y.-M. and Chuang, S.S., 1992. CATALYTIC HYDRODECHLORINATION OF 1, 2-DICHLOROETHANE AND TRICHLOROETHYLENE OVER Rh/Si0 2 CATALYSTS. Chemical Engineering Communications, 115(1): 1-11.

Chaplin, B.P. et al., 2012. Critical Review of Pd-Based Catalytic Treatment of Priority Contaminants in Water. Environmental Science & Technology, 46(7): 3655-3670.

Chen, N., 2003. Kinetics of the hydrodechlorination reaction of chlorinated compounds on palladium catalysts, Worcester Polytechnic Institute.

Crittenden, J.C., Trussell, R.R., Hand, D.W., Howe, K.J. and Tchobanoglous, G., 2012. MWH's Water Treatment: Principles and Design: Principles and Design. John Wiley & Sons.

Davie, M.G., Cheng, H., Hopkins, G.D., LeBron, C.A. and Reinhard, M., 2008. Implementing heterogeneous catalytic dechlorination technology for remediating TCE-contaminated groundwater. Environmental science & technology, 42(23): 8908-8915.

Dewulf, J., Drijvers, D. and Van Langenhove, H., 1995. Measurement of Henry's law constant as function of temperature and salinity for the low temperature range. Atmospheric Environment, 29(3): 323-331.

Dinglasan-Panlilio, M.J., Dworatzek, S., Mabury, S. and Edwards, E., 2006. Microbial oxidation of 1,2-dichloroethane under anoxic conditions with nitrate as electron acceptor in mixed and pure cultures. FEMS Microbiology Ecology, 56(3): 355-364.

Elliott, D.W. and Zhang, W.-X., 2001. Field assessment of nanoscale bimetallic particles for groundwater treatment. Environmental Science & Technology, 35(24): 4922-4926.

Fung, S.C. and Sinfelt, J.H., 1987. Hydrogenolysis of methyl chloride on metals. Journal of Catalysis, 103(1): 220-223.

Gómez-Lahoz, C., García-Herruzo, F., Rodríguez-Maroto, J.M. and Rodríguez, J.J., 1993. Cobalt(II) removal from water by chemical reduction with sodium borohydride. Water Research, 27(6): 985-992.

Gómez-Sainero, L.M., Seoane, X.L., Fierro, J.L. and Arcoya, A., 2002. Liquid-phase hydrodechlorination of CCl 4 to CHCl 3 on Pd/carbon catalysts: nature and role of Pd active species. Journal of Catalysis, 209(2): 279-288.

Heinrichs, B.t., Delhez, P., Schoebrechts, J.-P. and Pirard, J.-P., 1997b. Palladium–silver sol-gel catalysts for selective hydrodechlorination of 1, 2-dichloroethane into ethylene. Journal of Catalysis, 172(2): 322-335.

Huang, C.-C., Lo, S.-L., Tsai, S.-M. and Lien, H.-L., 2011. Catalytic hydrodechlorination of 1, 2-dichloroethane using copper nanoparticles under reduction conditions of sodium borohydride. Journal of Environmental Monitoring, 13(9): 2406-2412.

Humans, I.W.G.o.t.E.o.C.R.t., Cancer, I.A.f.R.o. and Organization, W.H., 1999. Re-evaluation of some organic chemicals, hydrazine and hydrogen peroxide. IARC, International Agency for Research on Cancer.

Job, N. et al., 2005. Hydrodechlorination of 1, 2-dichloroethane on Pd–Ag catalysts supported on tailored texture carbon xerogels. Catalysis today, 102: 234-241.

Kaminska, I.I. and Srebowata, A., 2015. Active carbon-supported nickel-palladium catalysts for hydrodechlorination of 1,2-dichloroethane and 1,1,2-trichloroethane. Research on Chemical Intermediates, 41: 9267-9280.

Kopinke, F.-D., Mackenzie, K., Koehler, R. and Georgi, A., 2004. Alternative sources of hydrogen for hydrodechlorination of chlorinated organic compounds in water on Pd catalysts. Applied Catalysis A: General, 271(1): 119-128.

Kovenklioglu, S., Cao, Z., Shah, D., Farrauto, R.J. and Balko, E.N., 1992. Direct catalytic hydrodechlorination of toxic organics in wastewater. AIChE Journal, 38(7): 1003-1012.

Kulkarni, P.P., Deshmukh, S.S., Kovalchuk, V.I. and d'Itri, J.L., 1999b. Hydrodechlorination of dichlorodifluoromethane on carbon-supported Group VIII noble metal catalysts. Catalysis letters, 61(3-4): 161-166.

Lambert, S., Ferauche, F., Brasseur, A., Pirard, J.-P. and Heinrichs, B., 2005. Pd–Ag/SiO 2 and Pd–Cu/SiO 2 cogelled xerogel catalysts for selective hydrodechlorination of 1, 2-dichloroethane into ethylene. Catalysis today, 100(3): 283-289.

Lambert, S., Polard, J.-F., Pirard, J.-P. and Heinrichs, B.t., 2004. Improvement of metal dispersion in Pd/SiO 2 cogelled xerogel catalysts for 1, 2-dichloroethane hydrodechlorination. Applied Catalysis B: Environmental, 50(2): 127-140.

Le, N. and Coleman, N., 2011. Biodegradation of vinyl chloride, cis-dichloroethene and 1,2-dichloroethane in the alkene/alkane-oxidising Mycobacterium strain NBB4. Biodegradation, 22(6): 1095-1108.

Legawiec-Jarzyna, M., Śrebowata, A., Juszczyk, W. and Karpiński, Z., 2004. Hydrodechlorination over Pd–Pt/Al 2 O 3 catalysts: A comparative study of chlorine removal from dichlorodifluoromethane, carbon tetrachloride and 1, 2-dichloroethane. Applied Catalysis A: General, 271(1): 61-68.

Li, L., Wang, X., Wang, A., Shen, J. and Zhang, T., 2009. Relationship between adsorption properties of Pt–Cu/SiO 2 catalysts and their catalytic performance for selective hydrodechlorination of 1, 2-dichloroethane to ethylene. Thermochimica Acta, 494(1): 99-103.

Lien, H.-L. and Zhang, W.-X., 2005. Hydrodechlorination of chlorinated ethanes by nanoscale Pd/Fe bimetallic particles. Journal of environmental engineering, 131(1): 4-10.

Liu, X., Vellanki, B.P., Batchelor, B. and Abdel-Wahab, A., 2014b. Degradation of 1,2-dichloroethane with advanced reduction processes (ARPs): Effects of process variables and mechanisms. Chemical Engineering Journal, 237(0): 300-307.

Lowry, G.V. and Reinhard, M., 1999. Hydrodehalogenation of 1-to 3-carbon halogenated organic compounds in water using a palladium catalyst and hydrogen gas. Environmental science & technology, 33(11): 1905-1910.

Luebke, D.R., Vadlamannati, L.S., Kovalchuk, V.I. and d'Itri, J.L., 2002. Hydrodechlorination of 1,2-dichloroethane catalyzed by Pt–Cu/C: effect of catalyst pretreatment. Applied Catalysis B: Environmental, 35(3): 211-217.

Mackenzie, K., Frenzel, H. and Kopinke, F.-D., 2006. Hydrodehalogenation of halogenated hydrocarbons in water with Pd catalysts: Reaction rates and surface competition. Applied Catalysis B: Environmental, 63(3): 161-167.

McNab Jr, W.W. and Ruiz, R., 1998. Palladium-catalyzed reductive dehalogenation of dissolved chlorinated aliphatics using electrolytically-generated hydrogen. Chemosphere, 37(5): 925-936.

Mcnab, W.W., Ruiz, R. and Reinhard, M., 2000. In-situ destruction of chlorinated hydrocarbons in groundwater using catalytic reductive dehalogenation in a reactive well: Testing and operational experiences. Environmental Science & Technology, 34(1): 149-153.

Meshesha, B.T. et al., 2013. PdCu alloy nanoparticles on alumina as selective catalysts for trichloroethylene hydrodechlorination to ethylene. Applied Catalysis A: General, 453(0): 130-141.

Nunez Garcia, A., Boparai, H.K. and O'Carroll, D.M., 2016b. Enhanced Dechlorination of 1,2-Dichloroethane by Coupled Nano Iron-Dithionite Treatment. Environmental Science & Technology, 50(10): 5243-5251.

O'Carroll, D., Sleep, B., Krol, M., Boparai, H. and Kocur, C., 2013. Nanoscale zero valent iron and bimetallic particles for contaminated site remediation. Advances in Water Resources, 51: 104-122.

Pardey, A. et al., 2005. Kinetics study of the hydrodechlorination of chlorobenzene catalyzed by immobilized copper complexes. Catalysis letters, 104(3-4): 141-150.

Schüth, C., Kummer, N.-A., Weidenthaler, C. and Schad, H., 2004. Field application of a tailored catalyst for hydrodechlorinating chlorinated hydrocarbon contaminants in groundwater. Applied Catalysis B: Environmental, 52(3): 197-203.

Smidt, H. and de Vos, W.M., 2004. Anaerobic microbial dehalogenation. Annu. Rev. Microbiol., 58: 43-73.

Song, H. and Carraway, E.R., 2005b. Reduction of Chlorinated Ethanes by Nanosized Zero-Valent Iron: Kinetics, Pathways, and Effects of Reaction Conditions. Environmental Science & Technology, 39(16): 6237-6245.

Śrębowata, A., Juszczyk, W., Kaszkur, Z. and Karpiński, Z., 2007. Hydrodechlorination of 1,2-dichloroethane on active carbon supported palladium–nickel catalysts. Catalysis Today, 124(1–2): 28-35.

Śrębowata, A., Lisowski, W., Sobczak, J.W. and Karpiński, Z., 2011. Hydrogen-assisted dechlorination of 1,2-dichloroethane on active carbon supported palladium–copper catalysts. Catalysis Today, 175(1): 576-584.

Tavoularis, G. and Keane, M.A., 1999. Gas phase catalytic dehydrochlorination and hydrodechlorination of aliphatic and aromatic systems. Journal of Molecular Catalysis A: Chemical, 142(2): 187-199.

Tobiszewski, M. and Namieśnik, J., 2012. Abiotic degradation of chlorinated ethanes and ethenes in water. Environmental Science and Pollution Research, 19(6): 1994-2006.

Ukisu, Y. and Miyadera, T., 1997. Hydrogen-transfer hydrodehalogenation of aromatic halides with alcohols in the presence of noble metal catalysts. Journal of Molecular Catalysis A: Chemical, 125(2): 135-142.

Urbano, F. and Marinas, J., 2001. Hydrogenolysis of organohalogen compounds over palladium supported catalysts. Journal of Molecular Catalysis A: Chemical, 173(1): 329-345.

USEPA, 2015. Priority pollutant list. United States Environmental Protection Agency. https://www.epa.gov/sites/production/files/2015-09/documents/priority-pollutant-list-epa.pdf. Accessed 19 May, 2016.

Vadlamannati, L.S., Kovalchuk, V.I. and d'Itri, J.L., 1999. Dechlorination of 1, 2-dichloroethane catalyzed by Pt–Cu/C: unraveling the role of each metal. Catalysis letters, 58(4): 173-178.

Vadlamannati, L.S., Luebke, D.R., Kovalchuk, V.I. and d'Itri, J.L., 2000. Olefins from chlorocarbons: Reactions of 1,2-dichloroethane catalyzed by Pt-Cu. In: F.V.M.S.M. Avelino Corma and G.F. José Luis (Editors), Studies in Surface Science and Catalysis. Elsevier, pp. 233-238.

VanStone, N., Elsner, M., Lacrampe-Couloume, G., Mabury, S. and Sherwood Lollar, B., 2007. Potential for Identifying Abiotic Chloroalkane Degradation Mechanisms using Carbon Isotopic Fractionation. Environmental Science & Technology, 42(1): 126-132.

Vilve, M. et al., 2010. Degradation of 1,2-dichloroethane from wash water of ion-exchange resin using Fenton's oxidation. Environmental Science and Pollution Research, 17(4): 875-884.

Wiener, H., Blum, J. and Sasson, Y., 1991. Transfer hydrogenolysis of aryl halides and other hydrogen acceptors by formate salts in the presence of palladium/carbon catalyst. The Journal of Organic Chemistry, 56(21): 6145-6148.

Xie, H. et al., 2008. Hydrodechlorination of 1,2-dichloroethane catalyzed by dendrimer-derived Pt–Cu/SiO2 catalysts. Journal of Catalysis, 259(1): 111-122.

Yuan, G. and Keane, M.A., 2003. Liquid phase catalytic hydrodechlorination of 2,4-dichlorophenol over carbon supported palladium: an evaluation of transport limitations. Chemical Engineering Science, 58(2): 257-267.

Zhang, M., He, F. and Zhao, D., 2015. Catalytic activity of noble metal nanoparticles toward hydrodechlorination: influence of catalyst electronic structure and nature of adsorption. Front. Environ. Sci. Eng., 9(5): 888-896.

Zhang, W.X., Wang, C.B. and Lien, H.L., 1998. Treatment of chlorinated organic contaminants with nanoscale bimetallic particles. Catalysis Today, 40(4): 387-395.

Zhao, Z.-F. et al., 2008. Synthesis of a nano-nickel catalyst modified by ruthenium for hydrogenation and hydrodechlorination. Catalysis Communications, 9(13): 2191-2194.

Chapter 2

2 Literature Review

2.1 Introduction

Chlorinated organic compounds (COCs) are a recalcitrant type of dense non aqueous phase liquids (DNAPL). Due to their intensive use in industrial applications, they are commonly found at brownfield and industrial sites (O'Carroll et al., 2013; Tobiszewski and Namieśnik, 2012). COCs include chlorinated methanes such as: trichloromethane (TCM), dichloromethane (DCM), chlorinated ethanes such as: 1,1,2-trichloroethane (1,1,2-TCA), 1,2-dichloroethane (1,2-DCA), and chlorinated ethenes such as: tetrachloroethene (PCE), trichloroethene (TCE), and vinyl chloride (VC) (Barnes et al., 2010; O'Carroll et al., 2013; Tobiszewski and Namieśnik, 2012; Zhang et al., 1998). These chemicals have been classified as priority pollutants with low drinking water allowable limits (i.e. ppb) by the U.S. Environmental Protection Agency and the Agency for Toxic Substances and Disease Registry due to their severe adverse health effects (ATSDR, 2015; USEPA, 2015). Due to their mobility in subsurface systems, possible carcinogenic effects and resistance to natural degradation processes, intensive research efforts are devoted into developing field applicable technologies for in-situ removal of these compounds.

Conventional groundwater treatment methods, such as sorption onto granular activated carbon (GAC), bioremediation, physio-chemical, and electrochemical degradation are in many cases not very effective. High costs, incomplete or slow degradation, as well as complex process control is what renders them impractical (Alpaslan Kocamemi and Cecen, 2010; Barbash and Reinhard, 1989b; Bejankiwar et al., 2005; Crittenden et al., 2012; Dinglasan-Panlilio et al., 2006; Le and Coleman, 2011; Smidt and de Vos, 2004; Vilve et al., 2010).

Reductive dechlorination of COCs by electron donors is thermodynamically feasible under ambient conditions (Atisha, 2011; O'Carroll et al., 2013). Thus, liquid phase nano metal based direct reduction technologies has received great interest (Atisha, 2011; Barnes et al., 2010; Lien and Zhang, 2005; O'Carroll et al., 2013; Song and Carraway, 2005b;

Tobiszewski and Namieśnik, 2012; Zhang et al., 1998). The dechlorination mechanism includes breakage of one or more carbon-chlorine bonds of a COC molecule where the chlorine atom is eliminated as a chloride ion (O'Carroll et al., 2013; Zhang et al., 1998). This cleavage requires an electron donor (i.e. zero valent iron or activated hydrogen gas) and possibly a proton donor depending on the reaction pathways (hydrogenolysis or dichloroelimination) (Arnold and Roberts, 2000a; Tobiszewski and Namieśnik, 2012; Yu, 2013). In the hydrogenolysis pathway, chlorine is replaced by hydrogen with simultaneous addition of two electrons to the molecule (Equation 2-1). In the dichloroelimination pathway, two electrons are transferred to the COC molecule and two chlorine atoms are released resulting in less saturated reaction products (Equation 2-2). Another reaction that usually takes place after the elimination step is called hydrogenation and it involves the addition of hydrogen to a double or triple C-C bond (Arnold et al., 1999; Arnold and Roberts, 2000a; O'Carroll et al., 2013; Tobiszewski and Namieśnik, 2012).

$$\boldsymbol{RCl + H^{+} + 2e^{-} \rightarrow RH + Cl^{-}} \qquad \text{(Equation 2-1)}$$

$$\boldsymbol{RCCl - CClR + 2e^{-} \rightarrow RC = CR + 2Cl^{-}} \qquad \text{(Equation 2-2)}$$

Where RCL is a chlorinated hydrocarbon.

The reductive dechlorination reaction is a surface mediated reaction where chemical and physical steps take place for the dechlorination reaction to occur. Firstly, reaction molecules diffuse within the interfacial region (active site). As soon as the molecule is adsorbed on the reactive site, the surface reaction can take place. Lastly, the product molecule desorbs from the active site and diffuses back to the solution (Deng et al., 1999; Wang et al., 2008).

Reductive dechlorination technologies includes: liquid phase reductive dechlorination by nano zero valent iron (nZVI) technology, gas phase catalyzed reductive dechlorination, and liquid phase catalyzed reductive dechlorination. nZVI is one of the most promising reductive dechlorination technologies proven capable of degrading a wide variety of COCs (O'Carroll et al., 2013). The very small dimensions of nZVI particles allow them to be injected in the form of a water slurry into the contaminated zone requiring treatment, which

makes it a very attractive remediation technology (Elliott and Zhang, 2001; O'Carroll et al., 2013). Nonetheless, so far 1,2-DCA has been found to be almost absolutely resistant to reduction by nZVI and palladized nZVI (Pd-nZVI) (Atisha, 2011; Nunez Garcia et al., 2016b; Song and Carraway, 2005b). Additionally, slow 1,2-DCA degradation rates have been observed when nZVI is coupled with strong reductants such as dithionite (Nunez Garcia et al., 2016b). On the other hand, gas phase reductive dechlorination technology has been proven capable of dechlorinating many COCs including 1,2-DCA (Borovkov et al., 2003; Job et al., 2005; Kaminska and Srebowata, 2015; Lambert et al., 2005; Lambert et al., 2004; Legawiec-Jarzyna et al., 2004; Li et al., 2009; Luebke et al., 2002; Śrębowata et al., 2007; Śrębowata et al., 2011; Xie et al., 2008). Nonetheless, gas-phase reductive dechlorination is carried out at high temperatures (>200°C) and uses a direct hydrogen gas (H_2) stream which makes it impractical for in-situ applications (Urbano and Marinas, 2001). Liquid-phase catalyzed dechlorination has been found to rapidly dechlorinate a variety of COCs without the formation of substantial amounts of chlorinated intermediate compounds (Aramendia et al., 2002; Chaplin et al., 2012; Kovenklioglu et al., 1992; Lowry and Reinhard, 1999; Mackenzie et al., 2006; McNab Jr and Ruiz, 1998). A few successful field applications of the technology were reported (Davie et al., 2008; Mcnab et al., 2000; Schüth et al., 2004) Yet, to date limited work has been devoted to the liquid-phase catalyzed reductive dechlorination of 1,2-DCA (Huang et al., 2011; Lowry and Reinhard, 1999; McNab Jr and Ruiz, 1998). Therefore, there is a pressing need to develop a liquid phase technology capable of degrading 1,2-DCA, and understanding the already existing reductive dechlorination technologies is essential and necessary to accomplish that.

2.2 Reductive Dechlorination by Nano Scale Zero Valent Iron Based Technologies

nZVI particles stand out as one of the most promising abiotic direct reduction remedial technologies due to their nano-sized dimensions leading to greater reactivity and potential for subsurface injection and transport to the contaminant zone (Atisha, 2011; Elliott and Zhang, 2001; He and Zhao, 2005; O'Carroll et al., 2013; Zhang et al., 1998). nZVI particles are easily synthesized without any need for highly specialized instruments, most commonly by borohydride reduction of the dissolved iron salt in aqueous phase at room temprature

(Equation 2-3) (Atisha, 2011; Liu et al., 2005a; Sun et al., 2006a; Zhang and Elliott, 2006). Usually, sodium borohydride is applied in excess amounts to accelerate the synthesis reaction as well as to ensure uniform growth of the metallic particle (Zhang, 2003).

$$2Fe^{2+} + BH_4^- + 3H_2O \rightarrow 2Fe^0 + H_2BO_3^- + 4H^+ + 2H_2 \uparrow \quad \text{(Equation 2-3)}$$

Due to van der Waals and magnetic forces, nZVI particles tend to agglomerate forming larger aggregates hindering their mobility and reducing available surface area for dechlorination reactions, consequently reducing dechlorination reaction rates (He and Zhao, 2005; Phenrat et al., 2007). To overcome this, usually stabilizers such as hydrophilic carbon and polyacrylic acid (PAA), starch, carboxymethyl cellulose (CMC), guar gum, and triblock copolymer (PMAA-PMMA-PSS) are added during or after the synthesis process to disperse the particles (He and Zhao, 2005; He and Zhao, 2007; Schrick et al., 2004; Tiraferri et al., 2008).

2.2.1 Reduction Mechanism

nZVI is a strong reductant with a redox potential of -0.44V (Equation 2-4), making it capable of reducing most of COCs (Atisha, 2011; O'Carroll et al., 2013). COCs reduction by nZVI involves electron transfer from nZVI to the COC resulting in breakage of the carbon chlorine bond with the release of chloride ion (Equation 2-5) (Zhang and Elliott, 2006). Moreover, nZVI produces H_2 gas by reduction of water (Equation 2-6) (O'Carroll et al., 2013).

$$Fe^0 \xrightarrow{E^0=-0.44V} Fe^{2+} + 2e^- \quad \text{(Equation 2-4)}$$

$$RCL + H^+ + Fe^0 \rightarrow RH + Fe^{2+} + Cl^- \quad \text{(Equation 2-5)}$$

$$Fe^0 + 2H_2O \rightarrow Fe^{2+} + H_2 \uparrow + 2OH^- \quad \text{(Equation 2-6)}$$

2.2.2 Reactivity with COCs

A wide variety of chlorinated compounds (e.g. TCM, 1,1,1-TCA, PCE etc.) can be degraded using nZVI (Lien and Zhang, 2001; Liu et al., 2005b; O'Carroll et al., 2013; Song and Carraway, 2005b; Song and Carraway, 2006; Tobiszewski and Namieśnik, 2012).

However, nZVI reactions with chlorinated ethanes are slower than chlorinated ethenes and may form toxic chlorinated byproducts (Lien and Zhang, 2005). Besides, although thermodynamically feasible, 1,2-DCA and DCM are found to be almost absolutely resistant to degradation by nZVI (Atisha, 2011; Song and Carraway, 2005b; Song and Carraway, 2006). Thus, to enhance nZVI reactivity, noble metals (e.g. Nickel, Palladium) are often doped on the nZVI surface forming bimetallic particles (Atisha, 2011; Barnes et al., 2010; Elliott and Zhang, 2001; O'Carroll et al., 2013; Zhang et al., 1998). Palladium (Pd), the most commonly doped metal, enhances nZVI reactivity by acting as a catalyst, adsorbing H_2 from water reduction by iron (Equation 2-7) and dissociating it into atomic $H^{\cdot}$ (Equation 2-8) (Atisha, 2011; Liu et al., 2014a; Nunez Garcia et al., 2016b). The activated hydrogen then attacks the chlorinated contaminants adsorbed on the iron surface leading to their dechlorination (Equation 2-8). Doping Pd on nZVI did enhance the dechlorination rates of many COCs (e.g. PCE, 1,1,2-TCA, Cis-DCE) without forming any toxic byproducts (Barnes et al., 2010; Lien and Zhang, 2005; Lim and Feng, 2007; O'Carroll et al., 2013; Zhang et al., 1998). However, even the Pd-nZVI bimetallic system has failed to degrade 1,2-DCA and DCM so far (Atisha, 2011; Lim and Feng, 2007; Wang et al., 2009).

$$\boldsymbol{H_2 \xrightarrow{Catalyst} 2H^{\cdot}} \qquad \text{(Equation 2-7)}$$

$$\boldsymbol{RCl + H_2 \xrightarrow{Catalyst} RH + HCl} \qquad \text{(Equation 2-8)}$$

It is not known yet the reason behind 1,2-DCA reduction resistance by nZVI or Pd-nZVI. Janada et al. suggested that adsorption of COCs on nZVI surface is the rate controlling step for the dechlorination reaction (Janda et al., 2004). As such, it is possible that nZVI or Pd doped on it is not providing adequate surface for adsorption of 1,2-DCA, preventing the dechlorination reaction from taking place. Infact, XPS studies point out that when Pd is impregnated on nZVI surface, Pd is totally reduced to Pd^0 due to nZVI action as a continuous source of electrons (Doong and Lai, 2005; Yan et al., 2010; Zhu and Lim, 2007). On the other hand, gas phase catalytic dechlorination reactions indicate that the adsorption of 1,2-DCA (COCs in general) takes place only on electron deficient sites of Pd (Choi et al., 1997; Gómez-Sainero et al., 2002). Thus, it is suggested that either nZVI

surface modification, or usage of Pd discretely is needed to facilitate adsorption of 1,2-DCA.

Recently, it was found that coupling nZVI with dithionite enhances nZVI reactivity towards 1,2-DCA (Nunez Garcia et al., 2016b). Sodium dithionite is a stronger reductant (E = -1.12 V) than nZVI, usually used to manipulate in-situ redox conditions to reduce subsurface ferric iron to ferrous iron for treating various organic and inorganic contaminants (Boparai et al., 2008; Boparai et al., 2006; Fruchter et al., 2000). Studies have also shown reduction of COCs by aqeuous solutions of dithionite (Boparai et al., 2006; Nzengung et al., 2001; Rodriguez and Rivera, 1997). In aqueous solutions, dithionite undergoes a disproportionation reaction producing two sulphoxyl radicals (Equation 2-9). Sulphoxyl radicals in turn also reacts with water yielding sulfite and thiosulfate reductants (Equation 2-10). Depending on the solution pH, a variety and a series of sulfur reductants are created (Deng et al., 2003). In the nZVI-dithionite treatment, dithionite enhances the reactivity of nZVI by providing additional electrons and coating the nZVI by an iron sulfide layer which preserves it from oxidation by water (Nunez Garcia et al., 2016b). In the study by Garcia et al., nZVI coupled with dithionite in bench scale experiments have yielded up to 92 % degradation of the initial 1,2-DCA concentration over the course of one year (Nunez Garcia et al., 2016b).

$$\boldsymbol{2S_2O_4^{2-} \rightleftarrows 4SO_2^*} \qquad \text{(Equation 2-9)}$$

$$\boldsymbol{2S_2O_4^{2-} + H_2O \rightarrow 2SO_3^{2-} + 2S_2O_3^{2-} + 2H^+} \qquad \text{(Equation 2-10)}$$

2.3 Reductive Dechlorination by Gas Phase Catalytic Hydrodechlorination Technology

Effective catalytic hydrodechlorination of organic wastes containing a variety of toxic and ozone-depleting compounds in the gas phase using direct H_2 gas has been shown (Li et al., 2009; Urbano and Marinas, 2001). The gas phase catalyzed hydrodechlorination reaction is carried out at high temperatures (+200^o C), using direct H_2 gas and supported nano/micro catalysts. The nano catalysts have the potential of very high reaction rates due to their high specific surface areas and low mass transfer restrictions (Hildebrand et al., 2009a). The

operation temperature is selected based on the desired byproducts, as the lower the operating temperature, the more partially chlorinated compounds are formed as byproducts (Kopinke et al., 2003; Urbano and Marinas, 2001).

2.3.1 Hydrodechlorination Metals

A variety of different catalysts from group VIII and Ib metals have been reported for effective gas phase hydrodechlorination reactions (Bozzelli et al., 1992; Heinrichs et al., 1997b; Śrębowata et al., 2007; Xie et al., 2008). These catalysts have different hydrodechlorination reaction activity and selectivity depending on their hydrogenation and C-Cl cleavage capabilities (Chen, 2003).

As for the hydrogenation characteristics, the bonding strength between hydrogen and the catalyst surface increases with an increase in vacant d-orbitals (Fogler, 1999), however according to the Sabatier Principle, maximum catalytic activity will not be realized if the bonding is too strong (Laursen et al., 2012). Thus, the maximum hydrogenation catalytic activity occurs when there is approximately one vacant d-orbital per atom (Bonarowska et al., 2010; Fogler, 1999). Therefore, group VIII metals (i.e.: Ni, Rh, Ru, Pd and Pt) are the most active metals for hydrogenation reactions (Bozzelli et al., 1992; Fogler, 1999; Lambert et al., 2005). Amongst group VIII metals, Pd is the most effective in hydrodechlorination reactions because of its efficiency in replacing chlorine atoms by hydrogen (Kulkarni et al., 1999b; Urbano and Marinas, 2001). It does not only promote C-Cl bond cleavage, but it is also the least affected by released chlorides ions poisoning (hydrogen halides in general) (Fung and Sinfelt, 1987; Kulkarni et al., 1999b; Urbano and Marinas, 2001). Therefore, Pd based catalysts are the most commonly used catalysts for gas and liquid phase catalytic hydrodechlorination experiments (Chaplin et al., 2012; Chen, 2003; Heck et al., 2009). The high activity of Pd catalysts is probably due to the relatively low chlorine coverage on their surface compared to other metals where the strongly adsorbed Cl atoms suppress the activity. That is because based on the direction of increasing nobility of the metals from left to right in the Periodic Table for group VIII metals, the chlorine coverage under hydrodechlorination conditions decreases towards the right in the series Ru > Rh > Pd and Os > Ir > Pt (Benitez and Del Angel, 2000; Urbano and Marinas, 2001). Platinum (Pt) based catalysts binds chlorine and chlorine-containing

organic intermediate species less strongly than Pd, and therefore show lower dehalogenation activity than Pd (Chaplin et al., 2012; Legawiec-Jarzyna et al., 2004). Ni is also a milder hydrogenation catalyst than Pd (Lingaiah et al., 2000; Murthy et al., 2004; Tavoularis and Keane, 1999). Group Ib metals (Cu, Ag, Au) are milder hydrogenation catalysts than group VIII metals, but are relatively cheaper, and can form stronger bonds with COCs (Bonarowska et al., 2010; Borovkov et al., 2003; Lambert et al., 2005; Luebke et al., 2002; Meshesha et al., 2013; Pardey et al., 2005; Vadlamannati et al., 1999; Vadlamannati et al., 2000; Xie et al., 2008).

Combining two catalysts (bimetallic catalysts) changes the adsorption energies of reactants and reaction products, which results in either higher activity or suppression of side reactions, depending on the specific metals combination (Borovkov et al., 2003). Studies on COCs demonstrated the ability of the bimetallic catalysts to selectively tailor byproducts to ethene or ethane, and/or less chlorinated alkenes, may be overcome poisoning, increase reactivity, and decrease process cost (Borovkov et al., 2003; Heck et al., 2009; Heinrichs et al., 1997b; Job et al., 2005; Lambert et al., 2005; Legawiec-Jarzyna et al., 2004; Li et al., 2009; Meshesha et al., 2013; Śrębowata et al., 2011; Vadlamannati et al., 1999; Xie et al., 2008). For instance, adding Au nano particles to Pd was found to enhance both Pd catalytic activity, and poisoning resistance to chlorine chemisorption onto Pd active sites, for trichloroethene hydrodechlorination (Heck et al., 2009). Also, modification of Ni surface with other metals, such as Au or Rh promoted its catalytic activity and stability in hydrodechlorination reactions against deactivation (Besenbacher et al., 1998; Zhao et al., 2008).

2.3.2 Reduction Mechanisms

The catalytic hydrodechlorination mechanisms involve activating the molecular hydrogen into atomic hydrogen (Catalyst-H$*$) which attacks the chlorinated organic molecule adsorbed on adjacent sites on the catalyst (Equations 2-7 & 2-8) (Álvarez-Montero et al., 2010; Tavoularis and Keane, 1999).

Catalysts participate in a catalytic cycle where COCs chlorinate their surface, then their surface is dechlorinated through reduction by the adsorbed hydrogen. Group Ib metals are

able to react with the COC and form a metal–chlorine bond as well as activate hydrogen gas in their zero valent state (Borovkov et al., 2003; Lambert et al., 2005; Luebke et al., 2002; Vadlamannati et al., 1999; Vadlamannati et al., 2000; Xie et al., 2008). However, for group VIII metals, dual electronic states are required in order for the hydrodechlorination reaction to take place: electron-deficient and metallic sites [M^{n+}, M^0]. H_2 chemisorbs and dissociates on M^0 to give the covalent adsorbed atom M–H. COCs chemisorbs dissociatively on M^{n+} site, leading to the formation of a highly reactive activated complex. Interaction between the two surface species leads to the byproducts (Choi et al., 1997; Choi et al., 1996). For instance, in the study by Choi et al., X-ray photoelectron spectroscopy (XPS) and X-ray absorption fine structure (XAFS) measurements indicate that Pt(II) species reacted with Cl ligands, while the bulk that remained as Pt metal were responsible for the H_2 chemisorption and dissociation (Choi et al., 1997). Therefore, the selectivity of the byproducts of the COCs hydrodechlorination reactions does not only depend on the type or ratio of the different metals (group VIII, and Ib), but also the synthesis/preparation method that leads to different ratios of electronic states of group VIII metals (Bai and Sachtler, 1991; Choi et al., 1996; Marchesini et al., 2008; Soares et al., 2011; Xie et al., 2011). Similarly, the support can also have an indirect effect on activity and selectivity by influencing the electronic state, size, and morphology of catalyst and thus the distribution of reactive sites (Henry, 1998; Kovenklioglu et al., 1992).

In the case of bimetallic particles, group Ib metals would be responsible for forming the metal chlorine bonds (as they form stronger bonds than group VIII metals) and group VIII metals would be responsible for supplying the hydrogen atoms (as they are stronger hydrogenation catalysts than group Ib metals) for the regeneration of the chlorinated surface of group Ib metal into the metallic form (Lambert et al., 2005; Xie et al., 2008).

2.3.3 1,2-Dichloroethane Reduction

Several gas-phase catalytic hydrodechlorination studies reported complete dechlorination of 1,2-DCA. The catalytic hydrodechlorination rate and extent of 1,2-DCA degradation as well as reaction pathways depend on operating temperatures and catalysts types (group VIII, or group Ib catalysts). At lower operating temperatures, production of chloroethane is reported as relatively stable byproduct.

Moreover, over strong hydrogenation catalysts (i.e. Pd, Pt, and Ru), ethane is the final byproduct detected from the dechlorination of 1,2-DCA through dissociative adsorption of 1,2-DCA followed by hydrogenation of the surface alkyl fragment to form ethane, with chloroethane being a possible secondary byproduct at temperatures < 250˚C (Borovkov et al., 2003; Bozzelli et al., 1992; Vadlamannati et al., 1999; Xie et al., 2008). On the other hand, over milder hydrogenation catalysts (group Ib metals), dechlorination selectivity shifts towards ethene, through dissociative adsorption of 1,2-DCA with successive breakage of the two C-Cl bonds followed by direct desorption of ethene (Heinrichs et al., 1997b; Job et al., 2005; Lambert et al., 2005; Li et al., 2009; Śrębowata et al., 2011; Vadlamannati et al., 1999; Xie et al., 2008). In other words, group Ib metals react with 1,2-DCA and picks up chlorine atoms, but does not hold firmly to the rest of the molecule which is then released as ethene (Heinrichs et al., 1997b). In addition to that, over bimetallic catalysts, selectivity to either ethene or ethane as well as dechlorination rates is a factor of the ratio between the two catalysts types. For example, Heinrichs et al. reported an increase in the selectivity of the byproducts for the reduction of 1,2-DCA to ethene on Ag rich Pd-Ag/SiO_2, and a shift in selectivity towards ethane on Pd rich Pd/Ag catalysts, where ethene is further hydrogenated to ethane by the adsorbed hydrogen on the Pd sites (Figure 2-1) (Heinrichs et al., 1997b). Similar results were reported in other studies for the dechlorination of 1,2-DCA on Pd/Ag catalysts (Heinrichs et al., 2001; Lambert et al., 2005). Also, Valdamannati et al., reported a 90% increase in selectivity towards ethene for a Cu/Pt ratio ⩾9 from the reduction of 1,2-DCA (Vadlamannati et al., 1999).

.

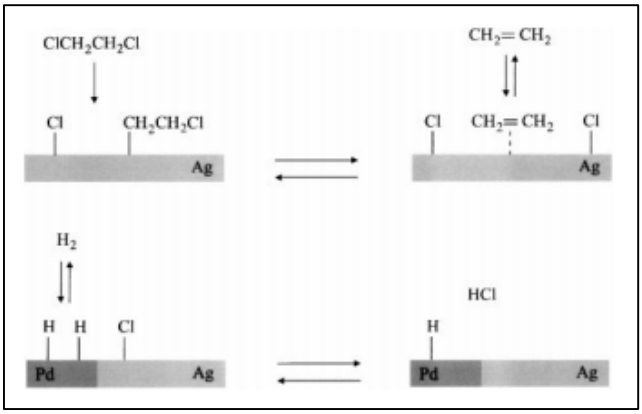

Figure 2-1: Reaction mechanism model for 1,2-DCA reduction on Ag rich Pd/Ag (Heinrichs et al., 1997b).

2.3.4 Catalysts Deactivation

Both group Ib and VIII catalysts are prone to poisoning by chlorides, sulfides, and hydrocarbons.

Group Ib metals are poor hydrogenation catalysts, thus lack the ability to dissociate enough hydrogen to clean their own sites from the adsorbed chlorides and are prone to rapid chlorine poisoning (e.g. (Lambert et al., 2005; Xie et al., 2008)). Even though group VIII metals are strong hydrogenation catalysts and are able to clean their own sites from the adsorbed chlorides, however if the halide acids (HCl) or chlorides produced during the reduction process are allowed to build up to high levels, inhibition or dissolution of catalyst takes place (Chaplin et al., 2012; Coq et al., 1993; Coq et al., 1986; Gómez-Sainero et al., 2004; Kulkarni et al., 1999b; Urbano and Marinas, 2001; Wiersma et al., 1998). For example, deactivation of Rh and Pd due to HCl derived from the hydrodechlorination of TCE, 1,2-DCA, and chlorobenzene have been reported (Bozzelli et al., 1992; Chang et al., 1999; Coq et al., 1986). In addition, Ordonez et al. reported poisoning of Pd nano (nPd) particles by the accumulation of HCl during the hydrodechlorination of TCE on Pd/C (Ordóñez et al., 2010). The authors proposed that the high Cl^- concentration and low pH possibly stabilize Pd^{2+} on the catalyst surface by the formation of $PdCl_3^-$ and $PdCl_4^{2-}$ species, suppressing sites responsible for TCE adsorption. Additionally, Formi et al., reported a 25% loss of Pd surface area after 20 h of hydrodechlorination of PCBs on Pd/C (Forni et al., 1997). Similarly, Choi et al. observed a drastic drop in the specific surface area of Pt/MgO catalysts during the hydrodechlorination of carbon tetrachloride which was also attributed to surface corrosion (Choi et al., 1996). Researchers suggest that the higher the operating temperatures, the more HCl discharge will be allowed, preventing chlorides poisoning of the catalyst (Benitez and Del Angel, 2000; Chaplin et al., 2012; Kopinke et al., 2003). For instance, in the study by Kopinke et al., increasing temperature from 200 ^oC to 250^oC resulted in complete restoration of Pd activity after deactivation through hydrodechlorination of different COCs due to adsorbed chlorides (Kopinke et al., 2003). Inhibiting concentrations of HCl or chlorides varies in the different studies up on the catalyst as well as substrate type, and operating conditions.

Group VIII catalysts usually suffer also from hydrocarbons depositions deactivating reactive sites (Legawiec-Jarzyna et al., 2004; Śrębowata et al., 2007; Śrębowata et al., 2011). The reason for deposition has been proposed to be due to low H_2/Substrate ratio (Urbano and Marinas, 2001). In addition to that, deactivation by H_2S and SO_2 (sulfur compounds) at very low concentrations as low as parts per million have been observed (Berube et al., 1987; L'Argentiere and Fi, 1990).

2.4 Reductive Dechlorination by Liquid Phase Catalyzed Hydrodechlorination Technology

Recently, liquid-phase catalyzed reductive hydrodechlorination has emerged as a water and wastewater treatment technology in the presence of direct H_2 gas (Aramendia et al., 2002; Chaplin et al., 2012; Davie et al., 2008; Gómez-Sainero et al., 2004; Gómez-Sainero et al., 2002; Heck et al., 2009; Hildebrand et al., 2009a; Hildebrand et al., 2009b; Janiak and Błażejowski, 2002; Kopinke et al., 2004; Kopinke et al., 2003; Lowry and Reinhard, 1999; Lowry and Reinhard, 2000; Lowry and Reinhard, 2001; Mackenzie et al., 2006; Mcnab et al., 2000; Ordóñez et al., 2010; Schreier and Reinhard, 1995; Schüth et al., 2004; Sun et al., 2011; Xia et al., 2004; Zhu and Lim, 2007), or hydrogen sources (e.g. potassium formate, formic acid, 2-propanol, sodium borohydride, and hydrazine) (Anwer et al., 1989; Aramendia et al., 2000; Huang et al., 2011; Kopinke et al., 2004; Ukisu and Miyadera, 1997; Wiener et al., 1991). Rapid catalyzed dehalogenation of a variety of commonly encountered halogenated groundwater contaminants including chlorinated ethenes (PCE, TCE, DCE, vinyl chloride), chlorinated methanes (carbon tetrachloride, chloroform), chlorinated aromatic compounds (1,2-dichlorobenzene), chlorinated biphenyls (4-chlorobiphenyl), chlorofluorocarbons (Freon-113), and even halogenated pesticides (1,2-dibromo-3-chloropropane (DBCP) and lindane) was found effective in the liquid phase at the bench scale without forming substantial amounts of halogenated intermediate compounds. In addition, a few effective pilot and field scale catalyzed reductive dechlorination applications were also reported effective (Davie et al., 2008; Mcnab et al., 2000; Schüth et al., 2004).

2.4.1 Hydrodechlorination Metals

Among all group VIII catalysts, Pd particles have proved to be well suited for promoting hydrodehalogenation reactions in the aqueous phase. For instance, Lowry et al. reported hydrodechlorination of 1-10 mg L^{-1} aqueous concentrations of PCE, TCE, cis -1,1-DCE trans-1,1-DCE, carbon tetrachloride, and 1,2-dibromo- 3-chloropropane on 0.22 g L^{-1} of Pd supported on Alumina, with only 4-6 mins half-lives, at nearly mass-transfer-limited rates (Lowry and Reinhard, 1999). Besides, unlike reductive dechlorination by nZVI, Pd catalyzed reductive dechlorination of TCE results in direct reduction to ethane without any formation of chlorinated intermediates (Figure 2-2) (Chaplin et al., 2012; Lowry and Reinhard, 1999; Lowry and Reinhard, 2000; McNab Jr and Ruiz, 1998; Nutt et al., 2005). The Pd catalyzed reductive dechlorination reactivity of COCs decreases in the order VC > TCE > TeCA >> DCA ~ DCM (Kopinke et al., 2003). On the other hand, other catalysts such as Pt, and Rh did not provide beyond 10% conversion for hydrodechlorination of COCs. (Kovenklioglu et al., 1992). Only one study in the literature reported successful reductive dechlorination utilizing a group Ib metal (unsupported nCu particles) (Huang et al., 2011). It is important to point out though that supporting the nano metals and the type of support plays an important role for the overall performance of the catalysts (Kovenklioglu et al., 1992).

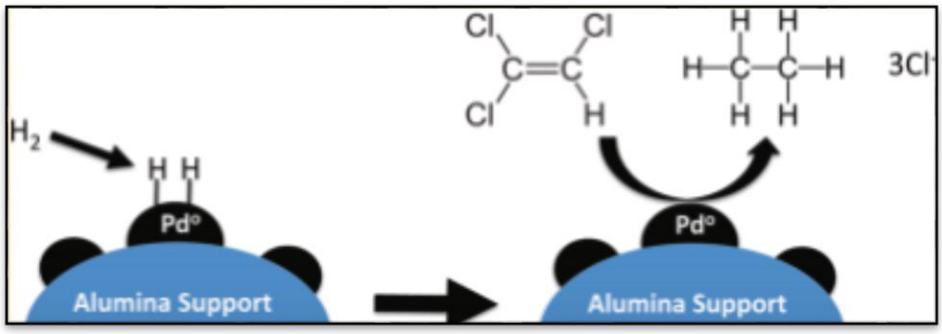

Figure 2-2: Reaction mechanism of TCE producing ethane during Pd catalyzed hydrodechlorination in the liquid phase (Chaplin et al., 2012).

2.4.2 Reduction Mechanism

The catalytic dechlorination reaction whether in the liquid or in the gas phase utilizes hydrodechlorination catalysts that can dissociatively adsorb H_2 gas into adsorbed surface atomic hydrogen ($Pd{-}H_{ads}$) which in turn reacts with dissociatively adsorbed COCs on adjacent sites (Chaplin et al., 2012).

Researchers dealing with this topic refer exclusively and extensively to gas phase reactions, as similarities between gas and liquid phase dechlorinations mechanisms are reported (Chaplin et al., 2012; Mackenzie et al., 2006). Similar to gas phase hydrodechloirnation mechanism, XPS studies have shown that the presence of dual species (electron-deficient Pd^{n+} and metallic palladium Pd^0) on the Pd surface is essential for the catalytic hydrodechlorination reaction to take place (Gómez-Sainero et al., 2002). H_2 dissociates on Pd^0, while the COC chemisorbs dissociatively on Pd^{n+} site. XPS results shows that the Pd^0/ Pd^{n+} ratio depends on the reduction temperature for the catalyst synthesis and the selection of the metal precursor, and that this ratio between the two sites controls the catalytic activity. The authors describe that catalysts having only one of these species are inactive (Gómez-Sainero et al., 2002).

Additionally, in agreement with gas phase studies, the correlation of C–Cl bond for chlorinated ethanes and chlorinated methanes was found inversely proportional to calculated C−Cl bond strengths on Pd and the hydrodechlorination rate. (Chaplin et al., 2012; Kovenklioglu et al., 1992; Mackenzie et al., 2006). This correlation suggests that the dissociative adsorption leading to C-Cl bond cleavage of chlorinated compounds is proposed to be the rate-determining step, indicating that the adsorption strength of the chlorinated ethanes with the catalyst is what facilitates bond cleavage. Moreover, liquid phase catalytic hydrodehalogenation rates of chloroethenes and halobenzenes were also found not to follow the order of the C–Cl bond strength, but rather with the number of Cl atoms, with the addition of an activated hydrogen species from the catalyst to the unsaturated hydrocarbon being the rate-determining step, as was observed for the gas phase (Chaplin et al., 2012; Kovenklioglu et al., 1992; Mackenzie et al., 2006). For instance, VC was found to be dechlorinated fastest, although it has the strongest C-Cl bond strength among chlorinated ethenes (Mackenzie et al., 2006), confirming that hydrogenation of the

C=C double bond being the rate limiting step for hydrodechlorination of chlorinated ethenes before C−Cl bond scission (Chaplin et al., 2012; Mackenzie et al., 2006). Density functional theory (DFT) studies found that the most energetically favorable adsorption configuration for chlorinated ethenes on Pd is through a C=C di-σ bond, and that the adsorption strength of chlorinated ethenes on Pd surface increases with decreasing the number of Cl atoms (Andersin and Honkala, 2011; Barbosa et al., 2002; Chaplin et al., 2012). It is important to point out though that other DFT studies and in situ surface-enhanced Raman spectroscopy (SERS) do indicate that the Cl atom in the chlorinated ethenes do adsorb to the catalyst surface (Chaplin et al., 2012; Heck et al., 2008). For instance, experimental results indicate dissociative adsorption of the C−Cl bonds of 1,1-DCE to form an adsorbed vinylidene intermediate before hydrogenation of the C=C bond (Heck et al., 2008).

Based on the above mentioned, the following factors influence the hydrodehalogenation rate at the Pd surface in the liquid phase: (1) the C–Cl bond strength and, (2) the presence or absence of a C=C double bond, which controls the reaction mechanism, (3) the bond strength between halogen and the catalyst, (4) the ratio between the different electronic states of the catalyst, (5) metallic precursor, catalysts synthesis method, catalyst support (Gómez-Sainero et al., 2002; Mackenzie et al., 2006; Urbano and Marinas, 2001).

2.4.3 1,2-Dichloroethane Reduction

Although liquid-phase catalyzed reductive hydrodechlorination show significant potential as a technology providing rapid destruction of halogenated groundwater contaminants, limited work has been devoted to hydrodechlorination of 1,2-DCA (Huang et al., 2011; Lowry and Reinhard, 1999; McNab Jr and Ruiz, 1998), with mostly unsuccessful results. In the study by Lowry and Reinhard, 1,2-DCA, methylene chloride, and 1,1-dichloroethane were found nonreactive via liquid-phase Pd-on-Al_2O_3 catalyzed hydrodechlorination among a variety of 1-3 carbon chlorinated compounds in the presence of direct H_2 gas (Lowry and Reinhard, 1999). Similarly, McNab et al. reported removal efficiency of > 95% for pentachloroethene, trichloroethene, 1,1-dichloroethene, and carbon tetrachloride, however chloroform and 1,2-DCA were found unreactive via catalytic hydrodechlorination using Pd/alumina beads and electrolytically-generated H_2 gas (McNab Jr and Ruiz, 1998).

Furthermore, Huang et al. also found that 1,2-DCA did not undergo any reduction via liquid phase Pd/alumina catalyzed hydrodechlorination using borohydride as a hydrogen source (Huang et al., 2011).

It should be noted that catalyst support plays an important role in the overall performance of the catalytic system, impacting catalyst morphology, electronic state, size, geometry, and adsorption or repulsion of the studied COC, and therefore affects dechlorination rates and pathways (Kovenklioglu et al., 1992). Consequently, it is possible that supporting Pd on alumina might have affected the catalytic efficiency of Pd in the aforementioned studies. The significant effect of the type of catalyst support was demonstrated in the study by Kovenklioglu et al. (Kovenklioglu et al., 1992). The authors reported that Pd/Al_2O_3 used for catalytic hydrodechlorination of 1,1,2-trichloroethane (1,1,2-TCA) exhibited almost no activity as compared to Pd/carbon. This was attributed to the inability of 1,1,2-TCA to adsorb on alumina due to the repulsion forces. Also, while testing different types of carbon supports, the authors further found that the hydrodechlorination rates dropped significantly when the carbon support could not readily adsorb 1,1,2-TCA.

To the best of our knowledge, only one study reported effective catalyzed hydrodechlorination of 1,2-DCA, however using Cu rather than Pd (Huang et al., 2011). In that study, sodium borohydride was used as the hydrogen donor instead of direct H_2 gas. The study however did not provide any justification for 1,2-DCA reduction on Cu surface rather than Pd.

2.4.4 Catalysts Deactivation

One of the main drawbacks of catalytic hydrodechlorination technology is catalyst deactivation. Pd deactivation has been related to several processes such as: the inhibitory and corrosive effect of hydrogen halide formed as byproduct, site blockage due to high surface species concentrations, carbon depositions during reaction, natural groundwater constituents (e.g. HCO_3^-, HS^- , Cl^-), redox active metals, mineral precipitates, sulfur poisoning, and interference with biological processes such as growth of sulfate-reducing bacteria (e.g. (Aramendía et al., 1999; Heck et al., 2008; Kopinke et al., 2010; Lecloux,

1999; Lowry and Reinhard, 2000; Mackenzie et al., 2006; Munakata and Reinhard, 2007; Ordóñez et al., 2010; Sun et al., 2011; Urbano and Marinas, 2001)).

Chlorides is one of the most commonly encountered Pd deactivators (Chaplin et al., 2012; Mackenzie et al., 2006; Ordóñez et al., 2010; Sun et al., 2011; Urbano and Marinas, 2001). As the desired reaction product, they are unavoidable under all reaction conditions. Chloride species released during dechlorination reactions, or coming from the metals precursor itself, as well as freely-dissolved chloride ions compete with the COCs for Pd surface sites, and form metal chlorides species and can also corrode catalysts and supports (Aramendia et al., 2002; Aramendía et al., 1999; Hoke et al., 1992; Mackenzie et al., 2006; Urbano and Marinas, 2001). For instance, Hoke et al. detected Pd solubilization during liquid-phase hydrodechlorination of chlorophenols over Pd/C by the HCl formed in the reaction medium (Hoke et al., 1992). Also, Aramendia et al. reported Pd/MgO deactivation and dissolution due to HCl production as the dechlorinating product from chlorobenzene reduction reaction, and premature cessation of the reaction (Aramendía et al., 1999). Furthermore, the authors reported poisoning of Pd particles during the hydrodechlorination of chlorobenzene on Pd/SiO_2-$AlPO_4$ due to chlorides produced from the metal precursor. The authors compared the performance of catalysts prepared from palladium chloride and palladium acetylacetonate and found out a remarkable difference in the reactivity due to the chlorides poisoning. This deactivation and corrosion was reported to be possibly minimized through the addition of a base (e.g. NaOH, NH_4OH) compound to the reaction medium (Hoke et al., 1992; Sun et al., 2011; Urbano and Marinas, 2001). In this sense, literature studies reported that in the absence of a base compound the reaction does not take place (Hoke et al., 1992) or that if proceeds, it stops at low conversions (Aramendía et al., 1999; Balko et al., 1993). The role of the added base is to neutralize the acid and to keep the catalytic metal in a reduced state, free from chloride ions. Sodium, potassium, calcium, barium hydroxides, and sodium acetates are generally employed (Sun et al., 2011; Urbano and Marinas, 2001).

Groundwater anions are potential catalyst deactivators (McNab Jr and Ruiz, 1998). For instance, HCO_3^- was found to compete with TCE for active Pd catalyst sites promoting catalyst deactivation (Kramer et al., 1995). Moreover, sulfur compounds are one of the

major causes of catalyst deactivation as sulfide ions and sulfur organic compounds can deactivate the catalyst in the water phase irreversibly (Albers et al., 2001; Chaplin et al., 2006; Chaplin et al., 2007; Kopinke et al., 2003; Korte et al., 2000; Lowry and Reinhard, 2000; Mackenzie et al., 2006). XPS analysis have shown that reduced sulfur forms strong complexes with Pd which blocks reaction sites, and may also form adlayers with the sulfur compounds preventing COCs adsorption and transformations at concentrations as low as 0.06 mmol S g^{-1} catalyst resulting in catalyst deactivation (Chaplin et al., 2007). Lowry et al. reported that in the presence of 30 mg L^{-1} SO_3^{2-} Pd deactivates after 5 min of exposure. Also, presence of 87 mg L^{-1} SO_3^{2-} or 0.4 mg L^{-1} HS^- caused rapid catalyst deactivation, presumably due to chemisorption to active sites (Lowry and Reinhard, 2000). Additionally, abundance of H_2 gas in the catalyzed hydrodechlorination technology creates favorable conditions for the growth sulfate reducing bacteria which indirectly poisons catalysts by producing sulfides (Lowry and Reinhard, 2000; Schüth et al., 2004). Sulfur-poisoned catalysts can be regenerated by strong oxidants, including $HOCl/OCl^-$, H_2O_2, $KMnO_4$, dissolved oxygen, and air exposure (for dried catalysts) (Angeles-Wedler et al., 2008; Angeles-Wedler et al., 2009; Chaplin et al., 2006; Chaplin et al., 2007; Chaplin et al., 2009; Munakata and Reinhard, 2007).

The presence of redox active metals in water can also lead to catalyst poisoning (Hildebrand et al., 2009b). For example, Hildebrand et al. reported that Cu^{2+} (80 μM), Pb^{2+} (0.5 μM), Sn^{2+} (40 μM), and Hg^{2+} (0.5 μM) decreased rate constants of TCE reduction on Pd/Fe_2O_3 by 97.0, 76.0, 99.8, and 98.0%, respectively, compared to rate constants measured in deionized water (Hildebrand et al., 2009b). This is assumed to be due to reduction of the metal ions to their zero valent states and subsequent blockage of active sites. Also, catalyst deactivation due to dissolved organic matter (DOM) competition with COC on active sites has been reported (Chaplin et al., 2006). Researchers suggested pre-treating water from DOM with activated carbon prior to applying catalytic hydrodechlorination to overcome this deactivation type. Furthermore, trace amounts of CO can completely inhibit the hydrodechlorination activity (Kopinke et al., 2004). For instance, when applying formic acid as alternative hydrogen source in water, the produced CO was reported to poison the catalyst (Kopinke et al., 2004). Finally, Pd activity loss can also be caused by surface blockage due to mineral or salt precipitations, accumulation of

debris, inorganic oxides, and surface saturation of intermediate compounds (Albers et al., 2001; Chaplin et al., 2006).

A few research studies focused on designing poisoning resistant catalysts. Supporting Pd on zeolite, polymerizing Pd with hydrophobic polymers, and altering the electronic structure by ensembling with other metals are some of the strategies used to overcome the aforementioned poisoning effects (Fritsch et al., 2003; Heck et al., 2009; Kopinke et al., 2010; Schüth et al., 2000).

2.4.5 Hydrogen Donors

Liquid-phase catalyzed reductive dechlorination utilizing Pd along with direct H_2 gas emerged as a promising water and wastewater treatment strategy (e.g. (Chaplin et al., 2012; Gómez-Sainero et al., 2002; Kopinke et al., 2004; Kovenklioglu et al., 1992; Lowry and Reinhard, 1999; Mackenzie et al., 2006; McNab Jr and Ruiz, 1998; Yuan and Keane, 2003; Zhang et al., 2015; Zhao et al., 2008)). However, utilizing direct H_2 gas is troublesome to handle and potentially dangerous (Urbano and Marinas, 2001). Therefore, a few studies focused on replacing the direct H_2 gas stream by a hydrogen source (Anwer et al., 1989; Aramendia et al., 2000; Huang et al., 2011; Kopinke et al., 2004; Ukisu and Miyadera, 1997; Wiener et al., 1991), while others generated the H_2 gas directly from the treated groundwater itself (Janiak and Błażejowski, 2002). Sodium borohydride, formic acid, isopropanol, and hydrazine were among the studied alternatives. However, studies concluded that selection of the hydrogen donor is substrate dependent because of possible competition on active sites (Anwer et al., 1989; Wiener et al., 1991).

Kopinke et al. investigated formic acid, isopropanol and hydrazine as hydrogen donors for Pd-catalyzed hydrodechlorination of chlorobenzene in water (Kopinke et al., 2004). Formic acid was found to be as reactive as direct H_2 gas under acidic and neutral conditions, but less reactive under alkaline conditions. Isopropanol was reported to be less reactive by about five orders of magnitude than direct H_2 gas. Hydrazine was found to be effective as a hydrogen donor under alkaline conditions only, but slower than direct H_2 gas by a factor of 30. The observed kinetics implied two pH-controlled reaction mechanisms (possibly H-atom and hydride transfer). The authors conclude that, from the technical and economic

point of view, formic acid is a promising substitute for direct H_2 gas which requires extra investigation with other chlorinated organic compounds. Ukisu et al. studied dechlorination of 1,2,4-trichlorobenzene to benzene on Pd/C using 2-propanol as hydrogen donor, and found that the reaction does not proceed without the addition of a base (NaOH) to remove the released halogen (Ukisu and Miyadera, 1997). Aramendia et al. also studied hydrodehalogenation of different halogenated organic compounds using potassium formate as hydrogen donor over Pd (Aramendia et al., 2000). They found that potassium formate competes with the halogenated organic compounds to the Pd active sites, with some of the halogenated organic compounds inhibiting formate adsorption, while others are inhibited by formate adsorption (competitive adsorption). Similarly, Wiener et al. stated that the rate-determining step in the overall catalyzed liquid phase hydrodechlorination by a hydrogen donor process is the adsorption of the hydrogen donor on the catalyst surface (Wiener et al., 1991). Thus, researchers emphasis on the great importance of the order of addition of reagents when either substrate or hydrogen donors is strongly adsorbed on the catalysts surfaces (Anwer et al., 1989). Huang et al successfully utilized sodium borohydride as H_2 gas donor for the hydrodechlorination of 1,2-DCA on nCu particles (Huang et al., 2011). Direct H_2 gas is readily generated during the hydrolysis of borohydride (Gómez-Lahoz et al., 1993; Huang et al., 2011). However, the study did not provide any insight on the effectiveness of using borohydride compared to direct H_2 gas on the dechlorination rate.

In all the aforementioned studies, the hydrogen transfer mechanism from the hydrogen donor (except borohydride) is not fully understood (Huang et al., 2011; Kopinke et al., 2004; Ukisu and Miyadera, 1997). In terms of electronegativity, hydrogen occupies a central position in the periodic table. Therefore, in reactions involving its transfer, hydrogen may appear as a proton, atom, or hydride depending on reagents and conditions (Urbano and Marinas, 2001).

2.4.6 Field Applications

Liquid-phase catalyzed reductive dechlorination technology have shown promising results in dehalogenating a variety of haloorganics in contaminated groundwater and wastewater. However, only a few researchers investigated its application for groundwater remediation

in a full-scale field or pilot test installation (Davie et al., 2008; Mcnab et al., 2000; Schüth et al., 2004) .

Mcnab et al. presented an in situ reactive well approach of a pump and treat system utilizing dissolved H_2 gas and palladium-on-alumina catalyst based fixed bed reactors, to reduce TCE and PCE at a major Superfund site with promising results (Mcnab et al., 2000). The treatment unit consisted of a dual-screened well bore, allowing contaminated groundwater to be drawn from one water-bearing zone, treated within the well bore, and discharged to an adjacent zone with only one pass through the system. The system rapidly dechlorinated the COCs, with TCE concentrations of the effluent reduced to < 1 ppb from 3600 ppb. After one year of operation, catalyst partial deactivation was observed however with proper system management such as entailing periodic shutoff of the H_2 supply and aeration, the overall system removal efficiency could be maintained. Davie et al. reported testing catalytic reductive dechlorination technology in remediating groundwater contaminated with 500-1200 µg L^{-1} TCE at Edwards Air Force Base, California (Davie et al., 2008). Eggshell-coated Pd on alumina beads were packed in a fixed bed reactor, where the water was pumped through after amending with H_2 gas. A TCE removal of 99.8% was achieved with a final concentration of 4.1 µg L^{-1} for more than a 100 days of testing period. Based on a cost comparison study with other conventional remediation technologies, the authors stated that catalytic reductive dechlorination technology was found to be a viable treatment technically and economically competitive with conventional treatment technologies. Schüth et al. presented the application of Pd on zeolite catalyzed reductive dechlorination technology in a full-scale flow-through mode for two years operation period (Schüth et al., 2004). The system was proven successful in dechlorinating the COCs with typical reduction half-lives between 1.5 and 3 min. The authors stated that the system can be operated over extended periods with sustained efficiencies, if some conditions such as sufficient supply of hydrogen, flushing the system periodically with a dilute H_2O_2 solution are met.

The presented studies show the feasibility and the promising results of utilizing catalytic reductive dechlorination technology as a viable groundwater remediation technique. Hydrogen is low cost, and the catalysts are commercially available, making this technology

accessible to industrial and commercial applications. Besides, a few studies even reported electrochemically generating hydrogen from the water itself (e.g. (Janiak and Błażejowski, 2002)), in addition to possible hydrogen donors. In general, this system provides several advantages such as; direct reduction to ethane without the presence of chlorinated intermediate byproducts, rapid reaction rates (in the order of minutes), which could permit a compact design for treatment within a well bore or reactive barriers (Davie et al., 2008; Mcnab et al., 2000; Schüth et al., 2004).

To further develop catalytic reductive dechlorination technology into practice, it is necessary to make the technology applicable to a wider range of contaminants. For instance, bench scale studies lack information on dechlorination of the commonly found COC contaminants: 1,2-dichloroethane, and 1,2-dichloromethane.

2.5 Summary

The reduction of COCs in the presence of electron donors is thermodynamically feasible under ambient conditions. Reductive dechlorination technologies include: liquid-phase reductive dechlorination by nZVI, gas-phase catalyzed reductive dechlorination, and liquid-phase catalyzed reductive dechlorination. nZVI technology failed to break down 1,2-DCA and exhibited slow reaction rates when coupled with strong reductants such as dithionite. On the other hand, gas-phase catalyzed reductive dechlorination technology even though capable of reducing 1,2-DCA, is carried out at high temperatures under conditions making it field inapplicable. Liquid-phase catalyzed reductive hydrodechlorination technology emerged as a promising field applicable technology, with promising rapid removal rates of a variety of COCs. A few working groups do describe in situ field application of catalyzed reductive hydrodehalogenation of COCs contaminated groundwater and wastewater. However, so far bench scale studies lack information on liquid-phase catalyzed reductive hydrodechlorination of 1,2-DCA. Thus, there is a pressing need to investigate and develop a liquid phase catalyzed reductive dechlorination technique capable of reducing 1,2-DCA.

2.6 References

Albers, P., Pietsch, J. and Parker, S.F., 2001. Poisoning and deactivation of palladium catalysts. Journal of Molecular Catalysis A: Chemical, 173(1): 275-286.

Alpaslan Kocamemi, B. and Cecen, F., 2010. Cometabolic degradation and inhibition kinetics of 1, 2-dichloroethane (1, 2-DCA) in suspended-growth nitrifying systems. Environmental technology, 31(3): 295-305.

Álvarez-Montero, M., Gómez-Sainero, L., Juan-Juan, J., Linares-Solano, A. and Rodriguez, J., 2010. Gas-phase hydrodechlorination of dichloromethane with activated carbon-supported metallic catalysts. Chemical Engineering Journal, 162(2): 599-608.

Andersin, J. and Honkala, K., 2011. First principles investigations of Pd-on-Au nanostructures for trichloroethene catalytic removal from groundwater. Physical Chemistry Chemical Physics, 13(4): 1386-1394.

Angeles-Wedler, D., Mackenzie, K. and Kopinke, F.-D., 2008. Permanganate oxidation of sulfur compounds to prevent poisoning of Pd catalysts in water treatment processes. Environmental science & technology, 42(15): 5734-5739.

Angeles-Wedler, D., Mackenzie, K. and Kopinke, F.-D., 2009. Sulphide-induced deactivation of Pd/Al 2 O 3 as hydrodechlorination catalyst and its oxidative regeneration with permanganate. Applied Catalysis B: Environmental, 90(3): 613-617.

Anwer, M.K., Sherman, D., Roney, J.G. and Spatola, A.F., 1989. Applications of ammonium formate catalytic transfer hydrogenation. 6. Analysis of catalyst, donor quantity, and solvent effects upon the efficacy of dechlorination. The Journal of Organic Chemistry, 54(6): 1284-1289.

Aramendia, M. et al., 2002. Liquid-phase hydrodechlorination of chlorobenzene over palladium-supported catalysts: Influence of HCl formation and NaOH addition. Journal of Molecular Catalysis A: Chemical, 184(1): 237-245.

Aramendia, M. et al., 2000. Hydrodehalogenation of aryl halides by hydrogen gas and hydrogen transfer in the presence of palladium catalysts. Studies in Surface Science and Catalysis, 130: 2003-2008.

Aramendía, M.A. et al., 1999. Influence of the Reaction Conditions and Catalytic Properties on the Liquid-Phase Hydrodechlorination of Chlorobenzene over Palladium-Supported Catalysts: Activity and Deactivation. Journal of Catalysis, 187(2): 392-399.

Arnold, W.A., Ball, W.P. and Roberts, A.L., 1999. Polychlorinated ethane reaction with zero-valent zinc: pathways and rate control. Journal of Contaminant Hydrology, 40(2): 183-200.

Arnold, W.A. and Roberts, A.L., 2000a. Pathways and kinetics of chlorinated ethylene and chlorinated acetylene reaction with Fe (0) particles. Environmental Science & Technology, 34(9): 1794-1805.

Atisha, A., 2011. Degradation of 1,2-Dichloroethane With Nano-Scale Zero Valent Iron Particles, Western Ontario, 111 pp.

ATSDR, 2015. Detailed data table for the 2015 priority list of hazardous substances that will be the subject of toxicological profiles. Agency for Toxic Substances and Disease Registry, Atlanta, GA. https://www.atsdr.cdc.gov/spl/resources/atsdr_2015_spl_detailed_data_table.pdf. Accessed 19 May, 2016.

Bai, X. and Sachtler, W.M., 1991. Methylcyclopentane conversion catalysis by zeolite encaged palladium clusters and palladium-proton adducts. Journal of Catalysis, 129(1): 121-129.

Balko, E.N., Przybylski, E. and Von Trentini, F., 1993. Exhaustive liquid-phase catalytic hydrodehalogenation of chlorobenzenes. Applied Catalysis B: Environmental, 2(1): 1-8.

Barbash, J.E. and Reinhard, M., 1989b. Abiotic dehalogenation of 1,2-dichloroethane and 1,2-dibromoethane in aqueous solution containing hydrogen sulfide. Environmental Science & Technology, 23(11): 1349-1358.

Barbosa, L.A.M.M., Loffreda, D. and Sautet, P., 2002. Chemisorption of Trichloroethene on the PdCu Alloy (110) Surface: A Periodical Density Functional Study. Langmuir, 18(7): 2625-2635.

Barnes, R.J. et al., 2010. Optimization of nano-scale nickel/iron particles for the reduction of high concentration chlorinated aliphatic hydrocarbon solutions. Chemosphere, 79(4): 448-454.

Bejankiwar, R., Lalman, J.A., Seth, R. and Biswas, N., 2005. Electrochemical degradation of 1,2-dichloroethane (DCA) in a synthetic groundwater medium using stainless-steel electrodes. Water Research, 39(19): 4715-4724.

Benitez, J.L. and Del Angel, G., 2000. Effect of chlorine released during hydrodechlorination of chlorobenzene over Pd, Pt and Rh supported catalysts. Reaction Kinetics and Catalysis Letters, 70(1): 67-72.

Berube, M.N., Sung, B. and Vannice, M.A., 1987. Sulfur poisoning of supported palladium methanol synthesis catalysts. Applied Catalysis, 31(1): 133-157.

Besenbacher, F. et al., 1998. Design of a Surface Alloy Catalyst for Steam Reforming. Science, 279(5358): 1913-1915.

Bonarowska, M., Śrębowata, A. and Karpiński, Z., 2010. Synergistic effects in hydrodechlorination of organic compounds catalyzed by metals. Annales UMCS, Chemistry, 65(1): 1-8.

Boparai, H.K., Comfort, S.D., Shea, P.J. and Szecsody, J.E., 2008. Remediating explosive-contaminated groundwater by in situ redox manipulation (ISRM) of aquifer sediments. Chemosphere, 71(5): 933-941.

Boparai, H.K., Shea, P.J., Comfort, S.D. and Snow, D.D., 2006. Dechlorinating chloroacetanilide herbicides by dithionite-treated aquifer sediment and surface soil. Environmental Science & Technology, 40(9): 3043-3049.

Borovkov, V.Y., Luebke, D.R., Kovalchuk, V.I. and d'Itri, J.L., 2003. Hydrogen-assisted 1, 2-dichloroethane dechlorination catalyzed by Pt-Cu/SiO2: Evidence for different functions of Pt and Cu sites. The Journal of Physical Chemistry B, 107(23): 5568-5574.

Bozzelli, J.W., Chen, Y.-M. and Chuang, S.S., 1992. CATALYTIC HYDRODECHLORINATION OF 1, 2-DICHLOROETHANE AND TRICHLOROETHYLENE OVER Rh/Si0 2 CATALYSTS. Chemical Engineering Communications, 115(1): 1-11.

Chang, C.-C., Reo, C.M. and Lund, C.R.F., 1999. The effect of a membrane reactor upon catalyst deactivation during hydrodechlorination of dichloroethane. Applied Catalysis B: Environmental, 20(4): 309-317.

Chaplin, B.P. et al., 2012. Critical Review of Pd-Based Catalytic Treatment of Priority Contaminants in Water. Environmental Science & Technology, 46(7): 3655-3670.

Chaplin, B.P., Roundy, E., Guy, K.A., Shapley, J.R. and Werth, C.J., 2006. Effects of natural water ions and humic acid on catalytic nitrate reduction kinetics using an alumina supported Pd-Cu catalyst. Environmental science & technology, 40(9): 3075-3081.

Chaplin, B.P., Shapley, J.R. and Werth, C.J., 2007. Regeneration of sulfur-fouled bimetallic Pd-based catalysts. Environmental science & technology, 41(15): 5491-5497.

Chaplin, B.P., Shapley, J.R. and Werth, C.J., 2009. Oxidative regeneration of sulfide-fouled catalysts for water treatment. Catalysis letters, 132(1-2): 174-181.

Chen, N., 2003. Kinetics of the hydrodechlorination reaction of chlorinated compounds on palladium catalysts, Worcester Polytechnic Institute.

Choi, H.C., Choi, S.H., Lee, J.S., Lee, K.H. and Kim, Y.G., 1997. Effects of Pt Precursors on Hydrodechlorination of Carbon Tetrachloride over Pt/Al2O3. Journal of Catalysis, 166(2): 284-293.

Choi, H.C. et al., 1996. Hydrodechlorination of carbon tetrachloride over Pt/MgO. Journal of Catalysis, 161(2): 790-797.

Coq, B., Cognion, J.M., Figueras, F. and Tournigant, D., 1993. Conversion Under Hydrogen of Dichlorodifluoromethane over Supported Palladium Catalysts. Journal of Catalysis, 141(1): 21-33.

Coq, B., Ferrat, G. and Figueras, F., 1986. Conversion of chlorobenzene over palladium and rhodium catalysts of widely varying dispersion. Journal of Catalysis, 101(2): 434-445.

Crittenden, J.C., Trussell, R.R., Hand, D.W., Howe, K.J. and Tchobanoglous, G., 2012. MWH's Water Treatment: Principles and Design: Principles and Design. John Wiley & Sons.

Davie, M.G., Cheng, H., Hopkins, G.D., LeBron, C.A. and Reinhard, M., 2008. Implementing heterogeneous catalytic dechlorination technology for remediating TCE-contaminated groundwater. Environmental science & technology, 42(23): 8908-8915.

Deng, B., Burris, D.R. and Campbell, T.J., 1999. Reduction of Vinyl Chloride in Metallic Iron−Water Systems. Environmental Science & Technology, 33(15): 2651-2656.

Deng, B., Lan, L., Houston, K. and Brady, P.V., 2003. Effects of clay minerals on Cr (VI) reduction by organic compounds. Environmental monitoring and assessment, 84(1-2): 5-18.

Dinglasan-Panlilio, M.J., Dworatzek, S., Mabury, S. and Edwards, E., 2006. Microbial oxidation of 1,2-dichloroethane under anoxic conditions with nitrate as electron acceptor in mixed and pure cultures. FEMS Microbiology Ecology, 56(3): 355-364.

Doong, R.-A. and Lai, Y.-J., 2005. Dechlorination of tetrachloroethylene by palladized iron in the presence of humic acid. Water Research, 39(11): 2309-2318.

Elliott, D.W. and Zhang, W.-X., 2001. Field assessment of nanoscale bimetallic particles for groundwater treatment. Environmental Science & Technology, 35(24): 4922-4926.

Fogler, H.S., 1999. Elements of chemical reaction engineering.

Forni, P., Prati, L. and Rossi, M., 1997. Catalytic dehydrohalogenation of polychlorinated biphenyls part II: Studies on a continuous process. Applied Catalysis B: Environmental, 14(1-2): 49-53.

Fritsch, D., Kuhr, K., Mackenzie, K. and Kopinke, F.-D., 2003. Hydrodechlorination of chloroorganic compounds in ground water by palladium catalysts: Part 1. Development of polymer-based catalysts and membrane reactor tests. Catalysis today, 82(1): 105-118.

Fruchter, J.S. et al., 2000. Creation of a subsurface permeable treatment zone for aqueous chromate contamination using in situ redox manipulation. Ground Water Monitoring and Remediation, 20(2): 66-77.

Fung, S.C. and Sinfelt, J.H., 1987. Hydrogenolysis of methyl chloride on metals. Journal of Catalysis, 103(1): 220-223.

Gómez-Lahoz, C., García-Herruzo, F., Rodríguez-Maroto, J.M. and Rodríguez, J.J., 1993. Cobalt(II) removal from water by chemical reduction with sodium borohydride. Water Research, 27(6): 985-992.

Gómez-Sainero, L.M., Seoane, X.L. and Arcoya, A., 2004. Hydrodechlorination of carbon tetrachloride in the liquid phase on a Pd/carbon catalyst: kinetic and mechanistic studies. Applied Catalysis B: Environmental, 53(2): 101-110.

Gómez-Sainero, L.M., Seoane, X.L., Fierro, J.L. and Arcoya, A., 2002. Liquid-phase hydrodechlorination of CCl 4 to CHCl 3 on Pd/carbon catalysts: nature and role of Pd active species. Journal of Catalysis, 209(2): 279-288.

He, F. and Zhao, D., 2005. Preparation and characterization of a new class of starch-stabilized bimetallic nanoparticles for degradation of chlorinated hydrocarbons in water. Environmental science & technology, 39(9): 3314-3320.

He, F. and Zhao, D., 2007. Manipulating the size and dispersibility of zerovalent iron nanoparticles by use of carboxymethyl cellulose stabilizers. Environmental Science & Technology, 41(17): 6216-6221.

Heck, K.N., Janesko, B.G., Scuseria, G.E., Halas, N.J. and Wong, M.S., 2008. Observing metal-catalyzed chemical reactions in situ using surface-enhanced Raman spectroscopy on Pd− Au nanoshells. Journal of the American Chemical Society, 130(49): 16592-16600.

Heck, K.N., Nutt, M.O., Alvarez, P. and Wong, M.S., 2009. Deactivation resistance of Pd/Au nanoparticle catalysts for water-phase hydrodechlorination. Journal of Catalysis, 267(2): 97-104.

Heinrichs, B., Schoebrechts, J.P. and Pirard, J.P., 2001. Palladium-silver sol-gel catalysts for selective hydrodechlorination of 1,2-dichloroethane into ethylene: III. Kinetics and reaction mechanism. Journal of Catalysis, 200(2): 309-320.

Heinrichs, B.t., Delhez, P., Schoebrechts, J.-P. and Pirard, J.-P., 1997b. Palladium–silver sol-gel catalysts for selective hydrodechlorination of 1, 2-dichloroethane into ethylene. Journal of Catalysis, 172(2): 322-335.

Henry, C.R., 1998. Surface studies of supported model catalysts. Surface Science Reports, 31(7–8): 231-325.

Hildebrand, H., Mackenzie, K. and Kopinke, F.-D., 2009a. Highly active Pd-on-magnetite nanocatalysts for aqueous phase hydrodechlorination reactions. Environmental science & technology, 43(9): 3254-3259.

Hildebrand, H., Mackenzie, K. and Kopinke, F.-D., 2009b. Pd/Fe3O4 nano-catalysts for selective dehalogenation in wastewater treatment processes—Influence of water constituents. Applied Catalysis B: Environmental, 91(1–2): 389-396.

Hoke, J.B., Gramiccioni, G.A. and Balko, E.N., 1992. Catalytic hydrodechlorination of chlorophenols. Applied Catalysis B: Environmental, 1(4): 285-296.

Huang, C.-C., Lo, S.-L., Tsai, S.-M. and Lien, H.-L., 2011. Catalytic hydrodechlorination of 1, 2-dichloroethane using copper nanoparticles under reduction conditions of sodium borohydride. Journal of Environmental Monitoring, 13(9): 2406-2412.

Janda, V., Vasek, P., Bizova, J. and Belohlav, Z., 2004. Kinetic models for volatile chlorinated hydrocarbons removal by zero-valent iron. Chemosphere, 54(7): 917-925.

Janiak, T. and Błażejowski, J., 2002. Hydrogenolysis of chlorobenzene, dichlorobenzenes and chlorotoluenes by in situ generated and gaseous hydrogen in alkaline media and the presence of Pd/C catalyst. Chemosphere, 48(10): 1097-1102.

Job, N. et al., 2005. Hydrodechlorination of 1, 2-dichloroethane on Pd–Ag catalysts supported on tailored texture carbon xerogels. Catalysis today, 102: 234-241.

Kaminska, I.I. and Srebowata, A., 2015. Active carbon-supported nickel-palladium catalysts for hydrodechlorination of 1,2-dichloroethane and 1,1,2-trichloroethane. Research on Chemical Intermediates, 41: 9267-9280.

Kopinke, F.-D., Angeles-Wedler, D., Fritsch, D. and Mackenzie, K., 2010. Pd-catalyzed hydrodechlorination of chlorinated aromatics in contaminated waters—Effects of surfactants, organic matter and catalyst protection by silicone coating. Applied Catalysis B: Environmental, 96(3–4): 323-328.

Kopinke, F.-D., Mackenzie, K., Koehler, R. and Georgi, A., 2004. Alternative sources of hydrogen for hydrodechlorination of chlorinated organic compounds in water on Pd catalysts. Applied Catalysis A: General, 271(1): 119-128.

Kopinke, F.-D., Mackenzie, K. and Köhler, R., 2003. Catalytic hydrodechlorination of groundwater contaminants in water and in the gas phase using Pd/γ-Al 2 O 3. Applied Catalysis B: Environmental, 44(1): 15-24.

Korte, N. et al., 2000. Field application of palladized iron for the dechlorination of trichloroethene. Waste Management, 20(8): 687-694.

Kovenklioglu, S., Cao, Z., Shah, D., Farrauto, R.J. and Balko, E.N., 1992. Direct catalytic hydrodechlorination of toxic organics in wastewater. AIChE Journal, 38(7): 1003-1012.

Kramer, H., Levy, M. and Warshawsky, A., 1995. Hydrogen storage by the bicarbonate/formate reaction. Studies on the activity of Pd catalysts. International journal of hydrogen energy, 20(3): 229-233.

Kulkarni, P.P., Deshmukh, S.S., Kovalchuk, V.I. and d'Itri, J.L., 1999b. Hydrodechlorination of dichlorodifluoromethane on carbon-supported Group VIII noble metal catalysts. Catalysis letters, 61(3-4): 161-166.

L'Argentiere, P.C. and Fi, N.S., 1990. Regeneration of a sulfur poisoned Pd/Al 2 O 3 catalyst during the selective hydrogenation of styrene. Applied Catalysis, 61(1): 275-282.

Lambert, S., Ferauche, F., Brasseur, A., Pirard, J.-P. and Heinrichs, B., 2005. Pd–Ag/SiO 2 and Pd–Cu/SiO 2 cogelled xerogel catalysts for selective hydrodechlorination of 1, 2-dichloroethane into ethylene. Catalysis today, 100(3): 283-289.

Lambert, S., Polard, J.-F., Pirard, J.-P. and Heinrichs, B.t., 2004. Improvement of metal dispersion in Pd/SiO 2 cogelled xerogel catalysts for 1, 2-dichloroethane hydrodechlorination. Applied Catalysis B: Environmental, 50(2): 127-140.

Laursen, A.B. et al., 2012. Electrochemical hydrogen evolution: Sabatier's principle and the Volcano plot. Journal of Chemical Education, 89(12): 1595-1599.

Le, N. and Coleman, N., 2011. Biodegradation of vinyl chloride, cis-dichloroethene and 1,2-dichloroethane in the alkene/alkane-oxidising Mycobacterium strain NBB4. Biodegradation, 22(6): 1095-1108.

Lecloux, A.J., 1999. Chemical, biological and physical constrains in catalytic reduction processes for purification of drinking water. Catalysis Today, 53(1): 23-34.

Legawiec-Jarzyna, M., Śrebowata, A., Juszczyk, W. and Karpiński, Z., 2004. Hydrodechlorination over Pd–Pt/Al 2 O 3 catalysts: A comparative study of chlorine removal from dichlorodifluoromethane, carbon tetrachloride and 1, 2-dichloroethane. Applied Catalysis A: General, 271(1): 61-68.

Li, L., Wang, X., Wang, A., Shen, J. and Zhang, T., 2009. Relationship between adsorption properties of Pt–Cu/SiO 2 catalysts and their catalytic performance for selective hydrodechlorination of 1, 2-dichloroethane to ethylene. Thermochimica Acta, 494(1): 99-103.

Lien, H.-L. and Zhang, W.-X., 2001. Nanoscale iron particles for complete reduction of chlorinated ethenes. Colloids and Surfaces A: Physicochemical and Engineering Aspects, 191(1): 97-105.

Lien, H.-L. and Zhang, W.-X., 2005. Hydrodechlorination of chlorinated ethanes by nanoscale Pd/Fe bimetallic particles. Journal of environmental engineering, 131(1): 4-10.

Lim, T.T. and Feng, J., 2007. Iron-mediated reduction rates and pathways of halogenated methanes with nanoscale Pd/Fe: Analysis of linear free energy relationship. Chemosphere, 66(9): 1765-1774.

Lingaiah, N. et al., 2000. Vapour phase catalytic hydrodechlorination of chlorobenzene over Ni–carbon composite catalysts. Journal of Molecular Catalysis A: Chemical, 161(1–2): 157-162.

Liu, W.-J., Qian, T.-T. and Jiang, H., 2014a. Bimetallic Fe nanoparticles: Recent advances in synthesis and application in catalytic elimination of environmental ppollutants. Chemical Engineering Journal, 236: 448-463.

Liu, Y., Choi, H., Dionysiou, D. and Lowry, G.V., 2005a. Trichloroethene hydrodechlorination in water by highly disordered monometallic nanoiron. Chemistry of Materials, 17(21): 5315-5322.

Liu, Y., Majetich, S.A., Tilton, R.D., Sholl, D.S. and Lowry, G.V., 2005b. TCE Dechlorination Rates, Pathways, and Efficiency of Nanoscale Iron Particles with Different Properties. Environmental Science & Technology, 39(5): 1338-1345.

Lowry, G.V. and Reinhard, M., 1999. Hydrodehalogenation of 1-to 3-carbon halogenated organic compounds in water using a palladium catalyst and hydrogen gas. Environmental science & technology, 33(11): 1905-1910.

Lowry, G.V. and Reinhard, M., 2000. Pd-catalyzed TCE dechlorination in groundwater: Solute effects, biological control, and oxidative catalyst regeneration. Environmental Science & Technology, 34(15): 3217-3223.

Lowry, G.V. and Reinhard, M., 2001. Pd-catalyzed TCE dechlorination in water: effect of [H2](aq) and H2-utilizing competitive solutes on the TCE dechlorination rate and product distribution. Environmental science & technology, 35(4): 696-702.

Luebke, D.R., Vadlamannati, L.S., Kovalchuk, V.I. and d'Itri, J.L., 2002. Hydrodechlorination of 1,2-dichloroethane catalyzed by Pt–Cu/C: effect of catalyst pretreatment. Applied Catalysis B: Environmental, 35(3): 211-217.

Mackenzie, K., Frenzel, H. and Kopinke, F.-D., 2006. Hydrodehalogenation of halogenated hydrocarbons in water with Pd catalysts: Reaction rates and surface competition. Applied Catalysis B: Environmental, 63(3): 161-167.

Marchesini, F.A., Irusta, S., Querini, C. and Miró, E., 2008. Nitrate hydrogenation over Pt,In/Al2O3 and Pt,In/SiO2. Effect of aqueous media and catalyst surface properties upon the catalytic activity. Catalysis Communications, 9(6): 1021-1026.

McNab Jr, W.W. and Ruiz, R., 1998. Palladium-catalyzed reductive dehalogenation of dissolved chlorinated aliphatics using electrolytically-generated hydrogen. Chemosphere, 37(5): 925-936.

Mcnab, W.W., Ruiz, R. and Reinhard, M., 2000. In-situ destruction of chlorinated hydrocarbons in groundwater using catalytic reductive dehalogenation in a reactive well: Testing and operational experiences. Environmental Science & Technology, 34(1): 149-153.

Meshesha, B.T. et al., 2013. PdCu alloy nanoparticles on alumina as selective catalysts for trichloroethylene hydrodechlorination to ethylene. Applied Catalysis A: General, 453(0): 130-141.

Munakata, N. and Reinhard, M., 2007. Palladium-catalyzed aqueous hydrodehalogenation in column reactors: Modeling of deactivation kinetics with sulfide and comparison of regenerants. Applied Catalysis B: Environmental, 75(1–2): 1-10.

Murthy, K.V., Patterson, P.M., Jacobs, G., Davis, B.H. and Keane, M.A., 2004. An exploration of activity loss during hydrodechlorination and hydrodebromination over Ni/SiO2. Journal of Catalysis, 223(1): 74-85.

Nunez Garcia, A., Boparai, H.K. and O'Carroll, D.M., 2016b. Enhanced Dechlorination of 1,2-Dichloroethane by Coupled Nano Iron-Dithionite Treatment. Environmental Science & Technology, 50(10): 5243-5251.

Nutt, M.O., Hughes, J.B. and Wong, M.S., 2005. Designing Pd-on-Au Bimetallic Nanoparticle Catalysts for Trichloroethene Hydrodechlorination. Environmental Science & Technology, 39(5): 1346-1353.

Nzengung, V.A., Castillo, R.M., Gates, W.P. and Mills, G.L., 2001. Abiotic transformation of perchloroethylene in homogeneous dithionite solution and in suspensions of dithionite-treated clay minerals. Environmental Science & Technology, 35(11): 2244-2251.

O'Carroll, D., Sleep, B., Krol, M., Boparai, H. and Kocur, C., 2013. Nanoscale zero valent iron and bimetallic particles for contaminated site remediation. Advances in Water Resources, 51: 104-122.

Ordóñez, S., Vivas, B.P. and Díez, F.V., 2010. Minimization of the deactivation of palladium catalysts in the hydrodechlorination of trichloroethylene in wastewaters. Applied Catalysis B: Environmental, 95(3): 288-296.

Pardey, A. et al., 2005. Kinetics study of the hydrodechlorination of chlorobenzene catalyzed by immobilized copper complexes. Catalysis letters, 104(3-4): 141-150.

Phenrat, T., Saleh, N., Sirk, K., Tilton, R.D. and Lowry, G.V., 2007. Aggregation and sedimentation of aqueous nanoscale zerovalent iron dispersions. Environmental Science & Technology, 41(1): 284-290.

Rodriguez, J.C. and Rivera, M., 1997. Reductive dehalogenation of carbon tetrachloride by sodium dithionite. Chemistry Letters(11): 1133-1134.

Schreier, C.G. and Reinhard, M., 1995. Catalytic hydrodehalogenation of chlorinated ethylenes using palladium and hydrogen for the treatment of contaminated water. Chemosphere, 31(6): 3475-3487.

Schrick, B., Hydutsky, B.W., Blough, J.L. and Mallouk, T.E., 2004. Delivery vehicles for zerovalent metal nanoparticles in soil and groundwater. Chemistry of Materials, 16(11): 2187-2193.

Schüth, C., Disser, S., Schüth, F. and Reinhard, M., 2000. Tailoring catalysts for hydrodechlorinating chlorinated hydrocarbon contaminants in groundwater. Applied Catalysis B: Environmental, 28(3): 147-152.

Schüth, C., Kummer, N.-A., Weidenthaler, C. and Schad, H., 2004. Field application of a tailored catalyst for hydrodechlorinating chlorinated hydrocarbon contaminants in groundwater. Applied Catalysis B: Environmental, 52(3): 197-203.

Smidt, H. and de Vos, W.M., 2004. Anaerobic microbial dehalogenation. Annu. Rev. Microbiol., 58: 43-73.

Soares, O.S.G.P., Órfão, J.J.M. and Pereira, M.F.R., 2011. Nitrate reduction with hydrogen in the presence of physical mixtures with mono and bimetallic catalysts and ions in solution. Applied Catalysis B: Environmental, 102(3–4): 424-432.

Song, H. and Carraway, E.R., 2005b. Reduction of Chlorinated Ethanes by Nanosized Zero-Valent Iron: Kinetics, Pathways, and Effects of Reaction Conditions. Environmental Science & Technology, 39(16): 6237-6245.

Song, H. and Carraway, E.R., 2006. Reduction of chlorinated methanes by nano-sized zero-valent iron. Kinetics, pathways, and effect of reaction conditions. Environmental Engineering Science, 23(2): 272-284.

Śrębowata, A., Juszczyk, W., Kaszkur, Z. and Karpiński, Z., 2007. Hydrodechlorination of 1,2-dichloroethane on active carbon supported palladium–nickel catalysts. Catalysis Today, 124(1–2): 28-35.

Śrębowata, A., Lisowski, W., Sobczak, J.W. and Karpiński, Z., 2011. Hydrogen-assisted dechlorination of 1,2-dichloroethane on active carbon supported palladium–copper catalysts. Catalysis Today, 175(1): 576-584.

Sun, C. et al., 2011. A Highly Active Pd on Ni–B Bimetallic Catalyst for Liquid-Phase Hydrodechlorination of 4-Chlorophenol Under Mild Conditions. Catalysis letters, 141(6): 792-798.

Sun, Y.-P., Li, X.-q., Cao, J., Zhang, W.-x. and Wang, H.P., 2006a. Characterization of zero-valent iron nanoparticles. Advances in Colloid and Interface Science, 120(1–3): 47-56.

Tavoularis, G. and Keane, M.A., 1999. Gas phase catalytic dehydrochlorination and hydrodechlorination of aliphatic and aromatic systems. Journal of Molecular Catalysis A: Chemical, 142(2): 187-199.

Tiraferri, A., Chen, K.L., Sethi, R. and Elimelech, M., 2008. Reduced aggregation and sedimentation of zero-valent iron nanoparticles in the presence of guar gum. Journal of Colloid and Interface Science, 324(1): 71-79.

Tobiszewski, M. and Namieśnik, J., 2012. Abiotic degradation of chlorinated ethanes and ethenes in water. Environmental Science and Pollution Research, 19(6): 1994-2006.

Ukisu, Y. and Miyadera, T., 1997. Hydrogen-transfer hydrodehalogenation of aromatic halides with alcohols in the presence of noble metal catalysts. Journal of Molecular Catalysis A: Chemical, 125(2): 135-142.

Urbano, F. and Marinas, J., 2001. Hydrogenolysis of organohalogen compounds over palladium supported catalysts. Journal of Molecular Catalysis A: Chemical, 173(1): 329-345.

USEPA, 2015. Priority pollutant list. United States Environmental Protection Agency. https://www.epa.gov/sites/production/files/2015-09/documents/priority-pollutant-list-epa.pdf. Accessed 19 May, 2016.

Vadlamannati, L.S., Kovalchuk, V.I. and d'Itri, J.L., 1999. Dechlorination of 1, 2-dichloroethane catalyzed by Pt–Cu/C: unraveling the role of each metal. Catalysis letters, 58(4): 173-178.

Vadlamannati, L.S., Luebke, D.R., Kovalchuk, V.I. and d'Itri, J.L., 2000. Olefins from chlorocarbons: Reactions of 1,2-dichloroethane catalyzed by Pt-Cu. In: F.V.M.S.M. Avelino Corma and G.F. José Luis (Editors), Studies in Surface Science and Catalysis. Elsevier, pp. 233-238.

Vilve, M. et al., 2010. Degradation of 1,2-dichloroethane from wash water of ion-exchange resin using Fenton's oxidation. Environmental Science and Pollution Research, 17(4): 875-884.

Wang, X.Y., Chen, C., Chang, Y. and Liu, H.L., 2009. Dechlorination of chlorinated methanes by Pd/Fe bimetallic nanoparticles. Journal of Hazardous Materials, 161(2-3): 815-823.

Wang, Z., Huang, W., Fennell, D.E. and Peng, P.a., 2008. Kinetics of reductive dechlorination of 1, 2, 3, 4-TCDD in the presence of zero-valent zinc. Chemosphere, 71(2): 360-368.

Wiener, H., Blum, J. and Sasson, Y., 1991. Transfer hydrogenolysis of aryl halides and other hydrogen acceptors by formate salts in the presence of palladium/carbon catalyst. The Journal of Organic Chemistry, 56(21): 6145-6148.

Wiersma, A. et al., 1998. Comparison of the performance of activated carbon-supported noble metal catalysts in the hydrogenolysis of CCl 2F 2. Journal of Catalysis, 177(1): 29-39.

Xia, C., Xu, J., Wu, W. and Liang, X., 2004. Pd/C-catalyzed hydrodehalogenation of aromatic halides in aqueous solutions at room temperature under normal pressure. Catalysis Communications, 5(8): 383-386.

Xie, H. et al., 2008. Hydrodechlorination of 1,2-dichloroethane catalyzed by dendrimer-derived Pt–Cu/SiO2 catalysts. Journal of Catalysis, 259(1): 111-122.

Xie, Y., Cao, H., Li, Y., Zhang, Y. and Crittenden, J.C., 2011. Highly Selective PdCu/Amorphous Silica−Alumina (ASA) Catalysts for Groundwater Denitration. Environmental Science & Technology, 45(9): 4066-4072.

Yan, W., Herzing, A.A., Li, X.-q., Kiely, C.J. and Zhang, W.-x., 2010. Structural evolution of Pd-doped nanoscale zero-valent iron (nZVI) in aqueous media and implications for particle aging and reactivity. Environmental science & technology, 44(11): 4288-4294.

Yu, F., 2013. Abiotic Degradation of Chlorinated Hydrocarbons (CHCs) with Zero-Valent Magnesium (ZVM) and Zero-Valent Palladium/Magnesium Bimetallic (Pd/Mg)-Reductant, Wright State University.

Yuan, G. and Keane, M.A., 2003. Liquid phase catalytic hydrodechlorination of 2,4-dichlorophenol over carbon supported palladium: an evaluation of transport limitations. Chemical Engineering Science, 58(2): 257-267.

Zhang, M., He, F. and Zhao, D., 2015. Catalytic activity of noble metal nanoparticles toward hydrodechlorination: influence of catalyst electronic structure and nature of adsorption. Front. Environ. Sci. Eng., 9(5): 888-896.

Zhang, W.-x., 2003. Nanoscale Iron Particles for Environmental Remediation: An Overview. Journal of Nanoparticle Research, 5(3-4): 323-332.

Zhang, W.x. and Elliott, D.W., 2006. Applications of iron nanoparticles for groundwater remediation. Remediation Journal, 16(2): 7-21.

Zhang, W.X., Wang, C.B. and Lien, H.L., 1998. Treatment of chlorinated organic contaminants with nanoscale bimetallic particles. Catalysis Today, 40(4): 387-395.

Zhao, Z.-F. et al., 2008. Synthesis of a nano-nickel catalyst modified by ruthenium for hydrogenation and hydrodechlorination. Catalysis Communications, 9(13): 2191-2194.

Zhu, B.-W. and Lim, T.-T., 2007. Catalytic reduction of chlorobenzenes with Pd/Fe nanoparticles: reactive sites, catalyst stability, particle aging, and regeneration. Environmental science & technology, 41(21): 7523-7529.

Chapter 3

3 Liquid-Phase Nano Palladium Catalyzed Hydrodechlorination of 1,2-Dichloroethane

3.1 Abstract

1,2-Dichloroethane (1,2-DCA) is among the most frequently detected chlorinated organic compounds (COCs) at contaminated sites. Possible carcinogenicity and recalcitrance towards abiotic dechlorination has created considerable interest in developing remediation technologies to successfully treat 1,2-DCA. Recently, liquid-phase catalyzed hydrodechlorination has emerged as a field-applicable technology showing promising results in reducing various COCs. However, limited research has been completed on the liquid-phase catalyzed hydrodechlorination of 1,2-DCA, even on bench scale. In this study, the feasibility of liquid-phase catalyzed hydrodechlorination of 1,2-DCA using borohydride as a hydrogen source over Pd nanoparticles (nPd) was investigated. nPd particles were synthesized via aqueous chemical reduction by sodium borohydride. Complete removal of 1,2-DCA (32 mg L^{-1}) in <7 days was achieved on CMC stabilized nPd (1 g L^{-1}) coupled with hydrogen produced from excess borohydride present in solution after nPd synthesis. The catalyzed dechlorination reaction followed pseudo-first-order kinetics. Ethane was the main byproduct indicating hydrogenolysis as the major degradation pathway. Detailed surface characterization including TEM, SEM/EDX, XPS and XRD of nPd particles was conducted. Different synthesis parameters were found to affect the oxidation state, elemental composition and reactivity of nPd. nPd loading and initial 1,2-DCA concentration also influenced 1,2-DCA dechlorination kinetics. This study suggests that in-situ 1,2-DCA dechlorination is possible via liquid-phase nPd catalyzed dechlorination technology.

Keywords: 1,2-Dichloroethane, Hydrodechlorination, Borohydride, Nano, Palladium, Liquid-phase.

3.2 Introduction

1,2-Dichloroethane (1,2-DCA, $C_2H_4Cl_2$) is a chlorinated organic compound (COC) commonly used for the synthesis of vinyl chloride monomer (Atisha, 2011; Liu et al., 2014b). Excessive usage as well as improper handling, storage, and disposal of 1,2-DCA has caused widespread subsurface contamination. 1,2-DCA has been found at 412 National Priorities List sites in the United States alone (NIH, 2016). It is classified as a possible carcinogen and can cause circulatory and respiratory failure, neurological disorders, immune suppression, and kidney and liver damage in human beings (ATSDR, 2001; Liu et al., 2014b). Due to its pervasive contamination and severe health effects, significant research has been devoted to develop remediation technologies for 1,2-DCA degradation (Atisha, 2011; Borovkov et al., 2003; Huang et al., 2011; Liu et al., 2014b; Lowry and Reinhard, 1999; Luebke et al., 2002; Nunez Garcia et al., 2016a; Śrębowata et al., 2011).

Over the last decade, liquid-phase chemical reduction by nano zero valent iron (nZVI) has become a very promising subsurface remediation technology capable of degrading a wide range of COCs (O'Carroll et al., 2013). Thus far, even nZVI and palladium (Pd) doped nZVI have been unable to degrade 1,2-DCA (Atisha, 2011; Nunez Garcia et al., 2016a; Song and Carraway, 2005a). However, gas-phase catalyzed hydrodechlorination has been found to effectively dechlorinate 1,2-DCA via activated hydrogen gas on a catalyst surface (Borovkov et al., 2003; Job et al., 2005; Kaminska and Srebowata, 2015; Lambert et al., 2005; Lambert et al., 2004; Legawiec-Jarzyna et al., 2004; Li et al., 2009; Luebke et al., 2002; Śrębowata et al., 2007; Śrębowata et al., 2011; Xie et al., 2008). H_2 gas undergoes chemisorption and decomposition to two atomic hydrogen on the surface of the catalyst (Equation 3-1), acting as a robust dechlorinating reductant. The activated hydrogen then reduces adsorbed COCs on adjacent sites (Equation 3-2) (Chaplin et al., 2012; Conrad et al., 1974).

$$\boldsymbol{H_2 \xrightarrow{Catalyst} 2H^{\cdot}} \qquad \text{(Equation 3-1)}$$

$$\boldsymbol{RCl + H_2 \xrightarrow{Catalyst} RH + HCl} \qquad \text{(Equation 3-2)}$$

Group VIII catalysts (i.e. Pd, Ni, Pt), known for their hydrogenation ability, are often utilized to catalyze gas-phase hydrodechlorination reactions (Urbano and Marinas, 2001; Zhang et al., 2015). Among these, Pd is the most effective and commonly used catalyst as it has strong hydrogen adsorption and activation properties as well as greater ability to selectively replace adsorbed chlorine atoms with hydrogen (Kulkarni et al., 1999a; Urbano and Marinas, 2001). Moreover, it is the least catalyst affected by chloride ions poisoning released during dechlorination reactions (Kulkarni et al., 1999a). Nickel (Ni), a cheaper alternative to Pd, is a milder hydrogenation catalyst and usually requires higher temperatures to yield the same dechlorination efficiency as Pd (Lingaiah et al., 2000; Murthy et al., 2004).

Nonetheless, gas-phase reductive hydrodechlorination is carried out at high temperatures (>200°C) and uses a direct hydrogen gas (H_2) stream making it impractical for in-situ applications (Borovkov et al., 2003; Heinrichs et al., 1997a; Job et al., 2005; Kaminska and Srebowata, 2015; Kulkarni et al., 1999a; Lambert et al., 2005; Lambert et al., 2004; Legawiec-Jarzyna et al., 2004; Li et al., 2009; Luebke et al., 2002; Śrębowata et al., 2007; Śrębowata et al., 2011; Urbano and Marinas, 2001). Therefore, recent studies were directed towards applying catalyzed hydrodechlorination in the liquid phase under ambient conditions. Liquid-phase catalyzed hydrodechlorination has been found to rapidly dechlorinate a variety of COCs (i.e. chlorinated ethenes, chlorinated methanes, chlorinated aromatic compounds, chlorinated biphenyls, chlorofluorocarbon, and halogenated pesticides) without the formation of substantial amounts of chlorinated intermediate compounds (Aramendia et al., 2002; Chaplin et al., 2012; Gómez-Sainero et al., 2002; Kopinke et al., 2004; Kovenklioglu et al., 1992; Lowry and Reinhard, 1999; Mackenzie et al., 2006; McNab Jr and Ruiz, 1998; Yuan and Keane, 2003; Zhang et al., 2015; Zhao et al., 2008). Also, a range of hydrogen sources (i.e. formate, formic acid, 2-propanol, borohydride, and hydrazine) have been utilized to overcome the impracticality of direct use of H_2 gas (Anwer et al., 1989; Huang et al., 2011; Kopinke et al., 2004; Ukisu and Miyadera, 1997; Wiener et al., 1991).

To date limited work has been devoted to the liquid-phase catalyzed reductive hydrodechlorination of 1,2-DCA. Lowry and Reinhard found methylene chloride, 1,1-

DCA, and 1,2-DCA to be nonreactive via liquid-phase catalytic hydrodechlorination using Pd-on-Al_2O_3 and H_2 gas while studying the dechlorination of 1- to 3-carbon COCs (Lowry and Reinhard, 1999). Similarly, McNab Jr. and Ruiz reported >95% removal of pentachloroethene, 1,1-dichloroethene, and carbon tetrachloride but chloroform and 1,2-DCA were found unreactive using Pd/alumina beads and electrolytically-generated H_2 gas (McNab Jr and Ruiz, 1998). Similarly, Huang et al. also found 1,2-DCA to be resilient against liquid-phase catalytic dechlorination via Pd/alumina with borohydride as a hydrogen source (Huang et al., 2011). It is well known that catalyst support plays an important role in the overall performance of the catalytic system, impacting catalyst morphology, electronic state, size, geometry, and adsorption or repulsion of the studied COC (Kovenklioglu et al., 1992; Zhang et al., 2008). Consequently, it is possible that supporting Pd on alumina might have affected the catalytic efficiency of Pd in these studies. Kovenklioglu et al. reported that Pd/Al_2O_3 used for catalytic hydrodechlorination of 1,1,2-trichloroethane (1,1,2-TCA) exhibited almost no activity as compared to Pd/carbon (Kovenklioglu et al., 1992). This was attributed to the inability of 1,1,2-TCA to adsorb on alumina. Also while testing different types of carbon supports, they further found that the hydrodechlorination rates dropped significantly when the carbon support could not readily adsorb 1,1,2-TCA. Thus, unsupported catalysts need to be developed to overcome the inhibitory effect of catalytic support on the hydrodechlorination reactions.

Recently, nano sized metal catalysts have become quite popular due to their enhanced catalytic activity for hydrodechlorination. Moreover, stabilizing the nano catalysts can successfully replace the catalyst support role as it can overcome the immobilization issue with regards to subsurface application (Zhang et al., 2015). Therefore, the overall goal of this research was to study the effect of utilizing unsupported stabilized palladium nanoparticles coupled with borohydride as a hydrogen gas source to dechlorinate 1,2-DCA in the liquid phase under ambient conditions. Borohydride is often used in excess amounts for nano metal synthesis and this excess borohydride can additionally be utilized as the H_2 gas source (Equation 3-3) for the hydrodechlorination reactions, making this technology more economical and feasible (Huang et al., 2011; Rostamikia and Janik, 2010).

$$\boldsymbol{BH_4^- + 2H_2O \rightarrow BO_2^- + 4H_2\uparrow} \qquad \text{(Hydrolysis)} \qquad \text{(Equation 3-3)}$$

The specific objectives of this study were to (a) investigate unsupported Pd nano metal (nPd) coupled with residual borohydride as a hydrogen source for the liquid-phase catalytic dechlorination of 1,2-DCA, (b) assess the effect of nPd synthesis parameters and experimental conditions on 1,2-DCA dechlorination kinetics, and (c) characterize the surface of nPd particles. Additionally, Ni was also tested for the catalytic dechlorination of 1,2-DCA as it represents a possible cheaper alternative to Pd.

3.3 Experimental Section

3.3.1 Chemicals

The following chemicals were used as received: 1,2-dichloroethane (1,2-DCA, 99+%, Sigma-Aldrich), sodium borohydride ($NaBH_4$, 98+%, ACROS Organics), ferrous sulfate heptahydrate ($FeSO_4.7H_2O$, 99.5% ACROS Organics), potassium hexachloropalladate (K_2PdCl_6, 99%, Alfa Aesar, Pd min 26.69%), palladium acetate ($Pd(O_2CCH_3)_2$, 45.9-48.4%, Alfa Aesar), nickel nitrate ($Ni(NO_3)_2.6H_2O$, 98%, Alfa Aesar), sodium carboxymethyl cellulose (CMC, MW = 90K, ACROS Organics), sodium chloride (NaCl, EMD Chemicals Inc.), gas Mix (5% H_2 balance Ar, PRAXAIR), and N_2 gas (Ultra High Purity, PRAXAIR). Deionized deoxygenated water purged with ultrapure N_2 gas was used to prepare aqueous solutions.

3.3.2 Synthesis of Nano Metal Particles

Nano sized metal particles were synthesized via reduction of metal salts by sodium borohydride. For CMC-stabilized nanoparticles, the metal salt solution was well mixed with CMC solution to form a M^{2+}-CMC complex. Freshly prepared $NaBH_4$ solution was then added dropwise to the M^{2+}-CMC solution with continuous stirring. The used stoichiometric ratio of $NaBH_4$ to metal salt (BH_4^-/M^{2+}) was 3.5 rather than the actually required ratio of 0.5 (Equation 3-4). Excess borohydride is standardly added to accelerate metal synthesis and to ensure uniform growth of the particles, and in this study was utilized to provide H_2 for 1,2-DCA hydrodechlorination. The synthesis process was carried out in an anaerobic glove box maintaining an O_2-free environment by purging with O_2-free Ar (95% Ar: 5% H_2).

$$2M^{2+} + BH_4^- + 3H_2O \rightarrow 2M^0 + H_2BO_3^- + 4H^+ + 2H_2 \uparrow \quad \text{(Equation 3-4)}$$

Bare nPd particles were synthesized in the similar way but without adding CMC. Two batches of bare nPd particles were washed three times with deoxygenated deionized water to: 1- use as a control of only nPd particles (without borohydride), 2- study the effect of washing nPd particles on 1,2-DCA dechlorination kinetics. During the washing steps, the supernatant was removed resulting in loss of the excess borohydride. So 25 mM fresh $NaBH_4$ was added to the washed nPd particles directly in the reactor bottles to provide H_2 gas for the dechlorination reaction. nPd synthesized from potassium hexachloropalladate and palladium acetate will be denoted as nPd_H and nPd_A respectively and the washed nPd particles as nPd_{HW}. 'C-' and 'B-' will be used as prefixes for the CMC-stabilized and bare particles respectively. C-nZVI/Pd_H particles were prepared using a method previously reported by Sakulchaicharoen et al. (Sakulchaicharoen et al., 2010).

3.3.3 Particles Characterization

Transmission Electron Microscopy (TEM) - TEM was used to determine particle size and surface morphology of the CMC-stabilized nanoparticles. Analysis was performed using a Philips CM10 and a FEI Titan 80–300 Cryo-in-situ Transmission Electron Microscope (Philips Export B.V. Eindhove, Netherlands). The samples were prepared by diluting the freshly synthesized nanoparticle suspensions and then adding a drop of each on 400 mesh Formvar/Carbon copper grids in the anaerobic glove box. The grids were left to dry in the glove box for some time. Nanoparticle diameter was measured using a Hamamatsu CCD based camera system software (Advanced Microscopy Techniques, version AMTV542).

Scanning Electron Microscopy/Energy Dispersive X-Ray Spectroscopy (SEM/EDX) - SEM (Hitachi S-4500, 10 kV field emission with a Quartz PCI XOne SSD X-ray analyzer) was used to determine the particle size and surface morphology of bare nPd (B-nPd) particles. Solid sample was sprinkled onto adhesive carbon tape supported on a metallic disk. Elemental composition of the B-nPd particles was determined by randomly selecting areas on the solid surface and analyzing by EDX in conjunction with SEM.

Specific Surface Area - The average particle size from the representative sets of TEM and SEM micrographs for each sample was calculated by a weighted averages method. Assuming a spherical geometry for the nanoparticles, specific surface area (a_s) was calculated using the average particle size obtained from TEM and SEM data as in Equation 3-5 (Sun et al., 2006b):

$$\boldsymbol{a_s = \frac{Surface\ Area}{Mass} = \frac{\pi d^2}{\rho \frac{\pi}{6} D^3} = \frac{6}{\rho D}} \qquad \text{(Equation 3-5)}$$

where D is the average diameter of particles and ρ is the density of the metal particles (Pd: 11.9 g cm^{-3}, Ni: 8.9 g cm^{-3}).

X-Ray Diffraction (XRD) - B-nPd particles were also analyzed using a Rigaku RPT 300 RC X-ray diffractometer (Cu Kα radiation, step size 0.02°, 2θ range 10-90°) to determine the product phase composition. The identification of the phases was achieved by referring to the Joint Committee on Powder Diffraction Standards (JCPDS) database and published literature.

X-ray Photoelectron Spectroscopy (XPS) - XPS was performed on B-nPd particles to determine the elemental composition and oxidation state of the atoms present on the catalyst surface. The samples were prepared and introduced into the spectrometer via an anaerobic glove box. XPS analyses were carried out with a Kratos Axis Ultra spectrometer using a monochromatic Al Kα source (15mA, 14kV). The instrument work function was calibrated to give a binding energy (BE) of 83.96 eV for the Au $4f_{7/2}$ line for metallic gold and the spectrometer dispersion was adjusted to give a BE of 932.62 eV for the Cu $2p_{3/2}$ line of metallic copper. The Kratos charge neutralizer system was used on all specimens. Survey scan analyses were carried out using the following parameters: x-ray spot size = 300 µm x 700 µm, pass energy = 160 eV, and binding energy (BE) range = 1100-0 eV. High resolution spectra were taken for Pd 3d and Cl 2p with a pass energy of 20 eV. Spectra have been charge corrected to the main line of the carbon 1s spectrum (adventitious carbon) set to 284.8 eV. Spectra were analyzed and fittings were carried out using CasaXPS software (version 2.3.14) and compared with literature database (Chastain et al., 1995; Wagner et al., 2003). The ratios of Pd^{n+}/Pd^{o} were calculated by comparing the intensities

of the components of Pd $3d_{5/2}$ core-level after the deconvolution of the experimental spectra. Here Pd^{n+} consists of both Pd^{2+} and Pd^{4+} species.

Dynamic Light Scattering (DLS) - The mean hydrodynamic diameter of the stabilized nanoparticles was measured by a 90Plus DLS instrument (BIC, Holtsville, NY) at a measurement angle of 90º. The data were processed with Zeta PALS software measuring the hydrodynamic diameter on a number-weighted average. The zeta potentials of the particles were determined using Zeta Plus software incorporating the Smoluchowski method for determining zeta potential from electrophoretic mobility measurements.

3.3.4 1,2-DCA Dechlorination

Batch experiments were conducted using amber glass bottles (250 mL, VWR) sealed with Teflon mininert valves to create anaerobic batch reactors (40 mL solution/ 210 mL headspace). Freshly synthesized CMC-stabilized or bare nanoparticles (1 g L^{-1}) were used to catalyze the dechlorination of ~35mg L^{-1} 1,2-DCA, unless otherwise mentioned. All experiments, including controls (only 1,2-DCA and deionized water, or only B-nPd_w with 1,2-DCA and deionized water), were conducted in duplicates, with error bars on dechlorination profiles representing the standard deviation between the two duplicates. The reactor bottles were shaken using an arm wrist action shaker (Model 75, Burrell Inc.) at room temperature.

Table 3-1 summarizes the experimental conditions and dechlorination kinetics for each reactivity experiment. Experiments 1 and 2 represents catalyzed dechlorination experiments of 1,2-DCA by C-nPd_H and nNi particles. Experiment 3 represents a control of B-nPd particles only, where the residual borohydride was removed from the synthesis slurry and washed off the surface of the nPd particles. Experiments 4 and 5 shows the effect of utilizing nPd particles solely as opposed to doping the same concentration of nPd on nZVI. Experiment 6 shows the effect of utilizing B-nPd_H particles on the dechlorination efficiency. Experiments 7 and 8 evaluates the effect of CMC coating on the catalytic efficiency of nP_A particles in reducing 1,2-DCA. Experiment 9 evaluates the effect of washing nPd_H particles on the dechlorination efficiency. Experiment 10 shows the effect of chlorides on the catalytic efficiency of nPdA in reducing 1,2-DCA. Experiments 11, 12,

and 13 shows the effect of Pd loading on 1, 2-DCA dechlorination kinetics. Experiments 14 and 15 indicates the effect of 1,2-DCA loading on the dechlorination kinetics.

3.3.5 Analytical Methods

Concentrations of 1,2-DCA were analyzed with an Agilent 7890 Gas Chromatograph (GC) equipped with a DB-624 capillary column (75 m x 0.45 mm x 2.55 μm) and an Electron Capture Detector (ECD) using modified EPA8021 method. The conditions of the GC method were as follows: N_2 as the carrier gas at a flow rate of 10 mL min^{-1}; a temperature ramp of 35 °C for 12 min, then 5 °C min^{-1} to 60 °C for 1 min and 17 °C min^{-1} to 200 °C for 5 min. 250 μL aliquot was collected from each reactor bottle at a selected sampling time and mixed with 1 mL n-Hexane in a 2-mL GC vial. The GC vials were vortex mixed, and allowed to equilibrate for two hours before extraction. One μL of the extract was injected into the GC using an auto sampler. Concentrations of chloroethane, ethane, and ethene were analyzed with an Agilent 7890A GC equipped with a GS-Gas Pro Column (3.0m x 320 μm), and Flame Ionization Detector (FID). The temperature program used was: 35 °C for 5 min, then 10 °C min^{-1} to 220 °C held for 7 min with He as the gas carrier. Samples were analyzed by manual injection of 250 μL headspace samples directly withdrawn from the headspace of the reactor bottles.

Chloride concentration in Experiment 5 was analyzed on a Waters 717 Plus Auto-sampler High Performance Liquid Chromatograph (HPLC) equipped with a conductivity detector and an IC PakTM anion column (4.6m x 50 mm). 100 μL sample was injected in an eluent mixture (12% acetonitrile in deionized water) with a flow rate of 1.2 mL min^{-1} at a pressure of 595 psi.

Table 3-1: Experimental conditions of dechlorination experiments and the summarized results.

Exp. No.	Metal	Metal Loading ($g\ L^{-1}$)	CMC (W/V) %	1,2-DCA ($mg\ L^{-1}$)	Degradation %	k_{obs} (d^{-1})	$k_{sa}*10^3$ ($L\ m^{-2}\ d^{-1}$)[f]
1	C-nPd_H	1	0.5	32	100 (7d)	0.940	11.8
2	C-nNi	1	0.5	37	35 (11d)	0.043	0.7
3[a]	B-Pd_{HW}	1	-	8	-	-	-
4[b]	C-nZVI/Pd_H	5	0.5	10	<5 (7d)	-	-
5	C-nPd_H	0.04	0.5	10	28 (7d)	0.044	13.8
6[c]	B-nPd_H	1	-	32	100 (10d)	0.713	25.6
7	C-nPd_A	1	0.5	33	100 (3d)	1.702	18.3
8	B-nPd_A	1	-	40	100 (10d)	0.400	13.4
9[d]	B-nPd_{HW}	1	-	40	32 (7d)	0.420	14.8
10[e]	B-nPd_A	1	-	40	100 (10d)	0.410	13.8
11	C-nPd_H	0.14	0.5	8	97 (32)	0.106	9.5
12	C-nPd_H	0.4	0.5	8	100 (19)	0.266	8.3
13	C-nPd_H	1	0.5	8	100 (7d)	0.887	11.1
14	C-nPd_H	1	0.5	65	90 (55d)	0.058	0.7
15	C-nPd_H	1	0.5	225	91 (55d)	0.067	0.8

[a] No borohydride was added after washing the particles nPd particles (B-Pd_{HW}).
[b] Bimetallic nZVI/Pd was used in this experiment. Pd loading was 0.04 $g\ L^{-1}$.
[c] Chloride balance of 93.7% was achieved.
[d] Fresh 25 mM $NaBH_4$ was injected to the reactor bottle as the excess borohydride from synthesis was lost during the washing steps. Rate constant for the first 0.29 days only as kinetics deviated to zero-order (k_{sa} = 0.22 $L\ m^2\ d^{-1}$) after this.
[e] 0.056M NaCl was added in this experiment.
[f] Surface area was calculated from Equation 3-5.

3.4 Results and Discussion

3.4.1 Particles Characterization

Catalytic dechlorination is a surface-mediated reaction and can be strongly influenced by the surface properties of nano metals. Thus, a detailed study of surface properties of the nano metals was conducted using TEM, SEM-EDX, XRD, XPS and DLS. Some chemical analyses for the different experiments were also done.

TEM - The particle size and morphology of CMC-stabilized particles (C-nPd_A, C-nPd_H, and C-nNi) were examined by TEM. The unreacted C-nPd_A and C-nPd_H consisted of individual quasi-spherical nanoparticles assembled in chains forming some tightly packed aggregates (Figures 3-1A-C). The mean diameters of nPd_A and nPd_H particles were 5.42±1.4 nm and 6.31±1.4 nm, respectively. Unreacted C-nNi particles were found to be better dispersed than nPd particles and were present mostly as individual spherical nanoparticles with an average particle size of 11.22 ± 4.3 nm (Figure 3-1D). Using the nanoparticle diameter from TEM data in Equation 3-5, the average specific surface areas for unreacted C-nPd_A, C-nPd_H, and C-nNi particles were calculated as 93.03, 79.91, and 60.08 $m^2 g^{-1}$, respectively.

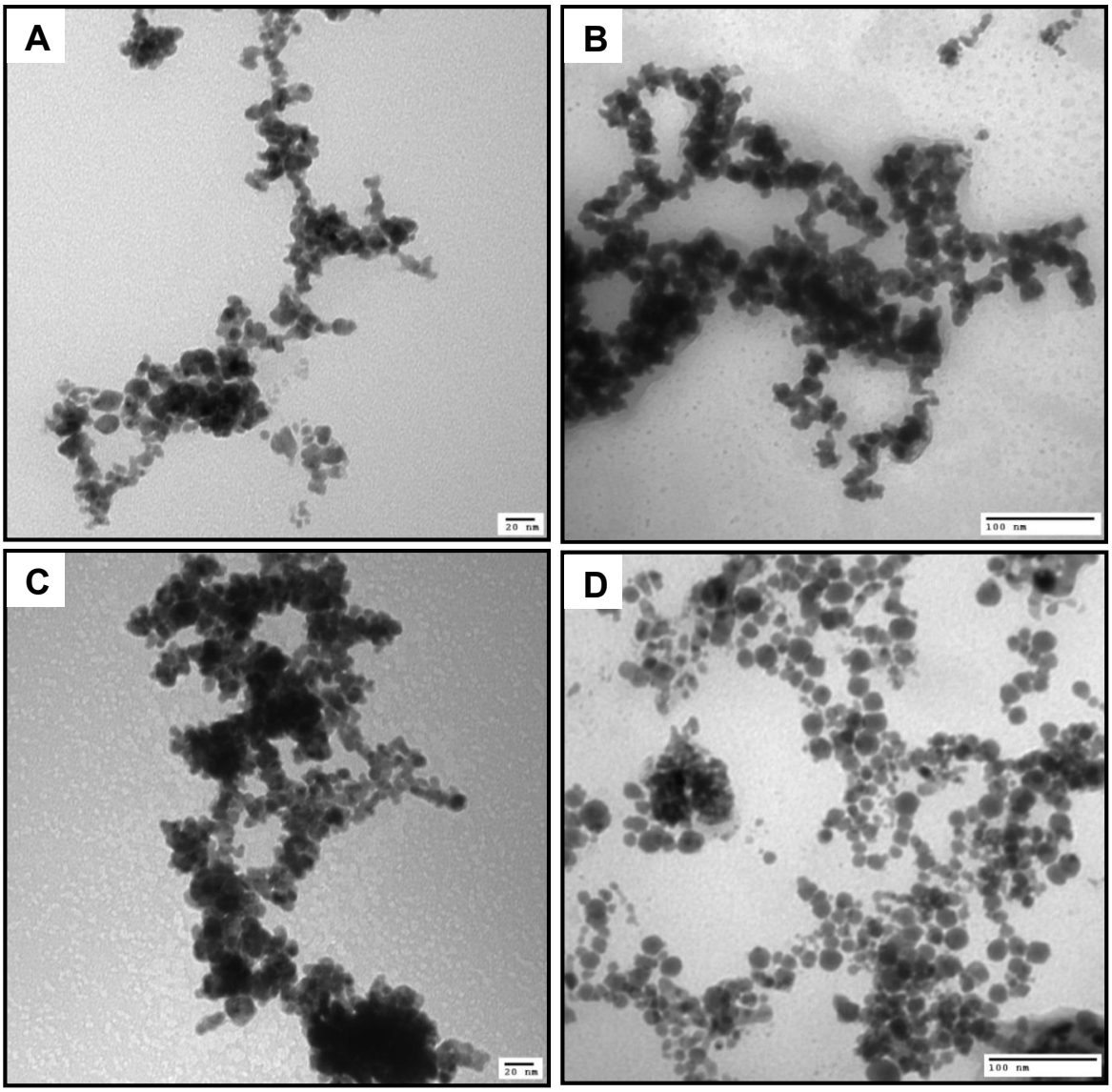

Figure 3-1: TEM images of unreacted (A) & (B) C-nPd$_A$, (C) C-nPd$_H$, and (D) C-nNi particles.

SEM/EDX - The bare nPd particles examined by SEM were found to agglomerate rapidly in the absence of CMC (Figures 3-2A-B & Appendix A, Figure 7-1A) as reported earlier (He et al., 2009). The micrographs revealed that particles were nearly spherical, uniform in shape and size, assembled in chains and tightly packed. The B-nPd particle diameters ranged between 11.19-22.64 nm, 14.04-22.11 nm, and 14.39-21.14 nm for the unreacted B-nPd_A, B-nPd_H, and B-nPd_{HW}, respectively and their specific surface areas were calculated as 29.81, 27.89, and 28.38 $m^2 g^{-1}$. The SEM analysis of reacted B-nPd_H particles (Figure 7-1B, Appendix A) also exhibited the presence of some bigger chunks indicating a slight change in palladium species after 1,2-DCA dechlorination. This could be due to oxidation of reacted B-nPd_H particles or the deposition of chlorides and/or hydrocarbons on their surface. EDX spectra showed that Pd was the major surface element (Figures 3-3 A-B and Figure 7-2A, Appendix A), accounting for 97, 94.9, and 98.3% (Table 3-2) of the mass of unreacted B-nPd_A, B-nPd_H, B-nPd_{HW}, respectively. The presence of small amounts of oxygen suggested minor formation of palladium oxides. Traces of chloride (0.2%) found in nPd_H (Figure 3-3B) came from the palladium precursor (potassium hexachloropalladate). However, when nPd_H was washed with deionized water to form B-nPd_{HW}, no chlorides were found. EDX spectrum for the reacted nPd_H particles also showed Pd as the major species with small amounts of oxygen, chloride and sodium (Figure 7-2B, Appendix A).

XRD - Diffractograms in Figure 3-4 showed characteristic peaks (2θ) of metallic Pd in the region of 40º, 47º, 68º, 82º, and 86º for all the tested B-nPd particles (Chen et al., 2005; Holade et al., 2016; Liu et al., 2008; Sekiguchi et al., 2011). These peaks were quite consistent with the standard metallic Pd XRD pattern (JCPDS 05-0681) in terms of their positions. Figure 3-4A for B-nPd_A showed an extra peak at 26.58º (2θ) corresponding to graphitic carbon (JCPDS 41-1487), probably coming from the Pd precursor (palladium acetate). The reacted B-nPd_H particles in Figure 3-4D also presented minor peaks (2θ) at 27.2º and 56.2º indicating the formation of some PdO (JCPDS 046-1211) (Sekiguchi et al., 2011).

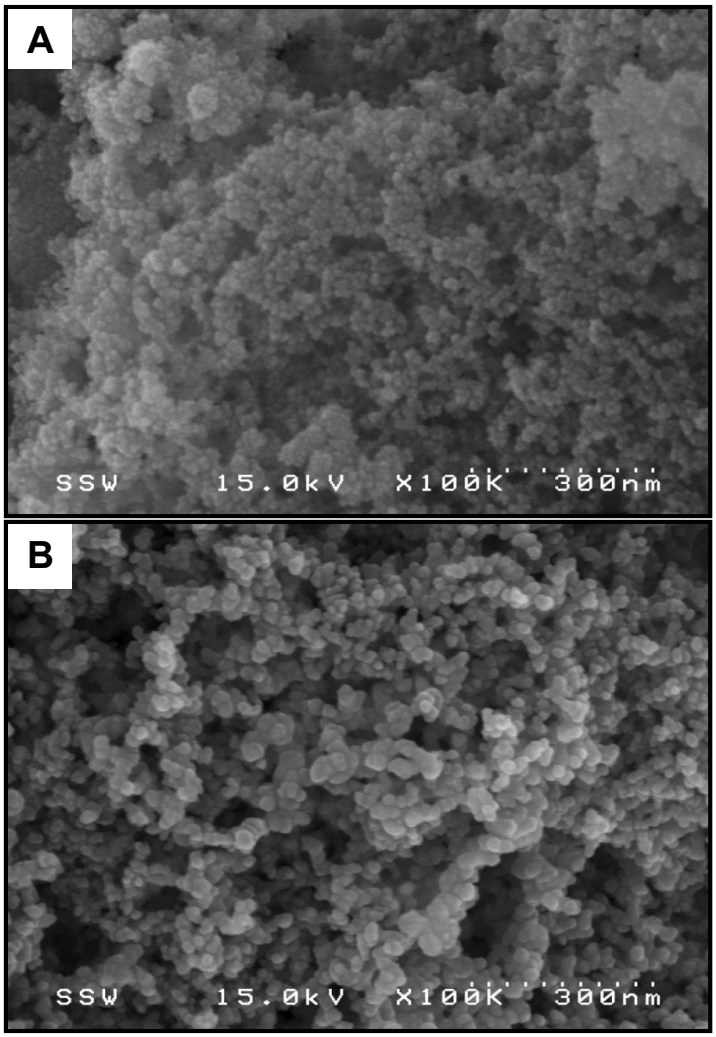

Figure 3-2: SEM images of unreacted (A) B-nPd$_A$ and (B) B-nPd$_H$ particles.

Table 3-2: EDX weight percent analysis of bare nPd particles.

Sample	Pd	O	Cl	Na
Unreacted B-nPd$_A$	97.0	3.0	-	-
Unreacted B-nPd$_H$	94.9	4.9	0.2	-
Unreacted B-nPd$_{HW}$	98.3	1.7	-	-
Reacted B-nPd$_H$	94.6	2.3	1.8	1.3

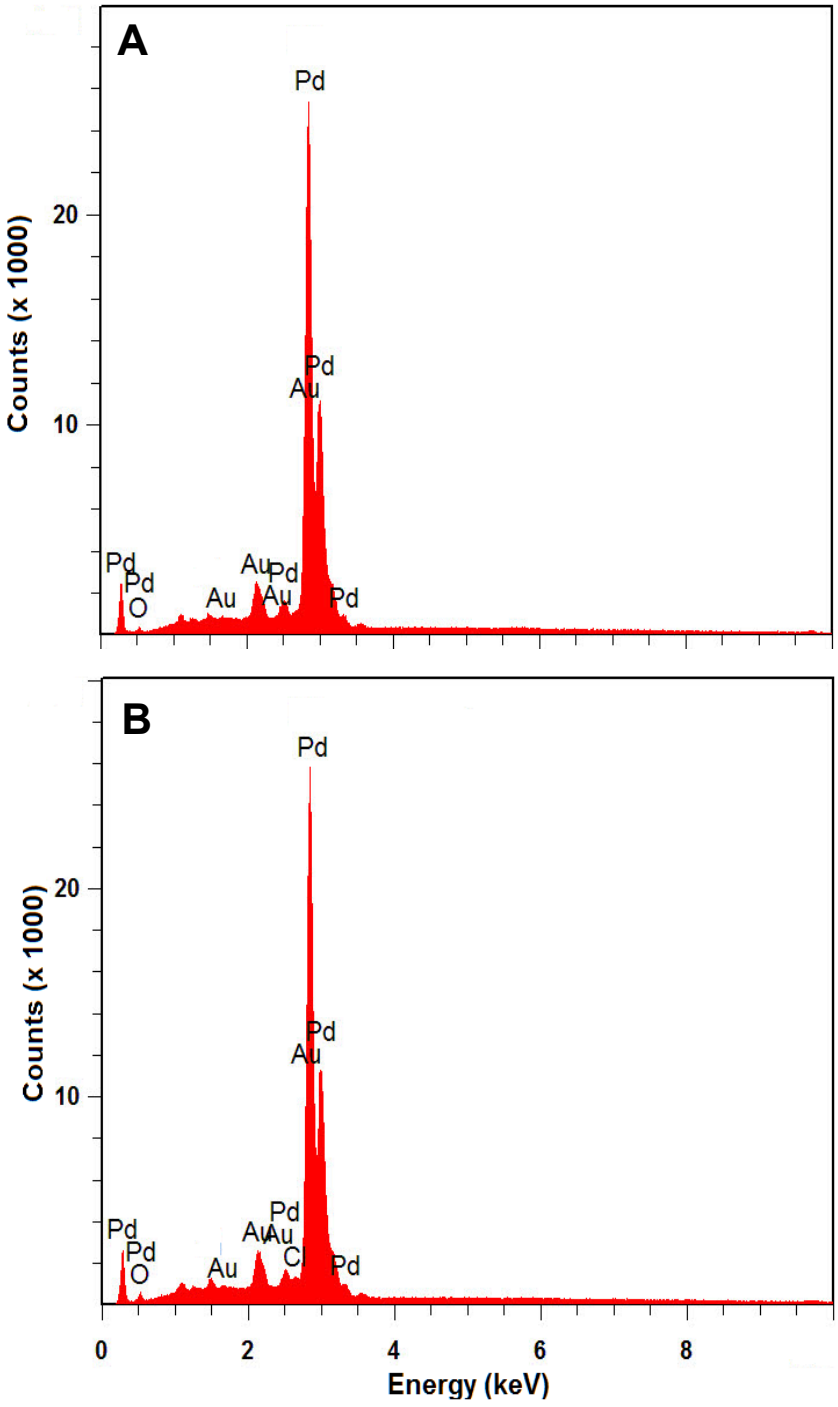

Figure 3-3: EDX spectra of unreacted (A) B-nPd$_A$ and (B) B-nPd$_H$ particles.

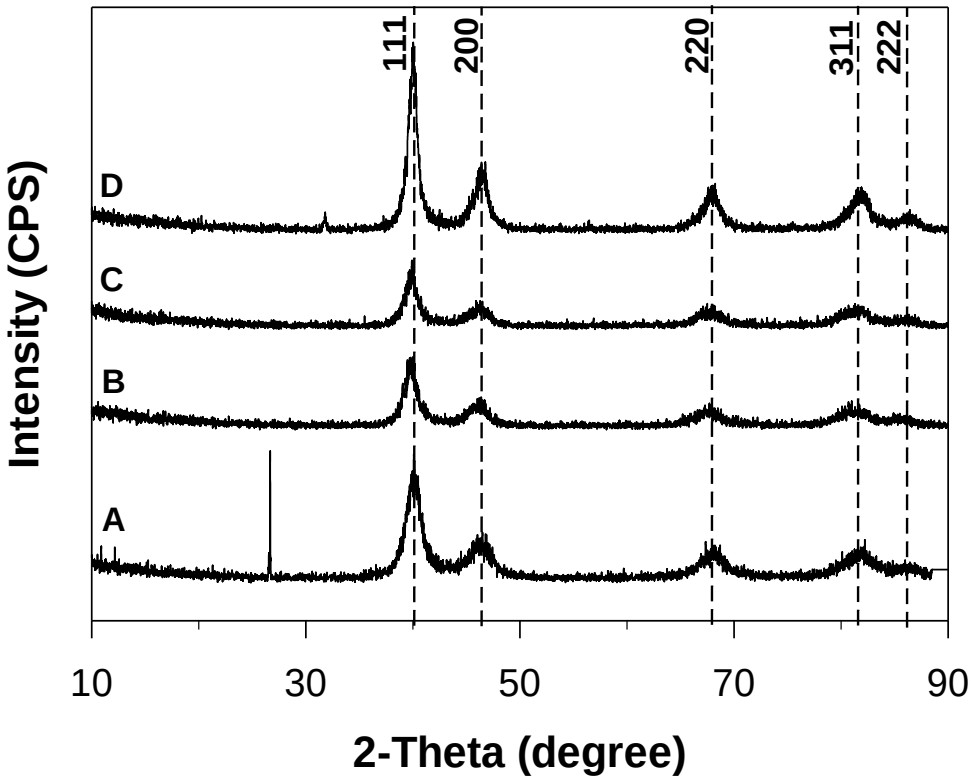

Figure 3-4: XRD patterns of unreacted (A) B-nPd$_A$, (B) B-nPd$_H$, (C) B-nPdH$_W$, and (D) reacted B-nPd$_H$ particles.

XPS – Unreacted B-nPd$_A$ and B-nPd$_H$ particles were further analyzed by XPS to determine their elemental composition and the valence state of Pd. The wide-scan survey revealed that the surface was mainly composed of palladium, oxygen, carbon, boron, and sodium (Figure 3-5 & Table 3-3). Sodium and boron peaks came from sodium borohydride used as the reductant for nPd synthesis. Carbon is likely originated from adventitious carbon contamination (Wielant et al., 2007). However, carbon would also have come from the Pd precursor (palladium acetate) in the case of B-nPd$_A$ particles, as also observed in XRD data. The chloride peak on B-nPd$_H$ surface came from the precursor potassium hexachloropalladate. O 1s line for oxygen is overlapped by the Pd ($3p_{3/2}$) core level, however, the O KLL line indicates the presence of oxygen in both B-nPd$_A$ and B-nPd$_H$.

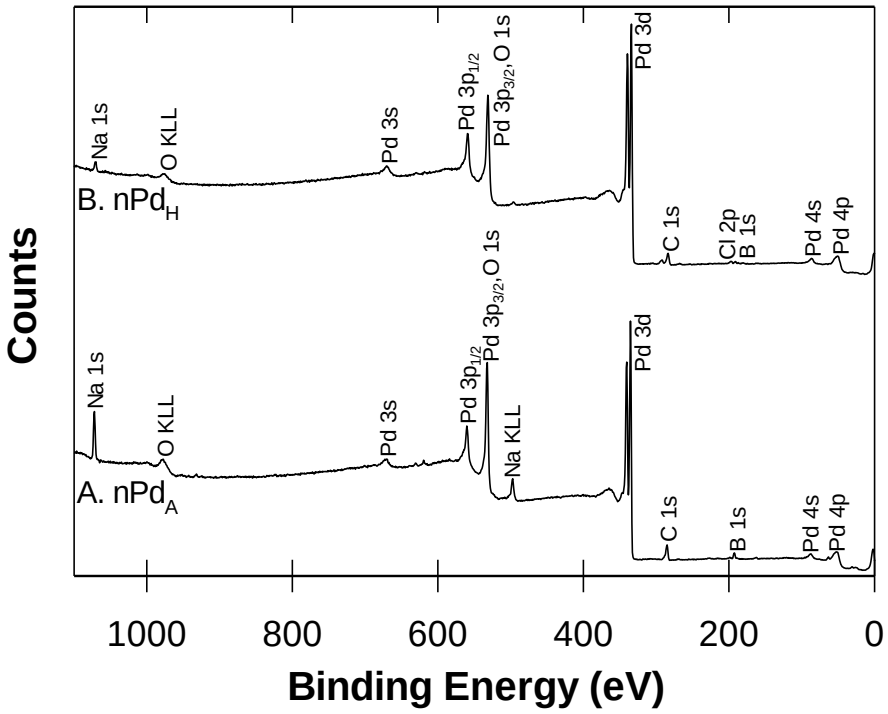

Figure 3-5: Wide-scan XPS survey spectra of unreacted (A) B-nPd$_A$ and (B) B-nPd$_H$.

Table 3-3 : Surface composition (atomic %) of nPd particles determined by XPS.

Nanoparticle/Element	Pd	O	C	Cl	B	Na	Other
B-nPd$_A$	26.8	24.2	24.6	0.4	13.1	9.2	1.7
B-nPd$_H$	38.1	27.3	23.2	1.5	4.9	2.5	2.5

The Pd 3d high resolution core level spectra for B-nPd$_A$ and B-nPd$_H$ and the fits of the curves are shown in Figure 3-6. The data for Pd species distribution is summarized in Table 3-4. Both B-nPd$_A$ and B-nPd$_H$ showed a major doublet peak at BEs of 335.2±0.2 eV ($3d_{5/2}$) and 340.4±0.2 eV ($3d_{3/2}$) which is in accordance with the literature values for Pd^0 (Chen et al., 2005; Gómez-Sainero et al., 2002; Holade et al., 2016; Kibis et al., 2012). This major

doublet contributed 96% and 78% to the total Pd 3d areas of B-nPd_A and B-nPd_H, respectively indicating metallic Pd as the dominant species in both the samples. The other sets of doublets at higher BEs in the Pd 3d region of these samples indicate the presence of non-zero valent/oxidized/electron-deficient Pd (Pd^{n+}). The Pd 3d spectra of B-nPd_H exhibited a doublet peak at 336.34 ($3d_{5/2}$) and 341.63 ($3d_{3/2}$) (Figure 3-6B) which is assigned to the Pd^{2+} present as PdO or $PdCl_2$ (Holade et al., 2016; Kibis et al., 2012). No PdO and $PdCl_2$ peaks were detected in this sample by XRD (Figure 3-4B), probably due to their amorphous nature or lower concentration. However, the EDX and XPS spectra clearly indicate the presence of Cl on the surface of B-nPd_H particles. The presence of significant amounts of Pd^{2+} (18%) suggests that this Pd species might have partially formed by interaction of Pd^0 with the electron-acceptor Cl^- (Xiong et al., 2007). This doublet was not significant in the Pd 3d spectra of nPd_A (Figure 3-6A) which can be attributed to the absence of Cl in this sample. Past research has reported the formation of significant amounts of Pd^{n+} species in catalysts prepared from chlorine-containing Pd precursors at low temperatures (Alvarez-Montero et al., 2010; Gómez-Sainero et al., 2002; Holade et al., 2016). The other set of minor doublet at higher BEs of 337.3±0.1 ($3d_{5/2}$) and 342.6±0.1 ($3d_{3/2}$) corresponding to the oxidized Pd species (Pd^{4+}) indicated the presence of small amounts of PdO_2 in both B-nPd_A and B-nPd_H. The presence of Pd^{4+} has also been reported by Holade et al. while completing XPS of palladium nanomaterials synthesized by $NaBH_4$ as a reductant. The Pd^{n+}/Pd^0 ratios were found to be 0.04 and 0.27 for B-nPd_A and B-nPd_H respectively, suggesting the favorability of chlorine-containing Pd precursor for forming Pd^{2+} species (Holade et al., 2016). Presence of both electron-deficient and metallic palladium [Pd^{n+}-Pd^0] sites on the Pd surface is essential for the catalyzed dechlorination reaction (Gómez-Sainero et al., 2002), as discussed later in the Reaction Mechanism Section.

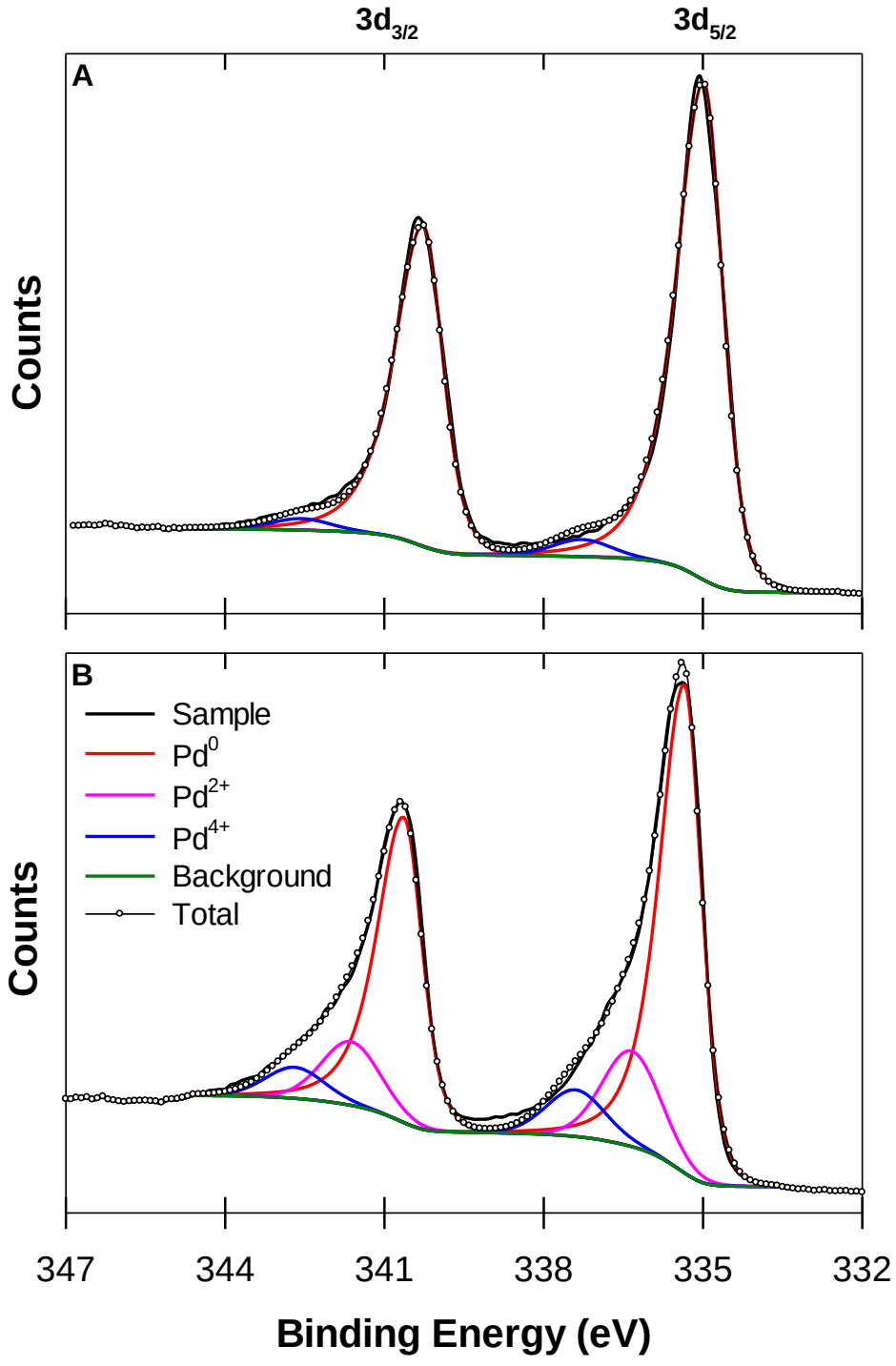

Figure 3-6: High resolution XPS for the Pd 3d region of unreacted (A) B-nPd$_A$ and (B) B-nPd$_H$.

Table 3-4: Pd 3d binding energies, percent area distribution, and Pd^{n+}/Pd^0 atomic ratio of unreacted bare nPd particles.

nPd Particle	Binding Energy (eV)	% Area	Pd^{n+}/Pd^0
B-nPd_A	Pd^0: 334.98 and 340.26 (Δ = 5.28)	96.0	0.04
	Pd^{2+}: 336.48 and 341.77 (Δ = 5.29)	0.2	
	Pd^{4+}: 337.27 and 342.56 (Δ = 5.29)	3.8	
B-nPd_H	Pd^0: 335.35 and 340.63 (Δ = 5.28)	73.1	0.27
	Pd^{2+}: 336.34 and 341.63 (Δ = 5.29)	18.1	
	Pd^{4+}: 337.40 and 342.69 (Δ = 5.29)	8.8	

Figure 7-3 (Appendix A) shows the high-resolution Cl 2p XPS spectrum for B-nPd_H which is fitted with doublet peaks (Cl $2p_{3/2}$ and Cl $2p_{1/2}$). The major doublet at 198.14 eV and 199.74 eV corresponds to inorganic chlorides making up 78.1% of the total area. The other doublet peak (199.89 and 201.49 eV) corresponds to covalent chlorocarbon (C-Cl bond) compounds. This indicates that the chlorines from the nPd_H precursor (potassium hexachloropalladate) were present on the surface of these nanoparticles, as also found earlier by EDX analysis. Past research has also reported similar findings for Pd synthesized from chlorine-containing precursors (Alvarez-Montero et al., 2010; Gómez-Sainero et al., 2002).

Table 3-5 summarizes some physical and chemical properties for the C-nPd_H, C-nPd_A, and C-nNi particles. The oxidation reduction potential (ORP) for the nanoparticles ranged between -860 to -710 mV further supporting the presence of reduced forms of nano metals. The pH values indicated all nano metal suspensions to be highly basic (9.25-10.44), which could be due to the formation of strongly basic metaborate (BO_2^-) ions during borohydride hydrolysis (Kong et al., 1999). The zeta potentials of all the stabilized nanoparticles

revealed their surfaces to be negatively charged, which is attributed to the net negative charge of CMC. This would favor nanoparticle transport in the subsurface by providing repulsive forces that would hinder their deposition on the negatively charged aquifer material (Yaron et al., 2012). DLS measurements were much larger for the stabilized particles (176-290 nm) in comparison to the TEM values. This is due to the fact that DLS also includes the hydrodynamic radius, both the metal particle as well as the outer CMC layer, yielding the overall size of the particle in aqueous solution. TEM measures only the inner electron-dense metal core and excludes the outer CMC layer (Lim et al., 2013; Liu et al., 2008).

Table 3-5: Properties of the unreacted CMC-stabilized nanoparticles.

Property	Analytical Technique	C-nPd$_A$	C-nPd$_H$	C-nNi
Particle Shape or Surface Morphology	TEM	Quasi-spherical particles, assembled in chains, forming some tightly packed aggregates	Quasi-spherical particles, assembled in chains, forming some tightly packed aggregates	Individual spherical particles, well dispersed
Average Particle Size (nm)	TEM	5.42±1.4	6.31±1.4	11.22±4.3
Specific Surface Area (m2 g-1)	Equation 3-5	93.03	79.91	60.08
ORP (mV)	Multimeter	-858.5	-860	-710.1
pH	pH-Meter	9.66	10.44	9.25
Zeta Potential	DLS	-53.82	-23.86	-42.2
Hydrodynamic Diameter (nm)	DLS	178.2	291.8	176

3.4.2 1,2-DCA Dechlorination

C-nPd$_H$ and C-nNi (1 g L^{-1}) particles were tested for catalyzing liquid-phase dechlorination of 1,2-DCA (~35 mg L^{-1}) at room temperature utilizing H_2 generated from excess $NaBH_4$ present in the system after particles synthesis (Exp. 1-2, Table 3-1). C-nPd$_H$ particles catalyzed complete and rapid removal of 1,2-DCA in <7 days (Figure 3-7A). However, C-nNi being a milder hydrogenation catalyst yielded incomplete and slower removal of 1,2-DCA, with only 35% 1,2-DCA dechlorinated in 11 days (Figure 3-7A). Past research has also reported higher and faster dechlorination of COCs when Pd or Ni/Pd was used as a catalyst rather than Ni (Kaminska and Srebowata, 2015; Śrębowata et al., 2007; Sun et al., 2011). In agreement with previous studies on liquid-phase catalyzed COCs hydrodechlorination (Davie et al., 2008; Hildebrand et al., 2009b; Mackenzie et al., 2006), 1,2-DCA dechlorination kinetics followed a pseudo-first-order kinetic model (Equation 3-6).

$$-\frac{d[1,2-DCA]}{dt} = k_{obs}[1,2-DCA] = k_{SA}a_s[1,2-DCA] \quad \text{(Equation 3-6)}$$

where *[1,2-DCA]* is the concentration of 1,2-DCA during reaction (mg L^{-1}), k_{obs} is the observed rate constant (d^{-1}), k_{SA} is the surface-area-normalized rate constant (L m^{-2} d^{-1}), and a_s is the specific surface area of nano metal (m^2 g^{-1}). k_{SA} values for C-nPd$_H$ and C-nNi treatments were 11.8 x 10^{-3} and 0.7 x 10^{-3} L m^{-2} d^{-1}, respectively (Figure 7-4, Appendix A). H_2 gas in the reactors far exceeded the stoichiometric H_2 demand for 1,2-DCA dechlorination, thus H_2 concentration in the aqueous phase was assumed to remain constant during the reaction.

Product analysis showed that ethane and chloroethane were the two main byproducts observed initially for the C-nPd$_H$ and C-nNi treatments (Exp. 1- 2, Table 3-1), following the same trend as the gas-phase 1,2-DCA hydrodechlorination catalyzed by group VIII catalysts (Borovkov et al., 2003; Heinrichs et al., 1997a; Lambert et al., 2004; Śrębowata et al., 2011; Xie et al., 2008). This suggests that 1,2-DCA was degraded through two successive hydrogenolysis steps (Figure 3-8). As ethane was observed immediately after 1,2-DCA injection into the reactors, the possibility of simultaneous direct reduction to ethane cannot be ignored. Ethane was the final byproduct for the C-nPd$_H$ treatment with

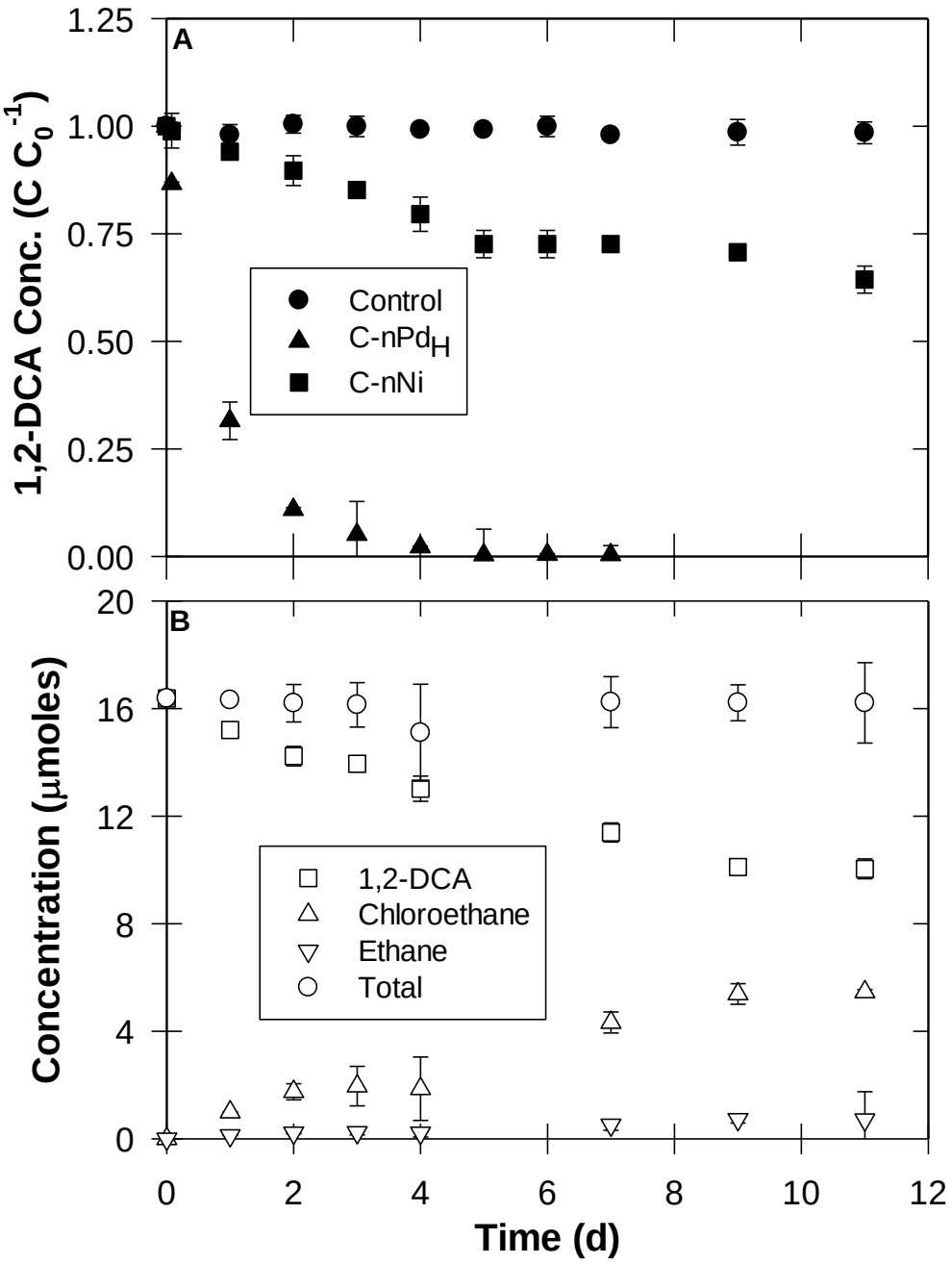

Figure 3-7: (A) 1,2-DCA dechlorination catalyzed by C-nPd$_H$ and C-nNi (Exp. 1-2, Table 3-1). (B) Distribution of dechlorination products for C-nNi treatment (Exp. 2, Table 3-1).

no chloroethane accumulation. A carbon mass balance (CMB) of 29.2% was achieved for this treatment, however a chlorides mass balance of 94 % could be achieved (for bare nPd treatment, Exp.6. Figure 7-5 in Appendix A shows byproducts distribution). The low CMB could be due to the deposition of hydrocarbons (i.e. ethane) on the Pd surface (Kaminska and Srebowata, 2015; Śrębowata et al., 2007). A much higher CMB (>90%) was achieved for the C-nNi particles (Figure 3-7B) which is attributed to incomplete dechlorination of 1,2-DCA, accumulation of chloroethane and comparatively less deposition of hydrocarbons on the Ni surface, presumably due to Ni being a milder hydrogenation catalyst. Accumulation of chloroethane in the C-nNi treatment suggests hydrogenolysis of chloroethane to ethane being a possible rate-limiting step in this treatment. Of note, in the absence of borohydride from the system, and in the presence of only B-nPd$_H$w (B-Pd$_H$ particles washed with deionized water and the supernatant was removed after synthesis), no 1,2-DCA dechlorination took place (Exp. 3, Table 3-1).

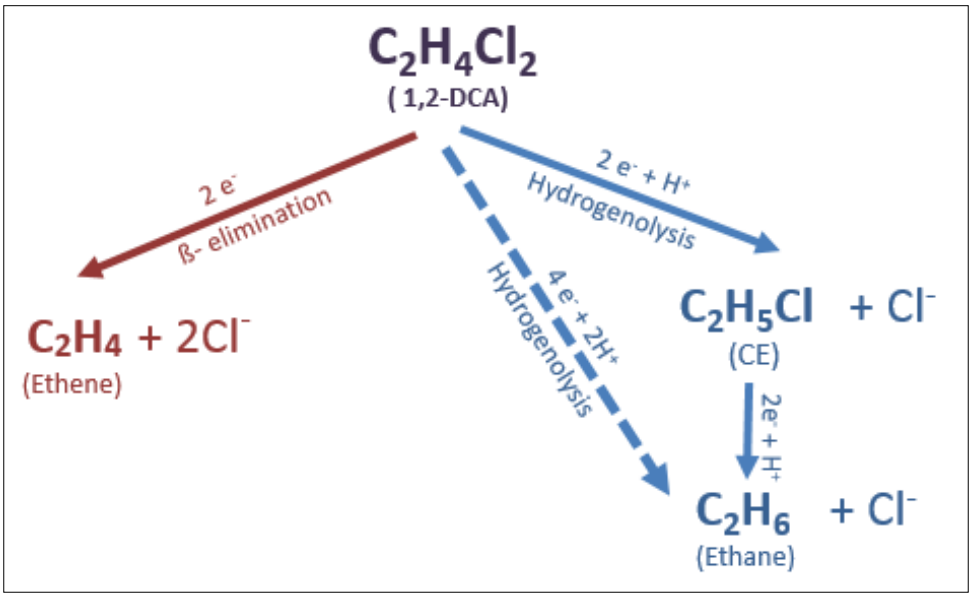

Figure 3-8: Abiotic 1,2-DCA dechlorination pathways.

Reaction Mechanism - Previous studies investigating liquid-phase catalyzed hydrodehalogenation suggest that the reductive reaction takes place through dissociative adsorption of the COC on the catalyst surface with successive breaking of C–Cl bonds (Chaplin et al., 2012; Kovenklioglu et al., 1992; Mackenzie et al., 2006). Considering the mechanisms mentioned in the literature and the degradation product results from the current study, it is proposed that 1,2-DCA molecules dissociatively adsorb on catalyst sites leading firstly to C-Cl bond scission. The adsorbed molecule is then hydrogenated by the dissociatively adsorbed hydrogen on adjacent sites and the resultant molecule finally desorbs as chloroethane. Thereafter, chloroethane adsorbs to the catalyst which is reduced to ethane through the same mechanism. However, the formation of ethane even at the very beginning of 1,2-DCA dechlorination in these experiments indicates that direct scission of the two C-Cl bonds on the catalyst surface also took place. For group VIII metals, the adsorption of 1,2-DCA (COCs in general) takes place on electron-deficient (M^{n+}) sites while H_2 activation takes place on adjacent metallic (M^0) sites (Bai and Sachtler, 1991; Gómez-Sainero et al., 2004; Gómez-Sainero et al., 2002; Sachtler and Stakheev, 1992). Past research reported that the presence of dual nature sites, consisting of both electron-deficient (Pd^{n+}) and zero valent (Pd^0) species, was essential for Pd to be catalytically active for liquid-phase hydrodechlorination in the presence of H_2 gas and the ratio between these two species affects the reaction rate (Alvarez-Montero et al., 2010; Gómez-Sainero et al., 2002). Based on XPS results, Gómez-Sainero also found that Pd catalysts having only one of these species were inactive for catalytic dechlorination reactions (Gómez-Sainero et al., 2002). In agreement with these studies, XPS analysis of Pd nanoparticles used in the current study also revealed that both these species were present on the nanoparticle surface (Figure 3-6, Table 3-4).

C-nZVI/nPd_H versus C-nPd_H - Following on the reaction mechanism explanation, it is worth mentioning that the borohydride remaining after particles synthesis in the aforementioned experiments is also present in the Pd doped on nZVI experiments (nZVI/Pd) reported incapable of dechlorinating 1,2-DCA (Atisha, 2011; Nunez Garcia et al., 2016a). Similarly, in Exp. 4, C-nZVI/Pd_H showed very little 1,2-DCA dechlorination (Figure 3-9) even though a high loading (5 g L^{-1}) of nZVI was used to dechlorinate 1,2-DCA (C_0 = 10 mg L^{-1}) and the H_2 generated from excess $NaBH_4$ was retained in the system.

The lack of nZVI reactivity towards 1,2-DCA, as compared to nPd and nNi, could be attributed to the inability of nZVI to break the C-Cl bond of 1,2-DCA, or adsorb 1,2-DCA (Huang et al., 2011). However, even the presence of Pd on nZVI could not effectively dechlorinate 1,2-DCA. One reason for this could be the much lower Pd concentration (0.04 g L^{-1}) in the C-nZVI/Pd_H system as compared to Pd (1 g L^{-1}) only experiment (Exp. 1, Table 3-1). To explore this, an additional experiment (Exp. 5, Table 3-1) was conducted using a lower C-nPd_H loading (0.04 g L^{-1}) which was same as the Pd dose in the C-nZVI/Pd_H experiment (Exp. 4, Table 3-1). This lower loading of C-nPd_H was able to catalyze 25% dechlorination of 1,2-DCA in 7 days even though there was much less H_2 available for the reaction as compared to the C-nZVI/Pd_H system (Figure 3-9). Negligible 1,2-DCA dechlorination in the C-nZVI/Pd_H treatment could be attributed to the absence of electron-deficient species (Pd^{n+}) of Pd in this system as Fe^0 continuously reduces Pd impregnated on nZVI to Pd^0 by acting as a continuous source of electrons. Moreover, Pd may also be covered underneath iron corrosion products during the reaction and becomes unavailable (Yan et al., 2010; Zhu and Lim, 2007). Importantly the C-nPd_H had both Pd^0 and Pd^{2+} species present as shown in the XPS results (Figure 3-6B).

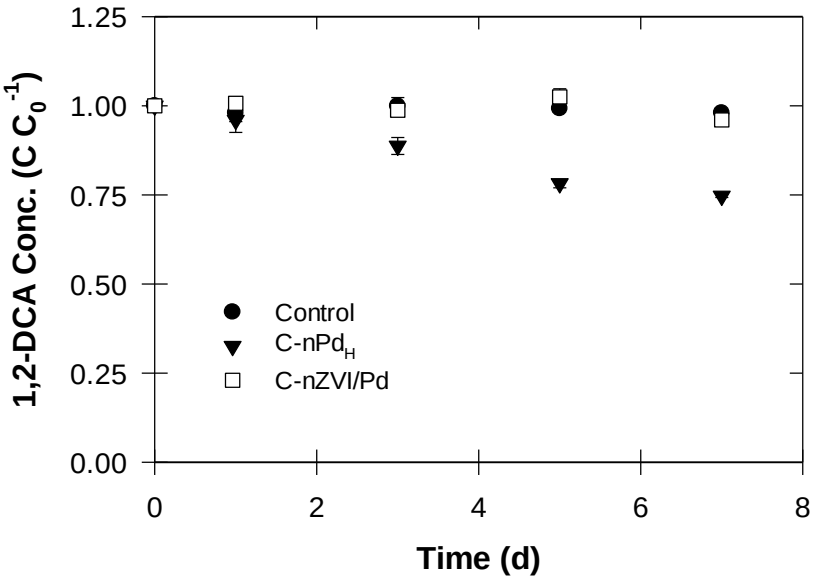

Figure 3-9: 1,2-DCA dechlorination by C-nPd_H and C-nZVI/Pd_H where Pd loading is 0.04 g L^{-1} (Exp. 4 & 5, Table 3-1).

3.4.3 Effect of Experimental Conditions

To our knowledge, this is the first time that Pd nanoparticles have shown successful catalytic dechlorination of 1,2-DCA in the liquid-phase. Thus, further research was conducted to study the effects of various experimental conditions including CMC coating, Pd precursors, nPd loading, and initial 1,2-DCA concentration on the catalytic dechlorination efficiency of these particles. Previous literature confirms that these parameters can have a strong influence on catalytic activity and dechlorination kinetics (He et al., 2009; Holade et al., 2016; Liu et al., 2008; O'Carroll et al., 2013; Sakulchaicharoen et al., 2010). Coating the nano metals with stabilizers/polymers prevents their agglomeration resulting in better subsurface mobility and possibly enhances dechlorination efficiency and consequently reaction rates by increasing the surface area (Liu et al., 2008; Sakulchaicharoen et al., 2010). However, it can also negatively impact the reactivity by blocking reactive surface sites (Phenrat et al., 2009). Metal precursors used for nanoparticle synthesis can also impact catalyst activity by changing the elemental composition, oxidation state and other properties (Alvarez-Montero et al., 2010; Chen et al., 2005; Gómez-Sainero et al., 2002). The effect of metal and substrate loading on dechlorination kinetics can be used to determine the rate limiting reaction step (Song and Carraway, 2005a). Figure 3-10 shows the effects of Pd precursors (potassium hexachloropalladate, palladium acetate), CMC coating (C-nPd$_H$ versus B-nPd$_H$, C-nPd$_A$ versus B-nPd$_A$) and washing of nPd$_H$ particles on 1,2-DCA dechlorination.

Effect of nPd Synthesis Parameters –Dechlorination data in Figure 3-10 suggests that the CMC coating slightly enhanced 1,2-DCA dechlorination for nPd$_H$ particles (C-nPd$_H$ versus B-nPd$_H$). However, normalizing the reaction rate constant by specific surface area suggests that CMC actually blocked some reactive sites and reduced k_{sa} by 50% (Exp. 1 & 6, Table 3-1). On the other hand, C-nPd$_A$ showed much higher apparent as well as surface-area-normalized rate constants than B-nPd$_A$ (Exp. 7 & 8, Table 3-1). This suggests that coating the nPd$_A$ particles, unlike the nPd$_H$ particles, did not block any reactive sites. This is further supported by the 'after dechlorination' images in Figure 7-6, Appendix A. C-nPd$_H$ particles were still uniformly suspended suggesting that the CMC coating was well attached to the Pd nanoparticles during dechlorination. However, the C-nPd$_A$ particles agglomerated into

bigger chunks indicating the detachment of CMC coating from Pd nanoparticles. Bhosale et al. reported that coated nPd particles synthesized from different precursors may interact differently with the coating agent due to variations in their surface/chemical properties (Bhosale et al., 2016).

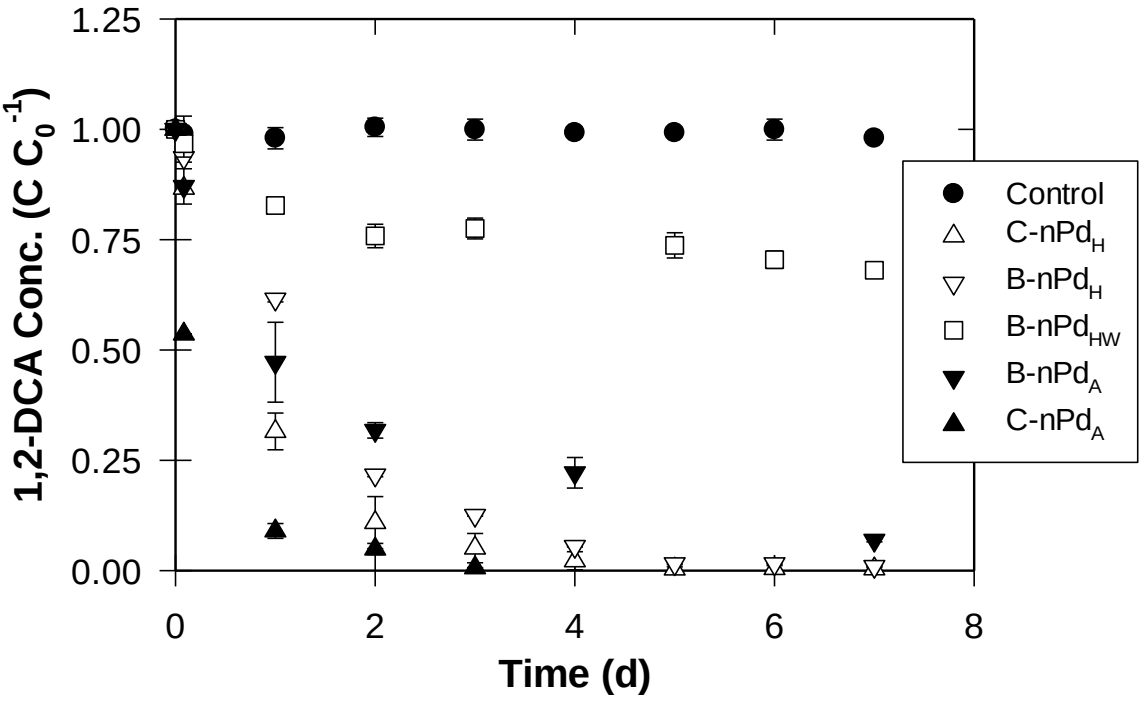

Figure 3-10: Effect of nPd (1 g L^{-1}) synthesis parameters (CMC coating, washing, and Pd precursor) on 1,2-DCA dechlorination (Exp. 1, 6, 7, 8, & 9, Table 3-1).

For the effect of Pd precursors on the catalytic activity of nPd particles, the dechlorination rate catalyzed by B-nPd_H was faster than that catalyzed by B-nPd_A with a k_{sa} value of 13.4 x 10^{-3} and 25.6 x 10^{-3} for C-nPd_A, and C-nPd_H, respectively (Figure 3-10, Exp. 6 & 8, Table 3-1). This could be attributed to the much higher Pd^{n+}/Pd^0 ratio for B-nPd_H (0.27), than that for B-nPd_A (0.04), which is comparatively closer to the value ($Pd^{n+}/Pd^0 \approx 1$) proposed for maximum hydrodechlorination activity (Gómez-Sainero et al., 2002). However, the precursor impact on the coated nanoparticles was the opposite, with C-nPd_A particles exhibiting faster dechlorination than C-nPd_H which could be due to the dominant inhibitory

effect of the coating rather than the Pd^{n+}/Pd^0 ratio. Past research also showed that nPd particles synthesized from different precursors had significant differences in their properties (e.g. dispersion, elemental composition, distribution of Pd species) which influenced their catalytic activity (Reddy et al., 2007; Xu et al., 2009).

In this study, EDX and XPS data indicates the presence of chlorides on the B-nPd_H surface coming from the Pd precursor (potassium hexachloropalladate), which would rather negatively influence the catalytic activity of B-nPd_H by surface poisoning (Mackenzie et al., 2006; Sun et al., 2011; Urbano and Marinas, 2001). To test the effect of chlorides on the catalytic efficiency of B-nPd_H, an additional experiment (Exp. 9, Table 3-1) was conducted where the particles were washed with deionized deoxygenated water to remove any residual chlorides from the system (both supernatant solution as well as particle surface). EDX spectra showed that no chlorides were present on the surface of washed Pd particles (B-nPd_{HW}). As the supernatant solution from the synthesis process was removed during washing, a fresh solution of 25 mM $NaBH_4$ was spiked to the system. Even after washing, the catalytic efficiency of B-nPd_{HW} was much lower than that of B-nPd_H, with incomplete 1,2-DCA dechlorination (Figure 3-10). It is possible that the addition of fresh 25 mM $NaBH_4$ inhibited nPd activity due to extensive surface coverage by H_2 gas, limiting surface sites for 1,2-DCA adsorption (Graham and Jovanovic, 1999; Jovanovic et al., 2005). Thus, it was not clear whether presence of chlorides in the elemental composition of nPd_H affected its catalytic performance. To further test the impact of chloride, an additional experiment (Exp. 10, Table 3-1) was conducted by spiking the B-nPd_A system with the same chloride concentration as that present in the B-nPd_H suspension (i.e., assuming chloride from the precursor is much greater than that evolved due to degradation). In this experiment 1,2-DCA dechlorination rate and efficiency were not affected by the presence of chlorides (Table 3-1).

All treatments shown in Figure 3-10 were found to follow pseudo-first-order (Figures 7-4 & 7-7, Appendix A) with an exception for the B-nPd_{HW}. In the B-nPd_{HW} treatment, deviation from pseudo-first-order to zero-order took place after the first two hours (Figure 7-8, Appendix A). This is assumed to be due to surface blockage by excessive H_2 gas. Deviation from a pseudo first order reaction rate to zero order has been observed in

previous studies with reductive dechlorination experiments due to surface blockage either by growth of surface species or poisoning and depositions (Hildebrand et al., 2009b; Song and Carraway, 2005a).

Effect of C-nPd$_H$ Loading - Heterogeneous catalytic dechlorination is a surface-mediated reaction involving multiple steps: diffusion and adsorption of the parent molecule to the catalyst surface, reaction on the surface, and desorption and diffusion of the daughter products from the surface (Chen et al., 2010; Yuan and Keane, 2003). According to the pseudo-first-order kinetic model, increased catalyst mass concentration is expected to provide a greater number of reactive sites which would enhance dechlorination rate provided mass transfer is not the rate-limiting step. In the current experiments, external mass transfer of 1,2-DCA or H_2 to the catalyst surface is unlikely to be the rate-limiting step due to the vigorous and continuous mixing of the reactor bottles. Nonetheless, to test for this possibility, the effect of C-nPd$_H$ loading in catalyzing 1,2-DCA dechlorination was studied (Exp. 5, 11, 12, and 13, Table 3-1, Figure 3-11A). Figure 3-11B presents a linear relationship between the pseudo-first-order rate constant and C-nPd$_H$ loading indicating mass transfer is not the rate limiting step under the studied conditions (Chen et al., 2010; Song and Carraway, 2005a; Yuan and Keane, 2003). It is important to note though that increased Pd loading would also result in increased $NaBH_4$ (H_2) concentrations in the system, as $NaBH_4$ is added in a stoichiometric ratio to the Pd concentration during nPd synthesis. As such, it is not possible to separate the impact of increased Pd loading and H_2 concentrations on the dechlorination rate, and that the linear relationship between k_{obs} and Pd loading could be due to increase in H_2 concentration. However, since the H_2 concentrations in all the treatments far exceeded the stoichiometric H_2 demand (~7-350 times) for 1,2-DCA dechlorination, H_2 concentration probably did not have significant effect on the 1,2-DCA dechlorination or the relation between k_{obs}, and Pd loading. This is further supported by the best fit of data for these Pd loadings to the pseudo-first-order kinetic model (Figure 7-9, Appendix A). Nonetheless, as shown in Figure 3-11A, the 1,2-DCA catalyzed dechlorination by 0.04 g L^{-1} C-nPd$_H$ plateaued after seven days, which could either be due to the limited availability of sites/surface area/blockage of reactive sites or lower H_2 concentration compared to the higher loadings. Taking into consideration that

low H_2/ substrate ratio is known to cause surface blockage due to adsorpion of hydrocarbons.

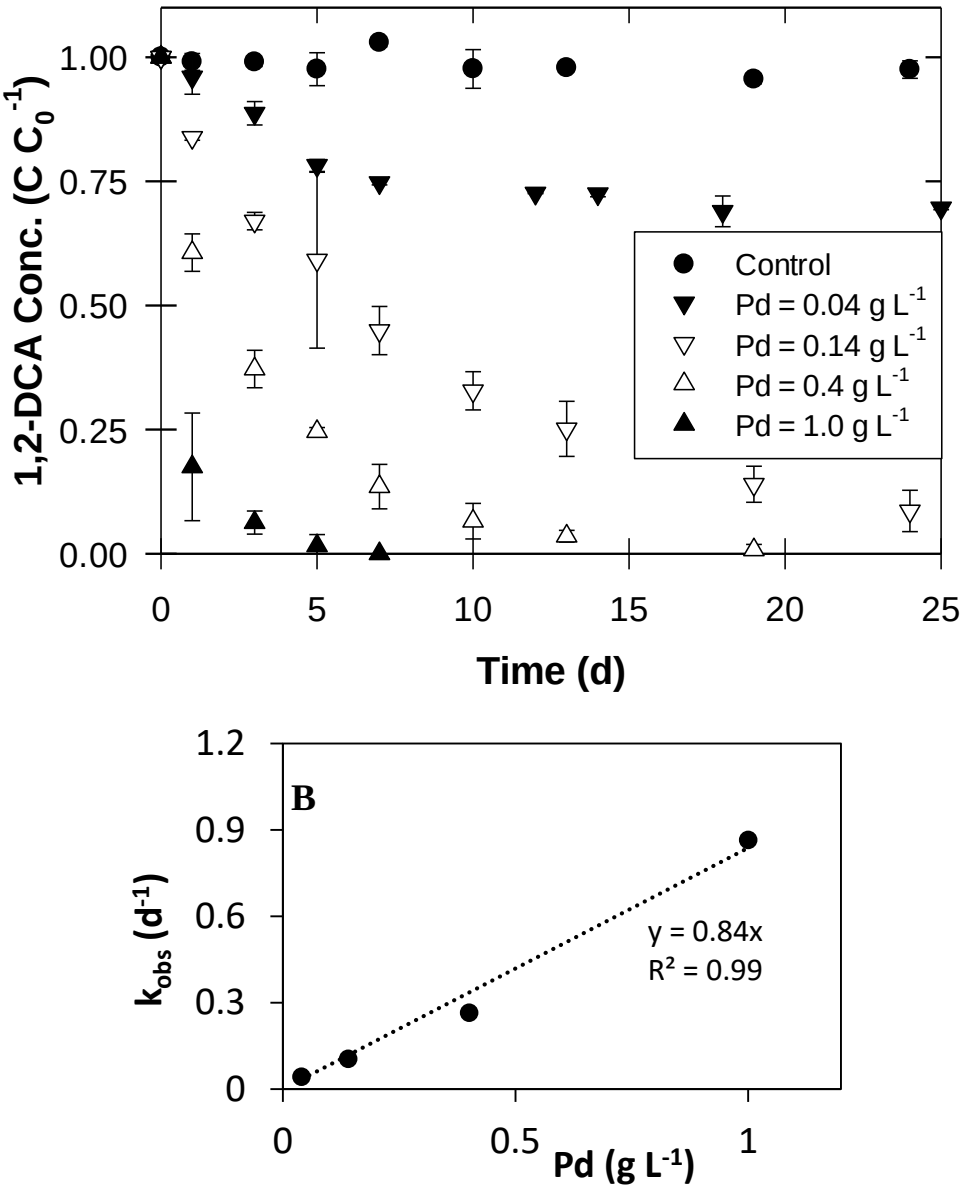

Figure 3-11: (A) Effect of C-nPd$_H$ loading on the catalytic dechlorination of 1,2-DCA (Exp. 5, 11, 12, & 13, Table 3-1), (B) C-nPd$_H$ loading versus k_{obs}.

Effect of Initial 1,2-DCA Concentration - The effect of initial 1,2-DCA concentration (8, 32, 65, and 225 mg L^{-1}) on the dechlorination rate catalyzed by C-nPd_H (1 g L^{-1}) is shown in Figure 7-10, Appendix A (Exp. 1, 13, 14, and 15). Good data fits were achieved using pseudo-first-order kinetic model for all initial concentrations (Figure 7-11, Appendix A). The dependence of reaction rate constant on the initial 1,2-DCA concentration is presented in Figure 3-12. As seen in Figure 3-12, the reaction rate constant is nearly constant for 1,2-DCA concentrations 8 and 32 mg L^{-1}, and then decreases to a nearly constant value for the higher initial concentrations. This is assumed to be due to blockage of some reactive sites due to the high 1,2-DCA concentration. It is suggested that due to adsorbed intermediate species or hydrocarbons, permanent blocking of some H_2 activation reactive sites took place and consequently reduced available surface area and therefore reaction rate constant decreased and remained constant for higher 1,2-DCA concentrations. This suggests that up to 32 mg L^{-1} reaction was limited by adsorption of 1,2-DCA, then at higher concentrations, reaction became limited by H_2 adsorption. At any case, this suggests that reaction was never limited by surface-reaction kinetics, as reaction rate constant did not decrease with increasing 1,2-DCA concentration >65 mg L^{-1}, but rather by adsorption before reaction takes place (Song and Carraway, 2005a). This also implies that the reaction rate constant was independent of 1,2-DCA concentration up to 32 mg L^{-1}, but above that it changed by a factor of 16 times. Similarly, Liu et al. studied the relationship between the reaction rate constant and TCE concentration for the reductive dechlorination of TCE over nZVI, and found that the reaction rate constant remained constant for low TCE concentrations (3.5, 14.5, 60.5 mg L^{-1}). However, at higher TCE concentrations the reaction rate constant decreased to the same value for all the studied concentrations (170.9, 1104.52 mg L^{-1}) due to reduction in available surface area for the reaction (Liu et al., 2007a).

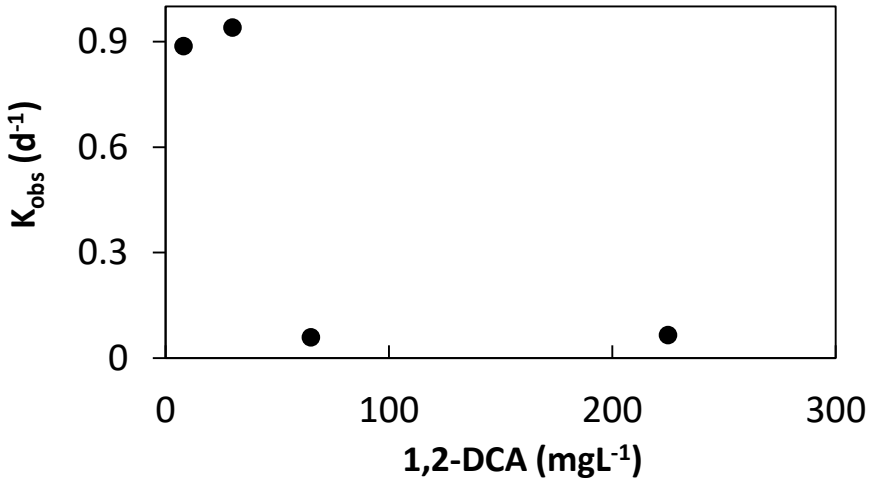

Figure 3-12: Plot of pseudo-first-order rate constant (k_{obs}) as a function of initial 1,2-DCA concentration where C-nPd_H = 1 g L^{-1} (Exp. 1, 13, 14, & 15, Table 3-1).

3.5 Conclusions

The feasibility of catalyzed reductive hydrodechlorination of 1,2-DCA in the liquid phase using $NaBH_4$ as a hydrogen source was investigated. For the first time, it is shown that nPd (1 g L^{-1}) can catalyze complete dechlorination of 1,2-DCA (32 mg L^{-1}) in <7 days, utilizing only residual borohydride after particles synthesis as the hydrogen source in the liquid phase. Ethane was the main byproduct indicating hydrogenolysis as the major pathway. The catalyzed dechlorination reaction followed a pseudo first order reaction rate with a surface area normalized rate constant (k_{sa}) of 11.76 x 10^{-3} L d^{-1} m^{-2}. A linear relationship between the pseudo-first-order rate constant (k_{obs}) and C-nPd_H loading was achieved, indicating mass transfer is not limiting the reaction. Increasing initial 1,2-DCA concentration > 32 mg L^{-1} resulted in more than a 16-fold reduction in k_{sa}, indicating blockage of some reactive sites. Synthesizing nPd particles from different precursors resulted in different particles surface species composition ratios as shown by XPS analysis and consequently different catalytic activities and dechlorination rates. The effect of coating on the catalytic activity of the nPd particles was found to be dependent on the Pd precursor used. For nPd_H particles (synthesized from potassium hexachloropalladate), CMC blocked some reactive sites even though it resulted in smaller particles (i.e., greater surface area per mass), but the K_{sa} was 0.46 times lower than that for bare particles. For

nPd_A particles (synthesized from palladium acetate), CMC did not block any reactive sites, with the K_{sa} being 1.4 times that of bare particles. nNi, as a milder hydrogenation catalyst, was found to catalyze the 1,2-DCA dechlorination reaction at a 0.06 times lower rate than that achieved by C-nPd_H.

Overall, a liquid-phase nano metal based technology capable of degrading 1,2-DCA with field application feasibility is developed. However, these reactivity experiments were carried out under ideal conditions not present at field sites. Real groundwater contains a range of constituents (e.g. NO_3^-, Cl^-, HCO_3^-, HS^-, HPO_4^{2-}, humic acid, and microbes) which can affect nano metal activity. Additionally, the continuous mixing of the treatment with contaminated water does not mimic real-field applications where contact time of treatment with groundwater is limited. Therefore, more research is needed to study these factors before taking this technology to the field.

3.6 References

Alvarez-Montero, M.A., Gomez-Sainero, L.M., Martin-Martinez, M., Heras, F. and Rodriguez, J.J., 2010. Hydrodechlorination of chloromethanes with Pd on activated carbon catalysts for the treatment of residual gas streams. Applied Catalysis B: Environmental, 96: 148-156.

Anwer, M.K., Sherman, D., Roney, J.G. and Spatola, A.F., 1989. Applications of ammonium formate catalytic transfer hydrogenation. 6. Analysis of catalyst, donor quantity, and solvent effects upon the efficacy of dechlorination. The Journal of Organic Chemistry, 54(6): 1284-1289.

Aramendia, M. et al., 2002. Liquid-phase hydrodechlorination of chlorobenzene over palladium-supported catalysts: Influence of HCl formation and NaOH addition. Journal of Molecular Catalysis A: Chemical, 184(1): 237-245.

Atisha, A., 2011. Degradation of 1,2-Dichloroethane With Nano-Scale Zero Valent Iron Particles, Western Ontario, 111 pp.

ATSDR, 2001. Toxicological profile for 1,2-dichloroethane. Agency for Toxic Substances and Disease Registry, Atlanta, GA. http://www.atsdr.cdc.gov/toxprofiles/index.asp. (accessed 13.09.2016).

Bai, X. and Sachtler, W.M., 1991. Methylcyclopentane conversion catalysis by zeolite encaged palladium clusters and palladium-proton adducts. Journal of Catalysis, 129(1): 121-129.

Bhosale, M.A., Sasaki, T. and Bhanage, B.M., 2016. Role of palladium precursors in morphology selective synthesis of palladium nanostructures. Powder Technology, 291: 154-158.

Borovkov, V.Y., Luebke, D.R., Kovalchuk, V.I. and d'Itri, J.L., 2003. Hydrogen-assisted 1, 2-dichloroethane dechlorination catalyzed by Pt-Cu/SiO2: Evidence for different functions of Pt and Cu sites. The Journal of Physical Chemistry B, 107(23): 5568-5574.

Chaplin, B.P. et al., 2012. Critical Review of Pd-Based Catalytic Treatment of Priority Contaminants in Water. Environmental Science & Technology, 46(7): 3655-3670.

Chastain, J., King, R.C. and Moulder, J., 1995. Handbook of X-ray photoelectron spectroscopy: a reference book of standard spectra for identification and interpretation of XPS data. Physical Electronics Eden Prairie, MN.

Chen, F., Zhong, Z., Xu, X.-J. and Luo, J., 2005. Preparation of colloidal Pd nanoparticles by an ethanolamine-modified polyol process. Journal of Materials Science, 40: 1517-1519.

Chen, H. et al., 2010. Aqueous bromate reduction by catalytic hydrogenation over Pd/Al2O3 catalysts. Applied Catalysis B: Environmental, 96(3–4): 307-313.

Conrad, H., Ertl, G. and Latta, E.E., 1974. Adsorption of hydrogen on palladium single crystal surfaces. Surface Science, 41(2): 435-446.

Davie, M.G., Cheng, H., Hopkins, G.D., LeBron, C.A. and Reinhard, M., 2008. Implementing heterogeneous catalytic dechlorination technology for remediating TCE-contaminated groundwater. Environmental science & technology, 42(23): 8908-8915.

Gómez-Sainero, L.M., Seoane, X.L. and Arcoya, A., 2004. Hydrodechlorination of carbon tetrachloride in the liquid phase on a Pd/carbon catalyst: kinetic and mechanistic studies. Applied Catalysis B: Environmental, 53(2): 101-110.

Gómez-Sainero, L.M., Seoane, X.L., Fierro, J.L. and Arcoya, A., 2002. Liquid-phase hydrodechlorination of CCl 4 to CHCl 3 on Pd/carbon catalysts: nature and role of Pd active species. Journal of Catalysis, 209(2): 279-288.

Graham, L.J. and Jovanovic, G., 1999. Dechlorination of p-chlorophenol on a Pd/Fe catalyst in a magnetically stabilized fluidized bed; Implications for sludge and liquid remediation. Chemical Engineering Science, 54: 3085-3093.

He, F., Liu, J., Roberts, C.B. and Zhao, D., 2009. One-step "green" synthesis of Pd nanoparticles of controlled size and their catalytic activity for trichloroethene hydrodechlorination. Industrial & Engineering Chemistry Research, 48(14): 6550-6557.

Heinrichs, B., Delhez, P., Schoebrechts, J.P. and Pirard, J.P., 1997a. Palladium-silver sol-gel catalysts for selective hydrodechlorination of 1,2-dichloroethane into ethylene: I. Synthesis and characterization. Journal of Catalysis, 172(2): 322-335.

Hildebrand, H., Mackenzie, K. and Kopinke, F.-D., 2009b. Pd/Fe3O4 nano-catalysts for selective dehalogenation in wastewater treatment processes—Influence of water constituents. Applied Catalysis B: Environmental, 91(1–2): 389-396.

Holade, Y. et al., 2016. High impact of the reducing agent on palladium nanomaterials: new insights from X-ray photoelectron spectroscopy and oxygen reduction reaction. RSC Adv., 6: 12627.

Huang, C.-C., Lo, S.-L., Tsai, S.-M. and Lien, H.-L., 2011. Catalytic hydrodechlorination of 1, 2-dichloroethane using copper nanoparticles under reduction conditions of sodium borohydride. Journal of Environmental Monitoring, 13(9): 2406-2412.

Job, N. et al., 2005. Hydrodechlorination of 1, 2-dichloroethane on Pd–Ag catalysts supported on tailored texture carbon xerogels. Catalysis today, 102: 234-241.

Jovanovic, G.N., Znidaršič Plazl, P., Sakrittichai, P. and Al-Khaldi, K., 2005. Dechlorination of p-chlorophenol in a microreactor with bimetallic Pd/Fe catalyst. Industrial & engineering chemistry research, 44(14): 5099-5106.

Kaminska, I.I. and Srebowata, A., 2015. Active carbon-supported nickel-palladium catalysts for hydrodechlorination of 1,2-dichloroethane and 1,1,2-trichloroethane. Research on Chemical Intermediates, 41: 9267-9280.

Kibis, L.S., Stadnichenko, A.I., Koscheev, S.V., Zaikovskii, V.I. and Boronin, A.I., 2012. Highly oxidixed palladium nanoparticles comprising Pd^{4+} species: Spectroscopic and structural aspects, thermal stability, and reactivity. The Journal of Physical Chemistry C, 116: 19342-19348.

Kong, V., Foulkes, F., Kirk, D. and Hinatsu, J., 1999. Development of hydrogen storage for fuel cell generators. i: Hydrogen generation using hydrolysis of hydrides. International Journal of Hydrogen Energy, 24(7): 665-675.

Kopinke, F.-D., Mackenzie, K., Koehler, R. and Georgi, A., 2004. Alternative sources of hydrogen for hydrodechlorination of chlorinated organic compounds in water on Pd catalysts. Applied Catalysis A: General, 271(1): 119-128.

Kovenklioglu, S., Cao, Z., Shah, D., Farrauto, R.J. and Balko, E.N., 1992. Direct catalytic hydrodechlorination of toxic organics in wastewater. AIChE Journal, 38(7): 1003-1012.

Kulkarni, P., Deshmukh, S., Kovalchuk, V. and d'Itri, J., 1999a. Hydrodechlorination of dichlorodifluoromethane on carbon-supported Group VIII noble metal catalysts. Catalysis Letters, 61(3-4): 161-166.

Lambert, S., Ferauche, F., Brasseur, A., Pirard, J.-P. and Heinrichs, B., 2005. Pd–Ag/SiO 2 and Pd–Cu/SiO 2 cogelled xerogel catalysts for selective hydrodechlorination of 1, 2-dichloroethane into ethylene. Catalysis today, 100(3): 283-289.

Lambert, S., Polard, J.-F., Pirard, J.-P. and Heinrichs, B.t., 2004. Improvement of metal dispersion in Pd/SiO 2 cogelled xerogel catalysts for 1, 2-dichloroethane hydrodechlorination. Applied Catalysis B: Environmental, 50(2): 127-140.

Legawiec-Jarzyna, M., Śrebowata, A., Juszczyk, W. and Karpiński, Z., 2004. Hydrodechlorination over Pd–Pt/Al 2 O 3 catalysts: A comparative study of chlorine removal from dichlorodifluoromethane, carbon tetrachloride and 1, 2-dichloroethane. Applied Catalysis A: General, 271(1): 61-68.

Li, L., Wang, X., Wang, A., Shen, J. and Zhang, T., 2009. Relationship between adsorption properties of Pt–Cu/SiO 2 catalysts and their catalytic performance for selective hydrodechlorination of 1, 2-dichloroethane to ethylene. Thermochimica Acta, 494(1): 99-103.

Lim, J., Yeap, S.P., Che, H.X. and Low, S.C., 2013. Characterization of magnetic nanoparticle by dynamic light scattering. Nanoscale Research Letters, 8(1): 381-381.

Lingaiah, N. et al., 2000. Vapour phase catalytic hydrodechlorination of chlorobenzene over Ni–carbon composite catalysts. Journal of Molecular Catalysis A: Chemical, 161(1–2): 157-162.

Liu, J., He, F., Durham, E., Zhao, D. and Roberts, C.B., 2008. Polysugar-stabilized Pd nanoparticles exhibiting high catalytic activities for hydrodechlorination of environmentally deleterious trichloroethylene. Langmuir, 24: 328-336.

Liu, X., Vellanki, B.P., Batchelor, B. and Abdel-Wahab, A., 2014b. Degradation of 1,2-dichloroethane with advanced reduction processes (ARPs): Effects of process variables and mechanisms. Chemical Engineering Journal, 237(0): 300-307.

Liu, Y., Phenrat, T. and Lowry, G.V., 2007a. Effect of TCE concentration and dissolved groundwater solutes on NZVI-promoted TCE dechlorination and H2 evolution. Environmental Science and Technology, 41(22): 7881-7887.

Lowry, G.V. and Reinhard, M., 1999. Hydrodehalogenation of 1-to 3-carbon halogenated organic compounds in water using a palladium catalyst and hydrogen gas. Environmental science & technology, 33(11): 1905-1910.

Luebke, D.R., Vadlamannati, L.S., Kovalchuk, V.I. and d'Itri, J.L., 2002. Hydrodechlorination of 1,2-dichloroethane catalyzed by Pt–Cu/C: effect of catalyst pretreatment. Applied Catalysis B: Environmental, 35(3): 211-217.

Mackenzie, K., Frenzel, H. and Kopinke, F.-D., 2006. Hydrodehalogenation of halogenated hydrocarbons in water with Pd catalysts: Reaction rates and surface competition. Applied Catalysis B: Environmental, 63(3): 161-167.

McNab Jr, W.W. and Ruiz, R., 1998. Palladium-catalyzed reductive dehalogenation of dissolved chlorinated aliphatics using electrolytically-generated hydrogen. Chemosphere, 37(5): 925-936.

Murthy, K.V., Patterson, P.M., Jacobs, G., Davis, B.H. and Keane, M.A., 2004. An exploration of activity loss during hydrodechlorination and hydrodebromination over Ni/SiO2. Journal of Catalysis, 223(1): 74-85.

NIH, 2016. TOXMAP: Environmental Health Maps. U.S. National Library of Medicine, Bethesda, MD. https://toxmap-classic.nlm.nih.gov/toxmap/main/index.jsp (accessed 13.09.2016).

Nunez Garcia, A., Boparai, H.K. and O'Carroll, D.M., 2016a. Enhanced dechlorination of 1,2-dichloroethane by coupled nano iron-dithionite treatment. Environmental Science & Technology, 50(10): 5243-5251.

O'Carroll, D., Sleep, B., Krol, M., Boparai, H. and Kocur, C., 2013. Nanoscale zero valent iron and bimetallic particles for contaminated site remediation. Advances in Water Resources, 51: 104-122.

Phenrat, T., Liu, Y., Tilton, R.D. and Lowry, G.V., 2009. Adsorbed polyelectrolyte coatings decrease Fe0 nanoparticle reactivity with TCE in water: conceptual model and mechanisms. Environmental Science & Technology, 43(5): 1507-1514.

Reddy, P.S.S., Babu, N.S., Lingaiah, N., Prasad, P.S.S. and Rao, I.V., 2007. Catalytic decomposition of nitrous oxide on nano sized palladium catalysts: The influence of precursor and the method of preparation, Proceedings of European Congress of Chemical Engineering (ECCE-6), Copenhagen.

Rostamikia, G. and Janik, M.J., 2010. Direct borohydride oxidation: mechanism determination and design of alloy catalysts guided by density functional theory. Energy & Environmental Science, 3(9): 1262-1274.

Sachtler, W. and Stakheev, A.Y., 1992. Electron-deficient palladium clusters and bifunctional sites in zeolites. Catalysis today, 12(2): 283-295.

Sakulchaicharoen, N., O'Carroll, D.M. and Herrera, J.E., 2010. Enhanced stability and dechlorination activity of pre-synthesis stabilized nanoscale FePd particles. Journal of contaminant hydrology, 118(3): 117-127.

Sekiguchi, Y., Hayashi, Y. and Takizawa, H., 2011. Synthesis of Palladium Nanoparticles and Palladium/Spherical Carbon Composite Particles in the Solid-Liquid System of Palladium Oxide-Alcohol by Microwave Irradiation. Materials transactions, 52(5): 1048-1052.

Song, H. and Carraway, E.R., 2005a. Reduction of chlorinated ethanes by nanosized zero-valent iron: kinetics, pathways, and effects of reaction conditions. Environmental science & technology, 39(16): 6237-6245.

Śrębowata, A., Juszczyk, W., Kaszkur, Z. and Karpiński, Z., 2007. Hydrodechlorination of 1,2-dichloroethane on active carbon supported palladium–nickel catalysts. Catalysis Today, 124(1–2): 28-35.

Śrębowata, A., Lisowski, W., Sobczak, J.W. and Karpiński, Z., 2011. Hydrogen-assisted dechlorination of 1,2-dichloroethane on active carbon supported palladium–copper catalysts. Catalysis Today, 175(1): 576-584.

Sun, C. et al., 2011. A Highly Active Pd on Ni–B Bimetallic Catalyst for Liquid-Phase Hydrodechlorination of 4-Chlorophenol Under Mild Conditions. Catalysis letters, 141(6): 792-798.

Sun, Y.P., Li, X.Q., Cao, J.S., Zhang, W.X. and Wang, H.P., 2006b. Characterization of zero-valent iron nanoparticles. Advances in Colloid and Interface Science, 120(1-3): 47-56.

Ukisu, Y. and Miyadera, T., 1997. Hydrogen-transfer hydrodehalogenation of aromatic halides with alcohols in the presence of noble metal catalysts. Journal of Molecular Catalysis A: Chemical, 125(2): 135-142.

Urbano, F. and Marinas, J., 2001. Hydrogenolysis of organohalogen compounds over palladium supported catalysts. Journal of Molecular Catalysis A: Chemical, 173(1): 329-345.

Wagner, C. et al., 2003. NIST Standard Reference Database 20: NIST X-ray Photoelectron Spectroscopy Database, *Version 3.4* (web version). Institute of Standards and Technology, Standard Reference Data Program, Gaithersburg, USA. https://srdata.nist.gov/xps/.

Wielant, J., Hauffman, T., Blajiev, O., Hausbrand, R. and Terryn, H., 2007. Influence of the iron oxide acid-base properties on the chemisorption of model epoxy compounds studied by XPS. Journal of Physical Chemistry C, 111(35): 13177-13184.

Wiener, H., Blum, J. and Sasson, Y., 1991. Transfer hydrogenolysis of aryl halides and other hydrogen acceptors by formate salts in the presence of palladium/carbon catalyst. The Journal of Organic Chemistry, 56(21): 6145-6148.

Xie, H. et al., 2008. Hydrodechlorination of 1,2-dichloroethane catalyzed by dendrimer-derived Pt–Cu/SiO2 catalysts. Journal of Catalysis, 259(1): 111-122.

Xiong, Y. et al., 2007. Synthesis and mechanistic study of palladium nanobars and nanorods. Journal of American Chemical Society, 129: 3665-3675.

Xu, S., Wang, L., Chu, W. and Yang, W., 2009. Influence of Pd precursors on the catalytic performance of Pd-$H_4SiW_{12}O_{40}/SiO_2$ in the direct oxidation of ethylene to acetic acid. Journal of Molecular Catalysis A: Chemical, 310: 138-143.

Yan, W., Herzing, A.A., Li, X.-q., Kiely, C.J. and Zhang, W.-x., 2010. Structural evolution of Pd-doped nanoscale zero-valent iron (nZVI) in aqueous media and implications for particle aging and reactivity. Environmental science & technology, 44(11): 4288-4294.

Yaron, B., Dror, I. and Berkowitz, B., 2012. Soil-subsurface change: Chemical pollutant impacts. Springer Science & Business Media.

Yuan, G. and Keane, M.A., 2003. Liquid phase catalytic hydrodechlorination of 2,4-dichlorophenol over carbon supported palladium: an evaluation of transport limitations. Chemical Engineering Science, 58(2): 257-267.

Zhang, F. et al., 2008. Size-Dependent Hydrogenation Selectivity of Nitrate on Pd−Cu/TiO2 Catalysts. The Journal of Physical Chemistry C, 112(20): 7665-7671.

Zhang, M., He, F. and Zhao, D., 2015. Catalytic activity of noble metal nanoparticles toward hydrodechlorination: influence of catalyst electronic structure and nature of adsorption. Front. Environ. Sci. Eng., 9(5): 888-896.

Zhao, Z.-F. et al., 2008. Synthesis of a nano-nickel catalyst modified by ruthenium for hydrogenation and hydrodechlorination. Catalysis Communications, 9(13): 2191-2194.

Zhu, B.-W. and Lim, T.-T., 2007. Catalytic reduction of chlorobenzenes with Pd/Fe nanoparticles: reactive sites, catalyst stability, particle aging, and regeneration. Environmental science & technology, 41(21): 7523-7529.

Chapter 4

4 Impact of Solution Chemistry on Nano Copper Catalyzed Dechlorination of 1,2-Dichloroethane

4.1 Abstract

1,2-Dichloroethane (1,2-DCA) is a persistent groundwater contaminant causing adverse health effects and is quite resistant to most remediation technologies. Recently, catalytic dechlorination of 1,2-DCA in the liquid-phase via copper nanoparticles (nCu) coupled with borohydride as a hydrogen (H_2) source at the bench scale has shown promising results. Implementation of this technology as a groundwater treatment requires understanding of the dechlorination kinetics under real-field conditions. Therefore, the current study has investigated the effects of the treatment synthesis parameters, initial 1,2-DCA concentrations, and common groundwater solutes (oxygen, sulfides, chlorides, and humic acid) on 1,2-DCA dechlorination kinetics. Surface characterization was carried out to confirm the particles were nano sized, elemental composition and oxidation state. nCu particles were found incapable of utilizing H_2 formed from borohydride during their synthesis process, and rather direct injections of borohydride in reactor bottles were found essential. Rinsing the nCu particles with deionized water was found to change their surface composition, and enhance their catalytic activity in reducing 1,2-DCA. Coating the nCu particles with carboxymethyl cellulose blocked reactive sites and consequently reduced 1,2-DCA dechlorination efficiency. 1,2-DCA dechlorination reaction was found to follow a pseudo-first-order kinetic model under all the studied 1,2-DCA concentrations. The presence of sulfides ($\geq$ 0.4 mg L^{-1}), chlorides (1000-2000 mg L^{-1}), humic acid (10-30 mg L^{-1}), as well as dissolved oxygen affected the catalytic activity of nCu particles in reducing 1,2-DCA and reduced the reaction rate by >18%. However, an additional injection of borohydride compensated for the poisoning/deactivation of nCu particles by these groundwater solutes and restarted 1,2-DCA dechlorination. This study provides insight on how the treatment synthesis parameters and groundwater solutes influence its performance and thus can aid in upscaling the treatment from ideal laboratory conditions to real-field application as a remediation tool.

Keywords: 1,2-Dichloroethane, Borohydride, Dechlorination, Nano Copper, Humic Acid, Chlorides, Sulfides, Dissolved Oxygen, Liquid-Phase.

4.2 Introduction

1,2-Dichloroethane (1,2-DCA, $C_2H_4Cl_2$), a chlorinated organic compound (COC) with extensive industrial applications and usage, has caused widespread subsurface contamination (Atisha, 2011; Liu et al., 2014b). It can cause adverse health effects including: circulatory and respiratory failure, neurological disorders, in addition to being a probable human carcinogen (ATSDR, 2001; Humans et al., 1999; Liu et al., 2014b; Water et al., 2011). Due to its persistent nature and adverse health effects, significant research has been devoted to the development of field-applicable remediation technologies for removing 1,2-DCA from water sources (Atisha, 2011; Huang et al., 2011; Liu et al., 2014b; Lowry and Reinhard, 1999; Luebke et al., 2002; Nunez Garcia et al., 2016a; Śrębowata et al., 2011).

Recently, liquid-phase catalyzed reductive hydrodechlorination has emerged as a possible field-applicable technology showing promising results in reducing COCs, including 1,2-DCA, at the bench scale (Chaplin et al., 2012; Huang et al., 2012; Huang et al., 2011; Kopinke et al., 2003; Mackenzie et al., 2006). Huang et al. (2011) reported complete and rapid dechlorination of 1,2-DCA following sequential injections of borohydride to a suspension of bare water-rinsed Cu nanoparticles (nCu). Borohydride ($NaBH_4$) was used as the H_2 source eliminating the need for direct H_2 gas, as H_2 gas is generated through the hydrolysis of borohydride (Equation 4-1) (Huang et al., 2012; Rostamikia and Janik, 2010). The suggested mechanism for dechlorination of COCs implies that the catalysts activate H_2 gas into a robust reductant which then reduces the dissociatively adsorbed COC molecules on adjacent sites (Equation 4-2) (Chaplin et al., 2012; Huang et al., 2012; Kopinke et al., 2003; Kovenklioglu et al., 1992; Mackenzie et al., 2006).

$$\boldsymbol{BH_4^- + 2H_2O \rightarrow BO_2^- + 4H_2\uparrow} \qquad \text{(Equation 4-1)}$$

$$\boldsymbol{RCl + H_2 \xrightarrow{Catalyst} RH + HCl} \qquad \text{(Equation 4-2)}$$

The development of a field-applicable technology capable of degrading recalcitrant compounds like 1,2-DCA utilizing a relatively cheap catalyst such as nCu is an important breakthrough for the remediation world. However, the literature study that investigated nCu catalyzed dechlorination of 1,2-DCA was carried out at one 1,2-DCA concentration on idealized nCu particles (bare and rinsed with water after synthesis) under conditions that are not representative of those in the field (Huang et al., 2011). For example, at many field sites oxygen, typical groundwater (GW) solutes (e.g. HS^-, Cl^-) and dissolved organic carbon (DOC) might be present at a range of concentrations. All of these constituents can impact nanoparticle surface composition and reactivity (Davie et al., 2008; Hutchings et al., 1994; Kim et al., 2014; Lecloux, 1999; Lowry and Reinhard, 2000; Schüth et al., 2004; Twigg and Spencer, 2001). Previous studies have indicated that Cu particles are known to spontaneously oxidize in air or aqueous solutions (Alsawafta et al., 2011; Coulman et al., 1990). Moreover, gas-phase Cu catalytic dechlorination studies have reported that Cu is very sensitive to chlorine and sulfur, especially at low operating temperatures, and is rapidly deactivated owing to its tendency to strongly adsorb chlorine or sulfur to its surface (Hutchings et al., 1994; Śrębowata et al., 2011; Twigg and Spencer, 2001). Furthermore, it has been reported that humic acid (as a surrogate to DOC) competes with COCs for reactive sites on metal surfaces, consequently reducing their dechlorination efficiency (Doong and Lai, 2005; Johnson et al., 1998; Tratnyek et al., 2001). Besides, our recent study investigating palladium nanoparticles (nPd) for catalytically dechlorinating 1,2-DCA, successfully demonstrated the use of residual borohydride present in the nano metal slurry after nanoparticles synthesis as the H_2 source. This eliminated the need for sequential borohydride injections, thus making the technology more economical and practical.

Therefore, in order to facilitate the transition of the Cu-borohydride technology from ideal laboratory conditions to field application as a remediation tool it is essential to understand the effects of solution chemistry on dechlorination kinetics of 1,2-DCA. Thus, the objectives of this study are to: (1) determine the possibility of utilizing the residual borohydride in the nCu slurry as a H_2 source, (2) evaluate the effects of nCu synthesis parameters on 1,2-DCA dechlorination kinetics, and (3) elucidate the effects of a typical range of concentrations of humic acid, sulfides, chlorides, and dissolved oxygen on 1,2-DCA dechlorination kinetics, and (4) characterize the surface of nCu particles under

different synthesis parameters. Additionally, 1,2-DCA dechlorination byproducts, and mechanisms, and the effect of initial 1,2-DCA concentrations on the reaction kinetics were also evaluated.

4.3 Experimental Methods

4.3.1 Chemicals and Materials

The following chemicals were used as received: 1,2-dichloroethane (1,2-DCA, 99+%, Sigma-Aldrich)), sodium borohydride ($NaBH_4$, 98+%, ACROS Organics), cupric sulfate ($CuSO_4$ (EMD)), sodium carboxymethyl cellulose (CMC, MW = 90K, ACROS Organics), sodium chloride (NaCl, EMD Chemicals Inc.)), humic acid (Sigma-Aldrich), sodium sulfide nonahydrate ($Na_2S.9H_2O$, 99.99%, Sigma-Aldrich), gas Mix (5% H_2 balance Ar, PRAXAIR), and N_2 (Ultra High Purity, PRAXAIR). Deionized deoxygenated water purged with ultrapure N_2 gas was used to prepare aqueous solutions.

4.3.2 Synthesis of Cu Nanoparticles

nCu and nCu/Pd particles were synthesized using the aqueous reduction method with sodium borohydride. To synthesize the bare particles (B-nCu) a freshly prepared solution of $NaBH_4$ was added dropwise to the Cu salt solution with a $NaBH_4$ to metal (BH_4^-/M^{2+}) ratio of 3.5 (Equation 4-3). Excess borohydride was added to accelerate the synthesis process and to ensure uniform growth of particles, and was used to provide H_2 for 1,2-DCA hydrodechlorination.

$$\boldsymbol{2Cu^{2+} + BH_4^- + 3H_2O \rightarrow 2M^0 + H_2BO_3^- + 4H^+ + 2H_2\uparrow} \qquad \text{(Equation 4-3)}$$

Washed bare particles (B-nCu_W) were prepared by removing the supernatant after the particles settled to the bottom of the synthesis vessel. The particles were then washed three times with deionized deoxygenated water. Since excess borohydride was removed during the washing step, 25 mM fresh $NaBH_4$ solution was injected directly to the reactor bottles to provide H_2 gas for the dechlorination reaction. CMC stabilized particles (C-nCu) were synthesized by mixing the CMC solution with the Cu salt solution to form a Cu^{2+}-CMC complex before the reduction step. Washed bare particles were stabilized to form C-nCu_W particles by mixing the CMC solution with the freshly synthesized B-nCu_W particles, and

then adding 25 mM fresh $NaBH_4$ solution directly to the reactor bottles. The CMC solution and deionized water used for synthesis were deoxygenated by purging with ultrapure N_2 unless otherwise mentioned. The synthesis was conducted in an anaerobic glove box maintaining an O_2-free environment by purging with Ar (95% Ar: 5% H_2).

4.3.3 Particles Characterization

Transmission Electron Microscopy (TEM) - A Philips CM10 and a FEI Titan 80–300 Cryo-in-situ TEM (Philips Export B.V. Eindhove, Netherlands) was used to determine surface morphology and size of CMC-coated nanoparticles before and after reaction. The samples were prepared in anaerobic glove box by adding a drop of freshly synthesized diluted nanoparticle suspension on 400 mesh Formvar/Carbon film grids, and then the the grids were left to dry overnight. A Hamamatsu CCD based camera system software (Advanced Microscopy Techniques, version AMTV542) was used to determine the diameters of the nanoparticles from obtained micrographs.

Scanning Electron Microscopy/Energy Dispersive X-Ray Spectroscopy (SEM/EDX) – To determine the particle size and surface morphology of bare nanoparticles, a SEM (Hitachi S-4500, 10 kV field emission with a Quartz PCI XOne SSD X-ray analyzer) was used. The samples were prepared by sprinkling solid samples onto adhesive carbon tape supported on a metallic disk. EDX was used in conjunction with SEM to determine the elemental composition of the nano metal particles by randomly selecting areas on the solid surface.

Specific Surface Area - The average particle size from the representative sets of TEM and SEM micrographs for each sample was calculated by a weighted averages method. Assuming a spherical geometry for the nanoparticles, specific surface area (a_s) was calculated using the average particle size obtained from TEM and SEM data as in equation 4-4 (Sun et al., 2006b):

$$a_s = \frac{Surface\ Area}{Mass} = \frac{\pi d^2}{\rho \frac{\pi}{6} D^3} = \frac{6}{\rho D} \qquad \text{(Equation 4-4)}$$

where D is the average diameter of particles and ρ is the density of the Cu particles (Cu: 8.92 g cm^{-3}).

X-Ray Diffraction (XRD) – A Rigaku RPT 300 RC diffractometer (Cu Kα radiation, step size 0.02°, 2θ rage 10-90°) was used to determine bare nCu particles product phase composition. The identification of the phases was carried out by correlating results with the Joint Committee on Powder Diffraction Standards (JCPDS) database and published literature.

X-ray Photoelectron Spectroscopy (XPS) - XPS was performed to analyze the chemical composition and oxidation state of bare nCu surface. A Kratos Axis Ultra spectrometer using a monochromatic Al K(alpha) source (15mA, 14kV) was used to carry out XPS analysis. XPS can detect all elements except hydrogen and helium, probing the surface of the sample to a depth of 5-7 nanometres, and has detection limits ranging from 0.1 to 0.5 atomic percent depending on the element. The instrument work function was calibrated to give a binding energy (BE) of 83.96 eV for the Au 4f7/2 line for metallic gold and the spectrometer dispersion was adjusted to give a BE of 932.62 eV for the Cu 2p3/2 line of metallic copper. The Kratos charge neutralizer system was used on all specimens. Survey scan analyses were carried out with an analysis area of 300 x 700 microns and a pass energy of 160 eV. High resolution analyses were carried out with an analysis area of 300 x 700 microns and a pass energy of 20 eV. Spectra have been charge corrected to the main line of the carbon 1s spectrum (adventitious carbon) set to 284.8 eV. Spectra were analyzed and fittings were carried out using CasaXPS software (version 2.3.14), and a literature database (Biesinger et al., 2007; Biesinger et al., 2010; Chastain et al., 1995; Wagner et al.).

Dynamic Light Scattering (DLS) - The mean hydrodynamic diameter on a number weighted average of the stabilized -nCu particles was analyzed by a 90 Plus light scattering instrument (Brookhaven Instrument Corporation, Holtsville, NY) coupled with Zeta PALS software. The zeta potential of the particles was determined from electrophoretic mobility measurements using the same aforementioned instrument coupled with Zeta Plus software incorporating the Smoluchowski method.

4.3.4 1,2-DCA Dechlorination

Batch reactivity experiments were carried out in amber glass bottles (250 mL, VWR) sealed with Teflon mininert caps and septa to minimize oxygen intrusion and create anaerobic batch reactors (40 mL solution/ 210 mL headspace). Tables 4-1 summarizes the experimental conditions and dechlorination results for each reactivity experiment. C-nCu (1 g L^{-1}) as well as C-nCu/nPd (1 g L^{-1} doped with 0.5% w/w nPd) were used to test the effectiveness of utilizing residual borohydride after particles synthesis as a H_2 source for the catalyzed dechlorination of ~35 mg L^{-1} 1,2-DCA, unless otherwise mentioned (Exp. 1-3). B-nCu_W (1 g L^{-1}) coupled with 25 mM borohydride was used to test the effect of washing nCu particles (Exp. 4 and 5), 1,2-DCA dosage (40, 65, and 225 mg L^{-1}, Exp.5, 7, and 8), as well as anions, humic acid, and dissolved oxygen on the catalyzed dechlorination reaction kinetics (Exp. 9-19). C-nCu_W coupled with 25 mM borohydride was used to test the effect of a coating on the catalytic efficiency in reducing 1,2-DCA (Exp. 6).

Concentrations of anions and humic acid used in the experiments were based on those observed at contaminated GW sites and previous studies (Angeles-Wedler et al., 2009; Davie et al., 2008; Doong and Lai, 2005; Heck et al., 2009; Kopinke et al., 2010; Liu and Lo, 2011a; Lowry and Reinhard, 2000; Yuan et al., 2013). For example, the average concentrations of anions and humic acid at field sites and from previous studies are: ~1500 mg L^{-1} for Cl^-, ~0.4 mg L^{-1} for sulfides, and ~20 mg L^{-1} for humic acid. To study the effect of dissolved oxygen in water on reactivity, deionized water was not purged with N_2 prior to use in reactivity experiments.

All experiments, including controls (only 1,2-DCA and deionized water), were conducted in duplicates, with error bars on dechlorination profiles representing the standard deviation between the two duplicates. The reactor bottles were shaken using an arm wrist action shaker (Model 75, Burrell Inc.) at room temperature.

Table 4-1: Experimental conditions of dechlorination experiments and the summarized results.

Exp.[a] No.	Metal (1 g L^{-1})	GW solute (mg L^{-1})	CMC (W/V) %	1,2-DCA (mg L^{-1})	Degradation % (7 hours)	k_{obs} (h^{-1})	k_{sa} (L m^{-2} d^{-1})
1	C-nCu	-	0.5	34	3	-	-
2[b]	C-nCu/nPd	-	0.5	34	6	-	-
3[c]	C-nCu/nPd	-	0.5	34	31.7, 81	-	-
4	B-nCu_W	-	-	40	92.7	0.345	0.3
5	B-nCu	-	-	40	44	0.158	0.1
6[d]	C-nCu_W	-	0.5	40	73.1	0.281	ND
7	B-nCu_W	-	-	65	92.2	0.340	0.3
8	B-nCu_W	-	-	225	90.6	0.347	0.3
9	B-nCu_W	-	-	45	93	0.345	0.3
10	B-nCu_W	Chlorides, 1000	-	45	77.3	0.206	0.2
11	B-nCu_W	Chlorides, 1500	-	45	75.7	0.191	0.2
12[e]	B-nCu_W	Chlorides, 2000	-	45	55.7, 94.6	0.11	0.1
13	B-nCu_W	Sulfides, 0.2	-	45	91.8	0.359	0.3
14	B-nCu_W	Sulfides, 0.4	-	45	70.5	0.158	0.1
15[e]	B-nCu_W	Sulfides, 4	-	45	43.1, 82.1	0.11	0.1
16	B-nCu_W	Humic Acid, 10	-	45	85	0.225	0.2
17	B-nCu_W	Humic Acid, 20	-	40	74.9	0.188	0.2
18[e]	B-nCu_W	Humic Acid, 30	-	45	65.3, 94	0.145	0.1
19	B-nCu_W	Dissolved Oxygen, 4.93	-	45	87	0.287	0.3

[a] 25 mM borohydride was initially spiked in reactor bottles of all experiments, except experiments number 1 and 2. Experiments from 3-18 had a chlorides mass balance > 90%, except experiment 6 where chlorides analysis was not conducted.

[b] nPd = 0.5% w/w of nCu.

[c] C-nCu/nPd (0.5 g L^{-1} doped with 0.5% nPd) coupled with two sequential injections of 25 mM borohydride. Total degradation after each injection is shown.

[d] no TEM imaging was carried out for C-nCu_W, and therefore k_{sa} was not calculated.

[e] an additional injection of 25 mM borohydride was spiked into reactor bottles after reaction ceased. Total degradation after each injection is shown.

4.3.5 Analytical Methods

Hexane extracts from 250 µL liquid sample mixed with 1 mL hexane were analyzed for 1,2-DCA using Agilent 7890 Gas Chromatograph (GC) equipped with a DB-624 capillary column (75 m x 0.45 mm x 2.55 µm) and an Electron Capture Detector (ECD). The gas carrier used was nitrogen at a flow rate of 10 mL min^{-1}. The oven temperature was set at 35 °C with a ramp for 12 min then 5 °C/min to 60 °C for 1 min and 17 °C/min to 200 °C for 5 min. Manual injection of 250 µL headspace samples directly withdrawn from the headspace of the batch bottles were used to analyze concentrations of chloroethane (CE), ethane, and ethene with an Agilent 7890 GC equipped with a GS-Gas Pro Column (3.0m x 320 µm), and Flame Ionization Detector (FID). The oven temperature was set at 35 °C for 5 min, then 10 °C/min to 220 °C held for 7 min with He as the gas carrier.

Chloride concentrations for bare particle experiments were analyzed on a Waters 717 Plus Auto-sampler High Performance Liquid Chromatograph (HPLC) equipped with a conductivity detector and an IC PakTM anion column (4.6m x 50 mm). 100 µL of sample was injected in an eluent mixture (12% acetonitrile in deionized water) with a flow rate of 1.2 mL min^{-1} at a pressure of 595 psi.

A Yellow Spring Instrument (YSI) probe Model number 85 was used to measure the dissolved oxygen. concentration in N_2 purged deionized water and unpurged deionized water.

4.4 Results and Discussion

4.4.1 Particles Characterization

The surface properties of the metals affect their catalytic characteristics, and consequently the dechlorination efficiency. As such the nCu particles was characterized using TEM, SEM-EDX, XRD, XPS and DLS.

TEM – The TEM image of unreacted C-nCu shows individual spherical nano sized particles (9.07 ± 2.36 nm) assembled in chains, forming some aggregates (Figure 4-1A). After dechlorination, most of the particles turned into larger chunks/aggregates with no particular shape and size. This could be due to oxidation or phase transformation of C-nCu particles during reaction. The inset to Figure 4-1B shows that there were still some individual spherical particles present after dechlorination.

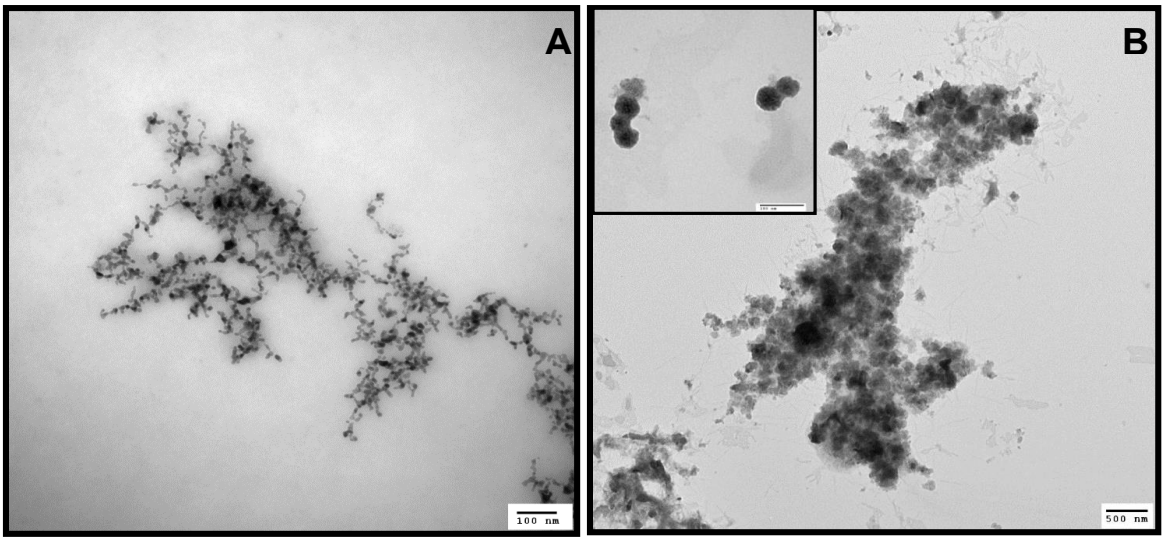

Figure 4-1: TEM images of (A) unreacted and (B) reacted C-nCu particles. Inset picture in (B) shows high resolution image of reacted C-nCu particles.

SEM/EDX - Figure 4-2A-B show SEM images of unreacted B-nCu and B-nCu$_W$ particles. The particles were found to agglomerate rapidly in the absence of the stabilizer as reported by (Huang et al. 2011). The particles were quasi spherical, with uniform size and shape, and assembled in chains forming tightly packed aggregates. The particle diameters ranged between 16.7-30.2 nm. Based on TEM and SEM derived nanoparticle diameter and Equation 4-4, the average specific surface areas for unreacted C-nCu, B-nCu, and B-nCu$_W$ particles were calculated as 74.16, 29.16, and 27.51 $m^2 g^{-1}$, respectively.

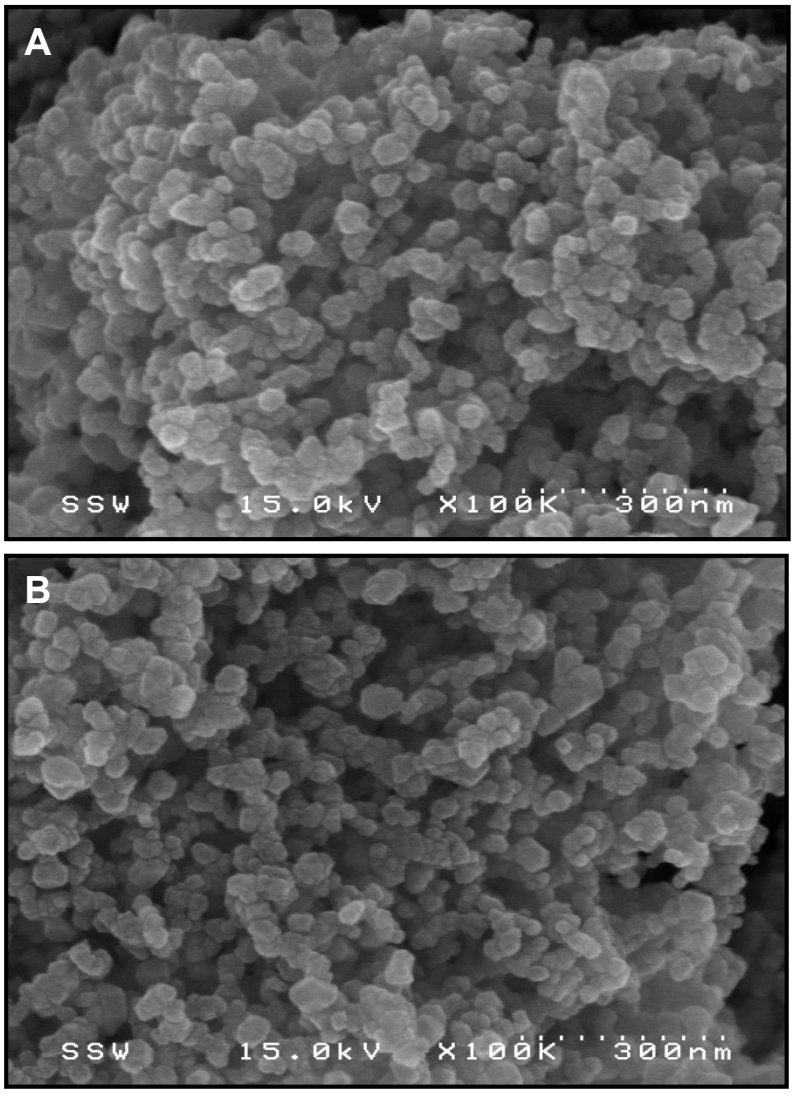

Figure 4-2: SEM images of unreacted (A) B-nCu and (B) B-nCu$_W$ particles.

The EDX spectra showed Cu as the major surface species accounting for 91.2 and 94.7% of the mass of B-nCu and B-nCu$_W$ nanoparticles, respectively (Figure 4-3, Table 4-2). Small amounts of oxygen can be attributed to the presence of copper oxide (Raut et al., 2016). Trace amounts of sulfur (0.5%) in B-nCu came from the Cu precursor (cupric sulfate). Washing the particles resulted in removal of sulfur in B-nCu$_W$ particles.

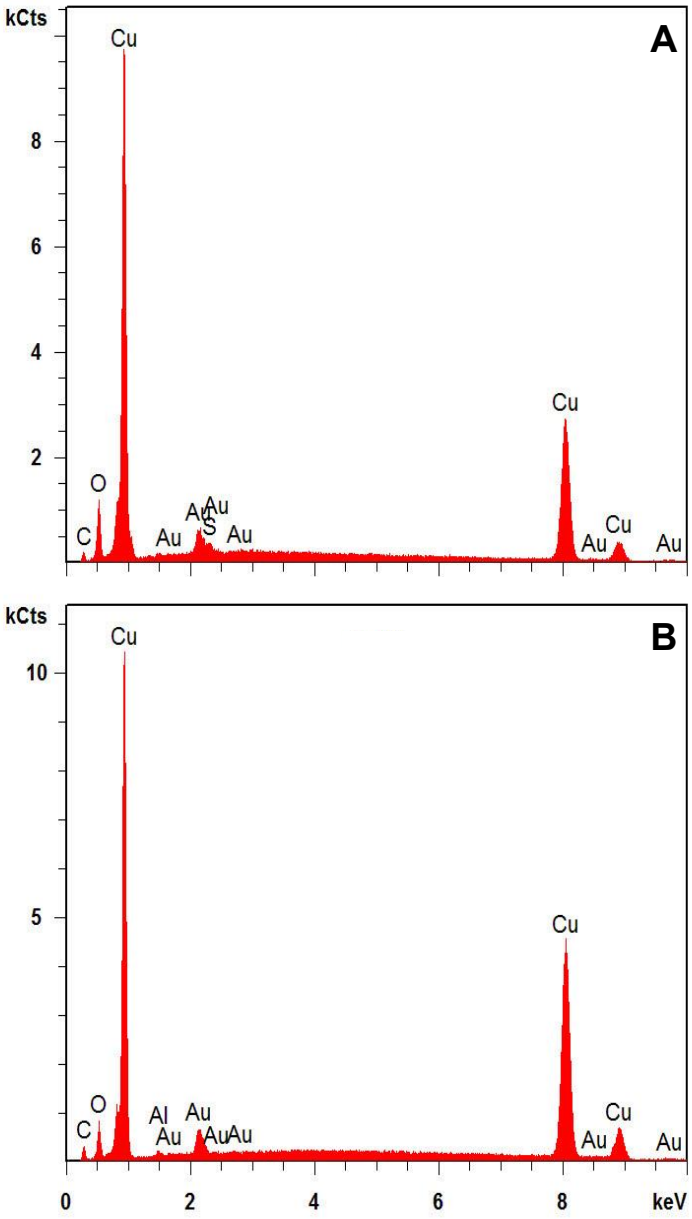

Figure 4-3: EDX spectra of unreacted (A) B-nCu and (B) B-nCu$_W$ particles.

Table 4-2: EDX weight percent analysis of B-nCu and B-nCu$_W$ particles.

Sample	C	O	S	Cu
B-nCu	3.1	5.2	0.5	91.2
B-nCu$_W$	3.4	2.0	-	94.7

XRD - Diffractograms indicate the presence of characteristic peaks of Cu metal for both B-nCu and B-nCu$_W$ particles (Figure 4-4). The peaks for Cu^0 matched with the Joint Committee on Powder Diffraction Standards database (JCPDS 04-0836) and published literature values (Table 8-1, Appendix B) confirming the formation of metallic Cu (Devaraj et al., 2016; Diaz-Droguett et al., 2011; Huang et al., 2011; Mondal et al., 2015). Cuprous oxide (Cu_2O) was also present in both samples, with peaks consistent with JCPDS 05-0667 and literature values (Tabe 8-1, Appendix B) (Devaraj et al., 2016; Diaz-Droguett et al., 2011; Huang et al., 2011). It is noteworthy that the intensities of the peaks for the B-nCu and B-nCu$_W$ nanoparticles were different which may indicate different ratios of Cu species in the two samples.

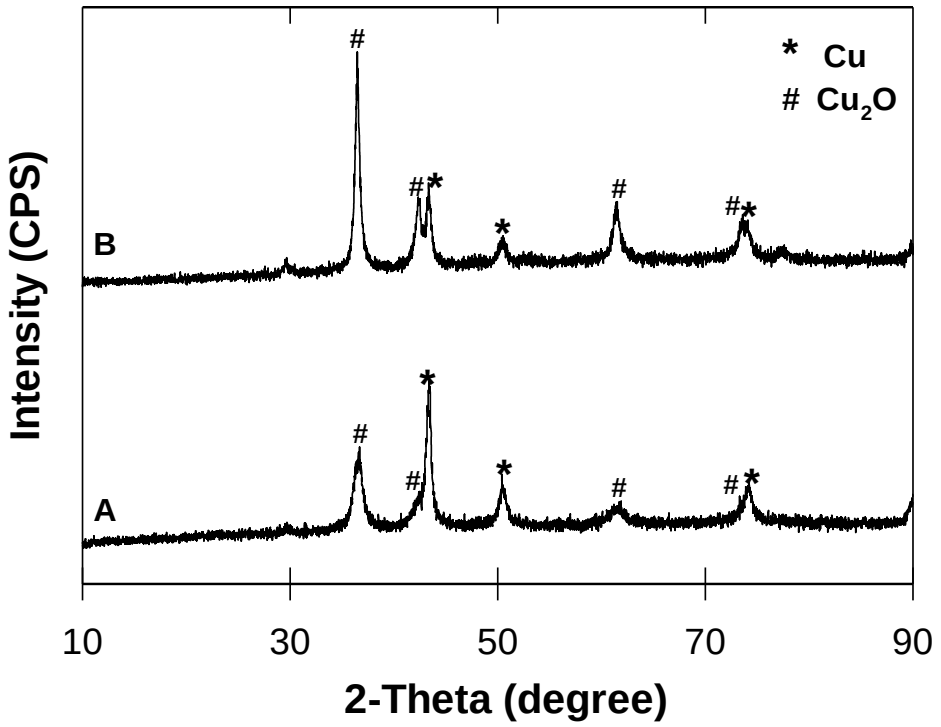

Figure 4-4: XRD patterns of unreacted (A) B-nCu and (B) B-nCu$_W$ particles.

XPS – XPS analysis was conducted to further confirm the formation of metallic Cu in both B-nCu and B-nCu$_W$ particles, and determine their elemental composition and valence state. The wide-scan survey revealed that the surface was mainly composed of copper, oxygen, carbon, and boron (Figure 4-5, Table 4-3). Carbon likely originated from adventitious carbon contamination (Wielant et al., 2007). Boron came from sodium borohydride used as the reductant for nCu synthesis. The presence of oxygen suggests the formation of some oxidized species of Cu.

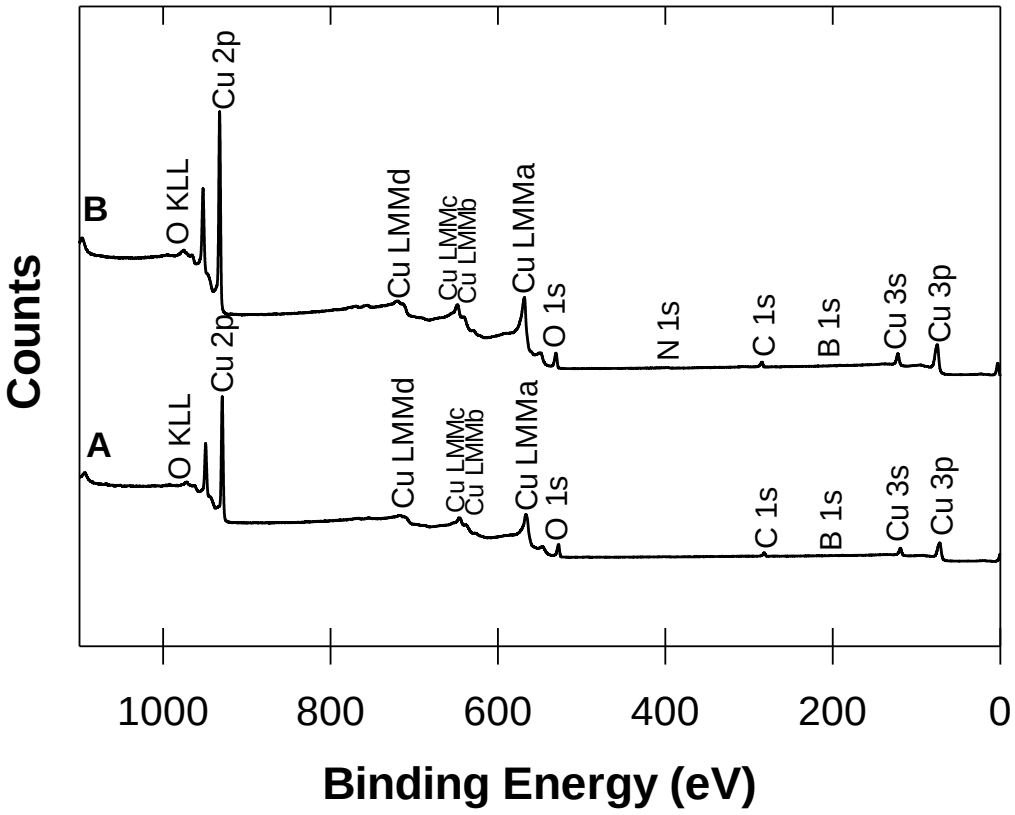

Figure 4-5: Wide-scan XPS survey spectra of unreacted (A) B-nCu and (B) B-nCu$_W$ particles.

Table 4-3: Surface composition (atomic %) of nCu particles determined by XPS.

Nanoparticle/Element	Cu	O	C	B	N
B-nCu	45.5	25.5	25.1	4	-
B-nCu$_W$	51.2	22.2	22.5	3.8	0.4

As depicted from the high resolution spectra of Cu 2p (Figure 4-6A, 4-7A), the binding energy values of Cu^+ and Cu^0 are almost identical, differing by less than 0.1 eV. Thus, it is not possible to distinguish between these two species on the catalyst surface on the basis of the Cu 2p level. The Cu^+ and Cu^0 species can be distinguished through the X-ray induced Auger (XAES) Cu LMM spectra (Devaraj et al., 2016; Marquez et al., 2001; Pan et al., 2013; Park et al., 2006; Yao et al., 2010; Zhang et al., 2013). The Cu LMM high resolution core-level spectra for B-nCu and B-nCu$_W$ and associated fitted curves are shown in Figures 4-6B and 4-7B, respectively. Both B-nCu and B-nCu$_W$ show the main peaks for Cu^0 at ~575.7, 572, 570, 568.5, 568, 567, and 565 eV, respectively (Marquez et al., 2001; Park et al., 2006). The spectra also revealed the presence of oxidized Cu in the form of $Cu(OH)_2$ at ~575 and 570 eV, and Cu_2O at ~ 574, 569.9, and 569 eV (Marquez et al., 2001; Park et al., 2006). The ratios of Cu^{n+}/Cu^0 were found to be 1.7 and 0.79 for B-nCu and B-nCu$_W$ particles, respectively (Table 8-2, Appendix B). This was calculated by comparing the intensities of the components of high resolution spectra of Cu LMM core-level (Zhang et al., 2013). Cu^{n+} comprised of both Cu^+ and Cu^{2+} species, with Cu^0, Cu^+, and Cu^{2+} making up 37 %, 44 %, and 19 %, of the B-nCu particles, respectively, and 56 %, 24%, and 20% the for B-nCu$_W$ particles, respectively. This suggests that rinsing the particles likely resulted in removal of some surface species increasing the proportion of Cu^0 sites responsible for the catalytic activity (Luebke et al., 2002).

The high resolution spectra for O1s is split into three peaks located at ~532.4, 531.5, and 530.4 eV, which are attributed to boron trioxide, surface-adsorbed oxygen species (O_2 or H_2O) and the lattice oxygen of Cu_2O, respectively (Figure 8-1, Table 8-3, Appendix B) (Pan et al., 2013; Yao et al., 2010). Given that B-nCu and B-nCu$_W$ particles have similar spectra this indicates that both particles have the same adsorbed oxygen species on their surfaces. Since the B-nCu particle surface contained a higher percent of boron trioxide than

B-nCu$_W$ it is assumed that washing the nCu particles resulted in removal of some of the boron trioxide from the B-nCu$_W$ surface.

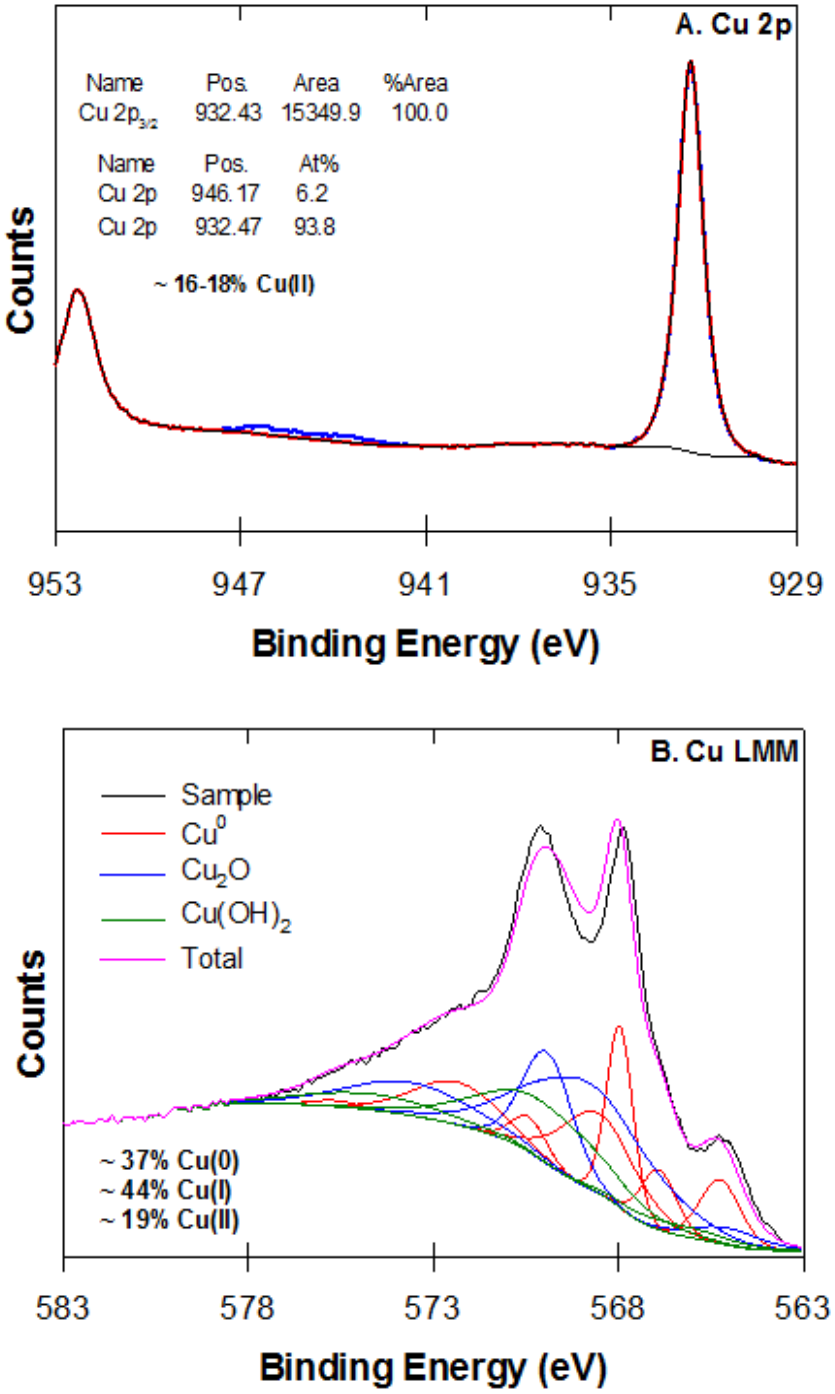

Figure 4-6: High resolution XPS for the Cu 2p and Cu LMM regions for unreacted B-nCu particles.

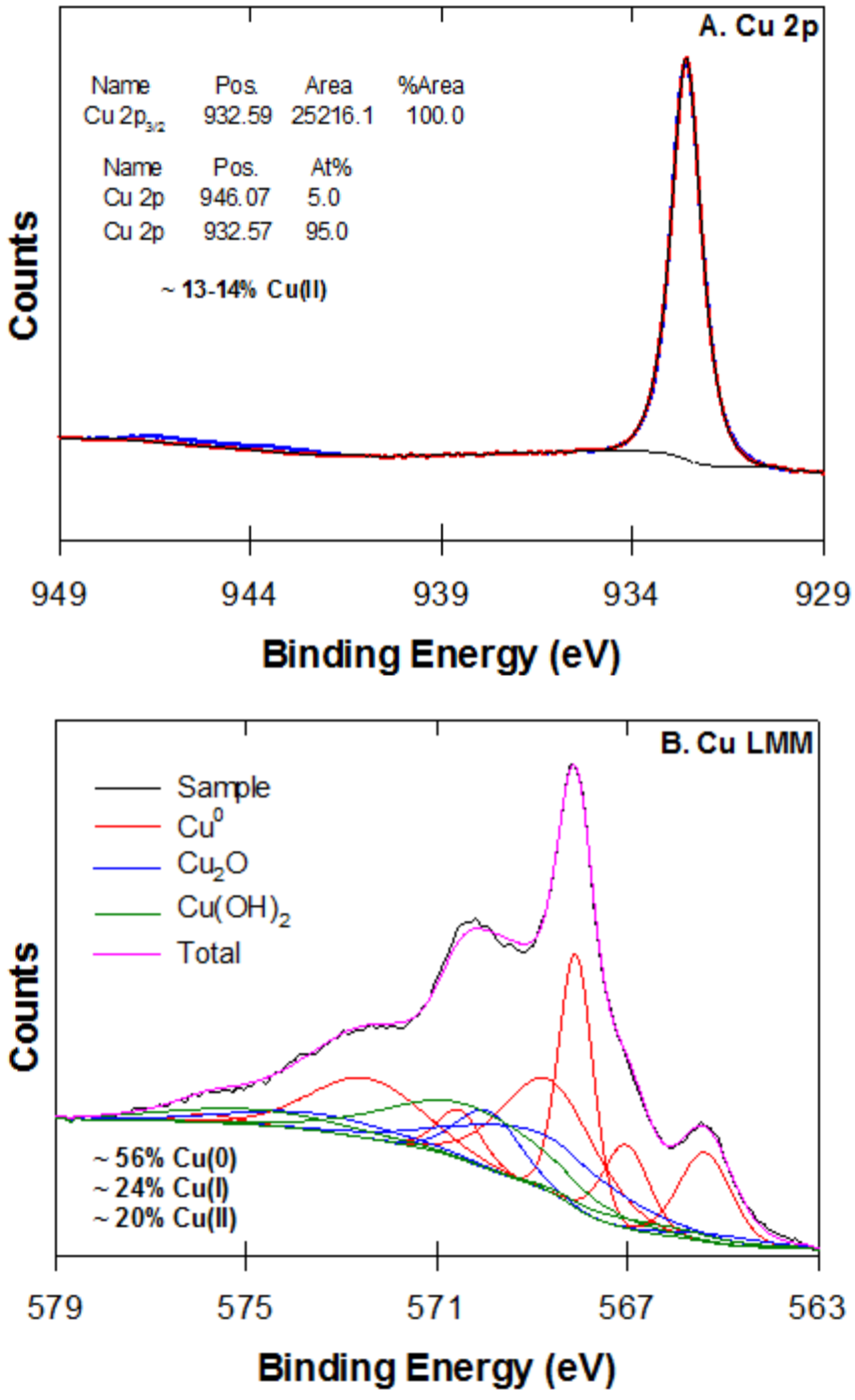

Figure 4-7: High resolution XPS for the Cu 2p and Cu LMM regions for unreacted B-nCuw particles.

Table 8-4 (Appendix B) summarizes some properties for selected experiments. All nanoparticle suspensions turned greenish at the end of the reactivity experiments indicating nCu oxidation. The oxidation reduction potential (ORP) ranged between -751 to -880 mV, which differs from the literature study that suggested a minimum ORP of -1100 mV for nCu coupled with borohydride to be able to catalytically reduce 1,2-DCA (Huang et al., 2011). All treatments solutions were still basic at the end of the reactivity experiments (pH: 10.45-10.83), presumbly due to borohydride forming basic solutions (Kong et al., 1999). CMC stabilized particles (C-nCu, and C-nCu/nPd) were negatively charged which yield unfavaorable interactions with subsruface soils as aquifer soil particles are usually negatively charged (Yaron et al., 2012). C-nCu particle hydrodynamic diameter was larger size than that measured by TEM imaging (65.5-145.5) nm. This is because TEM measures only the metallic core, while DLS measures the hydrodynamic diameter of both particle and the CMC layer (Lim et al., 2013; Liu et al., 2008).

4.4.2 1,2-DCA Dechlorination

C-nCu (1 g L^{-1}) particles were tested for catalyzing liquid phase dechlorination of 1,2-DCA (~35 mg L^{-1}), at room temperature utilizing only H_2 generated from excess $NaBH_4$ present in the system after particle synthesis (Exp. 1, Table 4-1). As depicted in Figure 4-8, the treatment failed to break down 1,2-DCA, with less than 5% removal. It is suggested that since Cu is a poor hydrogenation catalyst it was not able to retain/adsorb H_2 gas formed during synthesis so the H_2 gas escaped from solution as the synthesis process is conducted in open vessels (Lambert et al., 2005; Luebke et al., 2002; Meshesha et al., 2013; Śrębowata et al., 2011; Twigg and Spencer, 2001; Vadlamannati et al., 1999; Xie et al., 2008). To test for this hypothesis, 25 mM of borohydride was spiked into the reactor bottles, resulting in 27% removal of 1,2-DCA in the first few hours before the reaction ceased, supporting the aforementioned hypothesis.

Ethane and chloroethane were the two main byproducts, making up 55.2% and 43.4%, respectively of the total byproducts, along with trace amounts of ethene, acetylene, propane, butane, and n-butane, yielding a carbon mass balance of ~80%. This suggests that 1,2-DCA was degraded through two successive hydrogenolysis steps (Equation 4-5 & 4-6), and dichloroloelimination was a minor pathway (Equation 4-7) (Huang et al., 2011).

Nonetheless, formation of ethane through hydrogenation of ethene cannot be ruled out, suggesting that both hydrogenologysis and dichloroelimination were simultaneous dechlorination pathways. Previous studies have suggested that transition metals (e.g. Cu, Fe) holds to chlorine atoms only and do not hold the rest of the molecule (CH_2–CH_2) firmly enough, thus releasing ethene (dichloroelimination pathway) which is later hydrogenated to ethane (Arnold and Roberts, 2000b; Lambert et al., 2005). As for the other C_3 and C_4 byproducts, aqueous phase studies indicate that carbon−carbon coupling can also occur during hydrodechlorination reactions through a radical mechanism (Lowry and Reinhard, 1999).

$$\boldsymbol{C_2H_4Cl_2 + 2e^- + H^+ \rightarrow C_2H_5 + Cl^-} \quad \text{(Equation 4-5)}$$

$$\boldsymbol{C_2H_5Cl + 2e^- + H^+ \rightarrow C_2H_6 + Cl^-} \quad \text{(Equation 4-6)}$$

$$\boldsymbol{C_2H_4Cl_2 + 2e^- \rightarrow C_2H_4 + 2Cl^-} \quad \text{(Equation 4-7)}$$

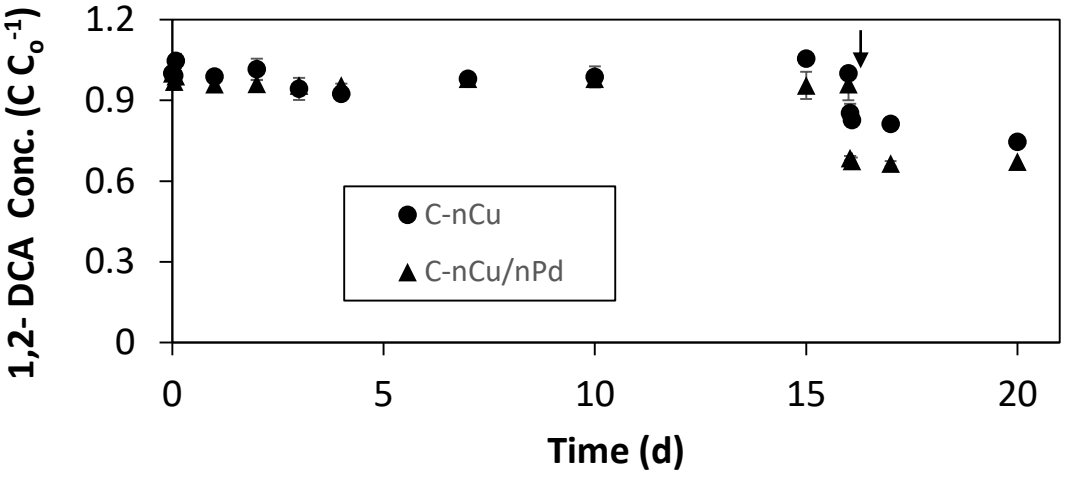

Figure 4-8: Dechlorination profiles of 1,2-DCA (34 mg L^{-1}) catalyzed by C-nCu (1 g L^{-1}) and C-nCu/nPd (1 g L^{-1} doped with 0.5% w/w nPd) (Exp. 1 & 2, Table 4-1). The arrow indicates spiking the reactors with 25 mM $NaBH_4$.

Interestingly, even when C-nCu particles were doped with nPd particles (0.5 w/w%) to help retain H_2 gas formed during the synthesis within the slurry (as observed earlier by nPd particles in the previous chapter), no appreciable dechlorination was observed without the addition of borohydride (Figure 4-8), likely due to the low nPd loading (Exp. 2). Sequential injections of 25 mM borohydride were able to boost the catalytic dechlorination reaction and a removal of >80% 1,2-DCA could be achieved (Exp.3, Table 4-1, Figure 8-2, Appendix B).

The efficiency of C-nCu particles in catalyzing the dechlorination of 1,2-DCA is much lower than that reported by (Huang et al., 2011). In that study, >80% removal of 1,2-DCA (30 mg L^{-1}) could be achieved in less than 8 hours, by coupling nCu (1 g L^{-1}) particles with 25 mM borohydride spiked in to reactor bottles. However, in that study the nCu particles were not stabilized and were rinsed with deionized water (after removal of the synthesis supernatant and residual borohydride) prior to spiking fresh borohydride. This suggests that nCu synthesis parameters (washing and stabilizing) affects its catalytic activity. Therefore, the effect of nCu synthesis parameters will be studied in the next section.

4.4.3 Effect of Cu Synthesis Parameters

Treatments of 1 g L^{-1} nCu particles coupled with 25 mM borohydride spiked directly into reactor bottles (as the H_2 source) were tested for the reductive dechlorination of 40 mg L^{-1} 1,2-DCA. Figure 4-9 shows the effect of rinsing nCu particles with deionized water (B-nCu_W versus B-nCu), as well as the effect of coating nCu_W particles (C-nCu_W versus B-nCu_W) on the dechlorination of 1,2-DCA (Exp. 4, 5, & 6, Table 4-1).

Effect of washing nCu particles - Rinsing nCu particles with deionized water significantly enhanced Cu catalytic activity in reducing 1,2-DCA, with more than 92 % removal of 1,2-DCA achieved on B-nCu_W compared to only 44% on B-nCu particles. The difference in the catalytic activity is proposed to be due to the rinsing action that washed off surface adsorbed elements (e.g. boron, sulfur, oxygen) which may have blocked reactive sites or oxidized them during the synthesis of the nanoparticles. EDX analysis (Table 4-2) showed the presence of sulfur (0.2 % of the weight) on the surface of B-nCu particles (produced from the precursor, cupric sulfate), that were not present in the surface of B-nCu_W particles.

Additionally, XPS analysis (Table 4-3) also revealed a higher atomic percentage of boron and oxygen at the surface of B-nCu particles than B-nCu$_W$ particles. In addition, XPS analysis also revealed that the atomic % of reduced Cu sites (Cu^0) - responsible for H_2 activation - in the B-nCu$_W$ particles is 1.5 times that of B-nCu particles (Table 8-2, Appendix B). Finally, B-nCu particles surface contained a higher % of boron trioxide than B-nCu$_W$ (Table 8-3, Appendix B). This may suggest that nCu particles are very sensitive towards elements present in the aqueous slurry during their synthesis process. Therefore, it is recommended to explore alternative nCu synthesis methods where the presence of problematic elements during synthesis is minimal. (i.e. radiation methods & sonochemical reduction).

Effect of Coating nCu$_W$ Particles - Coating B-nCu$_W$ particles with 0.5% (Wt./V) CMC negatively affected the dechlorination efficiency by 21% (Figure 4-9, Table 4-1). Previous studies reported that coatings may limit the adsorption of COCs by blocking reactive sites on the nanoparticle surface (Phenrat et al., 2009).

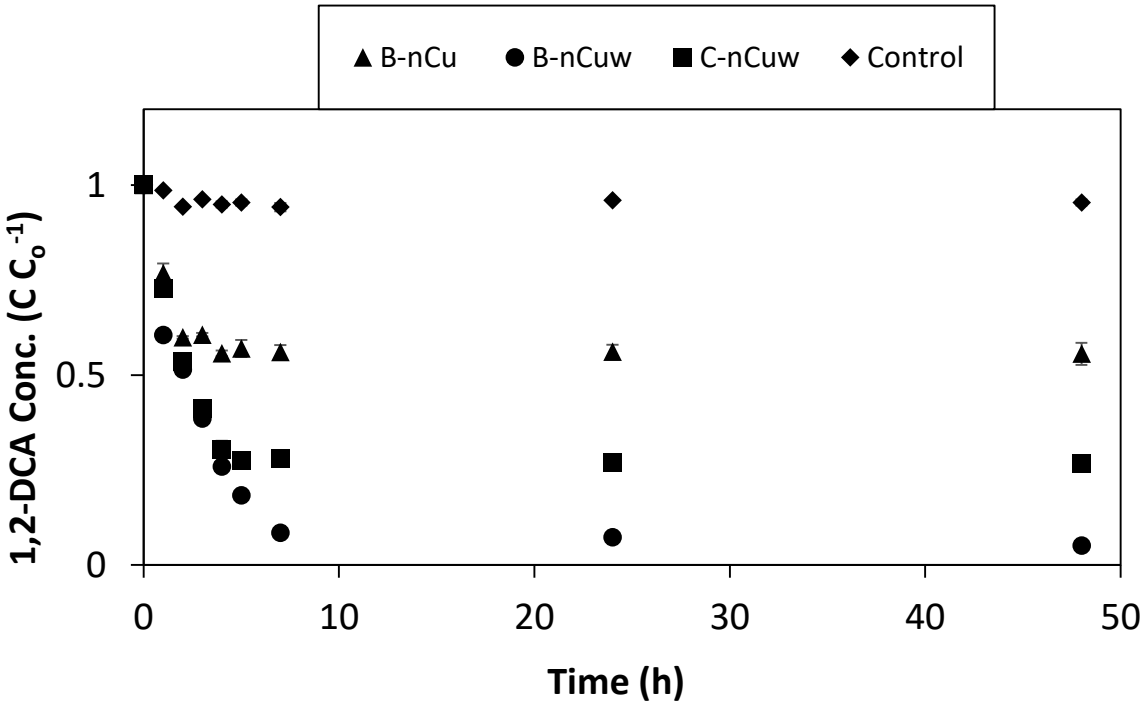

Figure 4-9: Effect of nCu (1 g L^{-1}) synthesis parameters (CMC coating & washing) on 1,2-DCA (40 mg L^{-1}) dechlorination (Exp. 4, 5, & 6).

It is worth mentioning that reductive dechlorination catalyzed by nCu_W yielded ethane as the main byproduct, with only trace amounts of ethene. Based on these results, it can be concluded that the catalytic activity of B-nCu_W is higher than the other nCu types investigated in this study. Thus, B-nCu_W particles are investigated further with regards to dechlorination reaction kinetics, as well as the effect of GW solutes on the catalytic activity.

4.4.4 Reaction Kinetics and Effect of 1,2-DCA Concentration

Reaction Kinetics- The dechlorination kinetics of 1,2-DCA catalyzed by B-nCu, B-nCu_W, and C-nCu_W (Exp. 4, 5, & 6), were found to follow a pseudo-first-order kinetic model (Equation 4-8, Figure 8-3, Appendix B), consistent with previous studies on liquid-phase catalyzed dechlorination (Davie et al., 2008; Huang et al., 2011; Mackenzie et al., 2006),

$$-\frac{d[1,2-DCA]}{dt} = k_{obs}[1,2-DCA] = k_{SA}a_s[1,2-DCA] \qquad \text{(Equation 4-8)}$$

In Equation (4-8), *[1,2-DCA]* is the concentration of 1,2-DCA during reaction (mg L^{-1}), k_{obs} is the rate constant (d^{-1}), k_{SA} is the surface-area-normalized rate constant (L m^{-2} d^{-1}), and a_s is the specific surface area of nano metal (m^2 g^{-1}). Linearization fittings are shown in Figure 8-2 in Appendix B. The k_{obs} values for 1,2-DCA reduction catalyzed by B- nCu_W, B-nCu, C-nCu_W were: 0.345, 0.158, and 0.281 h^{-1}, respectively, and the k_{sa} for B-nCu_W, and B-nCu were 0.3, and 0.1 L m^{-2} d^{-1}, respectively (Exp. 4, 5, & 6).

Effect of Initial 1,2-DCA Concentration – First-order kinetics imply that disappearance rates increase linearly with initial substrate concentration, however deviation from pseudo first order reaction rate kinetics may occur at elevated contaminant concentrations due to surface saturation (Johnson et al., 1998). The effect of initial 1,2-DCA concentration (40, 65, and 225 mg L^{-1}) on the dechlorination profile and kinetics catalyzed by B-nCu_W (1 g L^{-1}) coupled with 25 mM borohydride spiked directly into reactor bottles is shown in Figure 4-10 (Exp. 4, 7 & 8, Table 4-1). Pseudo-first-order kinetic model fit the degradation data well for all concentrations (Figure 8-4, Appendix B), with invariant reaction rate constant as shown in Figure 4-11. This suggests that surface saturation/coverage was not reached,

and that the reaction is not limited by surface-reaction, but rather by adsorption of 1,2-DCA (Liu et al., 2007b; Song and Carraway, 2005b).

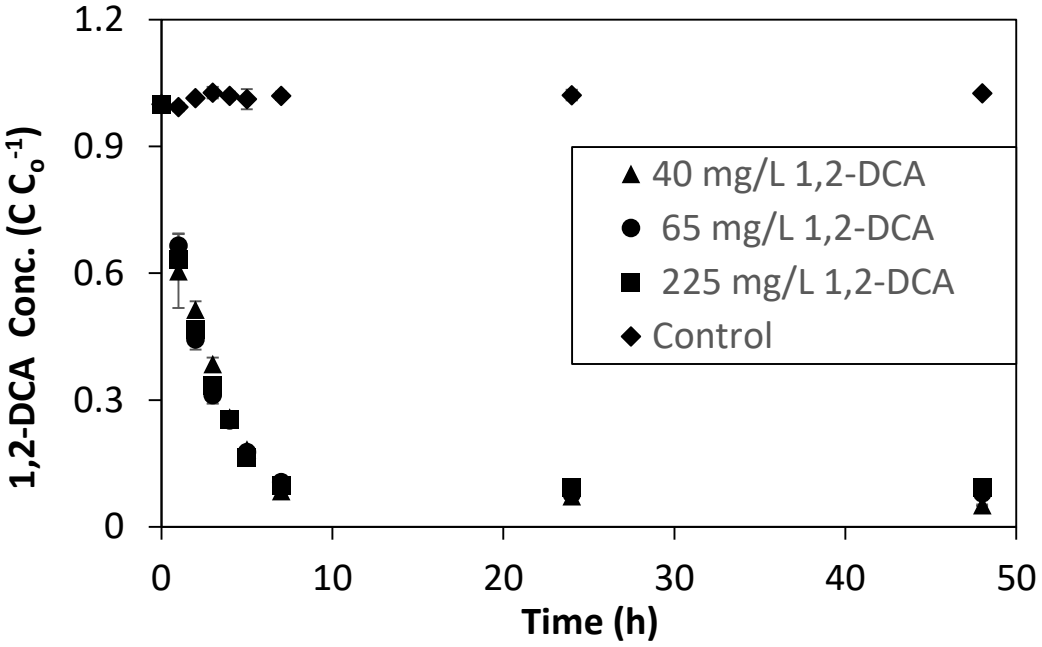

Figure 4-10: Dechlorination profiles of 40, 65, and 225 mg L^{-1} 1,2-DCA catalyzed by B-n Cuw (1 g L^{-1}) particles coupled with 25 mM $NaBH_4$ (Exp. 4, 7, & 8). All dechlorination profiles are overlapping.

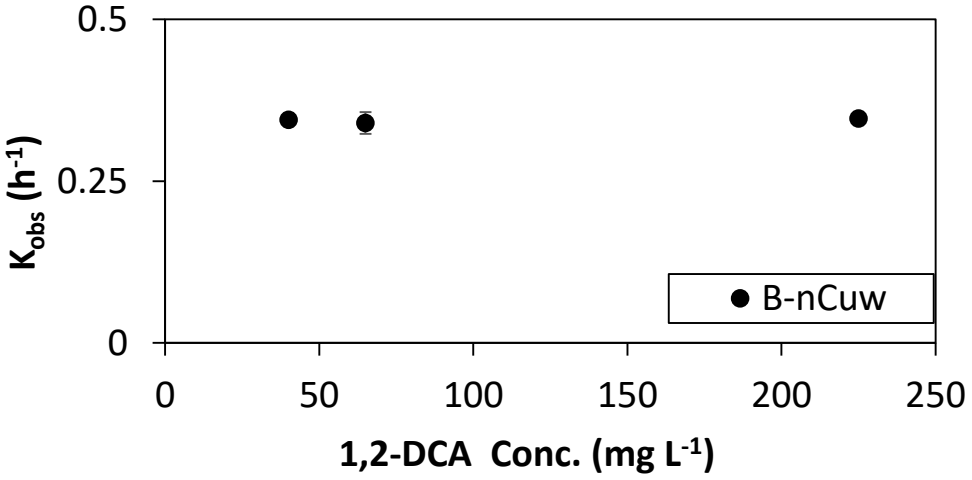

Figure 4-11: Effect of the initial concentration of 1,2-DCA concentration on the pseudo-first-order rate constant (Exp. 4, 7, & 8, Table 4-1).

4.4.5 Effect of Anions, Humic Acid, and Dissolved Oxygen

The effect of chlorides (1000, 1500, 2000 mg L^{-1}), sulfides (0.2, 0.4, 4 mg L^{-1}), humic acid (20, 20, 30 mg L^{-1}), and dissolved oxygen on dechlorination kinetics of 1,2-DCA (45 mg L^{-1}) catalyzed by B-nCu_W (1 g L^{-1}) coupled with 25 mM borohydride spiked directly into reactor bottles was evaluated (Exp. 9-19, Table 4-1). Figure 4-12 depicts the dechlorination profiles of 1,2-DCA in the presence of the different GW solutes. As shown in Figure 4-12, increasing concentrations of GW solutes generally decreased dechlorination rate and extent. Figure 4-13 presents the change in pseudo first order reaction rate constants due to the different solutes. Pseudo first order linearization fittings are shown in Figure 8-5 in Appendix B.

Effect of Chlorides - In the absence of the GW solutes, k_{obs} value was 0.345 h^{-1}, and the removal efficiency was 91.8% (Exp. 9, Table 4-1). In the presence of 1000 mg L^{-1} chlorides (Exp. 10, Table 4-1), the removal efficiency was reduced to 77.3% (Figure 4-12A) and the k_{obs} value was reduced by 40% (Figure 4-13A). Increasing chlorides concentration to 1500 or 2000 mg L^{-1} resulted in further decrease in dechlorination efficiency as well as k_{obs}. (Exp. 11 & 12, Table 4-1). This suggests partial deactivation of B-nCu_W particles by chlorides. In contrast, gas phase studies have shown that even when chlorides concentrations are below detection limits Cu can be completely deactivated (Hutchings et al., 1994; Śrębowata et al., 2011; Twigg and Spencer, 2001). Cu particles poisoning by chlorides can occur by several mechanisms. The only mechanism that can occur in the liquid phase is through reaction of Cu particles with the adsorbed chlorine atoms causing either physical blocking and/or modification of Cu sites by forming strong complexes (Twigg and Spencer, 2001). Previous XPS studies have shown that oxidized copper species is the species responsible for chemical reaction with chlorides, and that molecular adsorption (physical blocking) takes place in the absence of surface oxygen (Moroney et al., 1981). In the current study, XPS and XRD analysis confirmed formation of oxidized copper species, suggesting that chemical reaction of B-Cu_W particles with chlorides is possible.

Effect of Sulfides - As depicted in Figures 4-12B, 4-13B, 0.2 mg L^{-1} sulfides had no effect on the dechlorination rate and extent (Exp. 13, Table 4-1). However, higher concentrations

of sulfides of 0.4 mg L^{-1} and 4 mg L^{-1} reduced 1,2-DCA removal to 70.5, and 43.1%, respectively, and reduced k_{obs} by 54.2%, and 68.12%, respectively (Figure 4-13B), indicating poisoning of B-nCu_W particles (Exp. 14 & 15, Table 4-1). These results are consistent with gas phase catalyzed dechlorination studies which have suggested a maximum allowable sulfides concentration around 0.1 mg L^{-1} to prevent deactivation of Cu particles (Twigg, 1996). The deactivation of B-nCu_W particles is due to the accumulation of sulfides on the Cu surface (Twigg and Spencer, 2001). Similar to the Cu poisoning mechanism by chlorides, the accumulation of sulfides could be due to the formation of strong chemical bonds with Cu oxide sites or by physical adsorption (Moroney, Rassias and Roberts, 1981, Argyle and Bartholomew, 2015). For the chemical bonding, XPS studies indicated that sulfides easily replace chemisorbed oxygen at the Cu sites with negligible activation energies (Moroney et al., 1981). On the other hand, physical blocking would occur due to strong adsorption of sulfur atoms causing blocking of reactive sites (Argyle and Bartholomew, 2015). In the current study, both physical and chemical reaction of Cu sites with sulfides is possible as XPS and XRD analysis confirmed formation of Cu oxide species.

Effect of Humic Acid - Addition of humic acid to the treatment slurry decreased the dechlorination rate and efficiency of 1,2-DCA. Figures 4-12C and 4-13C illustrate the effect of 10-30 mg L^{-1} humic acid on the dechlorination of 1,2-DCA and the k_{obs} value, respectively (Exp. 16-18, Table 4-1). The k_{obs} values decreased by 34.5%, 45.5%, and 63.5 %, and 1,2-DCA removal efficiency also decreased to 85, 74.9, and 65.3% for humic acid concentrations of 10, 20, and 30 mg L^{-1}, respectively. Literature reports indicate that the various functional groups of humic acids can compete with contaminants for nano metals reactive surfaces and can form complexes blocking reactive sites (Balko and Tratnyek, 1998; Doong and Lai, 2005; Kim et al., 2014; Tratnyek et al., 2001). In addition, humic acid (dissolved organic matter in general) can directly coat (sorb) nanoparticles, consequently blocking reactive sites and increasing particle size, decreasing dechlorination rates (Feng et al., 2008; Giasuddin et al., 2007; Zhang et al., 2011). Previous EDX studies have shown increase in carbon concentrations in the elemental composition of nano metals upon introduction of humic acid to the system (Liu and Lo, 2011b).

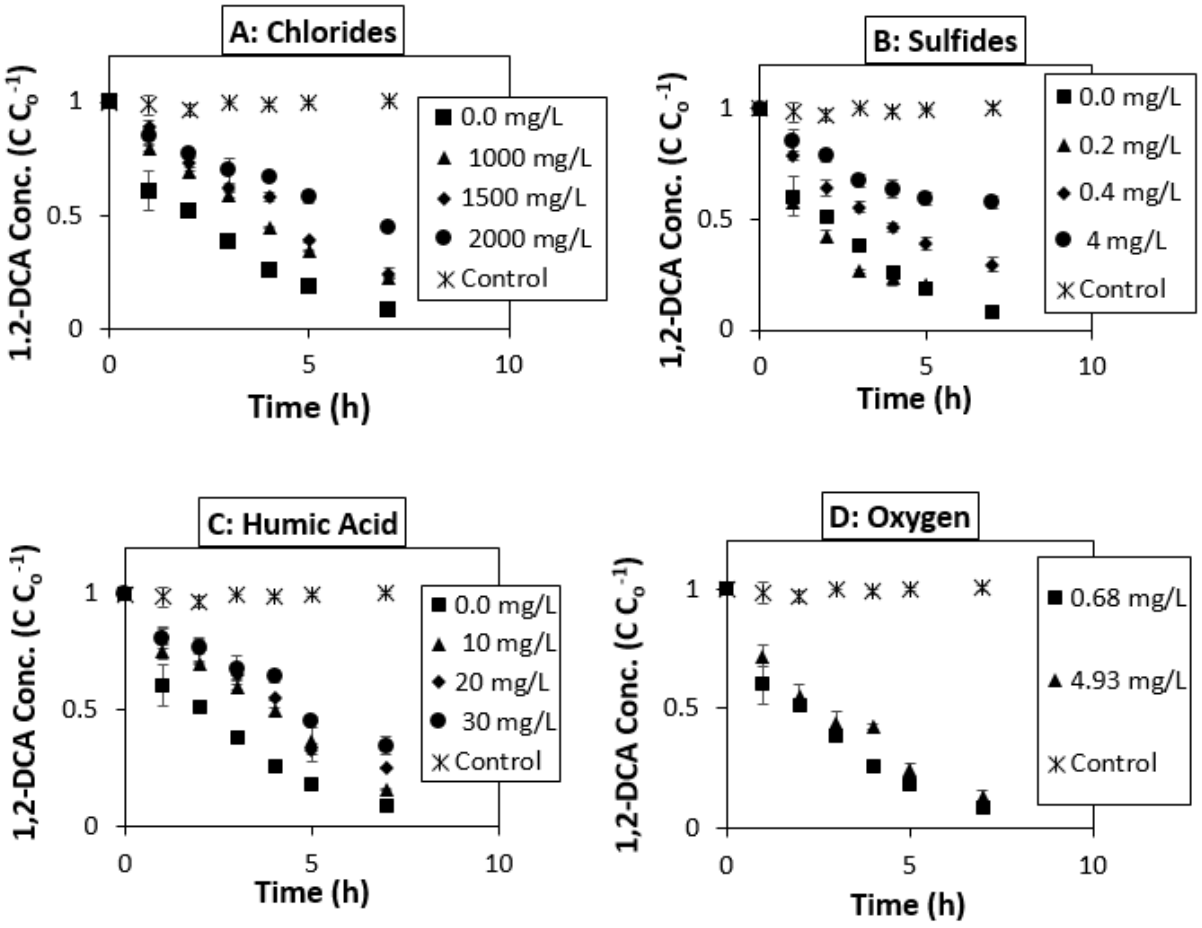

Figure 4-12: Dechlorination profile of 1,2-DCA (45 mg L^{-1}) catalyzed by B-nCuw (1 g L^{-1}) coupled with 25 mM $NaBH_4$ in the presence of: A) chlorides, B) sulfides, C) humic acid, and D) dissolved oxygen (Exp. 9-19, Table 4-1).

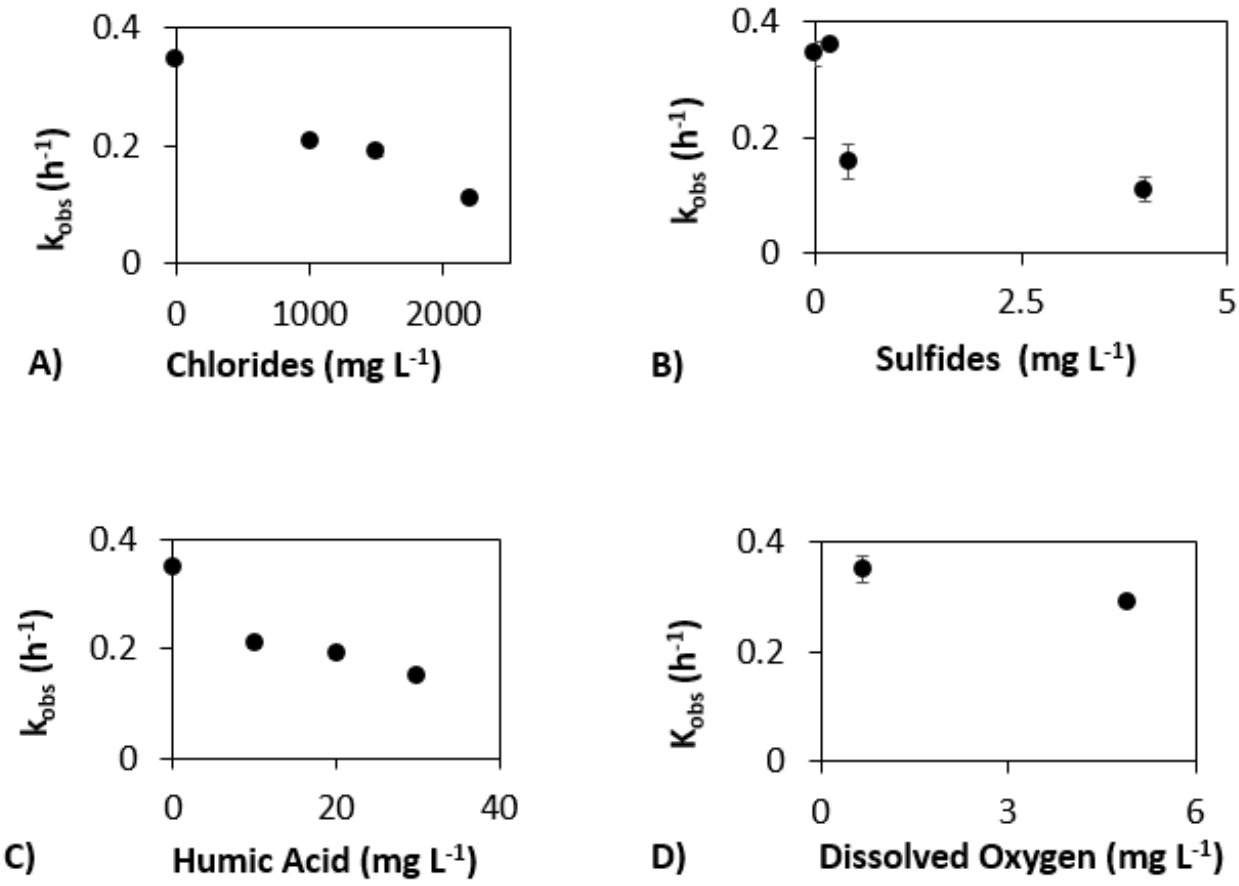

Figure 4-13: Pseudo-first-order constants (k_{obs}) changes in the presence of: a) chlorides, b) sulfides, d) humic acid, c) dissolved oxygen, in the dechlorination of 1.2-DCA (45 mg L^{-1}) catalyzed by B-nCuw (1 g L^{-1}) coupled with 25 mM $NaBH_4$ (Exp. 9-19, Table 4-1).

Effect of Dissolved Oxygen - The presence of dissolved oxygen had a relatively small effect on the efficiency of the treatment compared to the other GW solutes with a slight decrease in the k_{obs} (17%) and 1,2-DCA removal (87%) (Figures 4-12D & 4-13D, Exp. 19, Table 4-1). This is presumably due to one of two reasons, either reaction between nCu and oxygen is relatively slower than the dechlorination reaction, and/or the injected borohydride reduced oxidized sites. The aqueous oxidation of Cu is usually expressed by Equations 4-9, and 4-10 (Alsawafta et al., 2011).

$$2Cu + \frac{1}{2}O_2 + H_2O \rightarrow Cu_2O \quad \text{(Equation 4-9)}$$

$$Cu_2O + O_2 \rightarrow 2CuO \quad \text{(Equation 4-10)}$$

An additional injection of 25 mM borohydride into experiments containing 2000 mg L^{-1} chlorides, 4 mg L^{-1} sulfide, or 30 mg L^{-} Humic Acid (Figure 4-14), reactivated the catalytic dechlorination reaction in the same fashion as treatments utilizing unwashed nCu particles (Exp.3, Table 4-1), with a final 1,2-DCA removal of 94.6, 82.1, and 94%, respectively (Exp. 12, 15 & 18, Table 4-1). This implies that multiple reinjections of borohydride would compensate for the poisoned Cu sites.

The presence of oxygen, sulfides, chlorides, and humic acid did not change byproducts selectivity, with ethane still being the main byproduct along with trace amounts of ethene. This suggests that the dechlorination mechanism was not affected. This was further confirmed by the linear relationship observed between the reaction rate constant and the concentrations of the tested GW solutes (except sulfides) (Figure 4-13), suggesting that adsorption of these GW solutes was uniform and nonselective to active sites, and as a result the selectivity of the byproducts should not change (Forzatti and Lietti, 1999). However, since a complete CMB was not achieved, a change in byproduct selectivity cannot be conclusively ruled out.

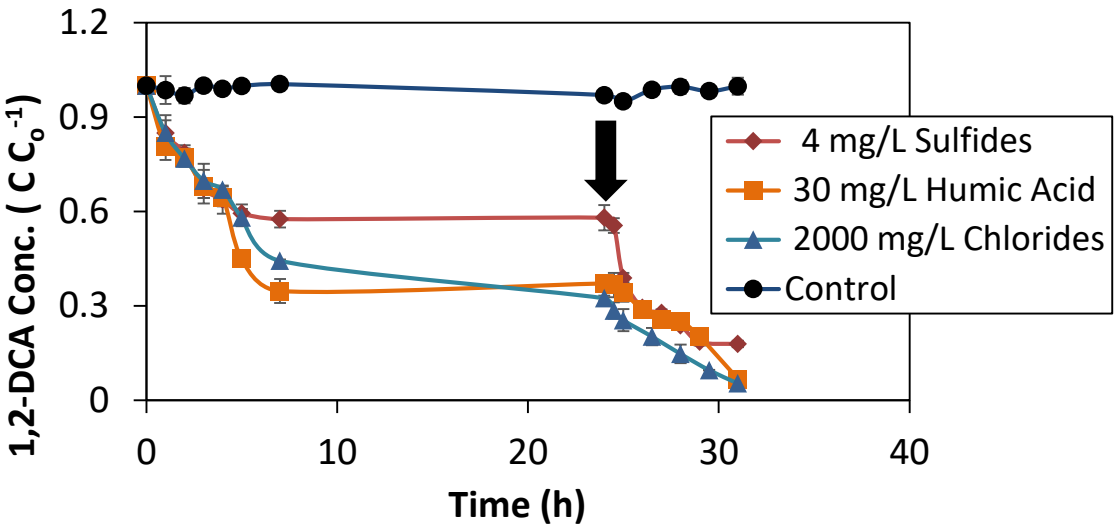

Figure 4-14: Effect of reinjecting 25 mM borohydride into treatments with lowest activities (2000 mg L^{-1} chlorides, 4 mg L^{-1} sulfides, and 30 mg L^{-1} humic acid) on the dechlorination profile of 1,2-DCA (45 mg L^{-1}) catalyzed by B-nCuw (1 g L^{-1}) coupled with 25 mM $NaBH_4$. The arrow indicates injection of 25 mM borohydride.

As indicated in Table 8-4 (Appendix B), the initial and final pH and ORP of experiments with and without GW solutes were similar. This suggests that pH and ORP are poor indicators of treatment reactivity and poisoning (Xie and Cwiertny, 2012).

4.5 Conclusions and Implications

Recently the catalytic dechlorination of 1,2-DCA in the liquid phase via nCu particles coupled with 25 mM borohydride as a H_2 source at the bench scale has shown promising results. The findings of this study provide insight on how nCu synthesis parameters, 1,2-DCA concentration, and GW solutes influence the dechlorination kinetics of 1,2-DCA. nCu particles were found incapable of utilizing H_2 formed during their synthesis process for the dechlorination of 1,2-DCA, and rather direct injections of borohydride in reactor bottles were found essential. Rinsing the nCu particles with deionized water prior to reactivity experiments resulted in altering their surface composition and enhanced 1,2-DCA dechlorination rate and efficiency. Coating nCu particles was found to decrease 1,2-DCA dechlorination rate probably due to reactive site blocking. The dechlorination

reaction was found to follow a pseudo first order reaction rate up to the studied 1,2-DCA concentration of 225 mg L^{-1}. Consistent with gas phase studies, the presence of small concentrations of sulfides (0.2 mg L^{-1}) did not affect Cu activity in catalyzing the dechlorination of 1,2-DCA. However, the presence of higher concentrations of sulfides as well as presence of chlorides (>1000 mg L^{-1}), humic acid (> 10 mg L^{-1}), and oxygen (>4.93 mg L^{-1}) partially deactivated the nCu particles resulting in reduction in 1,2-DCA dechlorination rate and extent. An additional injection of borohydride re-activated the dechlorination reaction and compensated for the reduction in catalytic activity.

There are several implications of this study regarding the effectiveness of nCu-borohydride treatment as a GW remediation technology. The fundamental knowledge on the potential roles of particles coating, synthesis method, and GW solutes will aid in extending the application of nCu coupled with borohydride treatment from laboratory scale to site remediation. The study shows that successful implementation of this technology to GW relies critically on determining the concentrations of the different solutes in GW, and consequently the corresponding required number of borohydride injections. Therefore, it would be recommended to assess GW characteristics and perform laboratory feasibility tests using actual water samples from the contaminated sites prior to applying the treatment in the field. Additionally, it is recommended to examine the changes in the oxidation state, elemental composition, and morphology of the particles aged in GW solutes. Besides, further research on the fate and risk of these nanoparticles should be conducted prior to field application. Following on that note, it is suggested to find an alternate to borohydride that is a more environmental friendly hydrogen donor.

4.6 References

Alsawafta, M., Badilescu, S., Packirisamy, M. and Truong, V.-V., 2011. Kinetics at the nanoscale: formation and aqueous oxidation of copper nanoparticles. Reaction Kinetics, Mechanisms and Catalysis, 104(2): 437-450.

Angeles-Wedler, D., Mackenzie, K. and Kopinke, F.-D., 2009. Sulphide-induced deactivation of Pd/Al 2 O 3 as hydrodechlorination catalyst and its oxidative regeneration with permanganate. Applied Catalysis B: Environmental, 90(3): 613-617.

Argyle, M.D. and Bartholomew, C.H., 2015. Heterogeneous catalyst deactivation and regeneration: A review. Catalysts, 5(1): 145-269.

Arnold, W.A. and Roberts, A.L., 2000b. Pathways and Kinetics of Chlorinated Ethylene and Chlorinated Acetylene Reaction with Fe(0) Particles. Environmental Science & Technology, 34(9): 1794-1805.

Atisha, A., 2011. Degradation of 1,2-Dichloroethane With Nano-Scale Zero Valent Iron Particles, Western Ontario, 111 pp.

ATSDR, 2001. Toxicological profile for 1,2-dichloroethane. Agency for Toxic Substances and Disease Registry, Atlanta, GA. http://www.atsdr.cdc.gov/toxprofiles/index.asp. (accessed 13.09.2016).

Balko, B.A. and Tratnyek, P.G., 1998. Photoeffects on the reduction of carbon tetrachloride by zero-valent iron. Journal of Physical Chemistry B, 102(8): 1459-1465.

Biesinger, M.C., Hart, B.R., Polack, R., Kobe, B.A. and Smart, R.S.C., 2007. Analysis of mineral surface chemistry in flotation separation using imaging XPS. Minerals engineering, 20(2): 152-162.

Biesinger, M.C., Lau, L.W., Gerson, A.R. and Smart, R.S.C., 2010. Resolving surface chemical states in XPS analysis of first row transition metals, oxides and hydroxides: Sc, Ti, V, Cu and Zn. Applied Surface Science, 257(3): 887-898.

Chaplin, B.P. et al., 2012. Critical Review of Pd-Based Catalytic Treatment of Priority Contaminants in Water. Environmental Science & Technology, 46(7): 3655-3670.

Chastain, J., King, R.C. and Moulder, J., 1995. Handbook of X-ray photoelectron spectroscopy: a reference book of standard spectra for identification and interpretation of XPS data. Physical Electronics Eden Prairie, MN.

Coulman, D.J., Wintterlin, J., Behm, R.J. and Ertl, G., 1990. Novel mechanism for the formation of chemisorption phases: The (2\ifmmode\times\else\texttimes\fi{}1)O-Cu(110) ``added row'' reconstruction. Physical Review Letters, 64(15): 1761-1764.

Davie, M.G., Cheng, H., Hopkins, G.D., LeBron, C.A. and Reinhard, M., 2008. Implementing heterogeneous catalytic dechlorination technology for remediating TCE-contaminated groundwater. Environmental science & technology, 42(23): 8908-8915.

Devaraj, M., Saravanan, R., Deivasigamani, R. and Gupta, V.K., 2016. Fabrication of novel shape Cu and Cu/Cu2O nanoparticles modified electrode for the determination of dopamine and paracetamol. Journal of Molecular Liquids, 221: 930-941.

Diaz-Droguett, D.E., Espinoza, R. and Fuenzalida, V., 2011. Copper nanoparticles grown under hydrogen: study of the surface oxide. Applied Surface Science, 257(10): 4597-4602.

Doong, R.-A. and Lai, Y.-J., 2005. Dechlorination of tetrachloroethylene by palladized iron in the presence of humic acid. Water Research, 39(11): 2309-2318.

Feng, J., Zhu, B.-w. and Lim, T.-T., 2008. Reduction of chlorinated methanes with nano-scale Fe particles: Effects of amphiphiles on the dechlorination reaction and two-parameter regression for kinetic prediction. Chemosphere, 73(11): 1817-1823.

Forzatti, P. and Lietti, L., 1999. Catalyst deactivation. Catalysis today, 52(2): 165-181.

Giasuddin, A.B.M., Kanel, S.R. and Choi, H., 2007. Adsorption of Humic Acid onto Nanoscale Zerovalent Iron and Its Effect on Arsenic Removal. Environmental Science & Technology, 41(6): 2022-2027.

Heck, K.N., Nutt, M.O., Alvarez, P. and Wong, M.S., 2009. Deactivation resistance of Pd/Au nanoparticle catalysts for water-phase hydrodechlorination. Journal of Catalysis, 267(2): 97-104.

Huang, C.-C., Lo, S.-L. and Lien, H.-L., 2012. Zero-valent copper nanoparticles for effective dechlorination of dichloromethane using sodium borohydride as a reductant. Chemical Engineering Journal, 203: 95-100.

Huang, C.-C., Lo, S.-L., Tsai, S.-M. and Lien, H.-L., 2011. Catalytic hydrodechlorination of 1, 2-dichloroethane using copper nanoparticles under reduction conditions of sodium borohydride. Journal of Environmental Monitoring, 13(9): 2406-2412.

Humans, I.W.G.o.t.E.o.C.R.t., Cancer, I.A.f.R.o. and Organization, W.H., 1999. Re-evaluation of some organic chemicals, hydrazine and hydrogen peroxide. IARC, International Agency for Research on Cancer.

Hutchings, G.J., King, F., Okoye, I.P. and Rochester, C.H., 1994. Influence of chlorine poisoning of copper/alumina catalyst on the selective hydrogenation of crotonaldehyde. Catalysis letters, 23(1-2): 127-133.

Johnson, T.L., Fish, W., Gorby, Y.A. and Tratnyek, P.G., 1998. Degradation of carbon tetrachloride by iron metal: Complexation effects on the oxide surface. Journal of Contaminant Hydrology, 29(4): 379-398.

Kim, H.-S., Ahn, J.-Y., Kim, C., Lee, S. and Hwang, I., 2014. Effect of anions and humic acid on the performance of nanoscale zero-valent iron particles coated with polyacrylic acid. Chemosphere, 113: 93-100.

Kong, V., Foulkes, F., Kirk, D. and Hinatsu, J., 1999. Development of hydrogen storage for fuel cell generators. i: Hydrogen generation using hydrolysis of hydrides. International Journal of Hydrogen Energy, 24(7): 665-675.

Kopinke, F.-D., Angeles-Wedler, D., Fritsch, D. and Mackenzie, K., 2010. Pd-catalyzed hydrodechlorination of chlorinated aromatics in contaminated waters—Effects of surfactants, organic matter and catalyst protection by silicone coating. Applied Catalysis B: Environmental, 96(3–4): 323-328.

Kopinke, F.-D., Mackenzie, K. and Köhler, R., 2003. Catalytic hydrodechlorination of groundwater contaminants in water and in the gas phase using Pd/γ-Al 2 O 3. Applied Catalysis B: Environmental, 44(1): 15-24.

Kovenklioglu, S., Cao, Z., Shah, D., Farrauto, R.J. and Balko, E.N., 1992. Direct catalytic hydrodechlorination of toxic organics in wastewater. AIChE Journal, 38(7): 1003-1012.

Lambert, S., Ferauche, F., Brasseur, A., Pirard, J.-P. and Heinrichs, B., 2005. Pd–Ag/SiO 2 and Pd–Cu/SiO 2 cogelled xerogel catalysts for selective hydrodechlorination of 1, 2-dichloroethane into ethylene. Catalysis today, 100(3): 283-289.

Lecloux, A.J., 1999. Chemical, biological and physical constrains in catalytic reduction processes for purification of drinking water. Catalysis Today, 53(1): 23-34.

Lim, J., Yeap, S.P., Che, H.X. and Low, S.C., 2013. Characterization of magnetic nanoparticle by dynamic light scattering. Nanoscale Research Letters, 8(1): 381-381.

Liu, J., He, F., Durham, E., Zhao, D. and Roberts, C.B., 2008. Polysugar-stabilized Pd nanoparticles exhibiting high catalytic activities for hydrodechlorination of environmentally deleterious trichloroethylene. Langmuir, 24: 328-336.

Liu, T. and Lo, I.M., 2011a. Influences of humic acid on Cr (VI) removal by zero-valent iron from groundwater with various constituents: implication for long-term PRB performance. Water, Air, & Soil Pollution, 216(1-4): 473-483.

Liu, T. and Lo, I.M.C., 2011b. Influences of Humic Acid on Cr(VI) Removal by Zero-Valent Iron From Groundwater with Various Constituents: Implication for Long-Term PRB Performance. Water, Air, & Soil Pollution, 216(1): 473-483.

Liu, X., Vellanki, B.P., Batchelor, B. and Abdel-Wahab, A., 2014b. Degradation of 1,2-dichloroethane with advanced reduction processes (ARPs): Effects of process variables and mechanisms. Chemical Engineering Journal, 237(0): 300-307.

Liu, Y., Phenrat, T. and Lowry, G.V., 2007b. Effect of TCE concentration and dissolved groundwater solutes on NZVI-promoted TCE dechlorination and H2 evolution. Environmental science & technology, 41(22): 7881-7887.

Lowry, G.V. and Reinhard, M., 1999. Hydrodehalogenation of 1-to 3-carbon halogenated organic compounds in water using a palladium catalyst and hydrogen gas. Environmental science & technology, 33(11): 1905-1910.

Lowry, G.V. and Reinhard, M., 2000. Pd-catalyzed TCE dechlorination in groundwater: Solute effects, biological control, and oxidative catalyst regeneration. Environmental Science & Technology, 34(15): 3217-3223.

Luebke, D.R., Vadlamannati, L.S., Kovalchuk, V.I. and d'Itri, J.L., 2002. Hydrodechlorination of 1,2-dichloroethane catalyzed by Pt–Cu/C: effect of catalyst pretreatment. Applied Catalysis B: Environmental, 35(3): 211-217.

Mackenzie, K., Frenzel, H. and Kopinke, F.-D., 2006. Hydrodehalogenation of halogenated hydrocarbons in water with Pd catalysts: Reaction rates and surface competition. Applied Catalysis B: Environmental, 63(3): 161-167.

Marquez, F., Palomares, A., Rey, F. and Corma, A., 2001. Characterisation of the active copper species for the NOx removal on Cu/Mg/Al mixed oxides derived from hydrotalcites: an in situ XPS/XAES study. Journal of Materials Chemistry, 11(6): 1675-1680.

Meshesha, B.T. et al., 2013. PdCu alloy nanoparticles on alumina as selective catalysts for trichloroethylene hydrodechlorination to ethylene. Applied Catalysis A: General, 453(0): 130-141.

Mondal, J., Biswas, A., Chiba, S. and Zhao, Y., 2015. Cu0 Nanoparticles Deposited on Nanoporous Polymers: A Recyclable Heterogeneous Nanocatalyst for Ullmann Coupling of Aryl Halides with Amines in Water. Scientific Reports, 5: 8294.

Moroney, L., Rassias, S. and Roberts, M.W., 1981. Chemisorption of HCl and H2S by Cu(111)-O surfaces. Surface Science, 105(1): L249-L254.

Nunez Garcia, A., Boparai, H.K. and O'Carroll, D.M., 2016a. Enhanced dechlorination of 1,2-dichloroethane by coupled nano iron-dithionite treatment. Environmental Science & Technology, 50(10): 5243-5251.

Pan, L. et al., 2013. Cu2O film via hydrothermal redox approach: morphology and photocatalytic performance. The Journal of Physical Chemistry C, 118(30): 16335-16343.

Park, J.Y., Jung, Y.S., Cho, J. and Choi, W.K., 2006. Chemical reaction of sputtered Cu film with PI modified by low energy reactive atomic beam. Applied Surface Science, 252(16): 5877-5891.

Phenrat, T., Liu, Y., Tilton, R.D. and Lowry, G.V., 2009. Adsorbed polyelectrolyte coatings decrease Fe0 nanoparticle reactivity with TCE in water: conceptual model and mechanisms. Environmental Science & Technology, 43(5): 1507-1514.

Raut, S.S., Kamble, S.P. and Kulkarni, P.S., 2016. Efficacy of zero-valent copper (Cu^0) nanoparticles and reducing agents for dechlorination of mono chloroaromatics. Chemosphere, 159: 359-366.

Rostamikia, G. and Janik, M.J., 2010. Direct borohydride oxidation: mechanism determination and design of alloy catalysts guided by density functional theory. Energy & Environmental Science, 3(9): 1262-1274.

Schüth, C., Kummer, N.-A., Weidenthaler, C. and Schad, H., 2004. Field application of a tailored catalyst for hydrodechlorinating chlorinated hydrocarbon contaminants in groundwater. Applied Catalysis B: Environmental, 52(3): 197-203.

Song, H. and Carraway, E.R., 2005b. Reduction of Chlorinated Ethanes by Nanosized Zero-Valent Iron: Kinetics, Pathways, and Effects of Reaction Conditions. Environmental Science & Technology, 39(16): 6237-6245.

Śrębowata, A., Lisowski, W., Sobczak, J.W. and Karpiński, Z., 2011. Hydrogen-assisted dechlorination of 1,2-dichloroethane on active carbon supported palladium–copper catalysts. Catalysis Today, 175(1): 576-584.

Sun, Y.P., Li, X.Q., Cao, J.S., Zhang, W.X. and Wang, H.P., 2006b. Characterization of zero-valent iron nanoparticles. Advances in Colloid and Interface Science, 120(1-3): 47-56.

Tratnyek, P.G., Scherer, M.M., Deng, B. and Hu, S., 2001. Effects of Natural Organic Matter, Anthropogenic Surfactants, and Model Quinones on the Reduction of Contaminants by Zero-Valent Iron. Water Research, 35(18): 4435-4443.

Twigg, M.V., 1996. Catalyst Handbook. Manson Pub.

Twigg, M.V. and Spencer, M.S., 2001. Deactivation of supported copper metal catalysts for hydrogenation reactions. Applied Catalysis A: General, 212(1): 161-174.

Vadlamannati, L.S., Kovalchuk, V.I. and d'Itri, J.L., 1999. Dechlorination of 1, 2-dichloroethane catalyzed by Pt–Cu/C: unraveling the role of each metal. Catalysis letters, 58(4): 173-178.

Wagner, C. et al., NIST Standard Reference Database 20, Version 3.4 (web version); http:/srdata. nist. gov/xps/, 2003. There is no corresponding record for this reference.

Water, O.o., Agency, U.S.E.P. and Washington, D., 2011. 2011 Edition of the Drinking Water Standards and Health Advisors.

Wielant, J., Hauffman, T., Blajiev, O., Hausbrand, R. and Terryn, H., 2007. Influence of the iron oxide acid-base properties on the chemisorption of model epoxy compounds studied by XPS. Journal of Physical Chemistry C, 111(35): 13177-13184.

Xie, H. et al., 2008. Hydrodechlorination of 1,2-dichloroethane catalyzed by dendrimer-derived Pt–Cu/SiO2 catalysts. Journal of Catalysis, 259(1): 111-122.

Xie, Y. and Cwiertny, D.M., 2012. Influence of Anionic Cosolutes and pH on Nanoscale Zerovalent Iron Longevity: Time Scales and Mechanisms of Reactivity Loss toward 1,1,1,2-Tetrachloroethane and Cr(VI). Environmental Science & Technology, 46(15): 8365-8373.

Yao, K.X., Yin, X.M., Wang, T.H. and Zeng, H.C., 2010. Synthesis, Self-Assembly, Disassembly, and Reassembly of Two Types of Cu2O Nanocrystals Unifaceted with {001} or {110} Planes. Journal of the American Chemical Society, 132(17): 6131-6144.

Yaron, B., Dror, I. and Berkowitz, B., 2012. Soil-subsurface change: Chemical pollutant impacts. Springer Science & Business Media.

Yuan, S., Chen, M., Mao, X. and Alshawabkeh, A.N., 2013. Effects of reduced sulfur compounds on Pd-catalytic hydrodechlorination of trichloroethylene in groundwater by cathodic H2 under electrochemically induced oxidizing conditions. Environmental science & technology, 47(18): 10502-10509.

Zhang, M., He, F., Zhao, D. and Hao, X., 2011. Degradation of soil-sorbed trichloroethylene by stabilized zero valent iron nanoparticles: Effects of sorption, surfactants, and natural organic matter. Water Research, 45(7): 2401-2414.

Zhang, Y., Zheng, N., Wang, K., Zhang, S. and Wu, J., 2013. Effect of copper nanoparticles dispersion on catalytic performance of Cu/SiO2 catalyst for hydrogenation of dimethyl oxalate to ethylene glycol. Journal of Nanomaterials, 2013.

Chapter 5

5 Nano metal Based Technologies for Treating Chlorinated Organic Compounds (COCs) Mixtures in Groundwater

5.1 Abstract

Chlorinated organic compounds (COCs) are amongst the most prevalent groundwater contaminants found at hazardous sites throughout the world. Given their pervasive contamination and adverse health effects, there is considerable interest in developing field-applicable technologies to treat these contaminants. Chemical reduction by nano zero valent iron, monometallic (nZVI) or bimetallic (Pd-nZVI), has proven to be a successful field applicable technology. However, this technology has failed to degrade recalcitrant compounds such as 1,2-dichloroethane (1,2-DCA). Recently, three novel field-applicable nano metal based technologies capable of successfully dechlorinating 1,2-DCA have been reported. These include nZVI coupled with dithionite and Pd or Cu nanoparticles combined with borohydride. However, reactivity studies of these novel technologies have been carried out under ideal laboratory conditions for degrading single contaminants only. At the field scale, there are usually diverse mixtures of COCs present, in addition to groundwater constituents which can significantly affect the performance of metal-based technologies. Thus, the objective of this study is to assess the effectiveness of these recently developed nano metal based technologies, along with nZVI and Pd-nZVI, to degrade a suite of COCs in a groundwater sample from an industrial site. The contaminants present in the groundwater sample included: trichloromethane, 1,1,2-trichloroethane, 1,2-dichloroethane, trichloroethene, and vinyl chloride, along with other secondary contaminants. Dechlorination efficiencies of each treatment for these COCs are studied and possible dechlorination pathways are proposed. Both nZVI and Pd-nZVI were found capable of breaking down all major contaminants with the exception of 1,2-DCA. nZVI-dithionite was able to break down all COCs including 1,2-DCA. Pd or Cu nanoparticles combined with multiple injections of borohydride were able to degrade 1,2-DCA, along

with complete removal of all other COCs. These results suggest that these nano metal based technologies can be effective remediation approaches depending upon site conditions.

Keywords: 1,2-Dichloroethane, Dechlorination, Nano Zero valent Iron, Copper, Palladium, Dithionite, Borohydride, Groundwater.

5.2 Introduction

Chlorinated organic compounds (COCs) are used extensively in various industrial applications (e.g. pesticides, detergents, wood preservation, paint removers, dyes, solvents) and as intermediates in the manufacture of other chemicals (Barnes et al., 2010; Tobiszewski and Namieśnik, 2012). Improper handling, storage and disposal, as well as their chemical stability, have caused widespread subsurface contamination of these chemicals. Trichloromethane (TCM), dichloromethane (DCM), 1,1,2-trichloroethane (1,1,2-TCA), 1,2-dichloroethane (1,2-DCA), tetrachloroethene (PCE), trichloroethene (TCE), and vinyl chloride (VC) are among the most prevalent COCs at contaminated sites (Barnes et al., 2010; Zhang et al., 1998). These known or suspected carcinogens have been classified as priority pollutants by the U.S. Environmental Protection Agency and the Agency for Toxic Substances and Disease Registry (ATSDR, 2015; USEPA, 2015). Due to their pervasive nature, severe adverse health effects, and the low drinking water guidelines, there is considerable interest in developing field-applicable technologies to degrade these contaminants.

Reductive dechlorination, biotic or abiotic, is a commonly employed technology for treating chlorinated compounds at the contaminated sites. This involves the cleavage of one or more carbon-chlorine bonds of a COC molecule, where the chlorine atom is eliminated as a chloride ion (Yu, 2013). This breakdown requires an electron donor (reductant) and may include a proton donor depending on the reaction pathways: hydrogenolysis or dichloroelimination (Arnold and Roberts, 2000a; Tobiszewski and Namieśnik, 2012). In the hydrogenolysis pathway, a chlorine atom is replaced by a hydrogen atom with simultaneous addition of two electrons to the molecule (Equation 5-1) (O'Carroll et al., 2013; Tobiszewski and Namieśnik, 2012; Yu, 2013). Dichloroelimination involves transfer of two electrons to the COC molecule, and release

of two chlorine atoms resulting in less saturated reaction products (Equation 5-2). Another reaction that usually happens after the elimination step is called hydrogenation, which involves the addition of hydrogen to a double or triple C-C bond. The dechlorination pathways for chlorinated methanes, ethanes and ethenes are shown in Figure 9-1 (Appendix C). The reduction of chlorinated aliphatic hydrocarbons in the presence of electron donors is thermodynamically feasible under ambient conditions (Dolfing et al., 2007). Thus, the degradation of COCs by liquid phase direct reduction has been the subject of some study (Atisha, 2011; Barnes et al., 2010; Sakulchaicharoen et al., 2010; Tobiszewski and Namieśnik, 2012; Yu, 2013; Zhang et al., 1998).

$$\boldsymbol{RCl + H^{+} + 2e^{-} \rightarrow RH + Cl^{-}} \qquad \text{(Equation 5-1)}$$

$$\boldsymbol{RCCl - CClR + 2e^{-} \rightarrow RC = CR + 2Cl^{-}} \qquad \text{(Equation 5-2)}$$

Nano zero valent iron (nZVI) particles stand out as one of the most promising abiotic direct reduction remedial technologies, due to their nano-sized dimensions leading to greater reactivity, and potential for subsurface injection and transport to the contaminant zone (Atisha, 2011; Elliott and Zhang, 2001; O'Carroll et al., 2013; Sakulchaicharoen et al., 2010; Song and Carraway, 2005a; Zhang et al., 1998). nZVI with a redox potential of -0.44V, can act as a strong reductant to dechlorinate COCs (Equation 5-3) (Atisha, 2011; O'Carroll et al., 2013). Moreover, nZVI can also produce hydrogen (H_2) gas by reduction of water (Equation 5-4) (O'Carroll et al., 2013), which can further act as a reductant. A wide variety of chlorinated compounds (e.g. TCM, 1,1,1-TCA, PCE, TCE) can be degraded using nZVI (Lien and Zhang, 2001; Liu et al., 2005a; O'Carroll et al., 2013; Song and Carraway, 2005a; Song and Carraway, 2006; Tobiszewski and Namieśnik, 2012). However, nZVI reactions with chlorinated ethanes are slower than chlorinated ethenes, and may form toxic chlorinated byproducts (Lien and Zhang, 2005). Also, although thermodynamically feasible, 1,2-DCA and DCM are found to be almost absolutely resistant to degradation by nZVI (Atisha, 2011; Song and Carraway, 2005a; Song and Carraway, 2006). Thus, noble metals (e.g. Ni, Pd) are often doped on the nZVI surface to increase its reactivity, forming bimetallic nZVI (Atisha, 2011; Barnes et al., 2010; Elliott and Zhang, 2001; O'Carroll et al., 2013; Sakulchaicharoen et al., 2010; Zhang et al., 1998). Palladium

(Pd), the most commonly doped metal, enhances nZVI reactivity by acting as a catalyst, adsorbing H_2 from water reduction by iron and dissociating it into the robst reductant atomic $H^{\cdot}$ (Equation 5-5) (Atisha, 2011; Liu et al., 2014a; Liu et al., 2001). The activated H_2 then attacks the chlorinated contaminants adsorbed on the iron surface leading to their dechlorination (Equation 5-6). Use of Pd doped nZVI significantly enhances the dechlorination efficiency of many COCs (e.g. PCE, 1,1,2-TCA, Cis-DCE) without the formation of any toxic byproducts (Lien and Zhang, 2001; Lien and Zhang, 2005; Lim and Feng, 2007; Zhang et al., 1998). However, even the Pd-nZVI bimetallic system has failed to degrade 1,2-DCA and DCM so far (Atisha, 2011; Lim and Feng, 2007; Wang et al., 2009).

$$Fe^0 \xrightarrow{E^0=-0.44V} Fe^{2+} + 2e^- \qquad \text{(Equation 5-3)}$$

$$Fe^0 + 2H_2O \rightarrow Fe^{2+} + H_2\uparrow + 2OH^- \qquad \text{(Equation 5-4)}$$

$$H_2 \xrightarrow{Catalyst} 2H^{\cdot} \qquad \text{(Equation 5-5)}$$

$$RCl + H_2 \xrightarrow{Catalyst} RH + HCl \qquad \text{(Equation 5-6)}$$

Recently, three novel liquid phase nano metal based technologies capable of successfully degrading 1,2-DCA have been reported. These include nZVI coupled with dithionite and Pd (nPd) or Cu (nCu) nanoparticles combined with borohydride (Huang et al., 2011; Nunez Garcia et al., 2016a).

Sodium dithionite, a strong reductant (E = -1.12 V), has been successfully used to manipulate in-situ redox conditions, to reduce subsurface ferric iron to ferrous iron for treating various organic and inorganic contaminants (Boparai et al., 2008; Boparai et al., 2006; Fruchter et al., 2000). In aqueous solutions, dithionite self-dissociates to form sulphoxyl radicals, sulfite and thiosulfate which can also act as reductants. Aqueous solutions of dithionite are also capable of degrading chlorinated organic compounds (Boparai et al., 2006; Nzengung et al., 2001; Rodriguez and Rivera, 1997). In the nZVI-dithionite treatment, dithionite enhances the reactivity of nZVI by providing additional

electrons, extending the reactive lifespan of nZVI and generating other reductants (e.g. hydrogen sulfide species and iron sulfides) (Nunez Garcia et al., 2016a).

The coupled nano metal-borohydride technology utilizes sodium borohydride ($NaBH_4$) as a H_2 source over nano scale Cu or Pd catalyst surfaces. Hydrogen gas is readily generated through the hydrolysis of borohydride (Equation 5-7) (Huang et al., 2012; Rostamikia and Janik, 2010). The nano sized catalyst dissociatively adsorbs 1,2-DCA and activates the H_2 gas into a robust reductant reducing the 1,2-DCA molecules adsorbed on adjacent sites (Equations 5-5 & 5-6) (Borovkov et al., 2003; Chaplin et al., 2012; Conrad et al., 1974; Kopinke et al., 2003; Lambert et al., 2005; Śrębowata et al., 2011; Vadlamannati et al., 1999). 1,2-DCA and DCM are reported to be almost completely and rapidly dechlorinated by Pd-borohydride and Cu-borohydride treatments, as seen in the previous chapters (Huang et al., 2012; Huang et al., 2011).

$$\boldsymbol{BH_4^- + 2H_2O \rightarrow BO_2^- + 4H_2\uparrow} \qquad \text{(Equation 5-7)}$$

The development of field applicable nano metal-based technologies capable of degrading recalcitrant compounds like 1,2-DCA is an important breakthrough for the environmental remediation world. So far the reactivity studies of these novel technologies have been carried out under ideal laboratory conditions for degrading a single contaminant, as such the degradation capabilities of these technologies under real field situations is still unknown. At the field scale, additional factors (e.g. inorganic co-contaminants, dissolved oxygen, humic acids, inorganic constituents (CO_3^{2-}, Cl^-, SO_4^{2-}) and microbial communities) can significantly affect the performance of metal-based technologies (Kim et al., 2014; Lowry and Reinhard, 2000; Mcnab et al., 2000; Schüth et al., 2004). Thus, the objective of this study is to assess the effectiveness of five nano metal-based technologies (nZVI, Pd-nZVI, nZVI-dithionite, nCu-borohydride, and nPd-borohydride) to degrade a suite of COCs in a groundwater sample recovered from an industrial site. Dechlorination efficiencies and the possible dechlorination pathways for all the treatments are discussed.

5.3 Experimental Methods

5.3.1 Chemicals and Groundwater matrix

All chemicals were used as received: sodium borohydride ($NaBH_4$, Venpure AF Granular, Dow Chemicals), ferrous sulfate heptahydrate ($FeSO_4.7H_2O$, A&K Petrochem Ind. Ltd., Vaughn, ON), copper sulfate ($CuSO_4$, EMD), potassium hexachloropalladate (K_2PdCl_6, Pd min 26.69%, Alfa Aesar), sodium carboxymethyl cellulose (CMC, MW = 90K, Walocel CRT 30PA, Dow Chemicals), sodium chloride (NaCl, EMD), sodium dithionite ($Na_2S_2O_4$, 85%, Sigma-Aldrich), gas mix (5% H_2 balance Ar, PRAXAIR), and N_2 (Ultra High Purity, PRAXAIR). All solutions were prepared using double deionized and deoxygenated water.

Groundwater samples were obtained from an industrial site at Altona, Australia. The samples were stored in a cold room (4 °C) prior to use to suppress any biological activity. The groundwater was characterized (Table 9-1, Appendix C) using standard procedures (NMI, Australia).

5.3.2 Synthesis of Stabilized Nano Metal Particles

The aqueous chemical reduction method was used for the synthesis of the CMC-stabilized nano metal particles as indicated in Equation 5-8 (Lien and Zhang, 2001; Lim and Feng, 2007; Sakulchaicharoen et al., 2010). Firstly, the metal salt solution was well mixed in the presence of CMC polymer to form M^{2+}-CMC complex. $NaBH_4$ was then added dropwise to the M^{2+}-CMC solution with continuous stirring. A BH_4^-/M^{2+} ratio of 3-4 was used to ensure uniform growth of the particles and to accelerate the synthesis process. Nano metal synthesis was conducted in an anaerobic glove box purged with O_2-free Ar (95% Ar : 5% H_2). Detailed information about synthesis of Pd and Cu nanoparticles is reported in the previous chapters. More details of nZVI synthesis are included in section 9-1 (Appendix C). For Pd-nZVI, K_2PdCl_6 (dissolved in NaCl) was added to the nZVI suspension which in turn reduced it to Pd^o (Equation 5-9). The Pd-nZVI suspension was mixed for 10 minutes. The Pd loading was 0.05% w/w of Fe.

$$2M^{2+} + BH_4^- + 3H_2O \rightarrow 2M^0 + H_2BO_3^- + 4H^+ + 2H_2\uparrow \qquad \text{(Equation 5-8)}$$

where M can be Fe, Pd or Cu.

$$Pd^{2+} + Fe^{0} \rightarrow Pd^{0} + Fe^{2+}$$ (Equation 5-9)

5.3.3 Reactivity Experiments

Reactivity experiments were conducted in 120 or 250 mL amber serum bottles sealed with Teflon mininert caps to minimize the oxidation of nano metals. The bottles were shaken using an arm wrist action shaker at room temperature (Model 75, Burrell Inc.). All the experiments were conducted in duplicates, with error bars on dechlorination profiles representing the standard deviation between the two duplicates. For each reactivity experiment, controls of groundwater only or groundwater and CMC were run (without nano metal suspension) to observe any losses of COCs due to adsorption, volatilization, etc.

For nZVI and Pd-nZVI treatments, 60 mL groundwater sample was added to 30 mL nano metal suspension in 120-mL bottles (90 mL solution/ 30 ml headspace). As such the final nano metal concentration in the reactor bottles was 2.5 g L^{-1} and the groundwater sample was diluted by 1.5 times. To study the effect of higher nZVI dosage, an additional experiment was conducted by adding 30 mL groundwater sample to 60 mL nZVI suspension, thus, increasing the final nZVI concentration to 5 g L^{-1} and diluting the COCs concentrations by 3 times. nZVI-dithionite treatment experiments were conducted in 250 mL bottles (90 mL solution/ 160 ml headspace) by mixing 60 mL groundwater with 30 mL nZVI-dithionite suspension making the final nZVI dose 2.5 g L^{-1} with a final dithionite concentration of 50 mM. The dithionite alone experiment was conducted in the same way but without nZVI suspension. Both nPd, and nCu treatments were conducted in 250 mL bottles (90 mL solution/ 160 ml headspace) by mixing 60 mL groundwater with 30 mL nPd or nCu suspension making the final nPd, and nCu dose 1 g L^{-1} in each reactor bottle (following experimental design from previous chapters). 25 mM borohydride is initiallyspiked into the nCu treatment slurry reactor bottle.

5.3.4 Analytical Methods

Concentrations of TCM, 1,1,2-TCA, 1,2-DCA, PCE, and TCE were analyzed with an Agilent 7890 Gas Chromatograph (GC) equipped with a DB-624 capillary column (75 m x 0.45 mm, 2.55 µm) and an Electron Capture Detector (ECD) following a modified EPA

8021 method. The oven temperature program was: 35°C for 12 min, increased to 60°C at 5°C min^{-1}, hold at 60°C for 1 min and then increased to 200°C at 17°C min^{-1} and hold at 200°C for 5 min. Nitrogen was used as the carrier gas at a flow rate of 10 mL min^{-1}. 250 μL liquid sample from each reactor bottle was collected at a selected sampling time and transferred to a 2-mL GC vial containing 1 mL hexane for COCs extraction.The GC vials were vortex-mixed and allowed to equilibrate for at least two hours before extraction. One μL of the extract was injected into the GC using an auto sampler. Concentrations of DCM, 1,1-DCA, chloroethane (CE), 1,1-dichloroethene (1,1-DCE), cis-1,2-dichloroethene (c-1,2-DCE), trans-dichloroethene (t-1,2-DCE), VC, ethane, ethene, and methane were measured with an Agilent 7890A GC equipped with a GS-Gas Pro Column (3.0 m x 0.32 mm) and Flame Ionization Detector (FID). The conditions of the GC method were as follows: a temperature ramp of 35°C for 5 min, then 10°C min^{-1} to 220°C held for 7 min with He as the carrier gas. 250 μL or 1 mL sample aliquots were collected in 2-mL GC vials, kept for equilibration, and then 250 μL headspace sample from the GC vial was injected into the GC either manually or using an autosampler (Agilent G4513A).

5.3.5 TEM Analysis

Surface morphology of the nanoparticles, before and after reaction, was performed using a Philips CM10 and a FEI Titan 80–300 Cryo-in-situ Transmission Electron Microscope (TEM, Philips Export B.V. Eindhove, Netherlands). The samples were diluted using deoxygenated water and then one drop was dried on a 400 mesh Formvar/carbon copper grid in an anaerobic chamber. A set of micrographs was obtained for each sample and the diameters of particles on these micrographs were measured using a Hamamatsu CCD based camera system software (Advanced Microscopy Techniques, version AMTV542).

5.4 Results and Discussion

5.4.1 TEM Analysis

The particle size and morphology of metal nanoparticles were examined by TEM. The fresh nCu is comprised of individual, spherical nanoparticles with particle size ranging from 6.7-11.4 nm and assembled in chains forming loose aggregates (Fiigure 5-1A). TEM images of nCu after reaction show the presence of some spherical nanoparticles still present

but majority of the particles transforming to long, thin rods indicating oxidation of nCu (Figures. 9-2A-B, Appendix C). The nCu suspension turned from black to light green (Figure 9-3A, Appendix C) at the end of reactivity experiment further suggesting oxidation (Scully and Graedel, 1987).

The nPd consists of individual spherical nanoparticles (4.9-7.7 nm) forming tightly packed aggregates (Figure 5-1B). After reaction, the size of nPd particles increased significantly, ranging between 50-600 nm (Figure 9-2C, Appendix C), and the suspension turned from black to greyish white (Figure 9-3B, Appendix C) which could be due to oxidation or surface poisoning by groundwater constituents.

TEM micrographs of fresh nZVI (Figure 5-1C) and Pd-nZVI (Figure 5-1D) suspensions indicate the presence of individual spherical particles with mean diameters of 34.1±7.1 nm and 39.6±8.0 nm, respectively. The fresh nZVI and Pd-nZVI suspensions were jet black in color (not shown) which turned greenish white towards the end of the experiments (Figure 9-3C, Appendix C), suggesting the complete oxidation of zerovalent iron to (oxy)(hydr)oxides. The TEM image of the nZVI-dithionite suspension after reaction (Figure 9-2D, Appendix C) show a significant change in morphology (almost spherical though flaky) and size (203±47 nm) of particles indicating the formation of FeS-nZVI due to their reaction with dithionite (Su et al., 2015). The nZVI-dithionite suspension was still jet black in color (Figure 9-3D, Appendix C) even after 120 days of reaction which could be attributed to preserved zero valent iron along with the formation of iron sulfides as reported earlier (Nunez Garcia et al., 2016a).

5.4.2 Dechlorination of Chlorinated Organic Compounds in Groundwater

Dechlorination of a mixture of COCs present in the contaminated groundwater from an industrial site by five nano metal-based technologies (nZVI, Pd-nZVI, nZVI-dithionite, nCu-borohydride, and nPd-borohydride) was studied. Additionally, a dithionite alone treatment was also tested. The primary contaminants present in the groundwater are TCM, 1,1,2-TCA, 1,2-DCA, TCE, and VC along with other secondary contaminants including DCM, PCE, 1,1-DCE, cis- and trans- 1,2-DCEs. A proposed dechlorination order based on

Gibb's free energy values for dechlorination reactions and carbon bearing chlorine atoms redox values is presented in section 9-2, Appendix 9. Dechlorination efficiencies and possible reaction pathways for each treatment are discussed. It is noted that it was not possible to close the carbon mass balance. DCM, and C-1,2-DCE were below detection limit in the nZVI-Dithionite, nCu-borohydride, and nPd borohydride reactivity experiments.

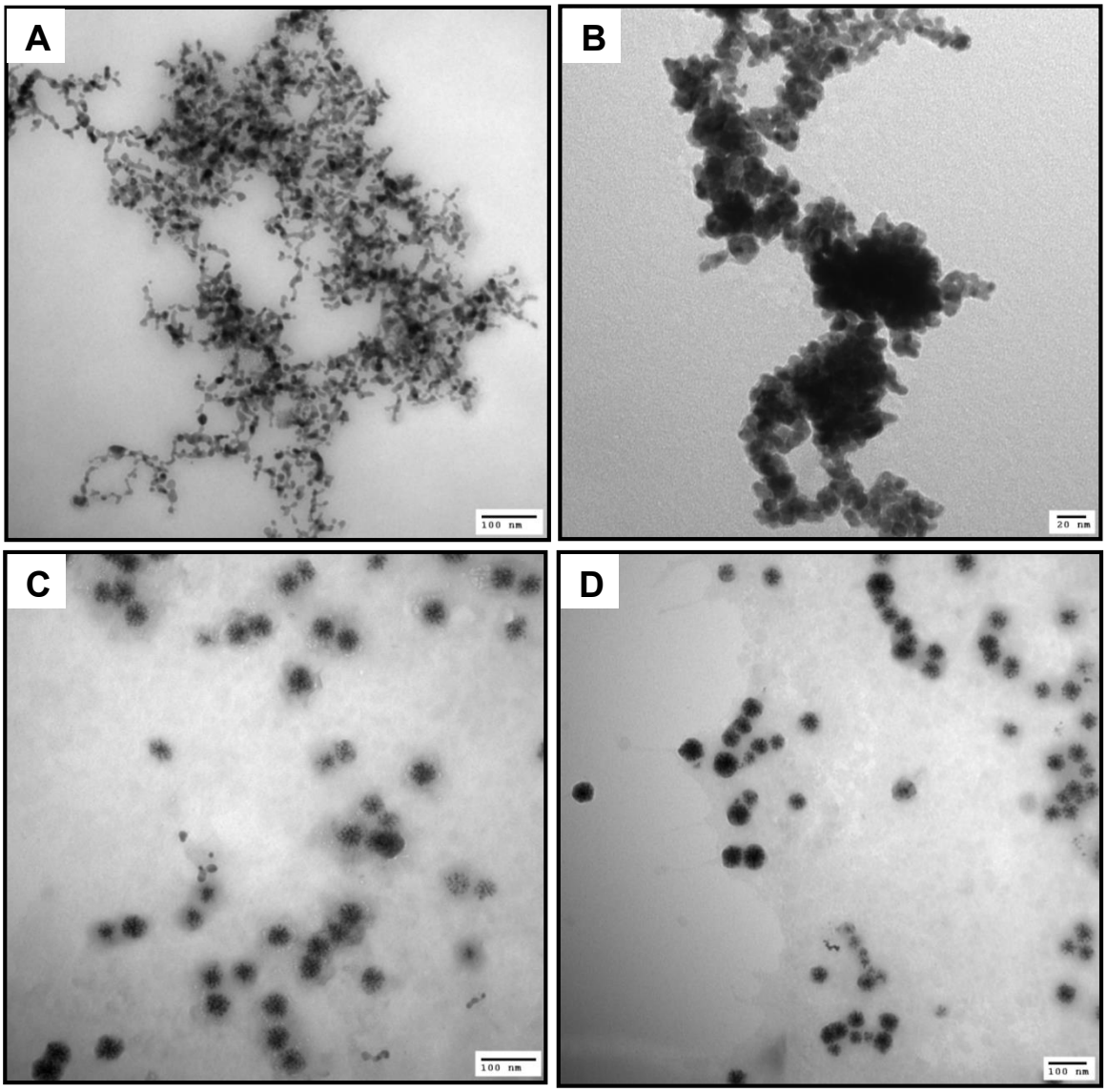

Figure 5-1: TEM images of fresh CMC-stabilized (A) nCu, (B) nPd, (C) nZVI, and (D) Pd-nZVI particles.

5.4.2.1 Dechlorination by nZVI and Pd-nZVI

The dechlorination profiles for the primary and secondary COCs treated by nZVI and Pd-nZVI are shown in Figures 5-2 and 9-4 (Appendix C). The initial and final concentrations of all the COCs are summarized in Table 5-1. Methane, ethane and ethene were detected in the nZVI and Pd-nZVI reactors following reaction. Direct reduction, sequential hydrogenolysis, dichloroelimination and hydrogenation are expected to be the degradation pathways for this multi-contaminant system as reported earlier for single contaminants (Lien and Zhang, 2001; Song and Carraway, 2005a; Song and Carraway, 2006). Most of the Fe^0 in both treatments was oxidized at 35 days of the reaction resulting in cessation of COCs' dechlorination. Consistent with previous research (Lien and Zhang, 2001; Lien and Zhang, 1999; Lim and Feng, 2007; Zhang et al., 1998) doping Pd on nZVI improved the rate and extent of dechlorination of the COCs.

Chlorinated Methanes – As expected, TCM dechlorination by Pd-nZVI was much faster than by nZVI (Figure 5- 2A). Complete dechlorination was achieved in 29 and 12 days by nZVI and Pd-nZVI, respectively, with simultaneous release of some DCM (Figure 9-4A, Appendix C). Both nZVI and Pd-nZVI failed to degrade DCM consistent with other studies (Feng and Lim, 2005; Lien and Zhang, 1999; Song and Carraway, 2006). For both treatments only 3-4 µM DCM evolved from the degradation of the ~47µM TCM (Table 5-1) representing <10% of the total TCM dechlorinated. This suggests direct reduction of TCM to methane as the major dechlorination pathway and transformation to DCM via hydrogenolysis as a minor pathway (Feng and Lim, 2005; Lien and Zhang, 1999; Song and Carraway, 2006; Wang et al., 2009)

Chlorinated Ethanes - 1,1,2-TCA dechlorination started after a lag phase (5 to 8 days) with 52 and 86% removal at 35 days in nZVI and Pd-nZVI respectively (Figure 5-2B). Some 1,1,2-TCA dechlorination could have occurred via hydrogenolysis yielding 1,2-DCA or chloroethane. Traces of chloroethane were detected in the Pd-nZVI treatment, and no significant change in 1,2-DCA concentration was observed, suggesting reduction to chloroethane, and resistance of 1,2-DCA to redcution (Figure 5-2C), consistent with previous research (Atisha, 2011; Lien and Zhang, 2005; Song and Carraway, 2005a). β-elimination of 1,1,2-TCA would have yielded VC as a dechlorination product, as reported

earlier for CMC-nZVI (Koenig et al., 2016). The slight increase in VC concentrations during the middle phase of the nZVI treatment experiment (Figure 5-2E) may be partially attributed to 1,1,2-TCA dechlorination, although VC increases could also be due to dechlorination of other chlorinated ethenes. In the case of Pd-nZVI, VC was dechlorinated without any accumulation, even if it was produced. Ethane and ethene are proposed as the end products. Song and Carraway has reported ethane as the sole observed product for 1,1,2-TCA dechlorination by bare nZVI (Song and Carraway, 2005a).

Chlorinated Ethenes – There was almost complete removal of PCE by Pd- nZVI, whereas only 55% PCE was removed by nZVI (Figure 9-4B, Appendix C). TCE dechlorination by nZVI started after a lag phase of 76 hours with total reduction of 94% at 35 days (Figure 5-2D). TCE removal by Pd-nZVI was much faster than nZVI and complete reduction occurred within 24 days. Significant VC removal by nZVI was noticed at t = 35d (Figure 5-2E) when the dechlorination of other more chlorinated compounds (1,1,2-TCA, TCE & PCE) ceased completely. 28% VC was removed at the end of the experiment. This delay in the VC dechlorination could either be due to a lag phase or the continuous release of VC as a dechlorination product but with its simultaneous removal. An immediate decrease in VC concentrations was observed in the Pd-nZVI treatment with 97% removal at 35 days (Figure 5-2E). Initial DCEs concentrations (≤12 μM) were much lower than the other chlorinated ethenes (Table 5-1). 1,1-DCE removal by nZVI was observed after a lag period of 12 days whereas 1,1-DCE dechlorination started immediately for Pd-nZVI (Figure 9-4C, Appendix C). Cis- and Trans- 1,2-DCE concentrations increased and decreased during the experiments for both treatments (Figure 9-4D-E, Appendix C). Traces of DCEs remain in both treatments at the end of the experiment. Dechlorination of chlorinated ethenes is assumed to occur primarily via direct reduction to hydrocarbons with ethane and/or ethene as major end products (Lien and Zhang, 2001; Liu et al., 2005a; Zhang et al., 1998). The fluctation in DCE concentration could be due to dechlorination of PCE and TCE via sequential hydrogenolysis forming lower chlorinated compounds (DCEs and VC) which finally dechlorinate to ethene and ethane (Figure 9-1, Appendix C).

The observed lag phases for some COCs might be due to their competition for reactive sites at the nZVI surface as the reactivity of nZVI towards COCs depends upon various

factors including structural and chemical properties of COCs, their initial concentrations and also environmental conditions (Atisha, 2011; Larson and Weber, 1994; Song and Carraway, 2005a; Song and Carraway, 2006). Dechlorination by nZVI is more favourable for chlorinated ethenes with a higher chlorine number and for chlorinated ethanes with a lower C-Cl bond strength (Lien and Zhang, 2005). Electron affinity of the C-Cl bond and the oxidation state of the carbon atoms in the COCs also affect their reduction by zero valent metals (De Wildeman and Verstraete, 2003; Larson and Weber, 1994).

At the end of the experiment 1,1,2-TCA, PCE, TCE, VC and 1,2-DCA concentrations were still high for the 2.5 g L^{-1} nZVI treatment. This could be due to the slower reactivity of nZVI towards the COCs, where a major portion of nZVI might have been utilized by water reduction. Therefore, another experiment with a higher nZVI loading (5 g L^{-1}) was conducted to treat the groundwater sample (diluted 3 times rather than 1.5 times). As shown in Figure 9-2 (Appendix C) the higher nZVI loading resulted in more complete dechlorination of most COCs although initial COC concentrations were also comparatively lower. The nZVI suspension was still black after 35 days.

Although not tested in this study incremental spiking of the nZVI suspension with borohydride may help limit oxidation and improve the rate and extent of COC dechlorination. Bae et al. reported that addition of $NaBH_4$ into an nZVI suspension resulted in complete reduction of *p*-nitrophenol even after re-using nZVI particles in four conscecutive tests (recycling) and also prevented the oxidation of nZVI in oxygen environments (Bae et al., 2016).

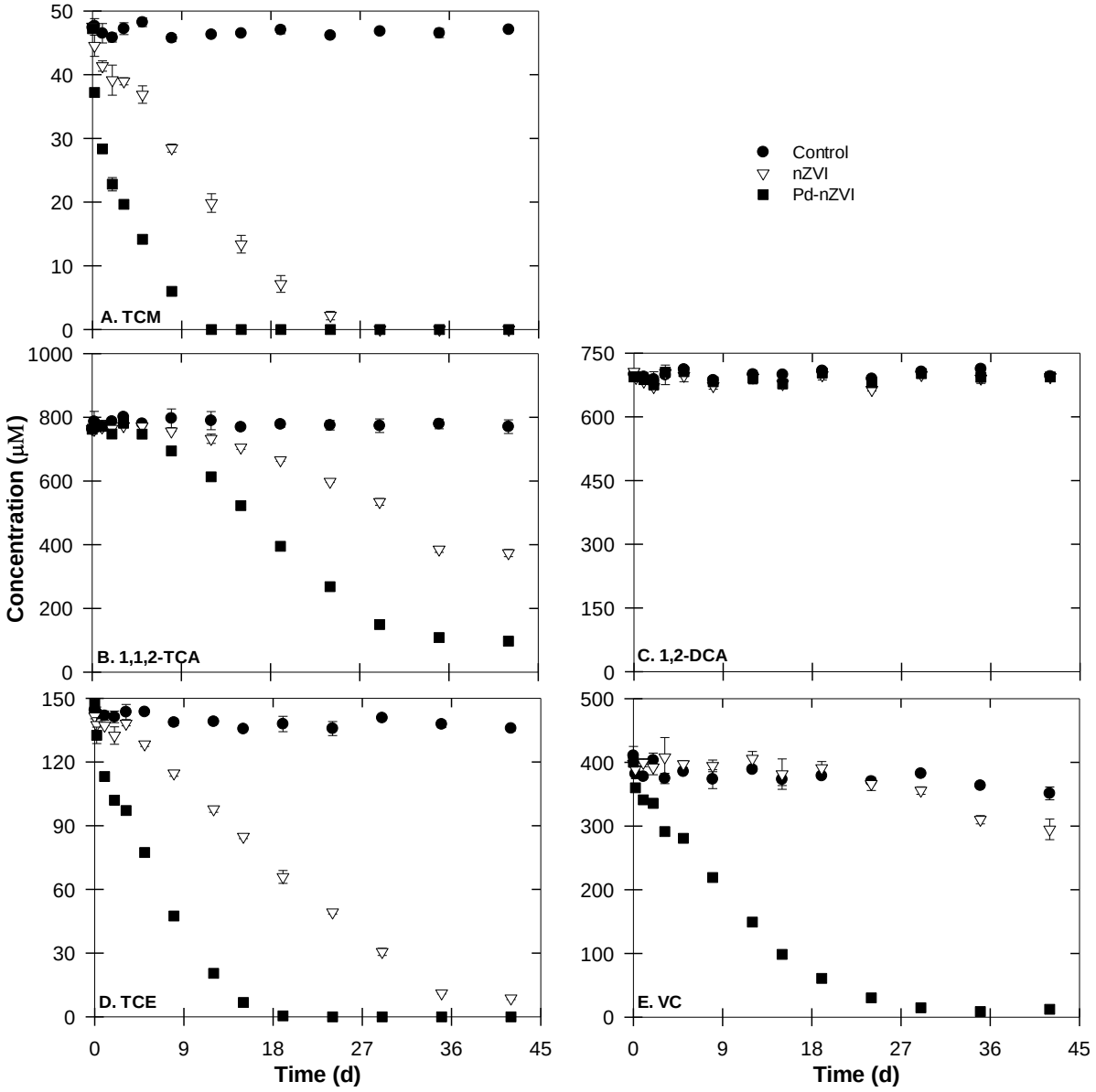

Figure 5-2: Changes in concentrations (µM) of (A) Trichloromethane, (B) 1,1,2-Trichloroethane, (C) 1,2-Dichloroethane, (D) Trichloroethene, and (E) Vinyl Chloride, after treatment with 2.5 g L^{-1} nZVI and Pd-nZVI.

Table 5-1: Concentrations of COCs in the groundwater sample after 42 days of its treatment with 2.5 g L^{-1} nZVI or Pd-nZVI.

Chlorinated Organic Compound	Concentration (µM)		
		Final	
	Initial*	nZVI	Pd-nZVI
Trichloromethane (TCM)	47.4	ND	ND
Dichloromethane (DCM)	1.47	5.24	4.42
1,1,2-Trichloroethane (1,1,2-TCA)	763	374	97.2
1,2-Dichloroethane (1,2-DCA)	700	694	694
Tetrachloroethene (PCE)	13.7	6.15	0.33
Trichloroethene (TCE)	145	8.70	ND
1,1-Dichloroethene (1,1-DCE)	11.2	3.09	2.22
trans-1,2-Dichloroethene (t-1,2-DCE)	2.06	1.85	ND
cis-1,2-Dichloroethene (c-1,2-DCE)	1.29	1.29	1.45
Vinyl Chloride (VC)	411	295	12.4

*Average concentrations in controls.

5.4.2.2 Dechlorination by nZVI-Dithionite and Dithionite alone

nZVI and Pd-nZVI treatments were able to dechlorinate most of the primary COCs with the exception of 1,2-DCA, which was not removed at all. Recently, Nunez Garcia et al. reported successful degradation of 1,2-DCA by coupling nZVI with dithionite (Nunez Garcia et al., 2016a). nZVI coupled with sulfur compounds has also shown enhanced removal of many other organic and inorganic contaminants (Fan et al., 2013; Lipczynskakochany et al., 1994; Rajajayavel and Ghoshal, 2015; Su et al., 2015; Xie and Cwiertny, 2010). Therefore, 2.5 g L^{-1} nZVI coupled with 50 mM dithionite was used to treat the contaminated groundwater sample in this study. Aqueous solutions of dithionite, alone, are also capable of degrading chlorinated solvents and herbicides (Boparai et al., 2006; Nzengung et al., 2001; Rodriguez and Rivera, 1997). Therefore, in order to evaluate the effect of dithionite alone, a treatment of 50 mM dithionite only (i.e. no nZVI) was tested. The dechlorination profiles for the primary and secondary COCs treated by nZVI-dithionite and dithionite alone are shown in Figures 5-3 and 9-5 (Appendix C). The initial and final concentrations of all the COCs are summarized in Table 5-2. COCs are expected to be degraded via both nucleophilic substitution and reductive dechlorination, as reported earlier for S-containing reductants and Fe-S systems (Barbash and Reinhard, 1989a; Boparai et al., 2006; Kuder et al., 2012; Nunez Garcia et al., 2016a; Nzengung et al., 2001; Roberts et al., 1992; Rodriguez and Rivera, 1997). Minor amounts of chloroethane, ethane and ethene were detected in the reactors. However, no detailed product analysis for organo sulfur compounds was performed for these treatments.

Chlorinated Methanes – Unlike nZVI and Pd-nZVI, TCM degradation was slower and incomplete for the nZVI-dithionite (52%) and dithionite (30%) treatments (Figure 5-3A, Table 5-2). TCM removal might be due to both nucleophilic substitution and reductive dechlorination. Since there was no increase in the DCM concentration, it is proposed that TCM reduction may have followed a dihaloelimination direct reduction to chloromethane, or methane, or nucleophilic substitution to organo-sulfur compounds. In the past, lower chlorinated compounds and organo-sulfur compounds have been reported as the degradation products for halomethanes treated by sulfides and Fe-S systems (Lipczynskakochany et al., 1994; Nriagu, 1987; Roberts et al., 1992). Due to storage, the

time lag between experiments, and sampling losses from the main groundwater storage bottle, DCM losses took place and was undetectable in the control as well as nZVI-dithionite, dithionite, nCu, and nPd treatments.

Chlorinated Ethanes - 1,1,2-TCA dechlorination started after a longer lag period (40 d) than by nZVI and Pd-nZVI, with 19 and 9% removal for nZVI-dithionite and dithionite, respectively (Figure 5-3B, Table 5-2). However, controls were also loosing mass with time (9%), suggesting part of the loss in the treatments might have been due to sampling losses. Different lag periods for nZVI, Pd-nZVI, and nZVI-dithionite are presumably due to changes in the surface chemistry of nZVI which can affect its affinity towards the COCs. Changes in surface composition of nZVI due to dithionite addition have been discussed in the literature (Kim et al., 2011; Nunez Garcia et al., 2016a). nZVI-dithionite and dithionite were able to remove 20 and 9% 1,2-DCA at 64d (Figure 5-3C, Table 5-2). Observed 1,2-DCA dechlorination was quite slow, consistent with the findings of Nunez Garcia et al., who observed 79% 1,2-DCA removal in 386 days using 2.5 g L^{-1} nZVI coupled with 44 mM dithionite (Nunez Garcia et al., 2016a). Removal of chlorinated ethanes is assumed to occur both via reductive dechlorination and nucleophilic substitution, as reported for haloethane degradation by sulfides and Fe-S systems (Barbash and Reinhard, 1989a; Kuder et al., 2012; Nunez Garcia et al., 2016a; Weintraub, 1989). Nunez Garcia et al. detected VC and ethene as the products for 1,1,2-TCA degradation by nZVI-dithionite and ethene for 1,2-DCA degradation (Nunez Garcia et al., 2016a). Unfortunately, unstable and complex organo-sulfur compounds in these relatively long-term experiments could not be monitored.

Chlorinated Ethenes – There was incomplete removal of PCE by both the nZVI-dithionite (36%) and dithionite (39%) treatments (Figure 9-5A, Table 5-2). Nzengung et al. also found incomplete and slow removal of PCE by dithionite alone with accumulation of some TCE (Nzengung et al., 2001). TCE dechlorination by nZVI-dithionite started immediately with 70% removal in 22 days and the reaction ceased thereafter (Figure 5-3D, Table 5-2). In contrast, rapid and complete degradation of TCE was observed by Nunez Garcia et al. which suggests that the presence of high concentrations of co-contaminants, oxygen and other inorganic constituents in groundwater significantly affected the rate and extent of

nZVI-dithionite reactivity (Nunez Garcia et al., 2016a). The dithionite alone treatment was even less effective, with only 25% TCE removal. There was rapid VC removal (35%) by nZVI-dithionite in the first two days with little concentration change thereafter (Figure 5-3E, Table 5-2). That could be due to continuous release and simultaneous dechlorination of VC as a degradation product from the dechlorination of PCE, TCE, and DCEs (Kim et al., 2011; Nunez Garcia et al., 2016a). As for the dithionite treatment, since production of VC as a byproduct from the dechlorination of other COCs was limited due to lower dechlorination efficiencies, there was continuous removal of VC with 70% VC removed in 64 days. Reduction of 1,1-DCE and t-1,2-DCE by both the treatments started immediately and the concentrations plateaued after two days of reaction, presumably due to production along with simultaneous dechlorination (Figure 5-3B-C). However, for the dithionite treatments, complete removal of 1,1-DCE was observed. Degradation of chlorinated ethenes by dithionite and Fe-S systems have been reported to follow a dichloroelimination pathway, with DCEs, VC, and hydrocarbons (ethane, ethene, and ethyne) as the degradation products (Hassan, 2000; Kim et al., 2011; Nzengung et al., 2001; Shiba et al., 2014).

It is worth mentioning that Nunez Garcia et al. were able to regain and boost reactivity of oxidized nZVI by reinjecting dithionite which resulted in continuous dechlorination of 1,2-DCA for over a year (Nunez Garcia et al., 2016a). Therefore, 50 mM dithionite was reinjected after 82 days in the current experiments in order to increase reactivity. However, the extra injected dithionite did not affect the reaction in the subsequent 25 days. Although the nZVI-dithionite suspension was still jet black at the end of the experiment, indicating the presence of zerovalent iron along with iron sulfides, it was comparatively less effective in treating this multi-contaminant system than nZVI and Pd-nZVI, with the exception of 1,2-DCA. nZVI reactivity is enhanced in the Fe-S system but it depends on the thickness and composition of the sulfide layer formed around Fe^0 core which is controlled by the Fe/S ratio, oxygen and solution pH (Fan et al., 2013; Kim et al., 2011; Rajajayavel and Ghoshal, 2015; Su et al., 2015; Xie and Cwiertny, 2010). This sulfide layer acts as an electron conductor for transferring electrons from the Fe^0 core to the contaminants on the surface, however if that layer thickness increases, it would suppress electrons transfer. The lower reactivity of nZVI-dithionite in the present study could be due to a high S/Fe ratio

and/or the presence of oxygen in the groundwater. The self-decomposition/disproportionation reactions of dithionite in aqueous solutions can also be influenced by the presence of dissolved oxygen, pH and other groundwater constituents forming undesired sulfur species which in turn affect the reactivity of nZVI-dithionite and dithionite alone treatments.

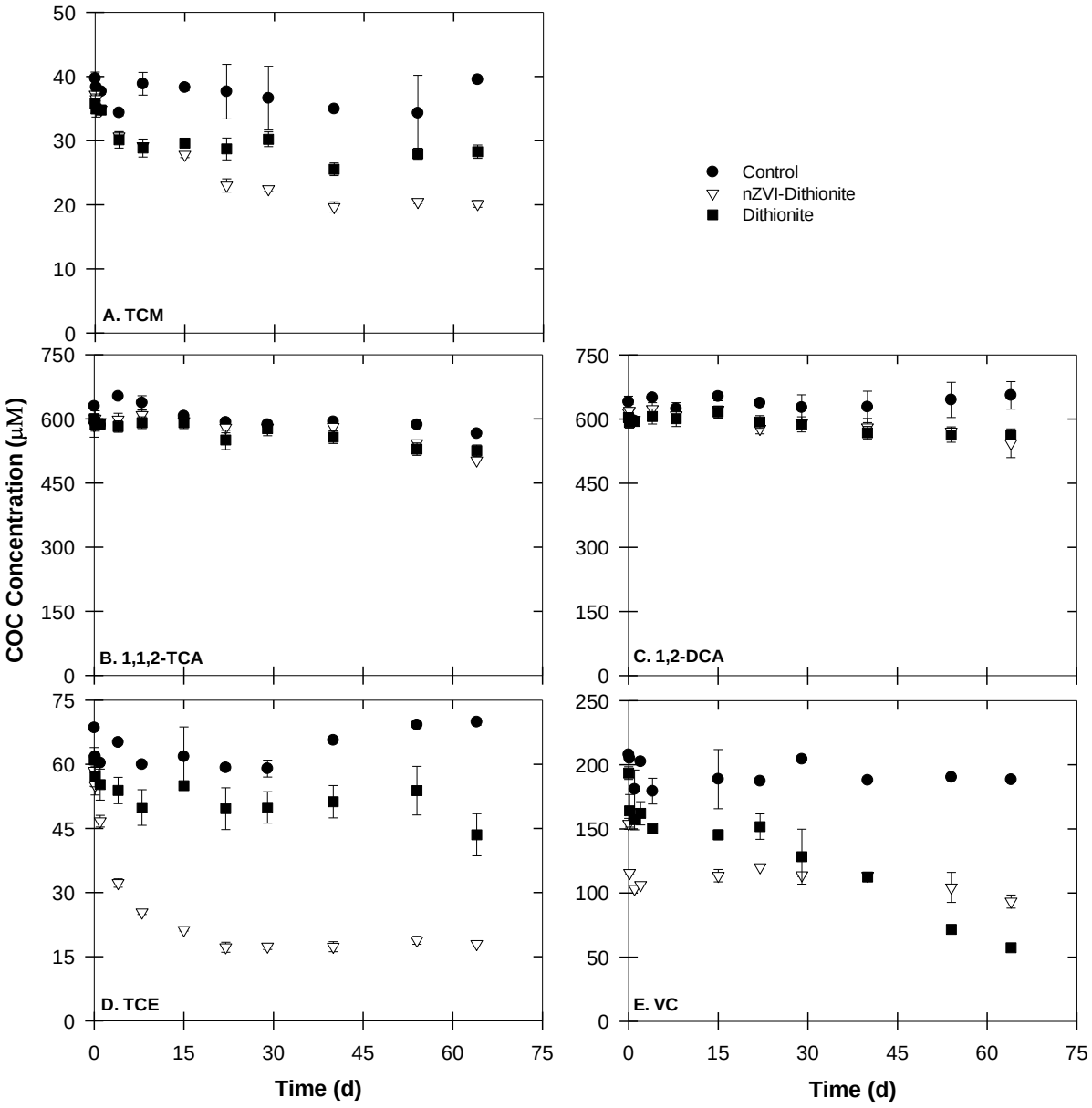

Figure 5-3: Changes in concentrations (µM) of (A) Trichloromethane, (B) 1,1,2-Trichloroethane, (C) 1,2-Dichloroethane, (D) Trichloroethene, and (E) Vinyl Chloride after treatment with 2.5 g L^{-1} nZVI-dithionite and 50 mM Dithionite.

Table 5-2: Concentrations of COCs in the groundwater sample after 64 days of its treatment with 2.5 g L^{-1} nZVI-dithionite or 50 mM Dithionite alone.

Chlorinated Organic Compound	Concentration (μM)		
		Final	
	Initial*	nZVI-dithionite[a]	Dithionite
Trichloromethane (TCM)	39.7	20.1	28.3
Dichloromethane (DCM)	ND	ND	ND
1,1,2-Trichloroethane (1,1,2-TCA)	630	503	526
1,2-Dichloroethane (1,2-DCA)	640	543	563
Tetrachloroethene (PCE)	5.68	2.71	3.72
Trichloroethene (TCE)	68.5	18.0	43.5
1,1-Dichloroethene (1,1-DCE)	5.71	1.69	ND
trans-1,2-Dichloroethene (t-1,2-DCE)	0.90	0.44	0.50
Vinyl Chloride (VC)	208	93.4	57.3

*Average concentrations in controls.
[a]50 mM dithionite was reinjected on t=82d but no further dechlorination of COCs was observed for next 25 days.

5.4.2.3 Dechlorination by nPd-borohydride and nCu-borohydride

Nano metal-borohydride systems utilize borohydride as a H_2 source over the nano metal (nPd or nCu) catalyst surface, where H_2 gas is readily generated through the hydrolysis of borohydride, as shown in the previous chapters and literature studies (Huang et al., 2012; Rostamikia and Janik, 2010). For the nPd-borohydride treatment, excess borohydride present in the solution during synthesis of Pd nanoparticles is utilized. However, the nCu-borohydride treatment is coupled with an additional 25 mM borohydride. These treatments were much faster than nZVI, Pd-nZVI and nZVI-dithionite and removed most of the COCs in less than two days without forming any chlorinated intermediates. Direct reduction to ethane was the observed pathway, in agreement with the previous studies (Huang et al., 2012; Huang et al., 2011; Liu et al., 2008). The dechlorination profiles are shown in Figure 5-4, and the initial and final COCs concentrations are summerzied in Table 5-3.

Chlorinated Methanes - There was complete removal of TCM by both treatments within two hours (Table 5-3). Previous studies have also reported this rapid degradation of chlorinated methanes by nCu catalyst via catalyzed reductive dechlorination (Huang et al., 2012; Huang et al., 2013; Lin et al., 2005). In the present study, TCM is assumed to degrade mainly via direct reduction to methane, as no increase in DCM concentration was observed.

Chlorinated Ethanes – 70% 1,1,2-TCA was removed in the first hour by nPd-borohydride (Figure 5-4A). The reaction continued for 24 hours resulting in 93% removal with the reaction ceasing thereafter. No significant dechlorination of 1,2-DCA was observed for the first six days (Figure 5-4B). These results are not consistent with the previously reported Pd catalyzed dechlorination of 1,2-DCA in deionized water where >43% of 1,2-DCA (C_0 = 65 mg L^{-1}) was dechlorinated within 7 days and 93% within 40 days (Chapter 3, Exp.15, Table 3-1). In the present study, the limited 1,2-DCA dechlorination might be due to the presence of co-contaminants which are more easily degraded preferentially consuming all H_2 present (De Wildeman and Verstraete, 2003). Therefore, a 25 mM borohydride (i.e., as the hydrogen source) was spiked into the treatment after 6 days. This resulted in removing the residual 7% of 1,1,2-TCA (Figure 5-4A, Table 5-3). Only 28% 1,2-DCA was removed in 40 days after spiking the H_2 source (Figure 5-4B). Therefore, another injection of 50 mM borohydride was spiked into the nPd-borohydride reactors on the 46th day. After this

injection degradation occurred over only one additional day, before ceasing, with an additional 15% 1,2-DCA removal. After another 9 days, 75 mM borohydride was spiked into the treatment (t = 56 d). This resulted in a further 11% (total 55%) removal of 1,2-DCA prior to reaction cessation. It was clear that the efficiency of the injected H_2 was decreasing with time and its concentration did not correlate with dechlorination efficiency.

nCu-borohydride was faster in removing 1,1,2-TCA with complete removal in two hours (Figure 5-4A). 1,2-DCA dechlorination ceased after one day with only 29% removal (Figure 5-4B), in agreement with previous findings (Chapter 4, Exp.1, Table 4-1). Additional injections of 25, 50, 75, and 75 mM on days 6, 10, 14 and 20 resulted in additional removal of 1,2-DCA with a final dechlorination of 95% in 22 days.

Ethane was detected as the immediate major, and final degradation product for these nano metal-borohydride treatments. Trace amounts of ethene and chloroethane were also detected during reaction. This indicates direct reduction to ethane as the major pathway for dechlorination by these nano metal-borohydride treatments. Some removal of these chlorinated ethanes might have occurred via sequential hydrogenolysis and dichloroelimination by forming chloroethane and ethene, respectively. Due to the presence of excessive H_2, hydrogenation of ethene to ethane cannot be ignored. Huang et al. also found ethane as the major product with traces of ethene while degrading 1,2-DCA with bare nCu particles coupled with borohydride (Huang et al., 2011).

Chlorinated Ethenes – All the chlorinated ethenes (PCE, TCE, 1,1-DCE, cis, trans 1,2-DCE, and VC) were completely removed within less than 48 hours by both nPd- and nCu-borohydride treatments, with some completely removed within the first hour (Table 5-3). It is assumed that these compounds are degraded via hydrogenolysis to form ethene (with or without producing any chlorinated intermediates) which then transforms to ethane via hydrogenation. Liu et al. also observed complete hydrodechlorination of TCE by nPd/H_2 gas within 10 minutes of reaction with no chlorinated intermediates formation (Liu et al., 2008).

In the nPd-borohydride treatment, Pd deactivation may be related to the inhibitory effect of hydrogen halides (HCl) formed as a byproduct, site blockage due to high concentrations

of surface species (adsorbed COCs), carbon depositions (such as ethane, ethene) during dechlorination reactions, groundwater constituents (HCO_3^-, CO_3^{2-}, SO_4^{2-}, Cl^-, S^{2-} etc.), redox active metals, mineral precipitates, organic matter, and microbial activity (Aramendia et al., 2002; Lecloux, 1999; Lowry and Reinhard, 2000; Mackenzie et al., 2006; Munakata and Reinhard, 2007; Sun et al., 2011; Urbano and Marinas, 2001). Many researchers have reported inhibition of Pd catalyst by HCl formed during dechlorination of COCs in liquid-phase processes, in addition to free chlorides present in the groundwater (Aramendia et al., 2002; Lowry and Reinhard, 2000; Mackenzie et al., 2006; Munakata and Reinhard, 2007; Sun et al., 2011; Urbano and Marinas, 2001). The extremely high Cl^- concentration (16,600 mg L^{-1}) of this groundwater might have affected the dechlorination activity of nPd particles by poisoning the reactive surface. Pd surfaces blocked by chlorides can be regenerated by addition of a base (e.g. NaOH, NH_3^-) to the reaction medium (Schüth et al., 2004; Sun et al., 2011; Urbano and Marinas, 2001). Sulfates (130 mg L^{-1}) in the groundwater, which might be reduced to sulfides by borohydride, can also inhibit Pd catalytic functions by forming a layer around the nPd particles and inhibiting COCs adsorption (Chaplin et al., 2006; Chaplin et al., 2007; Lowry and Reinhard, 2000; Mackenzie et al., 2006; Munakata and Reinhard, 2007). However, Pd can be successfully regenerated from sulfur poisoning by strong oxidants including $HOCl/OCl^-$, H_2O_2, $KMnO_4$, and dissolved oxygen (Chaplin et al., 2006; Chaplin et al., 2007; Lowry and Reinhard, 2000; Mcnab et al., 2000; Munakata and Reinhard, 2007; Schüth et al., 2004). The possibility of sulfate-reducing bacteria growing in the presence of H_2 gas producing sulfides which poisons Pd, is unlikely but cannot be ruled out (Davie et al., 2008; Lecloux, 1999; Lowry and Reinhard, 2000; Schüth et al., 2004). Lowry & Reinhard have reported that sulfate-reducing bacteria grew in a bench scale treatment of contaminated groundwater due to the abundance of H_2 gas producing sulfides that partially deactivated the Pd catalyst (Lowry and Reinhard, 2000). Reactivity could be restored through injections of dilute sodium hypochlorite solutions (Davie et al., 2008). Catalyst deactivation can also be caused by dissolved organic matter present in the groundwater which competes with COCs for active sites (Chaplin et al., 2006). Determining which groundwater constituents affect nano metal performance is important for implementation of this technology in the field.

In the nCu-borohydride treatment also, it was noticed that the increased concentration of $NaBH_4$ was not linearly correlated to the decrease in 1,2-DCA concentration. Groundwater constituents like chlorides, sulfates, humic acid and dissolved oxygen might have altered the chemical state or surface composition of nCu or sorb to its surface during reactivity experiments resulting in its deactivation, as indicated in the previous chapter and literature studies (Śrębowata et al., 2011; Twigg and Spencer, 2001).

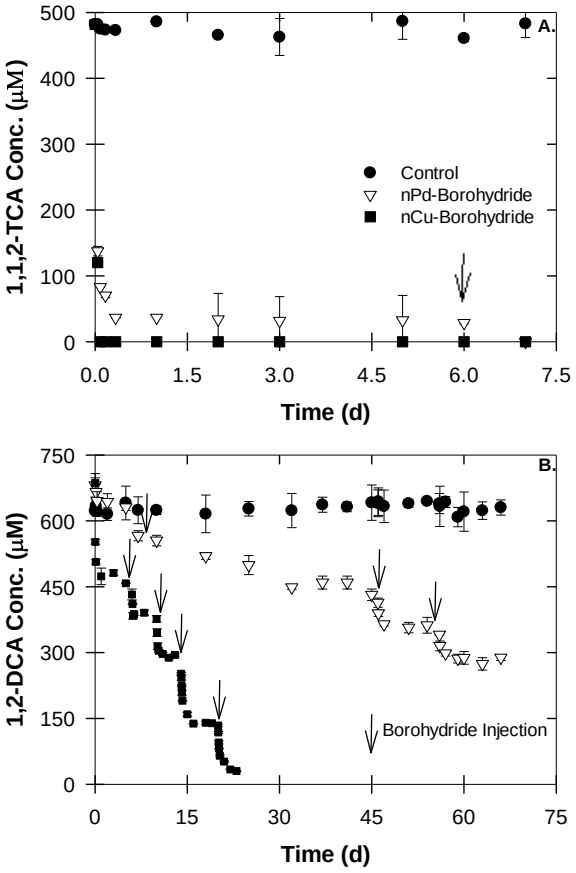

Figure 5-4: Changes in concentration Changes in concentrations (µM) of (A) 1,1,2-Trichloroethane and (B) 1,2-Dichloroethane after treatment with 1.0 g L^{-1} nPd Borohydride or nCu-Borohydride s (µM) of (A) 1,1,2-Trichloroethane and (B) 1,2-Dichloroethane after treatment with 1.0 g L^{-1} nPd-Borohydride or nCu-Borohydride. The arrows indicate borohydride injections.

Table 5-3: Concentrations of COCs in the groundwater sample after three days of its treatment with 1.0 g L^{-1} nPd-borohydride or nCu-borohydride.

Chlorinated Organic Compound	Concentration (µM)		
		Final	
	Initial *	nPd-borohydride[a]	nCu-borohydride[b]
Trichloromethane (TCM)	28.9	ND	ND
Dichloromethane (DCM)	ND	ND	ND
1,1,2-Trichloroethane (1,1,2-TCA)	482	31.8[c]	ND
1,2-Dichloroethane (1,2-DCA)	681	645[d]	482[e]
Tetrachloroethene (PCE)	10.1	ND	ND
Trichloroethene (TCE)	38.4	ND	ND
1,1-Dichloroethene (1,1-DCE)	1.32	ND	ND
trans-1,2-Dichloroethene (t-1,2-DCE)	0.32	ND	ND
Vinyl Chloride (VC)	54.5	ND	ND

*Average concentration in controls.
[a]Additional 25, 50, and 75 mM borohydride was injected on days 6, 46, and 56 respectively.
[b]Additional 25, 50, 75, and 75 mM borohydride was injected on days 6, 10, 14 and 20 respectively.
[c]1,1,2-TCA was completely removed on t = 7d.
[d] 1,2-DCA concentration decreased to 274 µM on t = 63d.
[e]1,2-DCA concentration decreased to 34 µM on t = 22d.

5.5 Conclusions and Recommendations

In the last two decades, many chemical remediation technologies have been developed and implemented at various contaminated sites to treat COCs. However, so far none of these technologies have been successful in degrading the recalcitrant compounds such as 1,2-DCA and DCM. The present study has tested five nano metal-based technologies to treat groundwater contaminated with a mixture of COCs. Both nZVI and Pd-nZVI were effective in breaking down the majority of the contaminants, with the exception of 1,2-DCA. Complete oxidation of nZVI, and Pd-nZVI treatments was observed at the end of the experiments. Although not tested in this study, respiking the oxidized nZVI suspension with borohydride may regenerate nZVI to its zerovalent state, making it reactive towards COCs. nZVI-dithionite was able to break down all COCs including 20% 1,2-DCA. Re-spiking of dithionite was unable to boost the reduction reaction. More work is therefore required to determine the cause of the reduced reactivity. Dithionite preserved nZVI in its reduced form even after 120 days. The novel technology of combining Pd or Cu nanoparticles with multiple injections of borohydride was able to significantly degrade 1,2-DCA along with rapid and complete dechlorination of all other COCs. The absence of any chlorinated intermediates is advantageous. Of concern is the deactivation of nPd and nCu requiring multiple borohydride injections. Given the significant reactivity of these nano metals there is the possibility of *in situ* manipulation of oxidized forms of these metals at sites co-contaminated with metallic ions (e.g. Cu^{2+}, Ni^{2+}). This would involve reducing these metals with borohydride, or other reductants, to their zero valent form and utilizing them for treating the COCs. Also, Given the high cost of nPd and nCu metals, applying these metals in reactive barriers along with injections of hydrogen donors (i.e. borohydride) up stream is suggested to be a promising extrapolation from these nano metals technologies.

To conclude, these findings suggest that these nano metal based technologies seems to be effective remediation approaches that need further investigation. Evaluating and understanding the effects of GW chemistry on the electronic state of the metals, on dithionite disproportion products, and on the thickness of iron sulfide layer in the nZVI-dithionite treatment is key to successful implementation of these treatments. The choice of

remediation technology to be implemented in the field strongly depends on the type and concentration of contaminant, presence of co-contaminants, geochemical properties of the water and microbial characteristics, timeline, and economical considerations.

5.6 References

Aramendia, M. et al., 2002. Liquid-phase hydrodechlorination of chlorobenzene over palladium-supported catalysts: Influence of HCl formation and NaOH addition. Journal of Molecular Catalysis A: Chemical, 184(1): 237-245.

Arnold, W.A. and Roberts, A.L., 2000a. Pathways and kinetics of chlorinated ethylene and chlorinated acetylene reaction with Fe (0) particles. Environmental Science & Technology, 34(9): 1794-1805.

Atisha, A., 2011. Degradation of 1,2-Dichloroethane With Nano-Scale Zero Valent Iron Particles, Western Ontario, 111 pp.

ATSDR, 2015. Detailed data table for the 2015 priority list of hazardous substances that will be the subject of toxicological profiles. Agency for Toxic Substances and Disease Registry, Atlanta, GA. https://www.atsdr.cdc.gov/spl/resources/atsdr_2015_spl_detailed_data_table.pdf. Accessed 19 May, 2016.

Bae, S., Gim, S., Kim, H. and Hanna, K., 2016. Effect of $NaBH_4$ on properties of nanoscale zero-valent iron and its catalytic activity for reduction of *p*-nitrophenol. Applied Catalysis B: Environmental, 182: 541-549.

Barbash, J.E. and Reinhard, M., 1989a. Abiotic Dehalogenation of 1,2-Dichloroethane and 1,2-Dibromoethane in Aqueous-Solution Containing Hydrogen-Sulfide. Environmental Science & Technology, 23(11): 1349-1358.

Barnes, R.J. et al., 2010. Optimization of nano-scale nickel/iron particles for the reduction of high concentration chlorinated aliphatic hydrocarbon solutions. Chemosphere, 79(4): 448-454.

Boparai, H.K., Comfort, S.D., Shea, P.J. and Szecsody, J.E., 2008. Remediating explosive-contaminated groundwater by in situ redox manipulation (ISRM) of aquifer sediments. Chemosphere, 71(5): 933-941.

Boparai, H.K., Shea, P.J., Comfort, S.D. and Snow, D.D., 2006. Dechlorinating chloroacetanilide herbicides by dithionite-treated aquifer sediment and surface soil. Environmental Science & Technology, 40(9): 3043-3049.

Borovkov, V.Y., Luebke, D.R., Kovalchuk, V.I. and d'Itri, J.L., 2003. Hydrogen-assisted 1, 2-dichloroethane dechlorination catalyzed by Pt-Cu/SiO2: Evidence for different functions of Pt and Cu sites. The Journal of Physical Chemistry B, 107(23): 5568-5574.

Chaplin, B.P. et al., 2012. Critical Review of Pd-Based Catalytic Treatment of Priority Contaminants in Water. Environmental Science & Technology, 46(7): 3655-3670.

Chaplin, B.P., Roundy, E., Guy, K.A., Shapley, J.R. and Werth, C.J., 2006. Effects of natural water ions and humic acid on catalytic nitrate reduction kinetics using an alumina supported Pd-Cu catalyst. Environmental science & technology, 40(9): 3075-3081.

Chaplin, B.P., Shapley, J.R. and Werth, C.J., 2007. Regeneration of sulfur-fouled bimetallic Pd-based catalysts. Environmental science & technology, 41(15): 5491-5497.

Conrad, H., Ertl, G. and Latta, E.E., 1974. Adsorption of hydrogen on palladium single crystal surfaces. Surface Science, 41(2): 435-446.

Davie, M.G., Cheng, H., Hopkins, G.D., LeBron, C.A. and Reinhard, M., 2008. Implementing heterogeneous catalytic dechlorination technology for remediating TCE-contaminated groundwater. Environmental science & technology, 42(23): 8908-8915.

De Wildeman, S. and Verstraete, W., 2003. The quest for microbial reductive dechlorination of C 2 to C 4 chloroalkanes is warranted. Applied microbiology and biotechnology, 61(2): 94-102.

Dolfing, J., Van Eekert, M., Seech, A., Vogan, J. and Mueller, J., 2007. In situ chemical reduction (ISCR) technologies: Significance of low Eh reactions. Soil & Sediment Contamination, 17(1): 63-74.

Elliott, D.W. and Zhang, W.-X., 2001. Field assessment of nanoscale bimetallic particles for groundwater treatment. Environmental Science & Technology, 35(24): 4922-4926.

Fan, D. et al., 2013. Reductive sequestration of pertechnetate ($^{99}TcO_4^-$) by nano zerovalent iron (nZVI) transformed by abiotic sulfide. Environmental Science & Technology, 47: 5302-5310.

Feng, J. and Lim, T.-T., 2005. Pathways and kinetics of carbon tetrachloride and chloroform reductions by nano-scale Fe and Fe/Ni particles: comparison with commercial micro-scale Fe and Zn. Chemosphere, 59: 1267-1277.

Fruchter, J.S. et al., 2000. Creation of a subsurface permeable treatment zone for aqueous chromate contamination using in situ redox manipulation. Ground Water Monitoring and Remediation, 20(2): 66-77.

Hassan, S.M., 2000. Reduction of halogenated hydrocarbons in aqueous media: I. Involvement of sulfur in iron catalysis. Chemosphere, 40(12): 1357-1363.

Huang, C.-C., Lo, S.-L. and Lien, H.-L., 2012. Zero-valent copper nanoparticles for effective dechlorination of dichloromethane using sodium borohydride as a reductant. Chemical Engineering Journal, 203: 95-100.

Huang, C.-C., Lo, S.-L. and Lien, H.-L., 2013. Synergistic effect of zero-valent copper nanoparticles on dichloromethane degradation by vitamin B_{12} under reducing condition. Chemical Engineering Journal, 219: 311-318.

Huang, C.-C., Lo, S.-L., Tsai, S.-M. and Lien, H.-L., 2011. Catalytic hydrodechlorination of 1, 2-dichloroethane using copper nanoparticles under reduction conditions of sodium borohydride. Journal of Environmental Monitoring, 13(9): 2406-2412.

Kim, E.J., Kim, J.H., Azad, A.M. and Chang, Y.S., 2011. Facile Synthesis and Characterization of Fe/FeS Nanoparticles for Environmental Applications. Acs Applied Materials & Interfaces, 3(5): 1457-1462.

Kim, H.-S., Ahn, J.-Y., Kim, C., Lee, S. and Hwang, I., 2014. Effect of anions and humic acid on the performance of nanoscale zero-valent iron particles coated with polyacrylic acid. Chemosphere, 113: 93-100.

Koenig, J.C. et al., 2016. Particles and enzymes: Combining nanoscale zero valent iron and organochlorine respiring bacteria for the detoxification of chloroethane mixtures. Journal of Hazardous Materials, 308: 106-112.

Kopinke, F.-D., Mackenzie, K. and Köhler, R., 2003. Catalytic hydrodechlorination of groundwater contaminants in water and in the gas phase using Pd/γ-Al 2 O 3. Applied Catalysis B: Environmental, 44(1): 15-24.

Kuder, T., Wilson, J.T., Philp, P. and He, Y.T., 2012. Carbon Isotope Fractionation in Reactions of 1,2-Dibromoethane with FeS and Hydrogen Sulfide. Environmental Science & Technology, 46(14): 7495-7502.

Lambert, S., Ferauche, F., Brasseur, A., Pirard, J.-P. and Heinrichs, B., 2005. Pd–Ag/SiO 2 and Pd–Cu/SiO 2 cogelled xerogel catalysts for selective hydrodechlorination of 1, 2-dichloroethane into ethylene. Catalysis today, 100(3): 283-289.

Larson, R.A. and Weber, E.J., 1994. Reaction mechanisms in environmental organic chemistry. CRC press, Boca Raton, FL.

Lecloux, A.J., 1999. Chemical, biological and physical constrains in catalytic reduction processes for purification of drinking water. Catalysis Today, 53(1): 23-34.

Lien, H.-L. and Zhang, W.-X., 2001. Nanoscale iron particles for complete reduction of chlorinated ethenes. Colloids and Surfaces A: Physicochemical and Engineering Aspects, 191(1): 97-105.

Lien, H.-L. and Zhang, W.-X., 2005. Hydrodechlorination of chlorinated ethanes by nanoscale Pd/Fe bimetallic particles. Journal of environmental engineering, 131(1): 4-10.

Lien, H.L. and Zhang, W.X., 1999. Transformation of chlorinated methanes by nanoscale iron particles. Journal of Environmental Engineering-Asce, 125(11): 1042-1047.

Lim, T.T. and Feng, J., 2007. Iron-mediated reduction rates and pathways of halogenated methanes with nanoscale Pd/Fe: Analysis of linear free energy relationship. Chemosphere, 66(9): 1765-1774.

Lin, C.J., Lo, S.L. and Liou, Y.H., 2005. Degradation of aqueous carbon tetrachloride by nanoscale zerovalent copper on a cation resin. Chemosphere, 59(9): 1299-1307.

Lipczynskakochany, E., Harms, S., Milburn, R., Sprah, G. and Nadarajah, N., 1994. Degradation of Carbon-Tetrachloride in the Presence of Iron and Sulfur-Containing-Compounds. Chemosphere, 29(7): 1477-1489.

Liu, J., He, F., Durham, E., Zhao, D. and Roberts, C.B., 2008. Polysugar-stabilized Pd nanoparticles exhibiting high catalytic activities for hydrodechlorination of environmentally deleterious trichloroethylene. Langmuir, 24: 328-336.

Liu, W.-J., Qian, T.-T. and Jiang, H., 2014a. Bimetallic Fe nanoparticles: Recent advances in synthesis and application in catalytic elimination of environmental ppollutants. Chemical Engineering Journal, 236: 448-463.

Liu, Y., Choi, H., Dionysiou, D. and Lowry, G.V., 2005a. Trichloroethene hydrodechlorination in water by highly disordered monometallic nanoiron. Chemistry of Materials, 17(21): 5315-5322.

Liu, Y., Yang, F., Yue, P. and Chen, G., 2001. Catalytic dechlorination of chlorophenols in water by palladium/iron. Water Research, 35: 1887-1890.

Lowry, G.V. and Reinhard, M., 2000. Pd-catalyzed TCE dechlorination in groundwater: Solute effects, biological control, and oxidative catalyst regeneration. Environmental Science & Technology, 34(15): 3217-3223.

Mackenzie, K., Frenzel, H. and Kopinke, F.-D., 2006. Hydrodehalogenation of halogenated hydrocarbons in water with Pd catalysts: Reaction rates and surface competition. Applied Catalysis B: Environmental, 63(3): 161-167.

Mcnab, W.W., Ruiz, R. and Reinhard, M., 2000. In-situ destruction of chlorinated hydrocarbons in groundwater using catalytic reductive dehalogenation in a reactive well: Testing and operational experiences. Environmental Science & Technology, 34(1): 149-153.

Munakata, N. and Reinhard, M., 2007. Palladium-catalyzed aqueous hydrodehalogenation in column reactors: Modeling of deactivation kinetics with sulfide and comparison of regenerants. Applied Catalysis B: Environmental, 75(1–2): 1-10.

Nriagu, J.O., 1987. Sulphur in the Environment. Part II. Wiley-Interscience Publications, New York.

Nunez Garcia, A., Boparai, H.K. and O'Carroll, D.M., 2016a. Enhanced dechlorination of 1,2-dichloroethane by coupled nano iron-dithionite treatment. Environmental Science & Technology, 50(10): 5243-5251.

Nzengung, V.A., Castillo, R.M., Gates, W.P. and Mills, G.L., 2001. Abiotic transformation of perchloroethylene in homogeneous dithionite solution and in suspensions of dithionite-treated clay minerals. Environmental Science & Technology, 35(11): 2244-2251.

O'Carroll, D., Sleep, B., Krol, M., Boparai, H. and Kocur, C., 2013. Nanoscale zero valent iron and bimetallic particles for contaminated site remediation. Advances in Water Resources, 51: 104-122.

Rajajayavel, S.R.C. and Ghoshal, S., 2015. Enhanced reductive dechlorination of trichloroethylene by sulfidated nanoscale zerovalent iron. Water Research, 78: 144-153.

Roberts, A.L., Sanborn, P.N. and Gschwend, P.M., 1992. Nucleophilic-Substitution Reactions of Dihalomethanes with Hydrogen-Sulfide Species. Environmental Science & Technology, 26(11): 2263-2274.

Rodriguez, J.C. and Rivera, M., 1997. Reductive dehalogenation of carbon tetrachloride by sodium dithionite. Chemistry Letters(11): 1133-1134.

Rostamikia, G. and Janik, M.J., 2010. Direct borohydride oxidation: mechanism determination and design of alloy catalysts guided by density functional theory. Energy & Environmental Science, 3(9): 1262-1274.

Sakulchaicharoen, N., O'Carroll, D.M. and Herrera, J.E., 2010. Enhanced stability and dechlorination activity of pre-synthesis stabilized nanoscale FePd particles. Journal of contaminant hydrology, 118(3): 117-127.

Schüth, C., Kummer, N.-A., Weidenthaler, C. and Schad, H., 2004. Field application of a tailored catalyst for hydrodechlorinating chlorinated hydrocarbon contaminants in groundwater. Applied Catalysis B: Environmental, 52(3): 197-203.

Scully, J. and Graedel, T.E., 1987. Copper Patina FormationCopper patinas formed in the atmosphere—II. A qualitative assessment of mechanisms. Corrosion Science, 27(7): 721-740.

Shiba, M., Uddin, M.A., Kato, Y. and Ono, T., 2014. Degradation of chlorinated organic compounds by mixed particles of iron/iron sulfide or iron/iron disulfide. Materials Transactions, 55(4): 708-712.

Song, H. and Carraway, E.R., 2005a. Reduction of chlorinated ethanes by nanosized zero-valent iron: kinetics, pathways, and effects of reaction conditions. Environmental science & technology, 39(16): 6237-6245.

Song, H. and Carraway, E.R., 2006. Reduction of chlorinated methanes by nano-sized zero-valent iron. Kinetics, pathways, and effect of reaction conditions. Environmental Engineering Science, 23(2): 272-284.

Śrębowata, A., Lisowski, W., Sobczak, J.W. and Karpiński, Z., 2011. Hydrogen-assisted dechlorination of 1,2-dichloroethane on active carbon supported palladium–copper catalysts. Catalysis Today, 175(1): 576-584.

Su, Y. et al., 2015. Magnetic sulfide-modified nanoscale zerovalent iron (S-nZVI) for dissolved metal ion removal. Water Research, 74: 47-57.

Sun, C. et al., 2011. A Highly Active Pd on Ni–B Bimetallic Catalyst for Liquid-Phase Hydrodechlorination of 4-Chlorophenol Under Mild Conditions. Catalysis letters, 141(6): 792-798.

Tobiszewski, M. and Namieśnik, J., 2012. Abiotic degradation of chlorinated ethanes and ethenes in water. Environmental Science and Pollution Research, 19(6): 1994-2006.

Twigg, M.V. and Spencer, M.S., 2001. Deactivation of supported copper metal catalysts for hydrogenation reactions. Applied Catalysis A: General, 212(1): 161-174.

Urbano, F. and Marinas, J., 2001. Hydrogenolysis of organohalogen compounds over palladium supported catalysts. Journal of Molecular Catalysis A: Chemical, 173(1): 329-345.

USEPA, 2015. Priority pollutant list. United States Environmental Protection Agency. https://www.epa.gov/sites/production/files/2015-09/documents/priority-pollutant-list-epa.pdf. Accessed 19 May, 2016.

Vadlamannati, L.S., Kovalchuk, V.I. and d'Itri, J.L., 1999. Dechlorination of 1, 2-dichloroethane catalyzed by Pt–Cu/C: unraveling the role of each metal. Catalysis letters, 58(4): 173-178.

Wang, X.Y., Chen, C., Chang, Y. and Liu, H.L., 2009. Dechlorination of chlorinated methanes by Pd/Fe bimetallic nanoparticles. Journal of Hazardous Materials, 161(2-3): 815-823.

Weintraub, R.A., 1989. Transformations of ethylene dibromide in aqueous systems and groundwater. Ph.D. Dissertation Thesis, University of Florida, Gainesville, FL.

Xie, Y. and Cwiertny, D.M., 2010. Use of Dithionite to Extend the Reactive Lifetime of Nanoscale Zero-Valent Iron Treatment Systems. Environmental Science & Technology, 44(22): 8649-8655.

Yu, F., 2013. Abiotic Degradation of Chlorinated Hydrocarbons (CHCs) with Zero-Valent Magnesium (ZVM) and Zero-Valent Palladium/Magnesium Bimetallic (Pd/Mg)-Reductant, Wright State University.

Zhang, W.X., Wang, C.B. and Lien, H.L., 1998. Treatment of chlorinated organic contaminants with nanoscale bimetallic particles. Catalysis Today, 40(4): 387-395.

Chapter 6

6 Conclusions, Implications, and Future Work

6.1 Summary and Conclusions

Chlorinated organic compounds (COCs) are amongst the most prevalent groundwater contaminants found at hazardous sites throughout the world. Possible carcinogenicity and recalcitrance towards abiotic dechlorination has created considerable interest in developing novel remediation technologies. Reductive dechlorination by monometallic nano zero valent iron (nZVI) or bimetallic (Pd-nZVI), has proven to be successful field applicable remediation approaches, nonetheless failed to break down 1,2-Dichlororethane (1,2-DCA). Gas-phase catalyzed reductive dechlorination has been found to effectively dechlorinate 1,2-DCA via activated hydrogen (H_2) gas on a catalyst surface, however due to high operating temperatures, this technology is impractical for field applications. On the other hand, limited research has been done on the liquid-phase catalyzed reductive dechlorination of 1,2-DCA. This thesis presents the development of nano metal catalyzed reductive dechlorination technology capable of reducing 1,2-DCA along with other COCs in the liquid phase.

In the first study, the feasibility of catalyzed hydrodechlorination of 1,2-DCA in the liquid phase using borohydride as a H_2 source over Pd nanoparticles (nPd) was investigated in batch reactivity experiments. nPd particles were synthesized via aqueous chemical reduction by sodium borohydride. The standard excess borohydride in solution after particle synthesis was used as a H_2 source for the dechlorination reaction. The influence of different particle synthesis parameters (coating, precursor), as well as other experimental conditions including nPd loading (0.04, 0.14, 0.4, and 1 g L^{-1}) and initial 1,2-DCA concentration (8, 32, 65, and 225 mg L^{-1}) on the dechlorination kinetics was studied. nNi particles were tested as a possible cheaper alternative to nPd particles for the catalyzed dechlorination of 1,2-DCA. The major conclusions from this study were:

- Complete removal of 1,2-DCA (32 mg L^{-1}) in <7 days was achieved by 1 g L^{-1} carboxymethyl cellulose (CMC) stabilized nPd (C-nPd_H, synthesized from

potassium hexachloropalladate) particles coupled with H_2 produced from excess borohydride present in the solution after nPd synthesis.

- Ethane was the main byproduct.
- The catalyzed dechlorination reaction followed a pseudo first order reaction rate with a surface area normalized rate constant (k_{sa}) of 11.76 x 10^{-3} L d^{-1} m^{-2}.
- A linear relationship between the pseudo-first-order rate constant (k_{obs}) and C-nPd_H loading was achieved, indicating mass transfer is not limiting the reaction.
- Increasing initial 1,2-DCA concentration > 32 mg L^{-1} resulted in more than 16-fold reduction in k_{sa}, indicating blockage of some reactive sites.
- Synthesizing nPd particles from different precursors resulted in different particle surface composition and consequently different catalytic activities and dechlorination rates.
- XPS studies showed that the ratio between reduced Pd sites and electron deficient ones changes by changing the Pd precursor, and affects the Pd catalytic activity and consequently 1,2-DCA dechlorination rate.
- Effect of coating on the catalytic activity of the nPd particles was found to be dependent on the Pd precursor used: for nPd_H particles, the coating resulted in the reduction in particles catalytic activity, with a 50% reduction in k_{sa} tcompared to bare particles. For nPd_A particles (synthesized from palladium acetate), the coating enhanced particles activity with the K_{sa} being 1.4 times that of bare particles.
- nNi as a milder hydrogenation catalyst was found to catalyze 1,2-DCA dechlorination reaction at a 0.06 times lower rate than that achieved by C-nPd_H
- TEM, and SEM imaging confirmed formation of spherical nano sized particles (<25 nm) for freshly synthesized particles.
- XPS, and XRD analysis confirmed formation of metallic particles for freshly synthesized particles.

Recently, catalytic dechlorination of 1,2-DCA in the liquid phase on copper nanoparticles (nCu) and borohydride as H_2 source at bench scale, have shown promising results. Implementation of this technology as a groundwater treatment requires optimization and understanding of the dechlorination kinetics under real-field

conditions. Therefore, in the second study the effect of treatment synthesis methods (borohydride source, particles coating, and particles water rinsing), variable 1,2-DCA loading (40, 65, and 225 mg L^{-1}), and common groundwater solutes (oxygen, sulfides, chlorides, and humic acid) on the dechlorination kinetics of 1,2-DCA was evaluated in batch reactivity experiments. The main findings from this study were:

- nCu particles were found unable to withhold H_2 gas formed during particles synthesis for use in the dechlorination reaction, and rather a direct fresh injection of borohydride into reactor bottles was found essential.
- Rinsing bare nCu particles (B-nCu_W) with deionized water prior to reactivity experiments enhanced the catalytic activity and the dechlorination efficiency of 1,2-DCA. XPS and EDX analysis showed that rinsing the nCu particles results in removal of surface elements and increase in the atomic % of reduced Cu^0 sites
- Coating the nCu_W particle with CMC (C-nCu_W) reduced the dechlorination efficiency by 21 % compared to treatments catalyzed by B-nCu_W probably due to site blockage.
- Near complete catalyzed dechlorination of 1,2-DCA (up to 225 mg L^{-1}) in < 7 hours was achieved via B-nCu_W (1 g L^{-1}) particles coupled with 25 mM borohydride with a k_{sa} value of 0.303 L d^{-1} m^{-2}.
- Presence of low concentrations of sulfides (<0.2 mg L^{-1}) did not affect B-nCu_W activity in catalyzing the dechlorination of 1,2-DCA (45 mg L^{-1}), however concentrations of 0.4, and 4 mg L^{-1} were found to partially inhibit the catalytic activity and reduce k_{obs} by 54%, and 68%, respectively.
- All the studied concentrations of humic acid (10-30 mg L^{-1}), chlorides (1000-2000 mg L^{-1}), and dissolved oxygen (4.93 mg L^{-1}) partially deactivated the B-nCu_W particles resulting in reduction in 1,2-DCA dechlorination rate, and extent.
- An additional injection of borohydride compensated for B-nCu_W particles partial poisoning and restarted the dechlorination reaction, with a final 1,2-DCA removal >80%.
- Presence of anions, humic acid and oxygen did not affect reaction rate order.

- TEM, and SEM imaging confirmed formation of spherical nano sized particles (< 35nm), and XPS, and XRD analysis confirmed formation of metallic Cu for freshly synthesized particles.

For the third study, the efficiency of the developed novel technology in remediating a suite of COCs including 1,2-DCA, in a groundwater sample from an industrial site in Australia, was assessed in batch reactivity experiments. Dechlorination efficiency of nZVI, nZVI-Pd, and nZVI-dithionite in remediating the same ground water sample was also evaluated. The primary contaminants present in the groundwater sample were: trichloromethane, 1,1,2-trichloroethane, 1,2-dichloroethane, trichloroethene, and vinyl chloride along with other secondary contaminants. The main conclusions from this part were:

- TEM imaging confirmed formation of spherical nano sized particles (<40 nm) before reaction, and agglomeration and morphology changes after reaction.
- Both nZVI and Pd-nZVI were found capable of significantly breaking down all major contaminants with the exception of 1,2-DCA.
- nZVI-dithionite was able to break down all COCs including < 20% removal of 1,2-DCA in 65 days. Re-spiking of dithionite was unable to boost the reduction reaction.
- C-nPd_H catalyzed reductive dechlorination treatment utilizing only residual borohydride after particles synthesis, was able to nearly completely remove all COCs in the first day, except 1,2-DCA. Sequential injections of borohydride were found essential to start and continue the dechlorination reaction of 1,2-DCA with a final 55% removal in 60 days.
- C-nCu particles coupled with an initial 25 mM borohydride was able to completely remove all COCs within the first couple of hours as well as a 30% removal of 1,2-DCA. Up on sequential injections of borohydride near complete removal of 1,2-DCA could be achieved in <25 days.
- Groundwater solutes were found to adversely affect the dechlorination efficiency of the treatments.

- At the end of the reactivity experiments, oxidation of all treatments indicated by change in their color was observed, with the only exception being the nZVI coupled with dithionite treatment which maintained its black color even after 120 days.

6.2 Implications

The results presented in this thesis have substantial implications for the remediation of groundwater from COCs. These implications include:

- For the first time, complete and rapid nPd catalyzed reductive dechlorination of 1,2-DCA in the liquid phase is shown feasible.
- Borohydride is an expensive chemical, typically used in excess amounts for the synthesis of nanoparticles (i.e. nZVI, Pd, Cu), thus making use of the excess amounts of borohydride as the H_2 source for the reductive dechlorination reaction is an important breakthrough.
- The results suggest that the developed nano catalyst based technology can be an effective remediation technology for a multi-COCs contaminated groundwater depending upon site conditions.
- The dechlorination rates for the different COCs (except 1,2-DCA) by C-nPd_H and C-nCu coupled with borohydride treatments is quite fast. Therefore, employment of nCu, or nPd particles in permeable reactive barriers coupled with injections of borohydride up stream, would be a promising extrapolation of the developed technology within this thesis.
- Resilience of nZVI-dithionite technology against oxidation suggests long term performance for field applications. However, understanding and evaluating the effect of dithionite on nZVI minerology on the fundamental level is a must for successful implementation.
- The study suggests that the choice of the remediation technology to be implemented in the field strongly depends on the type and concentration of contaminant, presence of co-contaminants, geochemical properties of the water and microbial characteristics, project's timeline, and economical considerations.

- Following on the previous note, it is suggested that key to successful choice of remediation technology to be applied, is running laboratory feasibility tests using different technologies and assessing groundwater characteristics prior to field application.

6.3 Research Gaps and Future Work

Different simplifications were employed in the reactivity experiments of this study, which may not adequately represent real field conditions. These simplifications include: continuous vigorous mixing of the reactor bottles, operating experiments at room temperature, use of synthetically contaminated deionized water, or groundwater filtered from soil grains, and spiking borohydride in a small closed confined well-sealed system. In addition, this thesis highlighted the effect of only a few groundwater constituents on the catalytic dechlorination efficiency of nCu-borohydride treatment performance in reducing 1,2-DCA, and did not address the effect on the minerology of the particles. Besides, effect of groundwater solutes on nPd, and nZVI in dithionite solution was not addressed. As such, future research needs to be expanded to consider more realistic field conditions, as well as explore the particles mineralogical changes.

Moreover, nPd and nCu particles are relatively expensive compared to nZVI, therefore optimization of the technology and the cost is a must in order to adequately present this technology as a viable remediation option.

Overall, future research should:

- Fundamentally examine the effect of the diverse groundwater solutes on the mineralogy and morphology of the nanoparticles (nCu, nPd, and nZVI in dithionite solution) as well as efficiency of treatments in reducing 1,2-DCA.
- Examine possible role of stabilizers in protecting nanoparticles against groundwater solutes, as well as mobility in different soil models.
- Run experiments at controlled temperatures similar to those found on site.
- Examine upscaling the experiments from batch reactors to column experiments with real groundwater samples and soil.

- Evaluate the relative efficiency of spiking borohydride in column reactors compared to batch reactors in terms of H_2 bubbles entrapment or losses.
- Investigate the effect of microbe presence on the catalytic dechlorination efficiency of the developed technologies.
- Since nPd and nCu particles are relatively expensive metals, possible cost reduction can be achieved by coupling the application of nZVI based technology with the developed catalyzed reductive dechlorination technology.
- Study replacing borohydride by environmentally friendly cheaper H_2 sources, as it would help bring down the cost of the technology.
- Examine the possibility of applying this technology using catalysts in the permeable reactive barrier coupled with injections of H_2 source up stream, from the practical, dechlorination efficiency, and economic point of view.
- Expand catalyzed reductive dehalogenation technology applications and testing to other halogenated compounds.
- Conduct research on fate and risk assessment of these nanoparticles.
- In this thesis, it has been shown that presence of dual species (Pd^{n+} and Pd^0) on Pd surface is essential for the catalyzed dechlorination reaction to take place, and decrease of Pd^{n+} sites from the surface of Pd doped on nZVI is suggested as the reason behind its incapability in reducing 1,2-DCA. As such, it is proposed that if nPd is coupled with nZVI in a different synthesis methodology, may be co-reduced with nZVI rather than deposited, those Pd^{n+} sites won't decrease and would facilitate the catalytic reduction of 1,2-DCA.

7 Appendix A: Supplementary Material for “Liquid-Phase Nano Palladium Catalyzed Hydrodechlorination of 1,2-Dichloroethane”

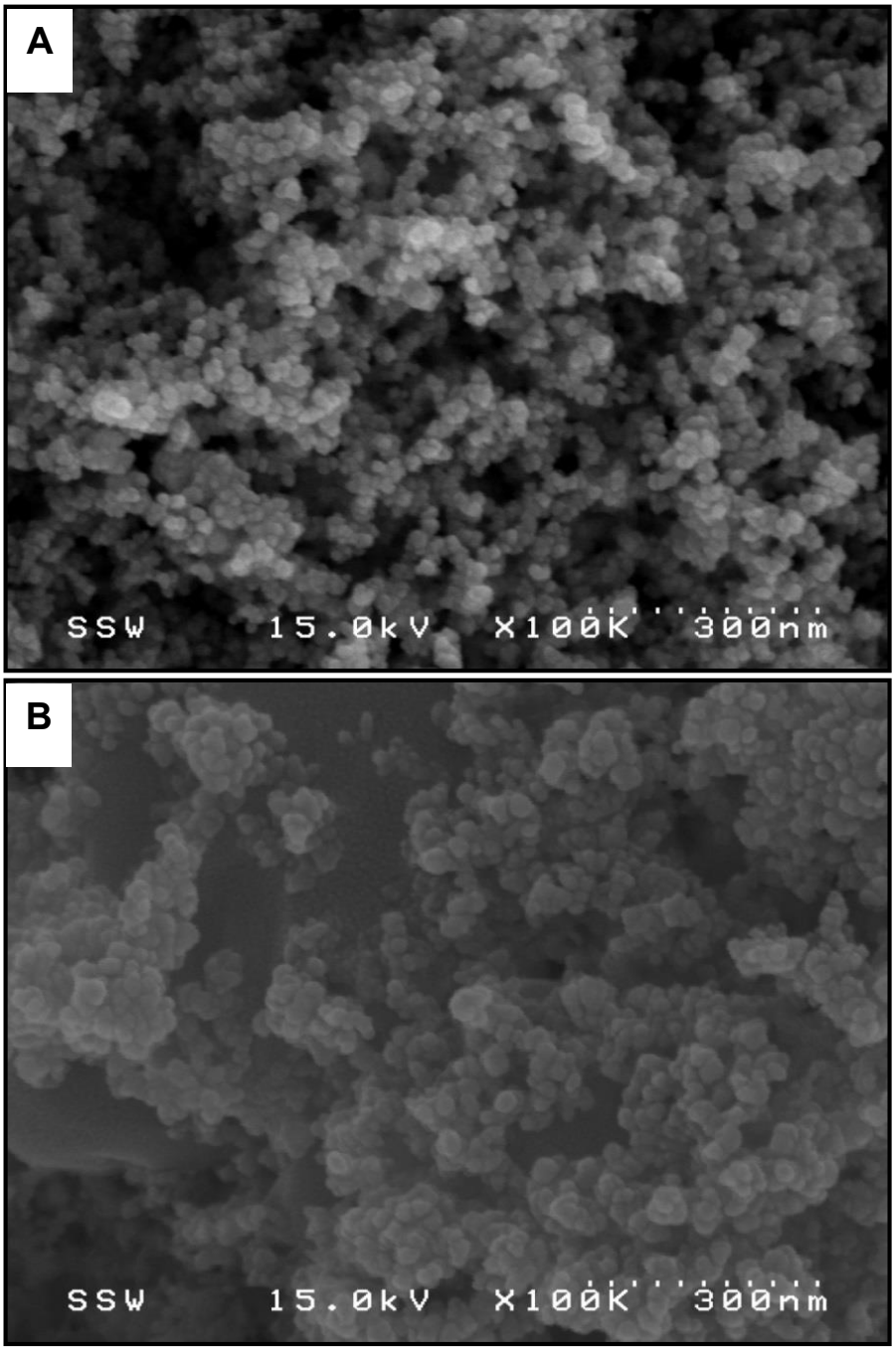

Figure 7-1: SEM images of (A) unreacted B-nPd$_{HW}$ and (B) reacted B-nPd$_{H}$ particles.

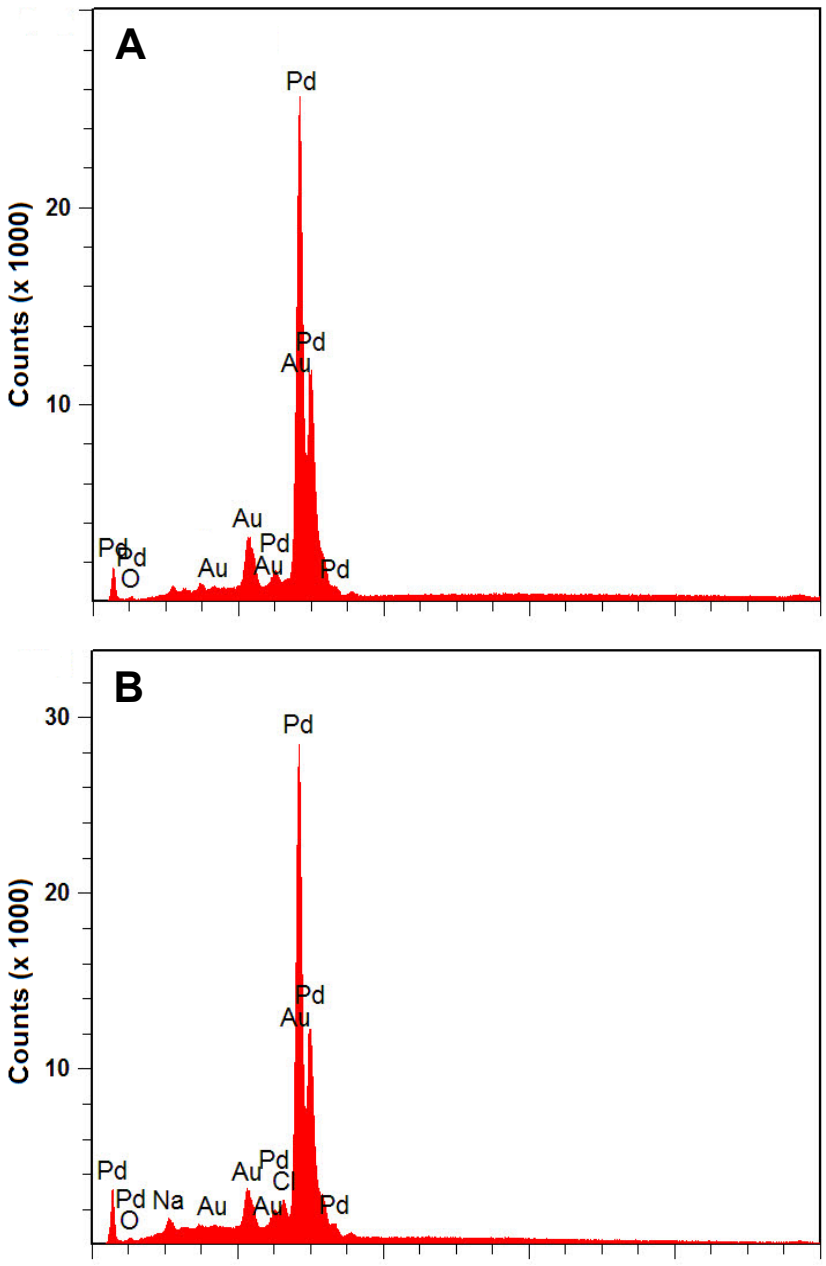

Figure 7-2: EDX analysis of (A) unreacted B-nPd$_{HW}$ and (B) reacted B-nPd$_{H}$ particles.

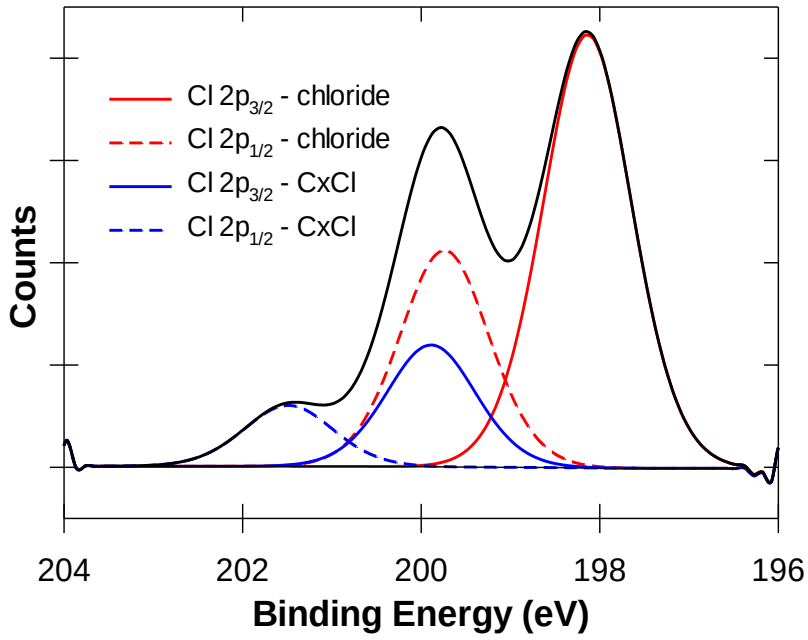

Figure 7-3: High resolution XPS for the Cl 2p region for unreacted B-nPd$_H$.

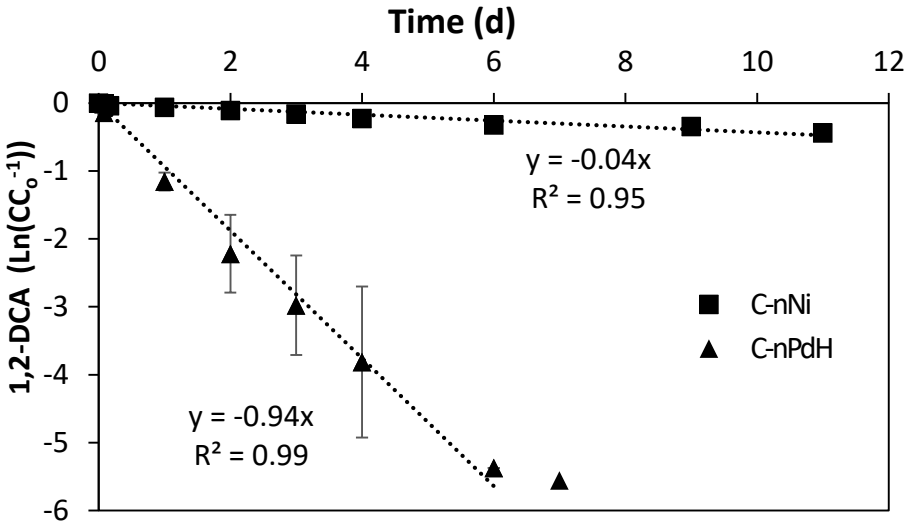

Figure 7-4: Pseudo-first-order linearization fittings of 1,2-DCA dechlorination catalyzed by C-nPd$_H$ and C-nNi (Exp. 1 & 2). Data point at t = 7d for linearization fit of C-nPd$_H$ was excluded due to the tailing effect (Johnson et al., 1996).

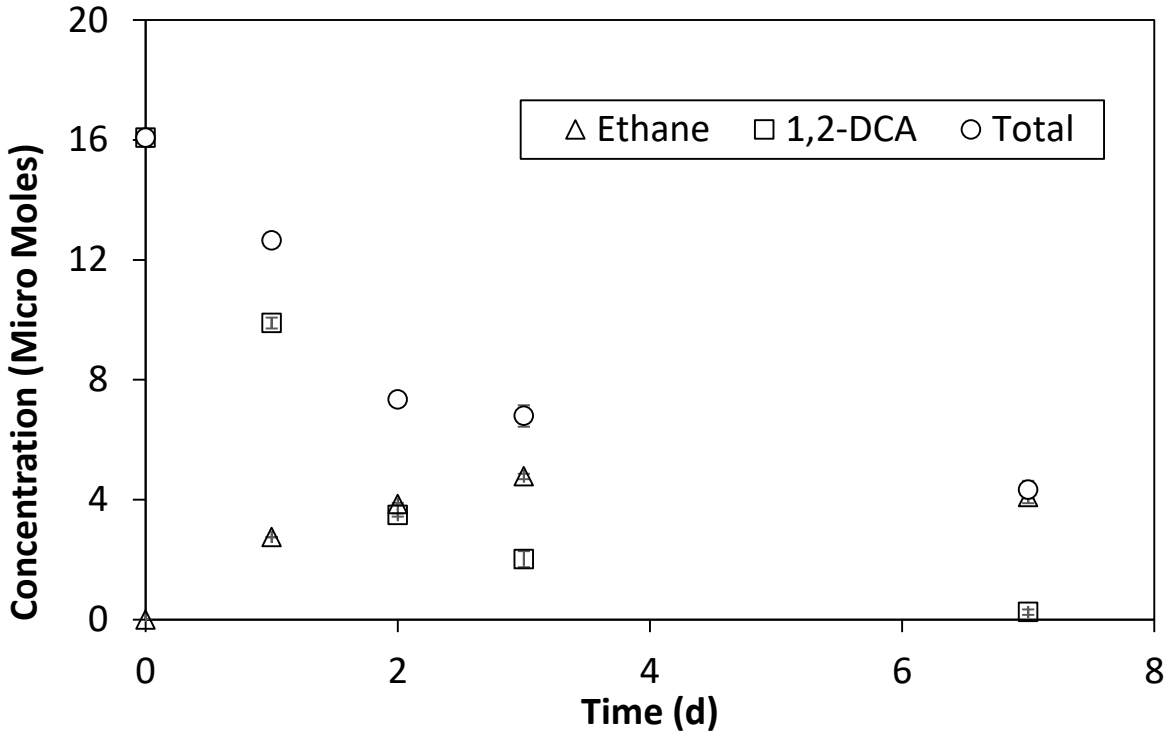

Figure 7-5: Distribution of dechlorination products for B-nPd treatment (Exp. 6, Table 3-1).

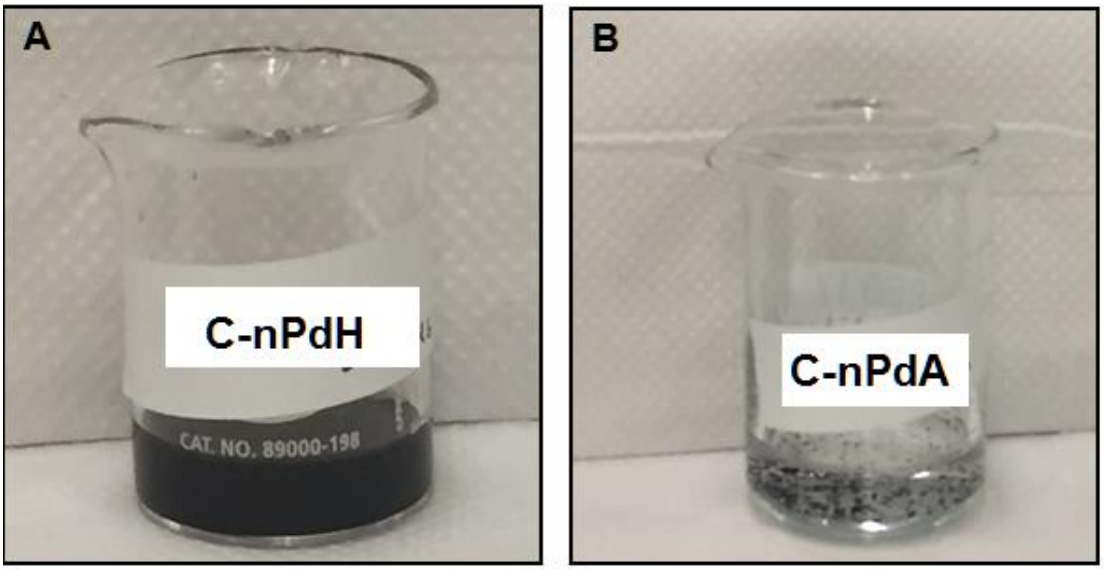

Figure 7-6: Photos of (A) C-nPd$_A$ and (B) C-nPd$_H$ suspensions after 1,2-DCA dechlorination.

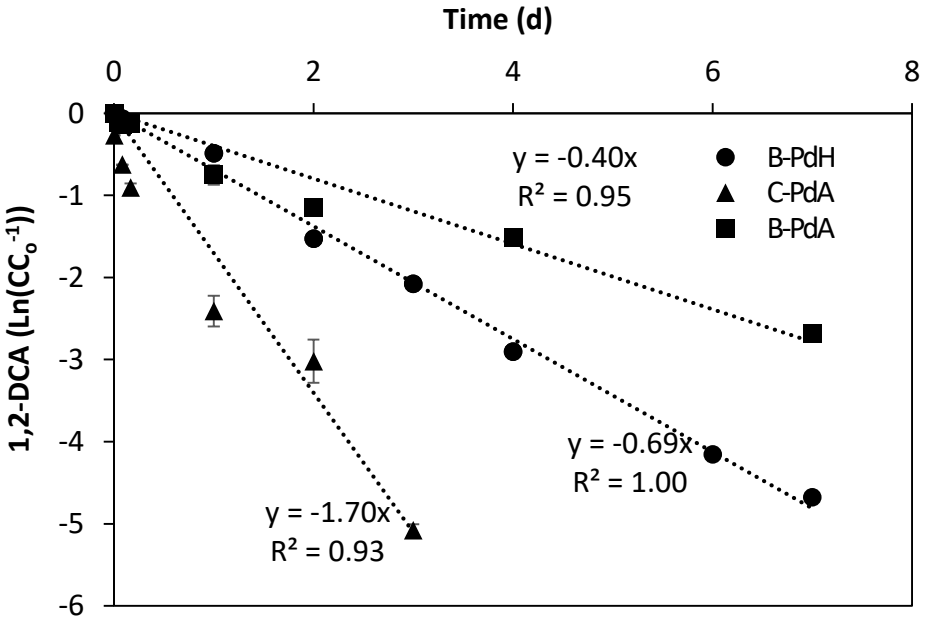

Figure 7-7: Pseudo-first-order linearization fittings of 1,2-DCA dechlorination catalyzed by B-nPd$_H$, C-nPd$_A$, and B-nPd$_A$ (Exp. 6, 7 & 8, Table 3-1).

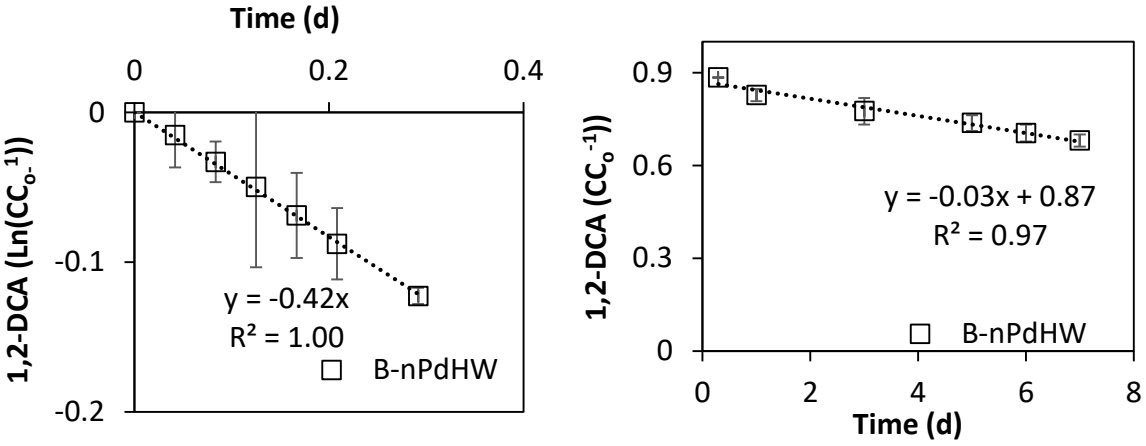

Figure 7-8: Linearization fitting of 1,2-DCA dechlorination catalyzed by B-nPd$_{HW}$ (Exp. 9) where (A) Pseudo-first-order linearization for t = 0 to 0.29 days and (B) Zero-order linearization fitting for t = 0.29 to 7 days. Reaction rate order change after 0.29 days due to blockage of reactive sites by excessive H_2 gas (Graham and Jovanovic, 1999; Jovanovic et al., 2005). Deviation from pseudo first order reaction rate to zero order have been observed earlier with reductive dechlorination experiments due to surface blockage either by growth of surface species or poisoning and depositions (Hildebrand et al., 2009b; Jovanovic et al., 2005; Song and Carraway, 2005a).

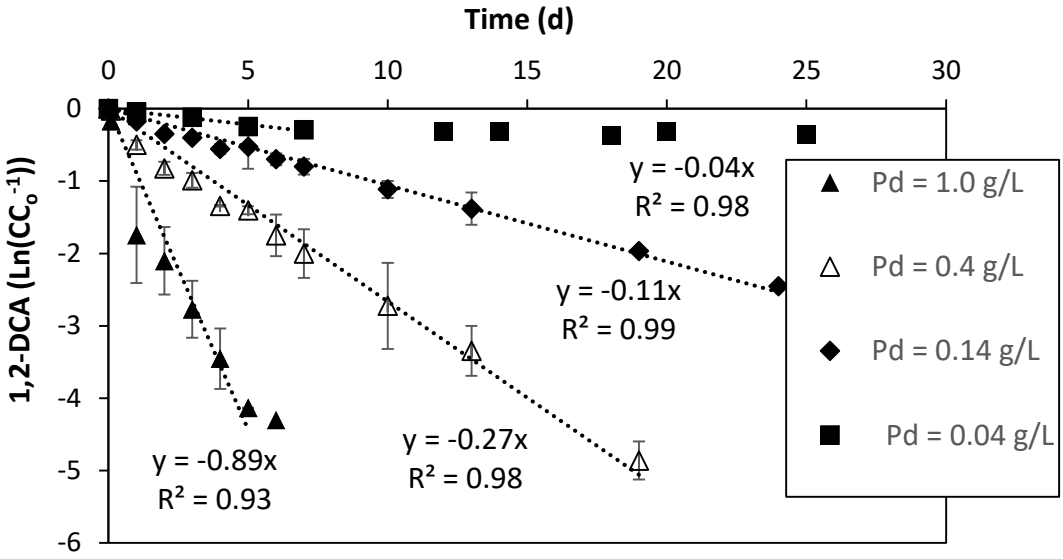

Figure 7-9: Pseudo-first-order linearization fittings of 1,2-DCA dechlorination catalyzed by C-nPd$_H$ (Exp. 5, 11, 12, &13). Data points after t = 7d were excluded for the linearization fit of C-nPd$_H$ = 1 g L^{-1} due to the tailing effect *(Johnson et al., 1996)*. Data points after t = 7d were also excluded for the linearization fit of C-nPd$_H$ = 0.04 g L^{-1} as the reaction almost ceased thereafter.

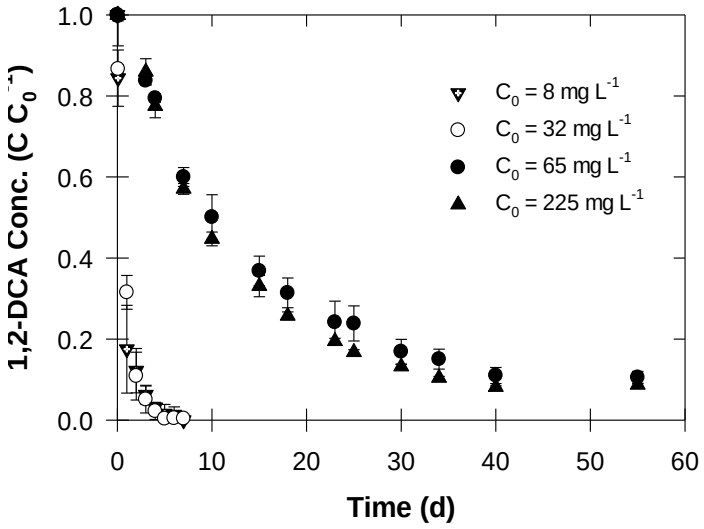

Figure 7-10: Effect of initial 1,2-DCA concentration on its catalytic dechlorination (Exp. 1, 13, 14, & 15, Table 3-1).

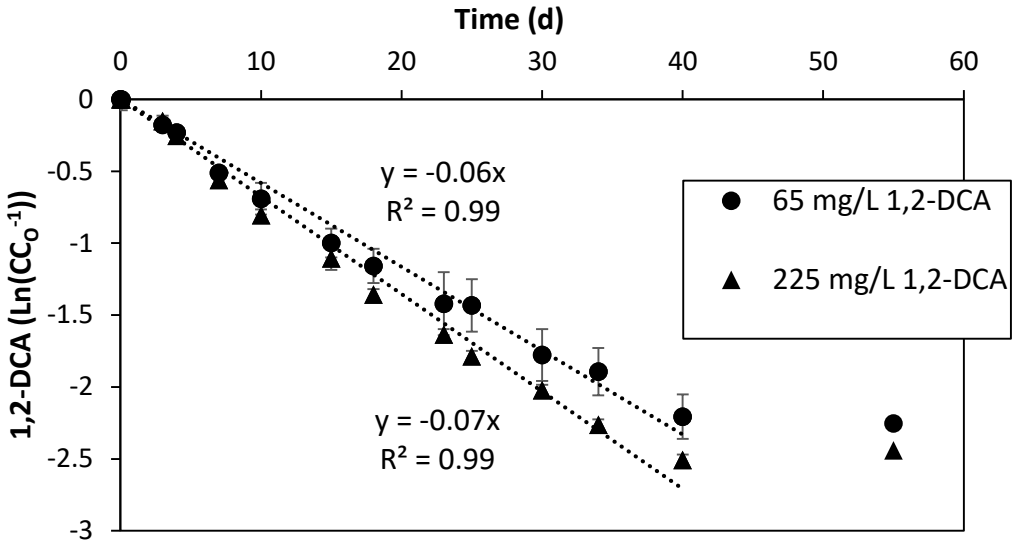

Figure 7-11: Pseudo-first-order linearization fittings of 1,2-DCA dechlorination catalyzed by C-nPd$_H$, where nano metal loading is 1 g L^{-1} (Exp. 14 & 15, Table 3-1). Last data point was excluded from both fittings due to the tailing effect (Johnson et al., 1996).

7.1 References

Graham, L.J. and Jovanovic, G., 1999. Dechlorination of p-chlorophenol on a Pd/Fe catalyst in a magnetically stabilized fluidized bed; Implications for sludge and liquid remediation. Chemical Engineering Science, 54: 3085-3093.

Hildebrand, H., Mackenzie, K. and Kopinke, F.-D., 2009b. Pd/Fe3O4 nano-catalysts for selective dehalogenation in wastewater treatment processes—Influence of water constituents. Applied Catalysis B: Environmental, 91(1–2): 389-396.

Johnson, T.L., Scherer, M.M. and Tratnyek, P.G., 1996. Kinetics of Halogenated Organic Compound Degradation by Iron Metal. Environmental Science & Technology, 30(8): 2634-2640.

Jovanovic, G.N., Znidaršič Plazl, P., Sakrittichai, P. and Al-Khaldi, K., 2005. Dechlorination of p-chlorophenol in a microreactor with bimetallic Pd/Fe catalyst. Industrial & engineering chemistry research, 44(14): 5099-5106.

Song, H. and Carraway, E.R., 2005a. Reduction of chlorinated ethanes by nanosized zero-valent iron: kinetics, pathways, and effects of reaction conditions. Environmental science & technology, 39(16): 6237-6245.

8 Appendix B: Supplementary Material for “Impact of Solution Chemistry on Nano Copper Catalyzed Dechlorination of 1,2-Dichloroethane“

Table 8-1: Experimental and literature studies diffraction angles for Cu species.

Experimental diffraction angle (2Θ in degrees)				Literature diffraction angle (2Θ in degrees)				
B-nCu		B-nCu$_W$		Huang et al.		Devaraj et al.		Mondal et al.
Cu^0	CuO_2	Cu^0	CuO_2	Cu^0	CuO_2	Cu^0	CuO_2	Cu^0
43.41	36.53	43.34	36.47	43.316	36.42	43.34	36.47	43.1
50.45	42.1	50.2	42.36	50.45	42.3	50.36	42.32	50.3
76.8	61.11	77.79	61.41	74.125	61.34	74.09	61.40	74.0
_	73.7	-	73.9	_	73.53	_	73.5	-

Table 8-2: % species content for B-n Cu particles and B-nCuw particles from Cu LMM spectra.

B-nCu			B-nCu$_W$		
Species (in Cu LMM)	Peak Position (eV)	%Area	Species (in Cu LMM)	Peak Position (eV)	%Area
Cu^0	575.67	0.5	Cu^0	575.79	0.7
Cu^0	572.35	6.7	Cu^0	572.47	10.1
Cu^0	570.41	2.2	Cu^0	570.53	3.3
Cu^0	568.52	10.5	Cu^0	568.64	15.8
Cu^0	567.97	8.6	Cu^0	568.09	13
Cu^0	566.91	3.9	Cu^0	567.03	5.7
Cu^0	565.26	4.6	Cu^0	565.37	6.9
Total % Area		37	Total % Area		55.5
$Cu(OH)_2$	574.66	4	$Cu(OH)_2$	574.86	4.2
Cu_2O	573.6	7.6	Cu_2O	573.6	4.2
$Cu(OH)_2$	570.07	13.5	$Cu(OH)_2$	570.27	14
Cu_2O	569.93	10	Cu_2O	569.93	5.6
Cu_20	568.84	23.9	Cu_2O	568.84	13.4
$Cu(OH)_2$	566.48	1.9	$Cu(OH)_2$	566.68	2
Cu_2O	565.05	2.1	Cu_2O	565.05	1.2
Total % Area		63	Total % Area		44.6

Table 8-3: Oxygen species % area distribution for Cu nanoparticles.

B-nCu			$B\text{-}nCu_W$		
Name	Position	%Area	Name	Position	%Area
O 1s – Organic O, B_2O_3	532.25	14.1	O 1s – Organic O, B_2O_3	532.76	10.6
O 1s – Hydroxide, Organic O	531.34	34.2	O 1s – Hydroxide, Organic O	531.69	33.1
O 1s – Lattice Oxide	530.38	51.6	O 1s – Lattice Oxide	530.46	56.3

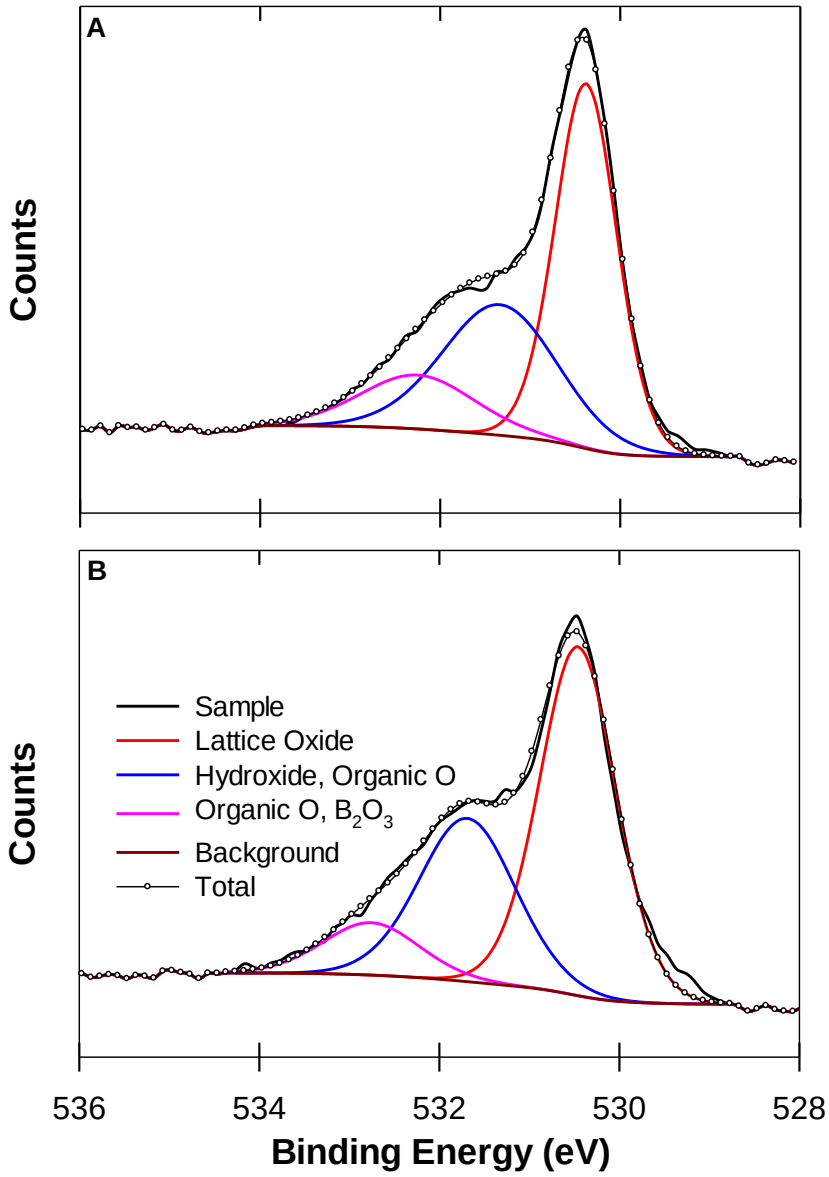

Figure 8-1: High resolution spectra for the O 1s region for nCu and nCu$_W$ particles.

Table 8-4: Properties for selected experiments.

Exp.	Description (particles + mg L^{-1} GW solute)	Zeta potential	Initial pH	Final pH	Initial ORP (mv)	Final ORP (mv)
1	C-nCu	-40.13	9.21	-	-816	-
2	C-nCu/nPd	-53.6	9.18	-	-751.8	-
5	B-nCu	-	9.77	10.74	-803	-104
9	B-nCu_W + 1000 Chlorides	-	9.75	-	-880	-170
10	B-nCu_W + 1500 Chlorides	-	9.69	-	-867	-168
11	B-nCu_W + 2000 Chlorides	-	9.71	-	-842	-100
12	B-nCu_W + 0.2 Sulfides	-	9.75	10.68	-780	-107
13	B-nCu_W + 0.4 Sulfides	-	9.91	10.83	-759	-95
14	B-nCu_W + 4 Sulfides	-	9.93	10.82	-754	-98
15	B-nCu_W +10 Humic Acid	-	9.71	10.55	-785	-114
16	B-nCu_W + 10 Humic Acid	-	9.87	10.45	-790	-121
17	B-nCu_W + 10 Humic Acid	-	9.60	10.62	-803	-130
18	B-nCu_W + 4.93 Dissolved Oxygen	-	9.28	10.68	-813	-123

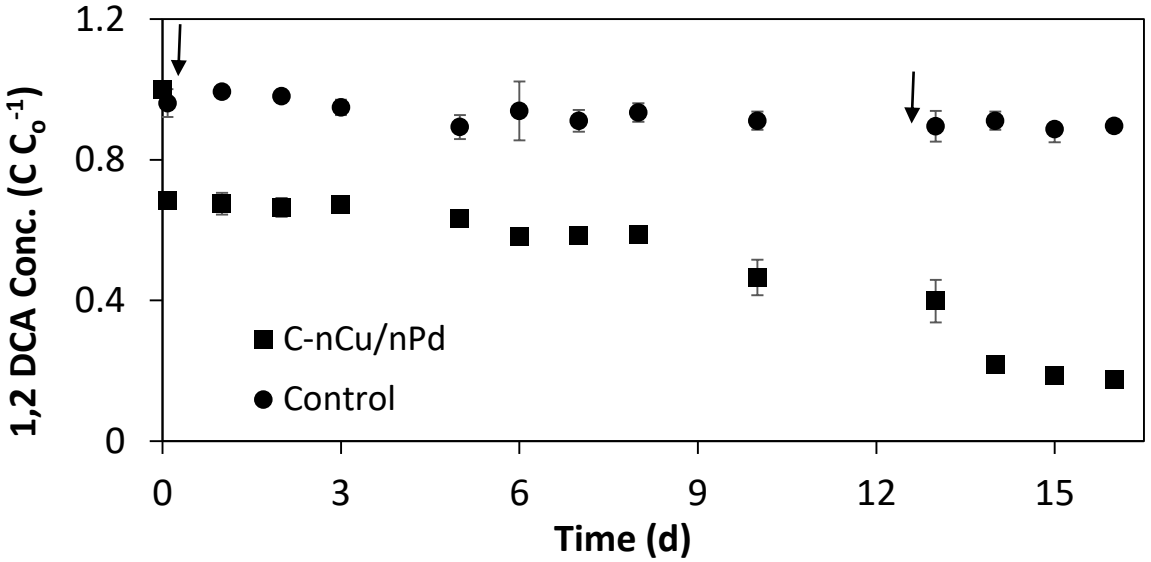

Figure 8-2: Dechlorination profile of 1,2-DCA (34 mg L^{-1}) catalyzed by C-nCu/nPd (0.5 g L^{-1} doped with 0.5% nPd). The arrow indicates spiking the reactors with 25 mM $NaBH_4$ (Exp. 3, Table 4-1).

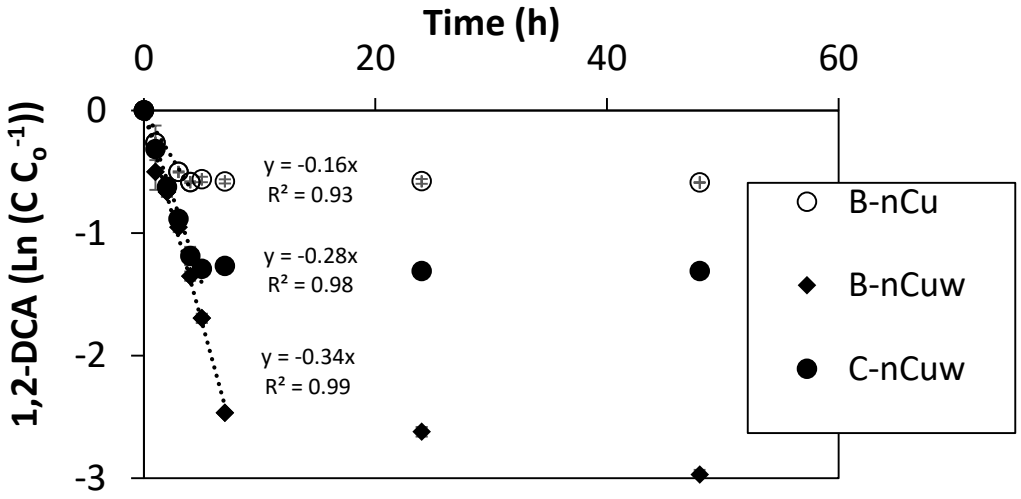

Figure 8-3: Pseudo-first-order linearization fittings of 1,2-DCA (40 mg L^{-1}) dechlorination catalyzed by 1 g L^{-1} of: C-nCu$_w$, B-nCuw, and B-nCu (Exp. 4, 5, &6). Data points after t = 7 or 5 h were also excluded for the linearization fit as the reaction ceased thereafter.

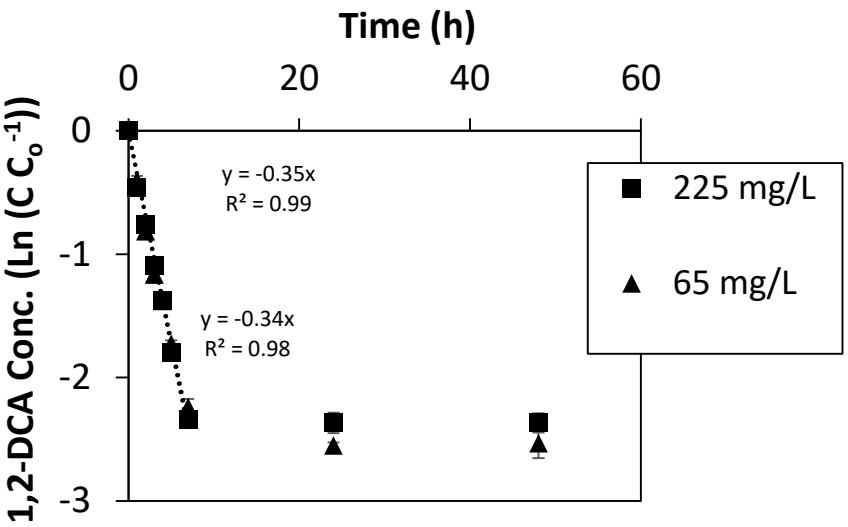

Figure 8-4: Pseudo-first-order linearization fittings of 1,2-DCA (65 & 225 mg L^{-1}) dechlorination catalyzed by 1 g L^{-1} B-nCuw (Exp. 7 & 8). Data points after t = 7 h were also excluded for the linearization fit as the reaction ceased thereafter.

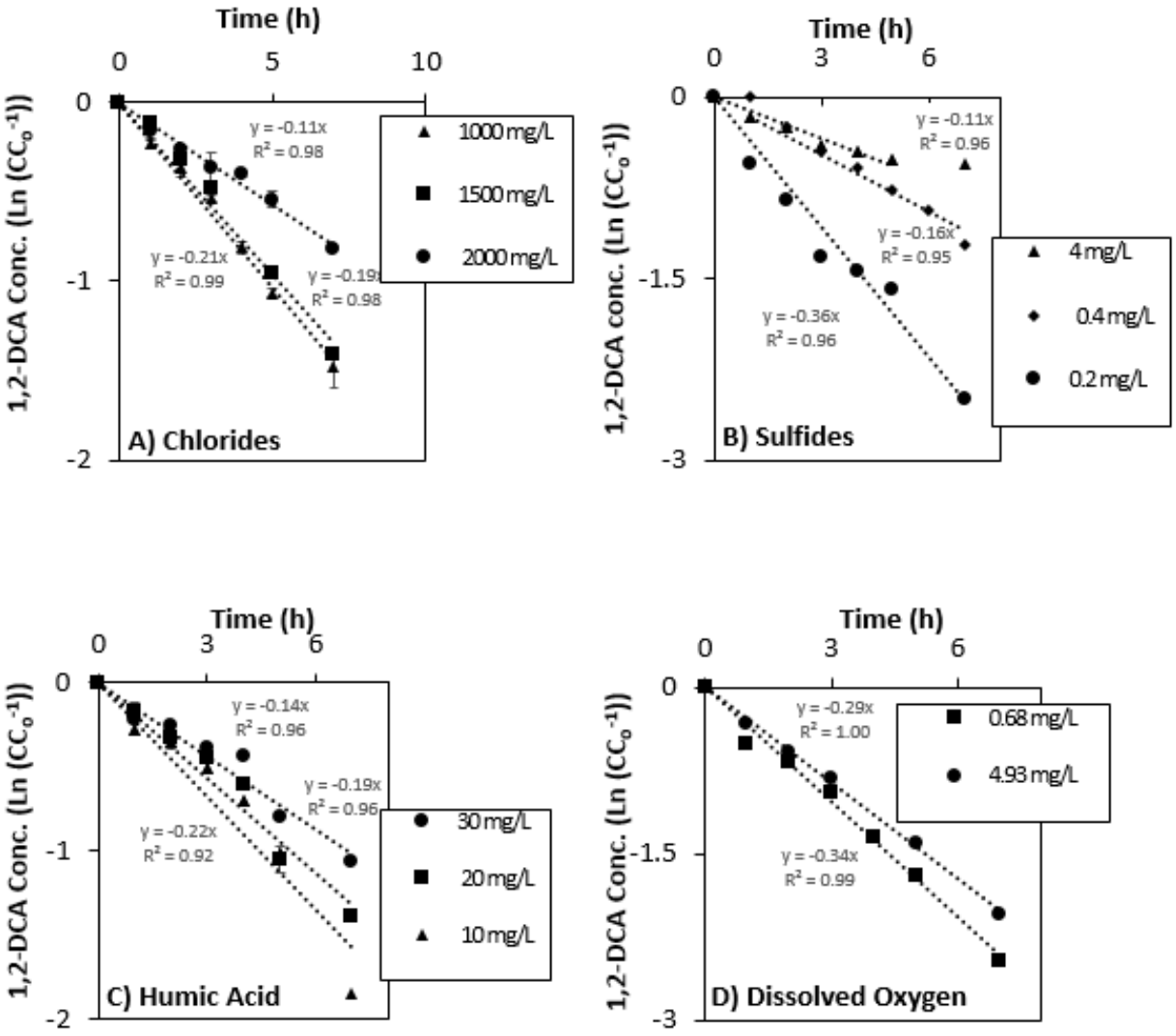

Figure 8-5: Pseudo first order Linearization curves for1,2-DCA dechlorination (45 mg L^{-1}) catalyzed by B-nCuw (1 g L^{-1}) coupled with 25 mM $NaBH_4$ in the presence of: A) chlorides, B) sulfides, C) humic acid, d) dissolved oxygen (Exp. 9-19, Table 4-1).

9 Appendix C: Supplementary Material for “Nano metal Based Technologies for Treating Chlorinated Organic Compounds (COCs) Mixtures in Groundwater”

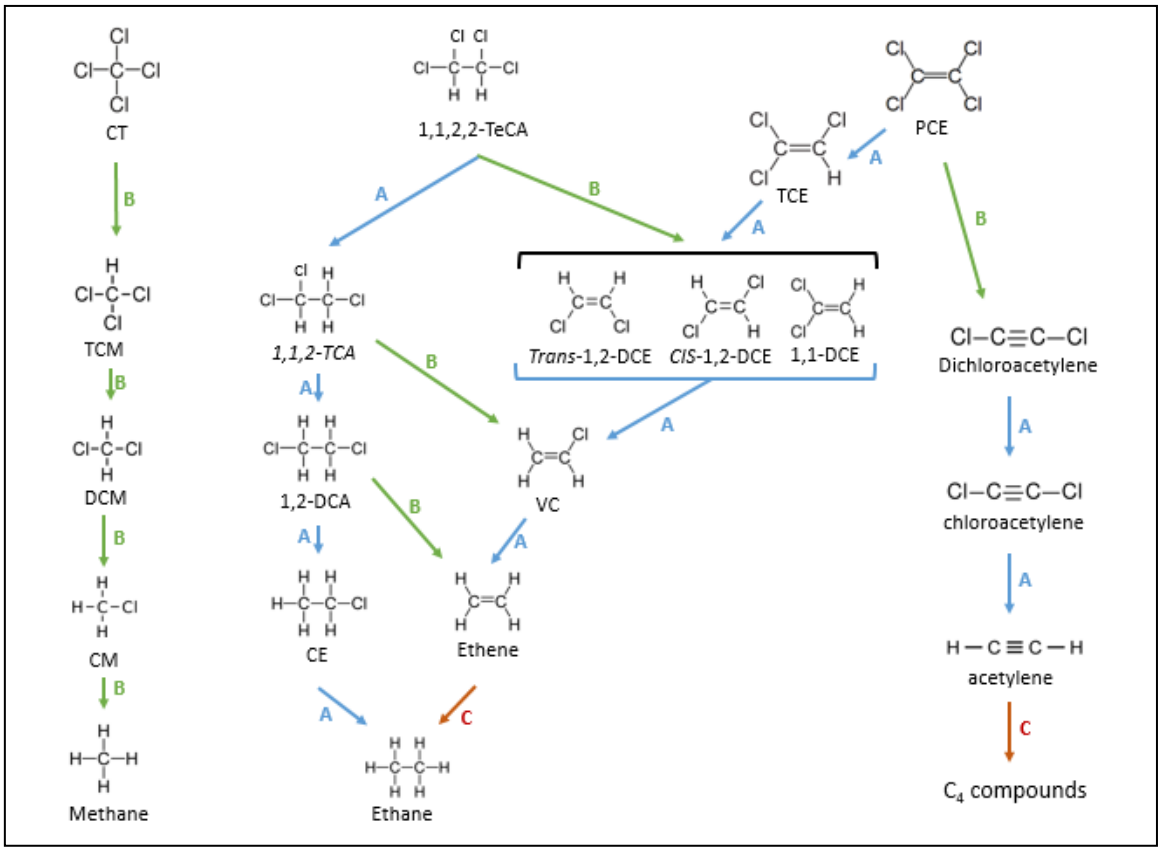

Figure 9-1: Abiotic degradation pathways for chlorinated methanes, chlorinated ethanes, and chlorinated ethenes, where: A: hydrogenolysis pathway, B: dichloroelimination pathway, and C: hydrogenation pathway (Arnold and Roberts, 2000a; Chen et al., 1996).

Table 9-1: Chemical composition of groundwater from the industrial site at Altona, Australia.

Constituent	Concentration (mg L^{-1})
Chloride (Cl^-)	16600
Sulfate (SO_4^{2-})	130
Nitrate (NO_3^-)	<0.02
Bromide (Br^-)	9.2
Mn^{2+}	34
Fe^{2+}	23
Total Organic Carbon (TOC)	41
Total Dissolved Solids (TDS)	26688
Dissolved Oxygen (DO)	0.65
pH	6.24

9.1 nZVI and Pd-nZVI Synthesis

nZVI was synthesized using a water-based approach (Lien and Zhang, 2001; Lim and Feng, 2007; Sakulchaicharoen et al., 2010). Carboxymethyl cellulose polymer (3% w/v) was dissolved overnight in deionized water and then deoxygenated with N_2 gas. Freshly prepared $FeSO_4.7H_2O$ was then added to the polymer solution to yield 7.5 g L^{-1} Fe^{2+} and 1.5% CMC (w/v). The Fe^{2+}-CMC complex solution was titrated to Fe^0 by dropwise addition of $NaBH_4$ solution (BH_4^-/M^{2+} molar ratio of 4) with continuous stirring. The solution was gently agitated for an additional 30 minutes to ensure complete nucleation of nZVI particles on the polymer.

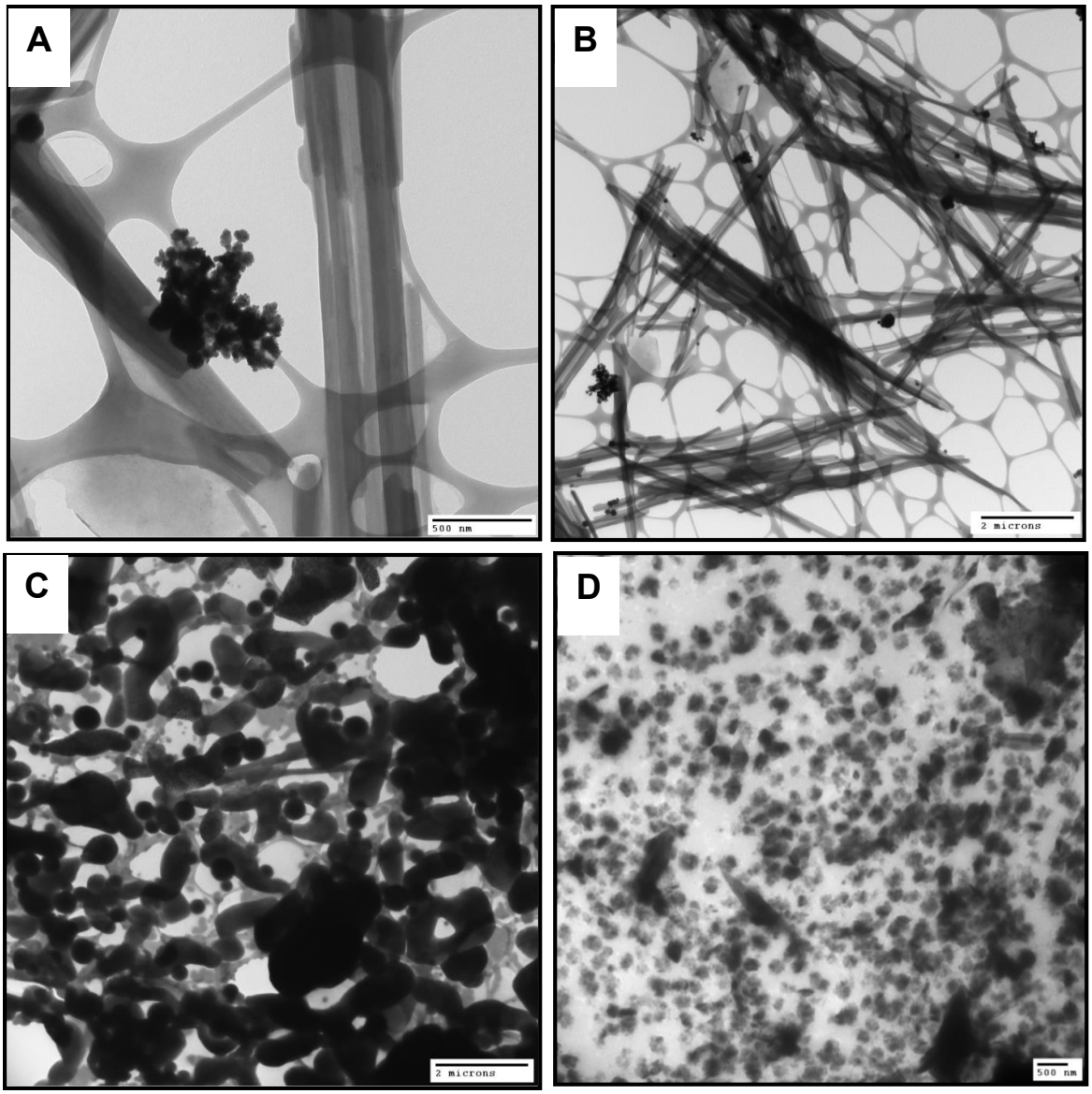

Figure 9-2: TEM images of CMC-stabilized (A) nCu (High resolution), (B) nCu, (C) nPd, and (D) nZVI-dithionite particles after reaction.

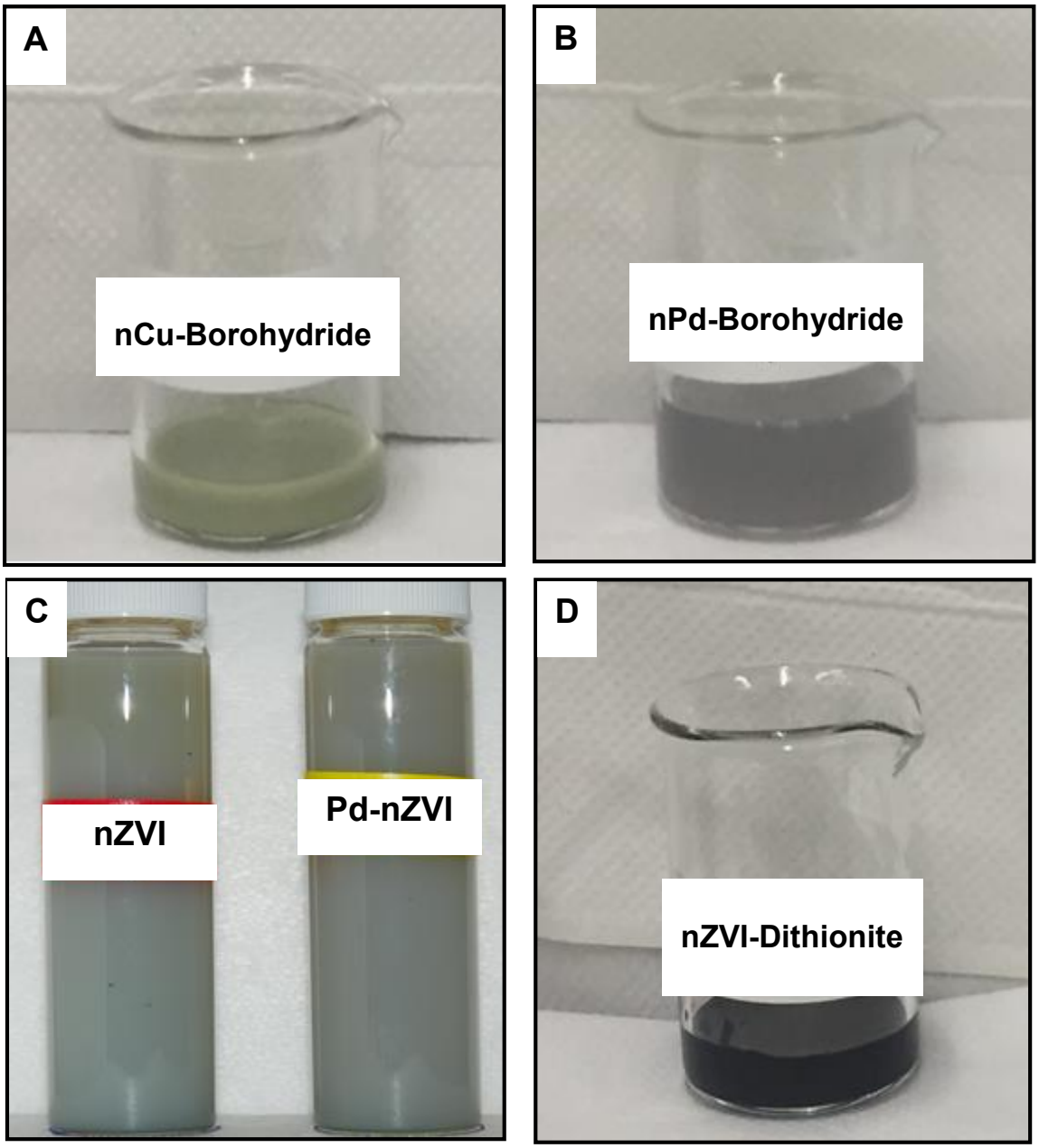

Figure 9-3: Pictures of (A) nCu, (B) nPd, (C) nZVI & Pd-nZVI, and (D) nZVI-dithionite suspensions after reaction.

9.2 Proposed COCs Dechlorination Order

The favorability of COCs to reduction can be rationalized by the Gibb's free energy for the reductive dechlorination reaction. The lower the Gibb's free energy value, the easier and more favorable the dechlorination (Dolfing et al., 2006). Therefore, the proposed dechlorination order for COCs based on the Gibb's free energy value at 25^{o} C and pH of 7 is: PCE > TCM> TCE > 1,1,2-TCA > DCM > VC > 1,2-DCE > 1,2-DCA. Besides, the lower the oxidation state of the carbon atoms bearing chlorine atoms, the less the favorability to dechlorination (De Wildeman and Verstraete, 2003). Therefore, the proposed dechlorination order for chlorinated ethanes, chlorinated ethenes, and chlorinated methanes is: 1,1,2-TCA > 1,2-DCA, PCE > TCE > 1,2-DCE > VC, and TCM > DCM, respectively.

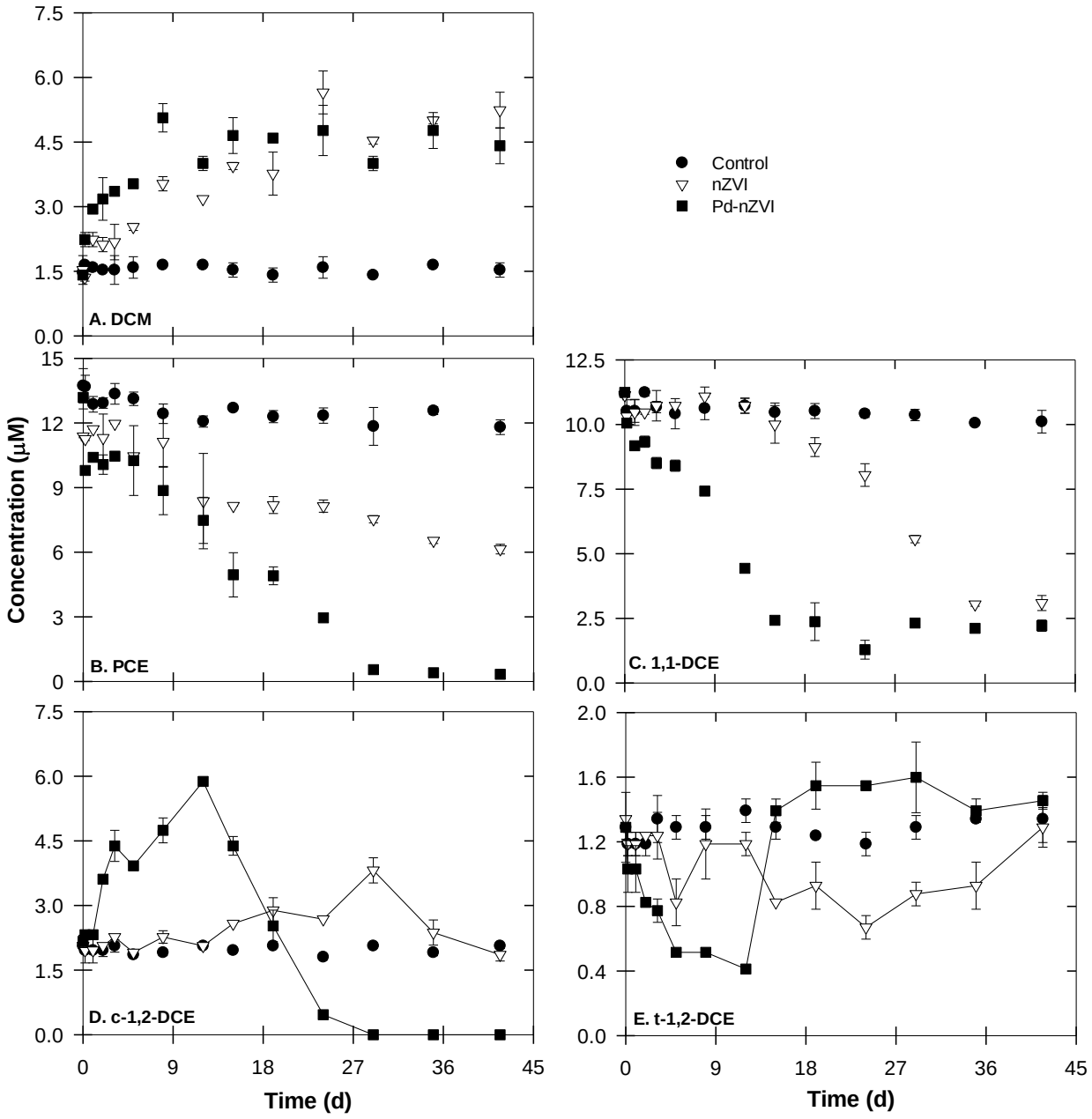

Figure 9-4: Changes in concentrations (μM) of (A) Dichloromethane, (B) Tetrachloroethene, (C) 1,1-Dichloroethene, (D) cis-1,2-Dichloroethene, and (E) trans-1,2-dichloroethene after treatment with 2.5 g L^{-1} nZVI and Pd-nZVI.

Table 9-2: Concentrations of COCs in the groundwater sample after 35 days of its treatment with 5 g L^{-1} nZVI.

Chlorinated Organic Compound	Concentration (µM)	
	Initial*	Final
Trichloromethane (TCM)	23.0	ND
Dichloromethane (DCM)	1.06	1.77
1,1,2-Trichloroethane (1,1,2-TCA)	414	54.8
1,2-Dichloroethane (1,2-DCA)	373	353
Tetrachloroethene (PCE)	7.11	0.06
Trichloroethene (TCE)	78.6	ND
1,1-Dichloroethene (1,1-DCE)	5.88	1.65
trans-1,2-Dichloroethene (t-1,2-DCE)	0.72	0.72
cis-1,2-Dichloroethene (c-1,2-DCE)	1.13	ND
Vinyl Chloride (VC)	209	3.84

*Average concentrations in controls.

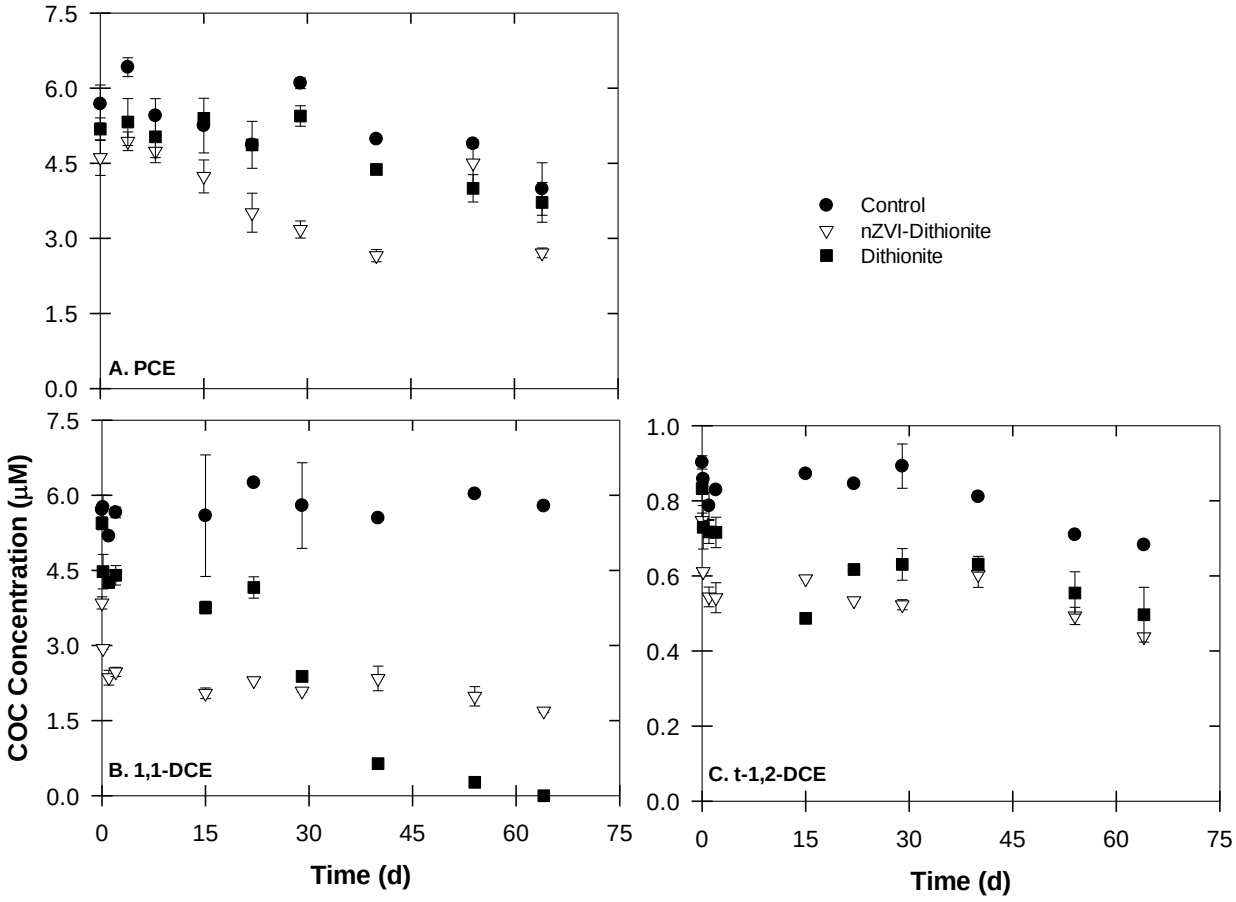

Figure 9-5: Changes in concentrations (µM) of (A) Tetrachloroethene, (B) 1,1-Dichloroethene, and (C) trans-1,2-dichloroethene after treatment with 2.5 g L^{-1} nZVI-dithionite and 50 mM Dithionite.

9.3 References

Arnold, W.A. and Roberts, A.L., 2000a. Pathways and kinetics of chlorinated ethylene and chlorinated acetylene reaction with Fe (0) particles. Environmental Science & Technology, 34(9): 1794-1805.

Chen, C., Puhakka, J.A. and Ferguson, J.F., 1996. Transformations of 1, 1, 2, 2-tetrachloroethane under methanogenic conditions. Environmental science & technology, 30(2): 542-547.

De Wildeman, S. and Verstraete, W., 2003. The quest for microbial reductive dechlorination of C 2 to C 4 chloroalkanes is warranted. Applied microbiology and biotechnology, 61(2): 94-102.

Dolfing, J., VanEckert, D. and Meuller, J., 2006. Thermodynamics of low Eh reactions, Battelle's Fifth International Conference on Remediation of Chlorinated and Recalcitrant Compounds. Citeseer.

Lien, H.-L. and Zhang, W.-X., 2001. Nanoscale iron particles for complete reduction of chlorinated ethenes. Colloids and Surfaces A: Physicochemical and Engineering Aspects, 191(1): 97-105.

Lim, T.T. and Feng, J., 2007. Iron-mediated reduction rates and pathways of halogenated methanes with nanoscale Pd/Fe: Analysis of linear free energy relationship. Chemosphere, 66(9): 1765-1774.

Sakulchaicharoen, N., O'Carroll, D.M. and Herrera, J.E., 2010. Enhanced stability and dechlorination activity of pre-synthesis stabilized nanoscale FePd particles. Journal of contaminant hydrology, 118(3): 117-127.

Curriculum Vitae

Name: Omneya El-Sharnouby

Post-secondary Education and Degrees:
University of Alexandria
Alexandria, Egypt
2004-2009 B.E.SC

Honors and Awards:
Ontario Trillium Scholarship
2012-2016
1st place "Three Minute Thesis Competition", Renew/Integarte Meeting

Related Work Experience
Teaching Assistant
The University of Western Ontario
2012-2016
Teaching and Research Assistant
Alexandria University
2009-2012

Publications:

a. Articles published or accepted in refereed journals

Omneya Elsharnouby, Hisham Hafez, George Nakhla, M. Hesham, El Naggar, 2013
"A critical literature review on biohydrogen production by pure cultures"
A review paper, Intentional journal of hydrogen energy, 38, (12), 4945-4966

b. Non-refereed contributions

Omneya El-Sharnouby, Hardiljeet Boparai, Denis M. O'Carroll, 2016
"Nano Metal Based Technologies for Treating Chlorinated Organic Compounds in Groundwater"
Oral Presentation, Integrate annual meeting, 30 September.

Omneya El-Sharnouby, Hardiljeet Boparai, Jose Herrera, Denis M. O'Carroll, 2015
"Liquid Phase Catalyzed Dechlorination of 1,2-Dichloroethane by Sodium Borohydride."
Oral Presentation, IAH-CNC 2015, Waterloo, 27-29 October.

Omneya El-Sharnouby, Hardiljeet Boparai, Jose Herrera, Denis M. O'Carroll, 2015
"Feasibility of Liquid Phase Metallic Catalyzed Dechlorination of 1,2-Dichloroethane by Sodium Borohydride."
Poster, Integrate/Renew, Western University, 1-2 October.

Omneya Elsharnouby, Denis O'Carroll, and Jose Herrera, 2014
"Feasibility of liquid phase Pd Catalyzed Reductive Dechlorination of 1,2-Dichloroethane." Oral Presentation, Integrate annual meeting, Toronto, 26 September.

c. Refereed Articles in Preparation

Omneya El-Sharnouby, Hardiljeet Boparai, Jose Herrera, Denis M. O'Carroll
"Liquid Phase Nano Palladium Catalyzed Reductive Dechlorination of 1,2-Dichlororethane".

Omneya El-Sharnouby, Hardiljeet Boparai, Jose Herrera, Denis M. O'Carroll
"Impact of Solution Chemistry on Nano Copper Catalyzed Dechlorination of 1,2-Dichloroethane".

Omneya El-Sharnouby, Hardiljeet Boparai, Denis M. O'Carroll
"Nano metal Based Technologies for Treating Chlorinated Organic Compounds Mixtures in Groundwater".